(12) INTERNATIONAL APPLICATION PUBLISHED UNDER THE PATENT COOPERATION TREATY (PCT)

(19) World Intellectual Property Organization
International Bureau

(43) International Publication Date
8 September 2017 (08.09.2017)

WIPO | PCT

(10) International Publication Number
WO 2017/147654 A1

(51) International Patent Classification:
A61K 38/17 (2006.01) *A61P 25/08* (2006.01)
A61P 25/28 (2006.01) *A61P 9/10* (2006.01)

(21) International Application Number:
PCT/AU2017/050180

(22) International Filing Date:
1 March 2017 (01.03.2017)

(25) Filing Language: English

(26) Publication Language: English

(30) Priority Data:
2016900764 1 March 2016 (01.03.2016) AU

(71) Applicant: **NEWSOUTH INNOVATIONS PTY LIMITED** [AU/AU]; Rupert Myers Building, Gate 14, Barker Street, UNSW, Sydney, New South Wales 2052 (AU).

(72) Inventors: **ITTNER, Lars Matthias**; 13 Ferndale Street, Chatswood, New South Wales 2067 (AU). **ITTNER, Arne Anselm**; 2/53-55B Frenchmans Road, Randwick, New South Wales 2031 (AU).

(74) Agent: **GRIFFITH HACK**; GPO Box 4164, North Sydney, New South Wales 2001 (AU).

(81) Designated States *(unless otherwise indicated, for every kind of national protection available)*: AE, AG, AL, AM, AO, AT, AU, AZ, BA, BB, BG, BH, BN, BR, BW, BY, BZ, CA, CH, CL, CN, CO, CR, CU, CZ, DE, DJ, DK, DM, DO, DZ, EC, EE, EG, ES, FI, GB, GD, GE, GH, GM, GT, HN, HR, HU, ID, IL, IN, IR, IS, JP, KE, KG, KH, KN, KP, KR, KW, KZ, LA, LC, LK, LR, LS, LU, LY, MA, MD, ME, MG, MK, MN, MW, MX, MY, MZ, NA, NG, NI, NO, NZ, OM, PA, PE, PG, PH, PL, PT, QA, RO, RS, RU, RW, SA, SC, SD, SE, SG, SK, SL, SM, ST, SV, SY, TH, TJ, TM, TN, TR, TT, TZ, UA, UG, US, UZ, VC, VN, ZA, ZM, ZW.

(84) Designated States *(unless otherwise indicated, for every kind of regional protection available)*: ARIPO (BW, GH, GM, KE, LR, LS, MW, MZ, NA, RW, SD, SL, ST, SZ, TZ, UG, ZM, ZW), Eurasian (AM, AZ, BY, KG, KZ, RU, TJ, TM), European (AL, AT, BE, BG, CH, CY, CZ, DE, DK, EE, ES, FI, FR, GB, GR, HR, HU, IE, IS, IT, LT, LU, LV, MC, MK, MT, NL, NO, PL, PT, RO, RS, SE, SI, SK, SM, TR), OAPI (BF, BJ, CF, CG, CI, CM, GA, GN, GQ, GW, KM, ML, MR, NE, SN, TD, TG).

Published:

— *with international search report (Art. 21(3))*

— *with sequence listing part of description (Rule 5.2(a))*

WO 2017/147654 A1

(54) Title: USE OF PHOSPHORYLATED TAU AND P38GAMMA TO TREAT A NEUROLOGICAL CONDITION

Figure 16

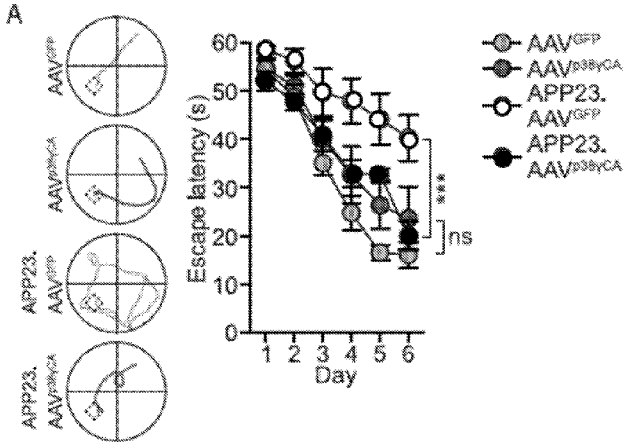

(57) Abstract: The present invention relates to a method of treating or preventing a neurological condition mediated by a tau-dependent signalling complex in neurons of a subject, comprising treating the subject to: (a) promote phosphorylation of one or more amino acid residues of tau, wherein the phosphorylation of the amino acid residues causes disruption of the tau-dependent signalling complex in neurons of the subject; or (b)introduce a variant of tau that causes disruption of the tau-dependent signalling complex in neurons of the subject. The invention also relates to vectors, compositions and kits for treating or preventing a neurological condition mediated by a tau-dependent signalling complex in neurons of a subject.

Use of phosphorylated tau and p38gamma to treat a neurological condition

Field

The present invention relates to a method of treating or preventing a neurological condition mediated by a tau-dependent signalling complex in neurons of a subject, to a vector for treating or preventing such neurological conditions, and to compositions comprising a vector for treating such conditions.

Background

Excitotoxicity of neurons is a pathological process by which neurons are damaged or killed by excessive stimulation. Such stimulation occurs when glutamatergic receptors, such as, for example, NMDA-type receptors (NR), are overactivated by neurotransmitters such as, for example, glutamic acid. Excitotoxicity can also be induced by excitotoxins such as amyloid-β (Aβ).

Excitotoxicity is believed to play a prominent role in neurological conditions such as various forms of neurodegenerative disease including Alzheimer's disease (AD), frontotemporal dementia, Huntington's disease, Parkinson's disease. Excitotoxicity is also associated with epilepsy, and neuronal damage which occurs following stroke.

Alzheimer's disease (AD) is the most prevalent form of dementia and is the most common neurodegenerative disease. AD is estimated to affect as many as 1% of adults 60 years of age and over.

AD is characterised by brain atrophy, neural loss, extracellular Aβ plaques, and intracellular neurofibrillary tangle (NFTs) containing aberrantly phosphorylated tau.

Tau is an axonal protein that, under non-pathological conditions, regulates microtubule stability and microtubule dependent processes. Tau has also been found to reside in a post-synaptic signalling complex that

mediates Aβ-induced excitotoxicity, and potentially other excitotoxicity. In AD, tau becomes aberrantly phosphorylated, and accumulates in the somatodendritic compartments of neurons, aggregates and eventually forms neurofibrilar tangles (NFT). Progression of NFT pathology throughout the brain correlates with disease progression in Alzheimer's disease.

The prevailing theory in AD is that Aβ triggers toxic events including tau phosphorylation causing neuronal dysfunction and death. In support, depleting tau prevents Aβ toxicity in AD mouse and cell culture models. Aβ-toxicity in AD is therefore considered in the art to be mediated by phosphorylated tau in the pathogenesis of AD.

It would be advantageous to provide alternative methods of treating AD and other neurological conditions.

Summary

The inventors have found that, contrary to the teaching in the art, phosphorylation of tau at particular amino acid residues causes disruption of tau-dependent signalling complexes, and prevents or reduces excitotoxicity and Aβ-induced toxicity.

A first aspect provides a method of treating or preventing a neurological condition mediated by a tau-dependent signalling complex in neurons of a subject, comprising treating the subject to:

(a) promote phosphorylation of one or more amino acid residues of tau, wherein the phosphorylation of the amino acid residues causes disruption of the tau-dependent signalling complex in neurons of the subject; or

(b) introduce a variant of tau that causes disruption of the tau-dependent signalling complex in neurons of the subject.

A second aspect provides a method of treating or

preventing a neurological condition mediated by a tau-dependent signalling complex in neurons of a subject, comprising administering an agent which:

(a) promotes phosphorylation of one or more amino acid residues of tau, wherein the phosphorylation of the amino acid residues causes disruption of the tau-dependent signalling complex in neurons of the subject; or

(b) introduces a variant of tau that causes disruption of the tau-dependent signalling complex in neurons of the subject.

An alternative second aspect provides an agent which: (a) promotes phosphorylation of one or more amino acid residues of tau, wherein the phosphorylation of the amino acid residues causes disruption of the tau-dependent signalling complex in neurons of the subject; or (b) introduces a variant of tau that causes disruption of the tau-dependent signalling complex in neurons of the subject, for use in the treating or preventing of a neurological condition mediated by a tau-dependent signalling complex in neurons of a subject, or use of an agent which: (a) promotes phosphorylation of one or more amino acid residues of tau, wherein the phosphorylation of the amino acid residues causes disruption of the tau-dependent signalling complex in neurons of the subject; or (b) introduces a variant of tau that causes disruption of the tau-dependent signalling complex in neurons of the subject, in the manufacture of a medicament for the treating or preventing of a neurological condition mediated by a tau-dependent signalling complex in neurons of a subject.

A third aspect provides a method of treating or preventing a neurological condition mediated by a tau-dependent signalling complex in neurons of a subject,

comprising administering an agent which elevates p38γ activity, or the activity of a variant of p38γ, in the neurons of the subject.

An alternative third aspect provides an agent which elevates p38γ activity, or the activity of a variant of p38γ, in neurons of a subject, for use in the treating or preventing of a neurological condition mediated by a tau-dependent signalling complex in neurons of a subject, or use of an agent which elevates p38γ activity, or the activity of a variant of p38γ, in neurons of a subject, in the manufacture of a medicament for the treating or preventing of a neurological condition mediated by a tau-dependent signalling complex in neurons of a subject.

A fourth aspect provides a vector for treating or preventing a neurological condition mediated by a tau-dependent signalling complex in neurons of a subject, comprising:

(a) a nucleic acid sequence encoding p38γ or a variant thereof; or

(b) a nucleic acid sequence encoding a variant of tau that causes disruption of the tau-dependent signalling complex in neurons of the subject.

A fifth aspect provides an adeno-associated viral vector for treating or preventing a neurological condition mediated by a tau-dependent signalling complex in neurons of a subject, comprising:

(a) a nucleic acid sequence encoding p38γ or a variant thereof; or

(b) a nucleic acid sequence encoding a variant of tau that causes disruption of the tau-dependent signalling complex in neurons of the subject.

A sixth aspect provides a method of disrupting, or reducing formation of, a signalling complex comprising PSD-95, tau and FYN in a neuron, comprising contacting the neuron with an agent which:

(a) promotes phosphorylation of one or more amino acid residues of the tau, wherein the phosphorylation of the amino acid residues causes disruption of the signalling complex; or

(b) introduces a variant of tau that causes disruption of the tau-dependent signalling complex.

An alternative sixth aspect provides an agent which: (a) promotes phosphorylation of one or more amino acid residues of tau, wherein the phosphorylation of the amino acid residues causes disruption of the tau-dependent signalling complex in neurons of the subject; or (b) introduces a variant of tau that causes disruption of the tau-dependent signalling complex in neurons of the subject, for use in disrupting, or reducing formation of, a signalling complex comprising PSD-95, tau and FYN in a neuron, or use of an agent which (a) promotes phosphorylation of one or more amino acid residues of tau, wherein the phosphorylation of the amino acid residues causes disruption of the tau-dependent signalling complex in neurons of the subject; or (b) introduces a variant of tau that causes disruption of the tau-dependent signalling complex in neurons of the subject, in the manufacture of a medicament for disrupting, or reducing formation of, a signalling complex comprising PSD-95, tau and FYN in a neuron.

A seventh aspect provides a method of treating Alzheimer's disease in a subject comprising administering an agent which:

(a) promotes phosphorylation of one or more amino acid residues of tau, wherein the phosphorylation of the

amino acid residues causes disruption of the tau-dependent signalling complex in neurons of the subject; or

(b) introduces a variant of tau that causes disruption of the tau-dependent signalling complex in neurons of the subject.

An alternative seventh aspect provides an agent which: (a) promotes phosphorylation of one or more amino acid residues of tau, wherein the phosphorylation of the amino acid residues causes disruption of the tau-dependent signalling complex in neurons of the subject; or (b) introduces a variant of tau that causes disruption of the tau-dependent signalling complex in neurons of the subject, for use in treating Alzheimer's disease in a subject, or use of an agent which (a) promotes phosphorylation of one or more amino acid residues of tau, wherein the phosphorylation of the amino acid residues causes disruption of the tau-dependent signalling complex in neurons of the subject; or (b) introduces a variant of tau that causes disruption of the tau-dependent signalling complex in neurons of the subject, in the manufacture of a medicament for treating Alzheimer's disease in a subject.

An eighth aspect provides a method of treating Alzheimer's disease in a subject comprising introducing into neurons of the subject:

(a) a nucleic acid capable of expressing p38γ, or variant thereof; or

(b) a nucleic acid capable of expressing a variant of tau that causes disruption of the tau-dependent signalling complex.

An alternative eighth aspect provides: (a) a nucleic acid capable of expressing p38γ, or variant thereof; or (b) a nucleic acid capable of expressing a variant of tau that causes disruption of the tau-dependent signalling complex, for use in treating Alzheimer's disease in a subject, or use of (a) a nucleic acid capable of expressing p38γ, or variant thereof; or (b) a nucleic acid capable of expressing a variant of tau that causes disruption of the tau-dependent signalling complex, in the manufacture of a medicament for treating Alzheimer's disease in a subject.

A ninth aspect provides a method of treating stroke in a subject comprising administering an agent which:

(c) promotes phosphorylation of one or more amino acid residues of tau, wherein the phosphorylation of the amino acid residues causes disruption of the tau-dependent signalling complex in neurons of the subject; or

(d) introduces a variant of tau that causes disruption of the tau-dependent signalling complex in neurons of the subject.

An alternative ninth aspect provides an agent which: (a) promotes phosphorylation of one or more amino acid residues of tau, wherein the phosphorylation of the amino acid residues causes disruption of the tau-dependent signalling complex in neurons of the subject; or (b) introduces a variant of tau that causes disruption of the tau-dependent signalling complex in neurons of the subject, for use in treating stroke in a subject, or use of an agent which (a) promotes phosphorylation of one or more amino acid residues of tau, wherein the phosphorylation of the amino acid residues causes

disruption of the tau-dependent signalling complex in neurons of the subject; or (b) introduces a variant of tau that causes disruption of the tau-dependent signalling complex in neurons of the subject, in the manufacture of a medicament for treating stroke in a subject.

A tenth aspect provides a method of treating stroke in a subject, comprising introducing into neurons of the subject:

(a) a nucleic acid capable of expressing p38γ, or variant thereof; or

(b) a nucleic acid capable of expressing a variant of tau that causes disruption of the tau-dependent signalling complex.

An alternative tenth aspect provides: (a) a nucleic acid capable of expressing p38γ, or variant thereof; or (b) a nucleic acid capable of expressing a variant of tau that causes disruption of the tau-dependent signalling complex, for use in treating stroke in a subject, or use of (a) a nucleic acid capable of expressing p38γ, or variant thereof; or (b) a nucleic acid capable of expressing a variant of tau that causes disruption of the tau-dependent signalling complex, in the manufacture of a medicament for treating stroke in a subject.

An eleventh aspect provides a method of treating epilepsy in a subject comprising introducing into neurons of the subject an agent which:

(a) promotes phosphorylation of one or more amino acid residues of tau, wherein the phosphorylation of the amino acid residues causes disruption of the tau-

dependent signalling complex in neurons of the subject; or

(b) introduces a variant of tau that causes disruption of the tau-dependent signalling complex in neurons of the subject.

An alternative eleventh aspect provides an agent which: (a) promotes phosphorylation of one or more amino acid residues of tau, wherein the phosphorylation of the amino acid residues causes disruption of the tau-dependent signalling complex in neurons of the subject; or (b) introduces a variant of tau that causes disruption of the tau-dependent signalling complex in neurons of the subject, for use in treating epilepsy in a subject, or use of an agent which (a) promotes phosphorylation of one or more amino acid residues of tau, wherein the phosphorylation of the amino acid residues causes disruption of the tau-dependent signalling complex in neurons of the subject; or (b) introduces a variant of tau that causes disruption of the tau-dependent signalling complex in neurons of the subject, in the manufacture of a medicament for treating epilepsy in a subject.

A twelfth aspect provides a method of treating epilepsy in a subject, comprising introducing into neurons of the subject:

(a) a nucleic acid capable of expressing p38γ, or variant thereof; or

(b) a nucleic acid capable of expressing a variant of tau that causes disruption of the tau-dependent signalling complex.

An alternative twelfth aspect provides: (a) a nucleic acid capable of expressing p38γ, or variant thereof; or (b) a nucleic acid capable of expressing a variant of tau that causes disruption of the tau-dependent signalling complex, for use in treating epilepsy in a subject, or use of (a) a nucleic acid capable of expressing p38γ, or variant thereof; or (b) a nucleic acid capable of expressing a variant of tau that causes disruption of the tau-dependent signalling complex, in the manufacture of a medicament for treating epilepsy in a subject.

A thirteenth aspect provides a composition for treating or preventing a neurological condition mediated by a tau-dependent signalling complex in neurons of a subject, comprising an agent which:

(a) promotes phosphorylation of one or more amino acid residues of tau, wherein the phosphorylation of the amino acid residues causes disruption of the tau-dependent signalling complex in neurons of the subject; or

(b) introduces a variant of tau that causes disruption of the tau-dependent signalling complex in neurons of the subject.

A fourteenth aspect provides a composition comprising a vector described herein.

A fifteenth aspect provides a kit for treating or preventing a neurological condition mediated by a tau-dependent signalling complex in neurons of a subject, comprising an agent which:

(a) promotes phosphorylation of one or more amino acid residues of tau, wherein the phosphorylation of the amino acid residues

causes disruption of the tau-dependent signalling complex in neurons of the subject; or

(b) introduces a variant of tau that causes disruption of the tau-dependent signalling complex in neurons of the subject.

A sixteenth aspect provides a kit comprising a vector described herein.

A seventeenth aspect provides a transgenic non-human animal comprising a transgenic nucleic acid sequence which is capable of expressing in neurons of the transgenic animal p38γ or a variant thereof, or a variant of tau that causes disruption of the tau-dependent signalling complex.

An eighteenth aspect provides a method of assessing whether a neurological condition can be treated or prevented by a method described herein, comprising the steps of:

(a) providing a test animal suffering from the neurological condition or exhibiting a phenotype which is a model for the neurological condition;

(b) crossing the test animal with a transgenic animal to obtain progeny, the transgenic animal comprising a transgenic nucleic acid sequence which is capable of expressing in neurons of the animal p38γ or a variant thereof, or a variant of tau that causes disruption of the tau-dependent signalling complex; and

(c) assessing the severity of the neurological condition or the phenotype which is a model for the neurological condition in progeny expressing the transgenic nucleic acid sequence.

Description of the Drawings

Figure 1A is a schematic diagram showing the domain structure of p38 MAP kinases including a dendrogram showing degree of similarity. As can be seen, *p38γ* has a unique C-terminal PDZ interaction motif.

Figure 1B shows the results of polymerase chain reaction (PCR) on genomic DNA from mice with targeted alleles for *p38α*, *p38β*, *p38γ* and *p38δ*. f, floxed allele, -, knockout allele, +, wild-type allele.

Figure 1C shows the results of western blots of cortical extracts of control mice (f/f or +/+) confirmed expression of p38α, p38β and p38γ, but not p38δ in brains. Antibody specificity was shown by probing extracts of mice with individual knockout or p38 MAPKs. Δneu, neuron-specific knockout of p38α. GAPDH showed equal loading. BM, bone marrow.

Figure 2A are graphs showing reduced seizure latency (left) and linear regression slopes (right) of $p38\gamma^{+/+}$ and $p38\gamma^{-/-}$ mice injected with 30mg/kg PTZ. Mean seizure severity was markedly increased in $p38\gamma^{-/-}$ compared to $p38\gamma^{+/+}$ mice injected with 30mg/kg PTZ (**$P < 0.01$; ****$P < 0.0001$; n=10-12).

Figure 2B are photographs showing co-localization of p38γ and post-synaptic PSD-95 (arrows), but not pre-synaptic synaptophysin (Syp) in neurons. Scale bar, 1μm.

Figure 2C is a graph showing early mortality in APP23.$p38\gamma^{+/+}$ (n=62) was further augmented in APP23.$p38\gamma^{-/-}$ (n=43) mice, while $p38\gamma^{+/+}$ (n=49) and $p38\gamma^{-/-}$ (n=48) mice presented with normal survival (****$P < 0.0001$, ***$P < 0.001$).

Figures 2D-F show the spatial working memory deficits in APP23.$p38\gamma^{+/+}$ (n=10), and more so APP23.$p38\gamma^{-/-}$ (n=8) compared to $p38\gamma^{+/+}$ (n=10) and $p38\gamma^{-/-}$ (n=10) mice using Morris-water-maze (MWM) (**P < 0.01; *P < 0.05).

Figure 2D is representative MWM path traces. Dashed squares, location of hidden platform.

Figure 2E is a graph showing escape latency was increased in APP23.$p38\gamma^{+/+}$, and more so in APP23.$p38\gamma^{-/-}$ mice, but comparable to $p38\gamma^{+/+}$ and $p38\gamma^{-/-}$ mice.

Figure 2F is a graph showing the time in quadrant (seconds) in a MWM test of p38$\gamma^{+/+}$, p38$\gamma^{-/-}$, APP23p38$\gamma^{+/+}$ and APP23p38$\gamma^{-/-}$ mice. APP23.$p38\gamma^{-/-}$ mice spent less time in the targeted (Q1) and more time in the opposite quadrant (Q4) during probe trials, compared to APP23.$p38\gamma^{+/+}$, $p38\gamma^{+/+}$ and $p38\gamma^{-/-}$ mice.

Figure 2G shows representative EEG traces of APP23.$p38\gamma^{+/+}$, APP23.$p38\gamma^{-/-}$, $p38\gamma^{+/+}$ and $p38\gamma^{-/-}$ mice, with bouts of hypersynchronicity (*green*) in APP23.$p38\gamma^{+/+}$ and APP23.$p38\gamma^{-/-}$, but not $p38\gamma^{+/+}$ and $p38\gamma^{-/-}$ mice.

Figure 2H is a graph showing markedly increased numbers of spike trains in APP23.$p38\gamma^{-/-}$ compared to APP23.$p38\gamma^{+/+}$ mice (n=6-8; **P < 0.01). No spike trains were detected in $p38\gamma^{+/+}$ and $p38\gamma^{-/-}$ recordings.

Figure 2I is a graph showing the number of spikes per minute was increased in APP23.$p38\gamma^{-/-}$ compared to APP23.$p38\gamma^{+/+}$ mice, but rare in $p38\gamma^{+/+}$ and $p38\gamma^{-/-}$ mice (n=6-8; ***P < 0.001 **P < 0.01, *P < 0.05).

Figure 2J shows a representative phase-amplitude comodulograms computed for interictal hippocampal LFPs recordings showing reduced cross-frequency coupling (CFC) around 8 Hz in APP23.$p38\gamma^{+/+}$ compared to $p38\gamma^{+/+}$ and $p38\gamma^{-/-}$ mice. CFC at ~8Hz was virtually lost in APP23.$p38\gamma^{-/-}$ mice.

Figure 2K is a graph showing the modulation index computed for phase-amplitude distributions was reduced in APP23.$p38\gamma^{+/+}$ (n=8) and more so in APP23.$p38\gamma^{-/-}$ (n=8) compared to $p38\gamma^{+/+}$ (n=6) and $p38\gamma^{-/-}$ (n=6) mice (***P < 0.001, **P < 0.01).

Figure 3A is a graph showing seizure latencies in p38$\gamma^{+/+}$, p38$\gamma^{-/-}$, Alz17.p38$\gamma^{+/+}$ and Alz17.p38$\gamma^{-/-}$ mice following i.p. administration of 30 mg/kg PTZ. Further reduction in seizure latencies following 30 mg/kg PTZ i.p. was observed in Alz17.$p38\gamma^{-/-}$ mice compared to those already reduced in $p38\gamma^{-/-}$ compared to $p38\gamma^{+/+}$ and Alz17.$p38\gamma^{+/+}$ mice (n=10-12; **P < 0.01; *P < 0.05; ns, not significant).

Figure 3B is a graph showing linear regression analysis of seizure latency curves in (3A) (n=10-12; ***P < 0.001; **P < 0.01).

Figure 3C is a graph showing further enhanced mean seizure severity after 30 mg/kg PTZ in Alz17.$p38\gamma^{-/-}$ mice compared to those already increased in $p38\gamma^{-/-}$ compared to $p38\gamma^{+/+}$ and Alz17.$p38\gamma^{+/+}$ mice (n=10-12; ***P < 0.001, **P < 0.01, *P < 0.05).

Figure 3D is a graph showing seizure latencies after 30mg/kg PTZ were profoundly reduced in $tau^{+/+}$.$p38\gamma^{-/-}$ compared to $tau^{+/+}$.$p38\gamma^{+/+}$ mice, and were markedly increased in both $tau^{-/-}$.$p38\gamma^{+/+}$ and $tau^{-/-}$.$p38\gamma^{-/-}$ mice (n=10-12; **P < 0.01; *P < 0.05).

Figure 3E is a graph showing a linear regression analysis of seizure latency curves in (D) (n=10-12; ***P < 0.001; **P < 0.01; ns, not significant)

Figure 3F is a graph showing mean seizure severity was increased in $tau^{+/+}$.$p38\gamma^{-/-}$ compared to $tau^{+/+}$.$p38\gamma^{+/+}$ mice, but was similarly reduced in $tau^{-/-}$.$p38\gamma^{+/+}$ and $tau^{-/-}$.$p38\gamma^{-/-}$ mice after 30 mg/kg PTZ injection (n=10-1; ***P < 0.001; **P < 0.01; *P < 0.05).

Figure 3G is a graph showing percent survival of APP23.p38$\gamma^{-/-}$.tau$^{-/-}$ mice compared with APP23.p38$\gamma^{+/+}$tau$^{-/-}$, APP23.p38$\gamma^{+/+}$ and APP23.p38$\gamma^{-/-}$ mice over 300 days.

Figure 3H is a graph showing escape latency of p38$\gamma^{+/+}$, p38$\gamma^{-/-}$,APP23.*p38*$\gamma^{+/+}$, APP23.*p38*$\gamma^{-/-}$, APP23.*p38*$\gamma^{+/+}$.*tau*$^{-/-}$ *and* APP23.*p38*$\gamma^{-/-}$.*tau*$^{-/-}$ mice following Morris Water Maze (MWM) test.

Figure 3I is a graph showing time in quadrant during MWM test for p38$\gamma^{+/+}$, p38$\gamma^{-/-}$,APP23.*p38*$\gamma^{+/+}$, APP23.*p38*$\gamma^{-/-}$, APP23.*p38*$\gamma^{+/+}$.*tau*$^{-/-}$ *and* APP23.*p38*$\gamma^{-/-}$.*tau*$^{-/-}$ mice.

Figure 4A is a photograph showing that more PSD-95/tau/Fyn complexes were immunoprecipitated from Alz17.*p38*$\gamma^{-/-}$ than Alz17.*p38*$\gamma^{+/+}$ brains, despite comparable total levels of PSD-95, tau and Fyn. GAPDH confirmed equal loading.

Figure 4B is a graph showing quantification of tau and Fyn bound to PSD-95 detected in (4A) (n=6; ***P < 0.001; *P < 0.05).

Figure 4C is a photograph showing the results of immunoprecipitation (IP) of PSD-95/tau/Fyn complexes from cells transfected with FLAG-PSD-95, tau and Fyn. Co-transfection of wild-type p38γ (WT) mitigated, and of constitutive active p38γ (CA) abolished, PSD-95/tau/Fyn interaction.

Figure 4D is a graph showing quantification of tau and Fyn bound to PSD-95 detected in (C) (n=6; ***P < 0.001; **P < 0.01; *P < 0.05).

Figure 4E shows that p38γ WT and CA p38γ failed to disrupt PSD-95/tau/Fyn complexes immunoprecipitated from cells in the presence of p38 inhibitor.

Figure 4F is a graph showing quantification of tau and Fyn bound to PSD-95 detected in (E) (n=6; ***P < 0.001; **P < 0.01; *P < 0.05).

Figure 4G shows that consistently more PSD-95/tau/Fyn complexes were immunoprecipitated from cortical lysates of *p38γ*$^{-/-}$ than *p38γ*$^{+/+}$ mice 0, 5 and 15 minutes after injection with 30 mg/kg PTZ.

Figure 4H is a graph showing quantification of tau and Fyn bound to PSD-95 detected in (4G) (n=6; ***$P < 0.001$; **$P < 0.01$; *$P < 0.05$).

Figure 4I shows more tau, Fyn, NMDA receptor subunits 1 (NR1) and 2B (NR2B) we immunoprecipitated in complexes with PSD-95 from brains of *p38γ*$^{-/-}$ than *p38γ*$^{+/+}$ mice. This was further enhanced in APP23.*p38γ*$^{-/-}$ compared to APP23.*p38γ*$^{+/+}$ mice. Total levels of APP (22C11), PSD-95, tau, Fyn, NR1, NR2B and p38γ were, however, comparable in *p38γ*$^{-/-}$, *p38γ*$^{+/+}$, APP23.*p38γ*$^{-/-}$ and APP23.*p38γ*$^{+/+}$ mice.

Figure 4J is a graph showing quantification of tau, Fyn, NR1 and NR2B bound to PSD-95 detected in (4I) (n = 6-8; ***$P < 0.001$; **$P < 0.01$; *$P < 0.05$).

Figure 5A shows cells transfected with tau and wild-type (WT) or constitutive active (CA) p38γ are predominantly being phosphorylated at T205 and less at S199, but virtually not at S396 and S404. GAPDH showed equal loading.

Figure 5B shows the results of immunoprecipitation of PSD95/tau/Fyn complexes from cells co-transfected with PSD95, Fyn and wild-type or mutant human tau (S199A, S199D, T205A, T205E). The results show that mimicking phosphorylation at T205 (T205E) quantitatively disrupted the interaction of PSD95, Fyn and tau, while the tau variant T205A increased it. Mutation of S199 had no effect on PSD-95/tau/Fyn complexes.

Figure 5C is a graph showing quantification of tau and Fyn bound to PSD-95 detected in (Fig. 5B) (n=6; ***P < 0.001; *P < 0.05; ns, not significant).

Figure 5D shows the results of imnmunoprecipitation of PSD95/tau/Fyn complexes from cells co-transfected with PSD95, Fyn, wild-type or mutant human tau, with or without p38γ^{CA}. Co-expression of PSD-95, Fyn and WT tau with p38γ^{CA} abolished PSD-95/tau/Fyn complex formation, while transfection of T205A tau completely prevented the effects of p38γ^{CA} on PSD-95/T205A tau/Fyn interaction.

Figure 5E is a graph showing quantification of tau and Fyn bound to PSD-95 detected in Figure 5D (n=4; ***P < 0.001; **P < 0.01).

Figure 5F is a graph showing the effect of tau variants on Aβ-induced toxicity as determined by LDH release in hippocampal neurons. Aβ (0.05 or 0.5μM)-induced toxicity (measured by LDH release) was reduced in T205E compared to WT and T205A tau-expressing neurons. Cytotoxicity induced by H_2O_2 (3μM) was similar for all tau variants. (n=6 independent experiments; **P < 0.01; *P < 0.05).

Figure 5G is an image showing localization of p38γ and p38γ^{CA} in cultured hippocampal neurons. Both, AAV-expressed WT and constitutive active (CA) p38γ localized to dendritic spines in cultured hippocampal neurons (β3Tub, β3-tubulin), similar to endogenous p38γ (see Fig. 2B). Control neurons expressed AAV18 GFP. Scale bar, 1 μm.

Figure 5H is a graph showing expression of p38γ WT and more so of p38γ^{CA} reduced toxicity induced by Aβ (0.05 or 0.5μM) but not H_2O_2 (3μM) in hippocampal neurons, determined by LDH release. (n=6 independent experiments; ***P < 0.001; **P < 0.01).

Figure 5I is a graph showing expression of p38γ and more so of p38γ^{CA} in C57Bl/6 brains increased seizure latencies

after administration of PTZ (50mg/kg i.p.) compared to mice that received AAV-GFP (n=8-10; **P < 0.01).

Figure 5J is a graph showing the results of linear regression analysis of seizure latency curves in Figure 5I (n=8-10;. ***P < 0.001; **P < 0.01).

Figure 5K is a graph showing the degree of improvement in seizure latencies (linear regression slopes) mediated by expression of both WT and CA p38γ positively correlated with level of p38γ expression in individual mice challenged with 50mg/kg PTZ (n=8-10; *P < 0.05).

Figure 6A is a graph showing the susceptibility of $p38\gamma^{-/-}$ knockout mice and $p38\gamma^{+/+}$ control mice to excitotoxic seizures induced following i.p injection of 50mg/kg body weight pentylenetetrazole (PTZ). Seizure latency was reduced in *p38γ* knockout ($p38\gamma^{-/-}$) as compared to control (*p38γ+/+*) mice following 50mg/kg PTZ (*P < 0.05; n=9-10).

Figure 6B is a graph showing the results of linear regression of analysis of seizure latency curves in Figure 6A (****P < 0.0001; n=9-10).

Figure 6C is a graph showing mean seizure severity in $p38\gamma^{+/+}$ and $p38\gamma^{-/-}$ mice following i.p. administration of 50 mg/kg PTZ. Mean seizure severity was reduced in $p38\gamma^{+/+}$ mice compared to $p38\gamma^{-/-}$ mice (*P<0.05).

Figure 7A is a graph showing the susceptibility of $p38\gamma^{-/-}$ knockout APP23 mice and $p38\gamma^{+/+}$ APP23 mice to excitotoxic seizures induced following i.p injection of 30mg/kg body weight PTZ. $p38\gamma^{-/-}$ and APP23.$p38\gamma^{+/+}$ presented similar reduced seizure latencies compared to non-transgenic $p38\gamma^{+/+}$ mice after PTZ injection. The seizure latency was even further reduced in APP23 $p38\gamma^{-/-}$ mice (n=10-12; **P < 0.01; *P < 0.05).

Figure 7B is a graph showing the results of linear regression analysis of seizure latency curves in Figure 7A (n=10-12; ***P < 0.001; *P < 0.05).

Figure 7C is a graph showing mean seizure severity following PTZ administration (30mg/kg BW i.p.). Seizure severity was significantly increased in $p38\gamma^{-/-}$ and APP23.$p38\gamma^{+/+}$ compared to non-transgenic $p38\gamma^{+/+}$ mice (n=10-12; ***P < 0.001; *P < 0.05). APP23.$p38\gamma^{-/-}$ mice showed a trend to even further enhanced seizure.

Figure 8A is a graph showing the length of swim paths of p38$\gamma^{+/+}$, p38$\gamma^{-/-}$, APP23.p38$\gamma^{+/+}$ and APP23.p38$\gamma^{-/-}$ *mice* in a Morris-water-maze (MWM) to assess memory impairment. Longer swim paths indicated memory acquisition deficits in APP23.$p38\gamma^{+/+}$, that were worse in APP23.$p38\gamma^{-/-}$ mice, compared to normal learning in $p38\gamma^{+/+}$ and $p38\gamma^{-/-}$ mice (**P < 0.01; *P < 0.05; ns, not significant).

Figure 8B is a graph showing escape latencies, and **Figure 8C** is a graph showing average speeds, of p38$\gamma^{+/+}$, p38$\gamma^{-/-}$, APP23.p38$\gamma^{+/+}$ and APP23.p38$\gamma^{-/-}$ *mice* in the Morris-water-maze (MWM). Escape latencies and average speeds were similar using visual cued platform, confirming visual and motor competency.

Figure 9A is a diagram of a representative raw interictal EEG (LFP), band pass filtered signals for theta (4-12 Hz) and gamma (25-100 Hz) oscillations, gamma amplitude envelope and theta phase in APP23.$p38\gamma^{+/+}$ and APP23.$p38\gamma^{-/-}$ and non-transgenic control $p38\gamma^{+/+}$ and $p38\gamma^{-/-}$ mice.

Figure 9B is a graph showing spectral power analysis of interictal EEGs showed a shift to lower theta frequencies in APP23.$p38\gamma^{+/+}$ and APP23.$p38\gamma^{-/-}$ compared to $p38\gamma^{+/+}$ and $p38\gamma^{-/-}$ recordings (n=6-8). Dashed boxes mark low and high theta bands.

Figure 9C is a graph showing quantification (area-under-curve, AUC) of spectral power of low frequency theta (4-8 Hz) in APP23.$p38\gamma^{+/+}$ and more so in APP23.$p38\gamma^{-/-}$ compared to $p38\gamma^{+/+}$ and $p38\gamma^{-/-}$ recordings (***P < 0.001).

Figure 9D is a graph showing that spectral power of high frequency theta power (8-12 Hz) in Figure 9B was decreased in APP23.$p38\gamma^{+/+}$ and APP23.$p38\gamma^{-/-}$ compared to $p38\gamma^{+/+}$ and $p38\gamma^{-/-}$ recordings (***P < 0.001; ns, not significant). Note that aberrant power of high frequency theta (8-12 Hz) in APP23 mice was not affected by deletion of *p38γ*.

Figure 9E is a graph showing gamma spectral power analysis of interictal EEG in APP23.$p38\gamma^{+/+}$, APP23.$p38\gamma^{-/-}$, $p38\gamma^{+/+}$ and $p38\gamma^{-/-}$ recordings (n=6-8). Dashed boxes mark gamma band.

Figure 9F is a graph showing quantification (AUC) of the graph shown in Figure 9E. The results showed increased spectral power of gamma (25-100 Hz) in APP23.*p38γ+/+* and APP23.$p38\gamma^{-/-}$ compared to $p38\gamma^{+/+}$ and $p38\gamma^{-/-}$ recordings (***P < 0.001).

Figure 9G is a graph showing phase-amplitude plot computed for interictal hippocampal LFPs recordings showing a reduction in APP23.$p38\gamma^{+/+}$ (n=8) and loss in APP23.$p38\gamma^{-/-}$ (n=8) of phase-amplitude coupling (CFC) compared to $p38\gamma^{+/+}$ (n=6) and *p38γ-/-* (n=6) mice.

Figure 10A shows immunoblots in which both full-length (FL) WT and CA p38γ precipitated together with PSD-95 from cells transfected with PSD-95 and p38γ variants. Notable, deletion of the C-terminal PDZ-binding motif (ΔPm) in both WT and CA p38γ abolished the interaction with PSD-95.

Figure 10B shows immunoblots in which both WT and CA p38γ precipitated together with tau from cells transfected with V5-tagged tau and p38γ variants. GAPDH confirmed equal loading.

Figure 10C shows immunoprecipitation (IP) of PSD-95/tau complexes from cells transfected with PSD-95 and tau (hTau40). Co-transfection of wild-type p38γ (WT) mitigated and of constitutive active p38γ (CA) abolished PSD-95/tau interaction. GAPDH confirmed equal loading. Figure 10C also shows a graph showing quantification of tau bound to PSD-95 as detected in IPs (n=5; ***$P < 0.001$; **$P < 0.01$).

Figure 10D is an immunoblot showing Fyn and both, WT and CA p38γ precipitated together with tau from cells transfected with V5-tagged tau, Fyn and p38γ variants. GAPDH confirmed equal loading.

Figure 11A is schematic diagram of tau domains and major phosphorylation sites, including non-SP/TP and SP/TP sites. N1/N2: N-terminal inserts encoded by exons 2/3; Pro: proline-rich domain; R1-4: microtubule-binding repeats.

Figure 11B is the results of an *in vitro* kinase assay using recombinant tau and p38γ in absence (-) or presence (+) of adenosinetriphosphate (ATP) and followed by immunoblotting for p38γ, tau (Tau13) and phosphorylation site specific antibodies showed phosphorylation of tau at S199, T205, S396 and S404, but not other sites tested by p38γ.

Figure 11C is the results of an in vitro kinase assay using recombinant wild-type tau or variants with indicated serines/threonines mutated to Alanine and p38γ in absence (-) or presence (+) of ATP which confirmed site-specific phosphorylation of S199, T205, S396 and S404 by p38γ.

Figure 12A shows hippocampal neurons with adeno-associated virus (AAV)-mediated expression of human wildtype (WT), T205A or T205E mutant tau which were exposed to 0.05 μM Aβ42 or vehicle. Cytotoxicity was detected 24 later by

EthD1 uptake in WT and T205A, but not T205E tau expressing neurons. Scale bar, 10 µm.

Figure 12B shows immunoblots in which similar expression of WT, T205A and T205E tau was observed in hippocampal neurons. GAPDH confirmed equal loading.

Figure 13 shows lower magnification of cells shown in Figure 5G: Both, AAV-expressed WT and constitutive active (CA) p38γ localized to dendritic spines in cultured hippocampal neurons (β3Tub, β3-tubulin), similar to endogenous p38γ (see Figure 1). Control neurons expressed AAV-GFP. Scale bar, 10µm. Broken lines indicated optical fields shown at higher magnification in Figure 5G.

Figure 14A shows forbrains of mice infected with AAV constructs. Brains show widespread AAV-mediated expression of GFP or HA-p38γ. NC, negative control. Scale bar, 250 µm. Broken lines indicate insets.

Figure 14B is an immunoblot of cortical lysates of mice intracranially injected with AAV carrying GFP, HA-tagged p38γ or HA-tagged p38γCA which shows higher expression of p38γ than p38γCA. GAPDH confirmed equal loading. Ctrl, lysate from cells transfected with HA-p38γ.

Figure 15 is a graph showing mean seizure severity was significantly reduced in C57Bl/6 mice with AAV-mediated expression of p38γCA challenged with PTZ (50mg/kg i.p.) compared to GFP-expressing controls (n=8-10; $*P < 0.05$).

Figures 16-18 show the spatial working memory deficits in APP23.AAV^{GFP}, AAV^{GFP}, $AAV^{p38\gamma CA}$, and APP23.$AAV^{p38\gamma CA}$ mice using Morris-water-maze (MWM).

Figure 16A is representative MWM path traces for APP23.AAV^{GFP}, AAV^{GFP}, $AAV^{p38\gamma CA}$, and APP23.$AAV^{p38\gamma CA}$ mice. Dashed squares is the location of hidden platform.

Also shown is a graph showing that escape latency was decreased in AAV^{GFP}, $AAV^{p38\gamma CA}$, and APP23.$AAV^{p38\gamma CA}$ as compared to APP23.AAV^{GFP} mice.

Figure 17 is a graph showing $AAV^{p38\gamma CA}$ mice spent more time in the targeted (Q1) and less time in the opposite quadrant (Q4) during probe trials, compared to APP23.AAV^{GFP} mice.

Figure 18 is a graph showing escape latency over 3 days was decreased in AAV^{GFP}, $AAV^{p38\gamma CA}$, and APP23.$AAV^{p38\gamma CA}$ as compared to APP23.AAV^{GFP} mice.

Figure 19 is graphs showing effect of AAV mediated expression of tau wild type ($tau^{-/-}$.AAV tau^{WT}), GFP ($tau^{-/-}$.AAV GFP), tauT205A ($tau^{-/-}$.AAV tau^{T205A}), or tau T205E ($tau^{-/-}$.AAV tau^{T205E}) in $tau^{-/-}$ mice on (A) seizure latency and seizure grade ((B) is a linear regression of the slopes of (A)); and (C) mean seizure severity, following PTZ-induced seizures by administration of 50mg/kg of PTZ.

Figure 20 is (A) an image of cross-frequency coupling (CFC); and (B) is a graph showing the modulation index, in APP23.AAVp38γ^{CA} mice compared with APP23.AAVGFP, AAV.GFP and AAV.p38γ^{CA} mice (n=5 to 6)(left). *P<0.05; ns: not significant. Error bars indicate SEM.

Figure 21 (A) shows stimulus image-location pairing possibilities in differential paired associate learning (dPAL) task in Bussey-Saksida touchscreen operant chamber used in pPAL trial in (B). + indicates the correct image location pairing and - indicates the incorect pairing. The 6 image location pairings were randomised across trials; (B) is a graph of the number of correct pPAL trials over time in APP23.p38$\gamma^{+/+}$, APP23.p38$\gamma^{-/-}$, p38$\gamma^{+/+}$ and p38$\gamma^{-/-}$ mice during touchscreen operant chamber testing; and (C) is a graph showing area under the curve analysis of correct

trials per minute curves in (B), (n=8-10); ***P<0.001, **P<0.01, *P<0.05, ns: not significant; (left) two-way ANOVA: F(3,941)=60.90; a=0.05; SAidak post-hoc; (right) one-way ANOVA: F(3,41)=11.43; a=0.05; Sidak post-hoc).

Figure 22 A-C shows the results of a pairwise discrimination task in Bussey-Saksida touchscreen operant chamber which shows minor impairment of discrimination memory in APP23.p38g-/- mice. (A) shows the stimulus used for the analysis of the pairwise discrimination task; (B) shows a graph of the number of correct trials per minute for consecutive testing days for APP23.p38$\gamma^{+/+}$, APP23.p38$\gamma^{-/-}$, p38$\gamma^{+/+}$ and p38$\gamma^{-/-}$ mice (n=8; *P<0.05 for APP23.p38$\gamma^{-/-}$ vs p38$\gamma^{-/-}$; α=0.05; F(3,100)=3.561; 2-way ANOVA with Sidak's multiple comparisons post-hoc test); and (C) is a graph showing area under the curve (AUC) analysis of correct trials per minute curves in (B)(n=8; *P<0.05 for APP23.p38$\gamma^{-/-}$ vs p38$\gamma^{-/-}$ α=0.05; F(3,28)=2.984; ANOVA with Sidak's multiple comparisons post-hoc test).

Figure 23 is (A) an image of a representative Western blot of brain extracts from human controls (Braak 0) and humans suffering from Alzheimer's Disease at different neuropathological disease stages (Braak I-VI) set out in Table 3, (B) is a graph showing the levels of p38γ in the western blot in (A) normalised to GAPDH, both (A) and (B) showing markedly reduced levels of p38γ as AD advances, and a trend towards reduction in early disease stages,(n=4-5/group; *P<0.05; ns, not significant; a=0.05; F(3,13)=5.435; ANOVA with Sidak's multiple comparisons post-hoc test).

Figure 24 is an image of representative EEG (LFP) traces in 4 month-old non-transgenic control *p38γ*$^{+/+}$ and *p38γ*$^{-/-}$, and APP23.*p38γ*$^{+/+}$, APP23.*p38γ*$^{-/-}$, APP23.*p38γ*$^{+/+}$.*tau*$^{-/-}$ and APP23.*p38γ*

$^{-/-}$.*tau*$^{-/-}$ mice. Note that deletion of *tau* results in absent hypersynchronous activity (grey boxes).

Figure 25 is a graph showing numbers of hypersynchronous epileptiform activity (spikes per minute) in *p38γ*$^{+/+}$,*p38γ*$^{-/-}$, APP23.*p38γ*$^{+/+}$, APP23.*p38γ*$^{-/-}$, APP23.*p38γ*$^{+/+}$.*tau*$^{-/-}$ and APP23.*p38γ*$^{-/-}$.*tau*$^{-/-}$ mice. Hypersynchronous epileptiform activity in APP23.*p38γ*$^{+/+}$.*tau*$^{-/-}$ and APP23.*p38γ*$^{-/-}$.*tau*$^{-/-}$ *mice* were similar to levels seen in nontransgenic control *p38γ*$^{+/+}$ and *p38γ*$^{-/-}$ mice (n=6-8; ***$P < 0.001$; ns, not significant; α=0.05; $F(5, 223)=45.12$; ANOVA with Sidak's multiple comparisons post-hoc test).

Figure 26 is graphs showing (A) spectral power analysis of theta frequencies (4 - 12 Hz) in interictal sections of APP23.*p38γ*$^{+/+}$, APP23.*p38γ*$^{-/-}$, APP23.*p38γ*$^{+/+}$.*tau*$^{-/-}$, APP23.*p38γ*$^{-/-}$.*tau*$^{-/-}$, *p38γ*$^{+/+}$ and *p38γ*$^{-/-}$ recordings (n=6-8). Note that theta shift to lower theta frequencies (4 - 8 Hz) in APP23 recordings was not reversed upon deletion of *tau* in APP23.*p38γ*$^{+/+}$.*tau*$^{-/-}$ and APP23.*p38γ*$^{-/-}$.*tau*-/-. Dashed boxes mark low and high theta bands; and (B) gamma spectral power (25 - 100 Hz) of interictal sections of APP23.*p38γ*$^{+/+}$ and more so APP23.*p38γ*$^{-/-}$ was reverted in APP23.*p38γ*$^{+/+}$.*tau*$^{-/-}$ and APP23.*p38γ*$^{-/-}$.*tau*$^{-/-}$ to levels of *p38γ*$^{+/+}$ and *p38γ*$^{-/-}$ recordings (n=6-8). Dashed boxes mark gamma band.

Figure 27 is an image of a representative phase-amplitude comodulograms of interictal hippocampal LFPs recordings showed reduced and virtually lost cross-frequency coupling (~8Hz) in APP23.*p38γ*$^{+/+}$ and APP23.*p38γ*$^{-/-}$ respectively compared to *p38γ*$^{+/+}$ and *p38γ*$^{-/-}$ mice. Deletion of *tau* resulted in restored cross-frequency coupling in both APP23.*p38γ*$^{+/+}$.*tau*$^{-/-}$ and APP23.*p38γ*$^{-/-}$.*tau*$^{-/-}$ recordings (n=6-8).

Figure 28 are graphs showing (A) the averaged modulation index for coupling of theta phase and gamma amplitude in

recordings from APP23.*p38γ*$^{+/+}$, APP23.*p38γ*$^{-/-}$, APP23.*p38γ*$^{+/+}$.*tau*$^{-/-}$, APP23.*p38γ*$^{-/-}$.*tau*$^{-/-}$, *p38γ*$^{+/+}$ and *p38γ*$^{-/-}$ mice (n=6-8; ***P < 0.001; **P < 0.01; ns, not significant; n=6-8; α=0.05; F(5, 111)=17.31; ANOVA with Sidak's multiple comparisons post-hoc test). Deletion of *tau* resulted in restored and similar levels of cross-frequency coupling in both APP23.*p38γ*$^{+/+}$.*tau*$^{-/-}$ and APP23.*p38γ*$^{-/-}$.*tau*$^{-/-}$ mice; and (B) a Phase-amplitude plot showing the relation of gamma amplitude across the theta phase computed for interictal hippocampal LFPs shows reduction in APP23.*p38γ*$^{+/+}$ (n=8) and loss in APP23.*p38γ*$^{-/-}$ (n=8) of phase-amplitude coupling (CFC) compared to *p38γ*$^{+/+}$ (n=6) and *p38γ-/-* (n=6) mice. However, deletion of *tau* results in restored coupling across the theta phase in both APP23.*p38γ*$^{+/+}$.*tau*$^{-/-}$ and APP23.*p38γ*$^{-/-}$.*tau*$^{-/-}$ recordings (α=0.05; F(5, 2790)=0.003418; 2-way ANOVA with Sidak's multiple comparisons post-hoc test per phase bin).

Figure 29 (A) to (C) is graphs showing details on effects of genetic deletion of *tau* on memory impairment in 12-month-old p38γ$^{+/+}$, p38γ$^{-/-}$, APP23. p38γ$^{+/+}$, APP23.*p38γ*$^{-/-}$, APP23.p38gγ$^{-/-}$.tau$^{-/-}$ and APP23.p38γ$^{+/+}$.tau$^{-/-}$ mice using the Morris water maze paradigm. (A) is a graph showing time in all 4 water maze quadrants (Q1-4) during probe trials (n=6-8; **P < 0.01; *P< 0.05; ns, not significant; α=0.05; F(5, 184)=0.002783; 2-way ANOVA with Sidak's multiple comparisons post-hoc test). (B) is a graph showing escape latencies were similar during visual cued platform testing, confirming visual competency (n=6-8; **P<0.01 (APP23.*p38γ*$^{-/-}$.*tau*$^{-/-}$ vs APP23.*p38γ*$^{-/-}$ in trial 1); ns, not significant (P=0.5092; APP23.*p38γ*$^{-/-}$.*tau*$^{-/-}$ vs APP23.*p38γ*$^{-/-}$ in trial 3); n=6-10; α=0.05; F(5, 145)=7.091; 2-way ANOVA with Sidak's multiple comparisons post-hoc test per

trial). (C) is a graph showing Average swimming speeds were similar between APP23.*p38γ*$^{+/+}$, APP23.*p38γ*$^{-/-}$, APP23.*p38γ*$^{+/+}$.*tau*$^{-/-}$, APP23.*p38γ*$^{-/-}$.*tau*$^{-/-}$, *p38γ*$^{+/+}$ and *p38γ*$^{-/-}$ mice during MWM testing, confirming motor competence (n=6-8; α=0.05; F(5, 169)=0.4651; ANOVA with Sidak's multiple comparisons post-hoc test).

Figure 30 (A) is a schematic of the transgene construct use for the generation of *p38γ*^{CA} mice by pronuclear injection into C57Bl/6 oocytes. HA-tagged p38γ containing the D179A mutation that renders it constitutively active was expressed under control of a neuronspecific murine Thy1.2 (mThy1.2) promoter, and followed by a bovine growth hormone poly-adenylation (pA) sequence. (B) Immunoblots of cortical (CTX), hippocampal (HC) and cerebellar (CB) brain extracts from non-transgenic (-) and of the *p38γ*^{CA}.3 (+) transgenic mouse line confirmed expression of HA-tagged p38γ^{CA}. HA-p38γ^{CA} expressed in 293T cells was used as a positive control. (C) Image showing immunoprecipitation of p38γ from nontransgenic (-) and of *p38γ*^{CA} (+) brains of transgenic p38γ^{CA} mice revealed active p38γ in all of *p38γ*^{CA} samples, as detected with an antibody to phosphorylated p38, indicating that the transgenic mice express active p38γ.

Figure 31 is (A) representative western blots of co-immunopreciptation of mutated tau variants with PSD-95/tau/Fyn complexes in 293T cells, co-expressing individual tau variants together with PSD-95 and Fyn. Only the T205E tau variant abolished complex formation with PSD-95 and Fyn.; and (B) is a graph showing quantification of 4 independent experiments as shown in (A). The PSD-95/tau/Fyn complex formation was only significantly disrupted in the presence of the T205E tau variant (n=4; *$P < 0.05$ (for WT vs T205E); ns, not significant; α=0.05;

F(18, 79)=1.003; ANOVA with Sidak's multiple comparisons test).

Figure 32 is (A) an image showing AAV-delivered WT tau, T205A and T205E (as indicated) is broadly expressed in the cortex of 4 month-old *tau*$^{-/-}$ mice injected intracranially at postnatal day 0. No tau was detected in *tau*$^{-/-}$ brains injected with AAV GFP (tau$^{-/-}$.AAVGFP). DAPI, nuclei. Scale bar, 50 µm; and (B) is an image showing staining of GFP or HA showing widespread neuronal AAV-mediated expression of GFP or HA-p38γ in brains of mice. Scale bar, 25 µm; and (C) is an immunoblot of cortical lysates of mice intracranially injected on postnatal day 0 with AAV carrying GFP, HA-tagged p38γ or HA-tagged p38γ$_{CA}$. HA-tagged p38γ showed higher expression of p38γ than p38γ$_{CA}$. GAPDH confirmed equal loading. Ctrl, lysate from cells transfected with HA-p38γ.

Figure 33 is an immunofluorescence image showing that AAV-delivered *p38γ*^{CA} is broadly expressed in murine cortex of 6 month-old APP23 mice injected intracranially with AAV at postnatal day 0. Immunofluorescence staining for HA showed expression of HA-tagged p38γ^{CA} throughout the cortex. DAPI, nuclei. Scale bar, 50 µm.

Figure 34 is graphs showing the results of Morris Water Maze testing of WT or APP23 mice expressing AAV-delivered GFP or p38γ^{CA}, in which (A) is a graph showing time in quadrant of mice, and shows that APP23 mice expressing AAV-delivered *p38γ*^{CA} (APP23.AAVp38γ^{CA}) show consolidated memory as compared with APP23 expressing control AAV (APP23.AAVGFP) when performing MWM probe trials. Time in all 4 water maze quadrants (Q1-4) during probe trials (day 7) is shown for APP23.AAVp38γ^{CA}, APP23.AAVGFP and non-transgenic AAVGFP, AAVp38γ^{CA} controls. APP23.AAVp38γ^{CA} mice spend significantly more time in target quadrant Q1 as

compared with APP23.AAVGFP mice. Note that AAVp38γ^{CA} mice show similar memory performance as AAVGFP mice (*P<0.05 (APP23.AAVp38γ^{CA} vs APP23.AAVGFP in Q1; F(3, 84)=3.494); n=6-10; α=0.05; F(3, 108)=4.454; 2-way ANOVA with Sidak's multiple comparisons post-hoc test per quadrant); (B) shows that APP23.AAVp38γ^{CA}, APP23.AAVGFP, AAVGFP, AAVp38γ^{CA} showed similar escape latencies after 3 visual cued trials in the MWM, indicating normal visuosensory function and motor-coordination competency (*P<0.05 (APP23.AAVp38γ^{CA} vs APP23.AAVGFP in trial 1; F(3, 84)=3.494); ns, not significant (P=0.5092; APP23.AAVp38γ^{CA} vs APP23.AAVGFP in trial 3); n=6-10; α=0.05; F(3, 84)=0.07474; 2-way ANOVA with Sidak's multiple comparisons post-hoc test per trial); and (C) shows that Average swimming speeds were similar between APP23.AAVp38γ^{CA}, APP23.AAVGFP, AAVGFP and AAVp38γ^{CA} mice during MWM testing, confirming motor competency (P=0.8389; n=6-10; α=0.05; F(3, 68)=0.2811; ANOVA with Sidak's multiple comparisons post-hoc test).

Figure 35 shows (A) reduced spontaneous spikes in EEG recording from APP23.AAVp38γ^{CA} mice compared to APP23.AAVGFP mice, and no spikes in EEG recording from AAVp38γ^{CA} or AAVGFP-treated wild-type mice (n=5-6; **P<0.01, *P<0.05; one-way ANOVA: F(3, 68)=301.1; a=0.05; Sidak post-hoc); and (B) is a graph showing the spikes/min for AAV.GFP, AAVp38γ^{CA}, APP23.AAV.GFP and APP23.AAVp38γ^{CA} mice, showing reduced spikes/min for APP23.AAVp38γ^{CA} compared to APP23.AAVGFP mice.

Figure 36 shows Theta oscillation power changes of APP23 mice at 4-8 (B) and 8-12Hz (C) were not affected by AAVp38γ^{CA} expression, with comparable levels in APP23.AAVp38γ^{CA} and APP23.AAVGFP recordings (*P<0.05; n=5-

6; α=0.05; F(3, 47)=3.038; ANOVA with Sidak's multiple comparisons post-hoc test).

Figure 37 shows gamma oscillation power (25-100Hz) in APP23.AAVp38γ^{CA} mouse recordings was significantly reduced compared with APP23.AAVGFP mouse recordings. (**P<0.01; *P<0.05; n=5-6; α=0.05; F(3, 26)=6.930; ANOVA with Sidak's multiple comparisons post-hoc test).

Figure 38 is a graph showing that AAV-delivered *p38γ^{CA}* results in normal cross-frequency coupling in EEG recordings of APP23 mice. Phase-amplitude correlation showed strong coupling of gamma amplitude along theta phase in APP23.AAVp38γ^{CA} and in AAVGFP and AAVp38γ^{CA} recordings, yet not in recordings from APP23.AAVGFP mice (**P<0.01 (APP23.AAVp38γ^{CA} vs APP23.AAVGFP); α=0.05; F(3, 20)=4.793; 2-way ANOVA with Sidak's multiple comparisons post-hoc test per phase bin).

Figure 39 A to E shows active neuronal p38γ protects APP23 mice from developing impaired memory function as tested by Morris water maze (MWM). (A) is representative traces of swim paths of WT(non tg), p38γ^{CA}.3, APP23 and APP23.p38γ^{CA}.3 mice in the MWM test showing that APP23.*p38γ^{CA}* mice swim shorter paths in the Morris water maze test (day 5) as compared with APP23 mice, indicative of non-impaired learning/memory in these mice. *p38γ^{CA}* single transgenic mice showed similar swim path lengths as non-transgenic controls, suggesting that active neuronal p38γ does not affect learning functions on a wild-type background. Representative swim path traces are shown (n=6-12). (B) is a graph of escape latencies over 6 days, and shows that, consistent with shorter swim paths, escape latencies in APP23.*p38γ^{CA}* mice were significantly lower than in APP23 mice, and similar to escape latencies seen in *p38γ^{CA}* and non-transgenic mice (*P<0.05; n=6-12; α=0.05; F(3,

168)=4.454; 2-way ANOVA with Sidak's multiple comparisons post-hoc test). (C) is a graph of time in quadrant, and shows that APP23.*p38γ*^{CA} *mice* spent significantly more time in the target quadrant during probe trials than APP23 mice, indicating consolidated memory in APP23.*p38γ*^{CA} *mice*, yet not in APP23 mice. APP23.*p38γ*^{CA} *mice*, single transgenic *p38γ*^{CA} and non-transgenic mice spent similar time in the target quadrant (**P*<0.05 F(3, 116)=7.028); n=6-12; α=0.05; 2-way ANOVA with Sidak's multiple comparisons post-hoc test per quadrant). (D) is a graph showing that escape latencies converged to similar levels after 3 visual cued trials in all experimental groups, indicating normal visuo-sensory function and motor-coordination in APP23.*p38γ*^{CA}, APP23, *p38γ*^{CA} and non-transgenic mice (**P*<0.05 (APP23.*p38γ*^{CA} vs APP23 in trial 1; F(3, 87)=3.690); ns, not significant (*P*=0.7190; APP23.*p38γ*^{CA} vs APP23 in trial 3); n=6-12; α=0.05; F(3, 87)=0.369; 2-way ANOVA with Sidak's multiple comparisons post-hoc test per trial). (E) is a graph showing that average swimming speeds were similar in APP23.*p38γ*^{CA}, APP23, *p38γ*^{CA} and nontransgenic mice during MWM testing, confirming motor competency (*P*=0.3221; n=6-12; α=0.05; F(3, 62)=1.187; ANOVA with Sidak's multiple comparisons post-hoc test).

Figure 40 is (A) EEG recordings from WT (non-tg), APP23 mice, single transgenic p38γ^{CA}.3, and APP23.p38γ^{CA}.3 mice, showing that APP23.*p38γ*^{CA}*.3* mice exhibited markedly lower epileptiform activity than APP23 recordings. (n=4-5). (B) is a graph showing that significantly fewer hypersynchronous epileptiform discharges were found in recordings from APP23.*p38γ*^{CA} mice compared with APP23 recordings. Single transgenic *p38γ*^{CA} and non-transgenic control recordings did not show hypersynchronous activity

(**P<0.01; n=4-5; α=0.05; F(3, 22)=11.38; ANOVA with Sidak's multiple comparisons post-hoc test). (C and D) are graphs showing increased theta oscillation power of APP23 was reduced to levels of $p38\gamma^{CA}$ and nontransgenic recordings in APP23.$p38\gamma^{CA}$ recordings. Specifically, the spectral distribution peak at 4-8Hz in APP23 power spectra was significantly lower in APP23.$p38\gamma^{CA}$ spectra (**P<0.01; *P<0.05; n=4-5; α=0.05; F(3, 26)=6.930; ANOVA with Sidak's multiple comparisons post-hoc test). (E and F) are graphs showing increased gamma oscillation power (25-100Hz) of APP23 was reduced to levels of $p38\gamma^{CA}$ and non-transgenic recordings in APP23.$p38\gamma^{CA}$ recordings (**P<0.01; *P<0.05; n=4-5; α=0.05; F(3, 47)=4.761; ANOVA with Sidak's multiple comparisons post-hoc test).

Figure 41 (A) is an image showing comodulogram analysis of cross-frequency coupling showed unaffected coupling of theta oscillations to gamma amplitude in recordings of APP23.$p38\gamma^{CA}$ mice in contrast to APP23 recordings. Representative comodulograms are shown (n=4-5) (B) is a graph in which phase-amplitude correlation showed strong coupling of gamma amplitude along theta phase in APP23.$p38\gamma^{CA}$ and in $p38\gamma^{CA}$ and non-transgenic recordings, yet not in recordings from APP23 mice. (**P<0.01 (APP23.AAVp38γ^{CA} vs APP23.AAVGFP); n=4-5; α=0.05; F(3, 162)=3.238; 2-way ANOVA with Sidak's multiple comparisons post-hoc test per phase bin). (C) is a graph showing average modulation index was significantly higher in APP23.$p38\gamma^{CA}$ recordings as compared with APP23 recordings and reached similar levels as in recordings from single transgenic $p38\gamma^{CA}$ and non-transgenic control mice (*P<0.05; n=4-5; α=0.05; F(3, 9)=6.370; ANOVA with Sidak's post-hoc test).

Figure 42 is an immunoblot of extracts from dendritic spines of hippocampal neurons showing p38γ enriched with NR1 and PSD-95 in PSD fractions of p38γ+/+ synaptosome preparations, yet not in non-PSD fractions (α-syn; α-synuclein).

Figure 43 shows (A) the nucleic acid sequence (SEQ ID NO: 1) and (B) the amino acid sequence (SEQ ID NO: 2) of full length human wild-type p38γ.

Figure 44 shows the amino acid sequence of $p38\gamma^{CA}$ (SEQ ID NO: 3). The location of the mutation from D to A (D179A) is underlined.

Figure 45 shows the amino acid sequence of full length human tau (top) (SEQ ID NO: 4) and tau T205E (SEQ ID NO: 5)(bottom). The location of the mutation from T to E in tau T205E is underlined.

Figure 46 is a map of adeno-associated viral vector pAM-CAG containing wild-type p38γ coding sequence. 1. Position 200-1120, CAG-promoter; 2. Position 1176-2372, 3xHA-p38γ-wt coding sequence; 3. Position 2395-2970, WPRE; 4. Position 3011-3238, bGH PA; 5. Position 3344-3453, ITR; 6. Position 3655-3459, SV40 promoter; 7. Position 3608-3531, SV40 ORI; 8. Position 4644-4016, ColE1 origin; 9. Position 5455-4796, AmpR; 10. Position 5723-5695, Amp prom; 11. Position 6546-6563, SP6.

Figure 47 is a map of adeno-associated viral vector pAM-CAG containing the coding sequence of $p38\gamma^{CA}$ (D179A)(constitutively active variant of p38γ). 1. Position 200-1120, CAG-promoter; 2. Position 1176-2372, 3xHA-$p38\gamma^{CA}$ coding sequence; 3. Position 2395-2970, WPRE; 4. Position 3011-3238, bGH PA; 5. Position 3344-3453, ITR; 6. Position 3655-3459, SV40 promoter; 7. Position 3608-3531, SV40 ORI; 8. Position 4644-4016, ColE1 origin; 9. Position 5455-

4796, AmpR; 10. Position 5723-5695, Amp prom; 11. Position 6546-6563, SP6.

Figure 48 is the nucleic acid sequence of adeno-associated viral vector pAM-CAG containing wild-type p38γ coding sequence (SEQ ID NO: 6).

Figure 49 is the nucleic acid sequence of adeno-associated viral vector pAM-CAG containing the coding sequence of $p38\gamma^{CA}$ (D179A)(constitutively active variant of p38γ) (SEQ ID NO: 7).

Detailed Description

The present invention relates to a method of treating or preventing a neurological condition mediated by a tau-dependent signalling complex in neurons of a subject. The inventors have found that promoting phosphorylation of one or more amino acid residues of tau, wherein the phosphorylation of the amino acid residues causes disruption of the tau-dependent signalling complex in neurons of the subject, or introducing a variant of tau that causes disruption of the tau-dependent signalling complex in neurons of the subject, can be used to treat or prevent neurological conditions mediated by a tau-dependent signalling complex, such as AD.

A tau-dependent signalling complex is a post-synaptic signalling complex, typically associated with the N-methyl-D aspartate receptor (NMDA receptor), which can mediate excitotoxicity in neurons. A signalling complex is a complex of proteins which are involved in transduction of a signal in a cell. A tau dependent signalling complex requires tau in order to transduce the signal. The tau-dependent signalling complex typically comprises tau as a component of the complex.

Excitotoxicity refers to the process by which neurons are damaged or killed by excessive stimulation of glutamatergic receptors, such as NMDA receptors, and is

mediated via signalling complexes in the postsynaptic space. Neural damage from excitotoxicity is associated with a number of neurological conditions. Neural damage in stroke patients is believed to be caused, at least in part, by overactivation of glutamatergic receptors and associated signalling complexes by excessive amounts of extracellular glutamate that are released immediately following ischaemic stroke. Neural damage in epilepsy is also thought to result from excitotoxicity caused by overactivation of glutamatergic receptors and associated signalling complexes following release of glutamate during epileptic events.

The tau-dependent signalling complex is also thought to mediate amyloid-β (Aβ) toxicity in Alzheimer's disease (AD). In Alzheimer's disease (AD), amyloid-β (Aβ) has been shown to induce toxicity in neurons through a signalling complex comprising NMDA receptors, PSD-95, tau and FYN.

The tau-dependent signalling complex typically comprises tau. In one embodiment, the tau-dependent signalling complex comprises PSD-95 and tau. In one embodiment, the tau-dependent signalling complex comprises PSD-95, FYN and tau. Typically, the tau-dependent signalling complex comprises NMDA receptors, PSD-95, tau and FYN.

The neurological condition may be any neurological condition mediated by a tau-dependent signalling complex. Typically, the neurological condition is caused by neuronal damage from overactivation of the tau-dependent signalling complex. Examples of such conditions include, for example, Alzheimer's disease, frontotemporal dementia, amyotrophic lateral sclerosis, Huntington's disease, Parkinson's disease, neural damage from stroke and neural damage from epilepsy.

In one embodiment, the neurological condition is Alzheimer's disease.

In one embodiment, the neurological condition is stroke.

In one embodiment, the neurological condition is epilepsy.

In one embodiment, the method comprises treating the subject to promote phosphorylation of one or more amino acid residues of tau, wherein the phosphorylation of the amino acid residues causes disruption of the tau-dependent signalling complex. As used herein, "disruption of the tau-dependent signalling complex" refers to an effect which prevents the tau-dependent signalling complex from mediating excitotoxicity and Aβ toxicity, and includes destabilising, dismantling or preventing formation of, the signalling complex. In one embodiment, the one or more amino acid residues of tau that are phosphorylated to cause disruption of the tau-dependent signalling complex are one or more amino acid residues that would be phosphorylated by the MAP kinase p38γ. In one embodiment, the one or more amino acid residues of tau that are phosphorylated to cause disruption of the tau-dependent signalling complex is threonine at position 205 (T205). In one embodiment, the one or more amino acid residues of tau that is phosphorylated to cause disruption of the tau-dependent signalling complex is threonine at position 205 (T205) and one or more amino acid residues selected from the group consisting of serine at position 199 (S199), serine at position 396 (S396) and serine at position (S404). In various embodiments, the amino acid residues of tau that are phosphorylated to cause disruption of the tau-dependent signalling complex are: (a) T205; (b) T205, S199; (c) T205,S199,S396; (d) T205,S199,S396,S404; (e) T205,S199,S404; (f) T205,S396,S404; (g) T205,S396; or (h)

T205,S404.

In one embodiment, the subject is treated to promote phosphorylation of tau at one or more amino acid residues, wherein phosphorylation of the amino acid residues causes disruption of the tau-dependent signalling complex in neurons of the brain of the subject.

In one embodiment, the subject is treated by administering an agent that elevates tau that has been phosphorylated at one or more amino acid residues, wherein the phosphorylation of the amino acid residues causes disruption of the tau-dependent signalling complex.

The agent may comprise, for example, a nucleic acid sequence, a nucleic acid analogue, a protein, a peptide, or a small molecule. Typically, administration of the agent introduces the agent into neurons of the subject. More typically, administration of the agent introduces the agent into neurons of the brain of the subject.

In some embodiments, the agent comprises a nucleic acid sequence which is introduced into neurons of the subject. The nucleic acid is then transcribed and translated in the neurons.

In some embodiments, the agent can cross the blood-brain barrier, or can be formulated to cross the blood-brain barrier.

As used herein, a “subject” is a mammal. The mammal can be a human, non-human primate, sheep, mouse, rat, dog, cat, horse, cow, pig, or any other mammals which can suffer from a neurological condition mediated by a tau-dependent signalling complex in neurons. Typically, the subject is a human.

In one embodiment, the subject is treated by administering an agent that elevates p38γ activity, or

activity of a variant of p38γ, in neurons of the subject. p38γ, also known as ERK6, SAPK3 and MAPK12, is a mitogen activated protein kinase (MAP Kinase). In one embodiment, the p38γ is from a mammal. For example, the p38γ may be from a human, mouse, dog, cat, pig, cow, rat, non-human primate, goat, sheep. Typically, the p38γ is human p38γ. Wild type p38γ is activated through phosphorylation of tyrosine and threonine residues in the motif TGY. Wild type p38γ phosphorylates tau following activation. Activation of p38γ is carried out by the MAP kinase kinases MKK3 and MKK6, which are in turn activated upon phosphorylation by the MAPK kinase MAP3K.

As described in the Examples, the inventors have found that phosphorylation of tau by p38**γ** results in disruption of NR/PSD-95/tau/FYN complexes in cultured neurons and in a mouse model of Alzheimer's disease; limits Aβ-induced toxicity in cultured neurons in a mouse model of Alzheimer's disease; and reduces the severity of pentylenetetrazole (PTZ) induced seizures in a mouse model of excitotoxicity and epilepsy. The inventors have shown that by introducing p38**γ,** or a constitutively active variant of p38**γ,** into neurons of mice, NR/PSD-95/tau/FYN complexes in neurons are disrupted and Aβ-induced excitotoxicity is reduced in a mouse model of Alzheimer's disease, and the severity of pentylenetetrazole (PTZ) induced seizures in a mouse model of excitotoxicity and epilepsy is reduced.

An agent that elevates p38γ activity, or the activity of a variant of p38γ, in a neuron may be an agent that: (a) elevates the amount of p38γ, typically the amount of active p38γ, in the neuron; and/or (b) elevates the amount of a

variant of p38γ, typically the amount of an active variant of p38γ, in the neuron; and/or (c) elevates the amount of p38γ activation in the neuron; and/or (d) elevates the amount of activation of the variant of p38γ in the neuron, if the variant if not an active variant. As used herein, "p38γ activity" is an activity of activated p38γ that causes disruption of the tau-dependent signalling complex. Typically, the activity of activated p38γ that causes disruption of the tau-dependent signalling complex is phosphorylation of tau at T205, and optionally phosphorylation of tau at one or more amino acid residues selected from the group consisting of, for example, S199, S396, and S404. The "activity of a variant of p38γ" refers to an activity of a variant of p38γ which is the same as, or substantially similar to, p38γ activity. The variant of p38γ may be capable of p38γ activity without activation (for example, an active variant, such as a constitutively active variant), or may exhibit p38γ activity following activation. p38γ activity is elevated in a neuron when the amount of p38γ activity in the neuron after treatment is increased relative to the amount of p38γ activity in the neuron prior to treatment. The activity of a variant of p38γ is elevated in a neuron when the amount of activity of the variant in the neuron after treatment is increased relative to the amount of activity of the variant in the neuron prior to treatment. The p38γ activity, or the activity of a variant of p38γ, may be elevated by administering an agent which elevates:

(a) the amount of endogenous p38γ in the neurons, such as increasing expression (transcription and/or translation) of endogenous p38γ; and/or

(b) the amount of exogenous p38γ in the neurons; and/or

(c) the amount of a variant of p38γ in the neurons; and/or

(d) the activation of endogenous p38γ, exogenous p38γ and/or variant of p38γ, in the neurons.

In one embodiment, the p38γ activity, or the activity of a variant of p38γ, is elevated by administering an agent which elevates the amount of exogenous p38γ, or a variant thereof, in neurons. The amount of exogenous p38γ, or a variant thereof, may be elevated by introducing into neurons p38γ, or a variant thereof, or by introducing into neurons a nucleic acid capable of expressing p38γ, or a variant thereof.

Thus, in one embodiment, the agent which elevates p38γ activity, or the activity of a variant of p38γ, in neurons of the subject, may comprise the p38γ protein or variant thereof, or a nucleic acid that is capable of expressing p38γ, or a variant thereof, in neurons of the subject. The nucleic acid sequence encoding full-length wild-type human p38γ, together with the amino acid sequence of full-length wild-type human p38γ, used in the Examples described herein is shown in Figure 43. Naturally occurring isoforms and variants of human p38γ are also known (e.g. Genbank accession nos. NP_001290181, CR456515). It is envisaged that natural isoforms or variants of p38γ that phosphorylate tau at an amino acid residue of tau which causes disruption of the tau-

dependent signalling complex could be used in the methods described herein.

In one embodiment, the agent which elevates p38γ activity, or the activity of a variant of p38γ, comprises a nucleic acid that encodes p38γ or a variant thereof. Those skilled in the art will be able to determine the appropriate nucleic acid sequence which encodes the amino acid sequence of the p38γ or variant thereof. For example, a nucleic acid sequence which encodes p38γ may comprise a nucleic acid sequence that is in the range of from about 60% to 100% identical to the wild-type coding sequence of human p38γ (SEQ ID NO: 1). For example, the nucleic acid encoding p38γ may have a sequence that has at least 60%, 61%, 62%, 63%, 64%, 65%, 66%, 67%, 68%, 69%, 70%, 71%, 72%, 73%, 74%, 75%, 76%, 77%, 78%, 79%, 80%, 81%, 82%, 83%, 84%, 85%, 86%, 87%, 88%, 89%, 90%, 91%, 92%, 93%, 94%, 95%, 96%, 97%, 98%, 99% or 100% sequence identity to the wild-type coding sequence of p38γ using one of the alignment programs described herein using standard parameters. Those skilled in the art will recognize that these values can be appropriately adjusted to determine corresponding identity of proteins encoded by a nucleotide sequence by taking into account codon degeneracy, reading frame positioning, and the like.

In one embodiment, the agent which elevates p38γ activity, or the activity of a variant of p38γ, comprises a variant of p38γ. In one embodiment, the agent which elevates p38γ activity, or the activity of a variant of p38γ, comprises a nucleic acid that encodes a variant of p38γ. As used herein, a variant of p38γ is a protein which differs from the wild-type human p38γ protein by one or

more amino acid substitutions, additions or deletion, and which is capable of phosphorylating an amino acid residue of tau which causes disruption of the tau-dependent signalling complex. Typically, the variant of p38γ phosphorylates tau at residue T205, and optionally one or more residues selected from the group consisting of S199, S396, S404. In one embodiment, the variant of p38γ comprises an amino acid sequence that is at least 60%, 65%, 70%, 75%, 80%, 85%, 90%, 95%, or 99% identical to the amino acid sequence of wild-type human p38γ. In one embodiment, the variant of p38γ comprises an amino acid sequence that is at least 60%, 65%, 70%, 75%, 80%, 85%, 90%, 95%, or 99% identical to the amino acid sequence represented by SEQ ID NO: 2.

As used herein, "% identity" with reference to a polypeptide, or "% identical to the amino acid sequence of a polypeptide", refers to the percentage of residues in the two sequences that are the same when aligned for maximum correspondence over a specified comparison window, as measured by sequence comparison algorithms or by visual inspection.

Sequence comparison algorithms for determining % identity between two polypeptides are known in the art. Examples of such algorithms are the algorithm of Myers and Miller (1988); the local homology algorithm of Smith et al. (1981); the homology alignment algorithm of Needleman and Wunsch (1970); the search-for-similarity-method of Pearson and Lipman (1988); the algorithm of Karlin and Altschul (1990), modified as in Karlin and Altschul (1993). Computer implementations of these algorithms for determining % identity between two polypeptides include, for example: CLUSTAL (available from Intelligenetics,

Mountain View, Calif.) (Pearson et al. (1994)).; the ALIGN program (Version 2.0) and GAP, BESTFIT, BLAST, FASTA, and TFASTA in the Wisconsin Genetics Software Package, Version 8 (available from Genetics Computer Group (GCG), 575 Science Drive, Madison, Wis., USA).

In some embodiments, the variant of p38γ may comprise a part of p38γ. In one embodiment, the variant of p38γ comprises a PDZ interaction motif. PSD-95 comprises a PDZ motif, and p38γ is believed to interact with PSD-95, at least in part, through the PDZ interaction motif. The PDZ interaction motif of p38γ is a short amino acid sequence in the C-terminal portion of the p38γ molecule (see Figure 1A). Typically, the PDZ interaction motif comprises the amino acid sequence ETPL or ETAL. In various embodiments, the variant of p38γ comprises an amino acid sequence selected from the group consisting of: ETPL (SEQ ID NO: 8), KETPL (SEQ ID NO: 9), SKETPL (SEQ ID NO: 10), VSKETPL (SEQ ID NO: 11), RVSKETPL (SEQ ID NO: 12), ARVSKETPL (SEQ ID NO: 13), GARVSKETPL (SEQ ID NO: 14), LGARVSKETPL (SEQ ID NO: 15), QLGARVSKETPL (SEQ ID NO: 16), RQLGARVSKETPL (SEQ ID NO: 17), PRQLGARVSKETPL (SEQ ID NO: 18), PPRQLGARVSKETPL (SEQ ID NO: 19), KPPRQLGARVSKETPL (SEQ ID NO: 20), FKPPRQLGARVSKETPL (SEQ ID NO: 21), SFKPPRQLGARVSKETPL (SEQ ID NO: 22), LSFKPPRQLGARVSKETPL (SEQ ID NO: 23), VLSFKPPRQLGARVSKETPL (SEQ ID NO: 24), EVLSFKPPRQLGARVSKETPL (SEQ ID NO: 25), KEVLSFKPPRQLGARVSKETPL (SEQ ID NO: 26), YKEVLSFKPPRQLGARVSKETPL(SEQ ID NO: 27), TYKEVLSFKPPRQLGARVSKETPL (SEQ ID NO: 28), VTYKEVLSFKPPRQLGARVSKETPL (SEQ ID NO: 29), RVTYKEVLSFKPPRQLGARVSKETPL (SEQ ID NO: 30), KRVTYKEVLSFKPPRQLGARVSKETPL (SEQ ID NO: 31), ETAL (SEQ ID

NO: 32), KETAL (SEQ ID NO: 33), PKETAL (SEQ ID NO: 34), VPKETAL (SEQ ID NO: 35), RVPKETAL (SEQ ID NO: 36), ARVPKETAL (SEQ ID NO: 37), GARVPKETAL (SEQ ID NO: 38), LGARVPKETAL (SEQ ID NO: 39), QLGARVPKETAL (SEQ ID NO: 40), RQLGARVPKETAL (SEQ ID NO: 41), PRQLGARVPKETAL (SEQ ID NO: 42), PPRQLGARVPKETAL (SEQ ID NO: 43), KPPRQLGARVPKETAL (SEQ ID NO: 44), FKPPRQLGARVPKETAL (SEQ ID NO: 45), SFKPPRQLGARVPKETAL (SEQ ID NO: 46), LSFKPPRQLGARVPKETAL (SEQ ID NO: 47), VLSFKPPRQLGARVPKETAL (SEQ ID NO: 48), EVLSFKPPRQLGARVPKETAL (SEQ ID NO: 49), KEVLSFKPPRQLGARVPKETAL (SEQ ID NO: 50), YKEVLSFKPPRQLGARVPKETAL (SEQ ID NO: 51), TYKEVLSFKPPRQLGARVPKETAL (SEQ ID NO: 52), VTYKEVLSFKPPRQLGARVPKETAL (SEQ ID NO: 53), RVTYKEVLSFKPPRQLGARVPKETAL (SEQ ID NO: 54), and KRVTYKEVLSFKPPRQLGARVPKETAL (SEQ ID NO: 55)..

In some embodiments, the variant of p38γ may comprise a part of p38γ but otherwise differ from the wild-type p38γ. In this regard, the inventors envisage that variants of p38γ may include protein in which the PDZ interaction motif of p38γ is fused to the carboxy-terminus of other kinases, such as MAP kinase or other serine/threonine kinases, or variants of other kinases that carry mutations to modify their activity. For example, the variant of p38γ may comprise the PDZ interaction motif of p38γ fused to the carboxy-terminus of a kinase selected from the group consisting of p38α, p38β and p38δ, or variants of p38α, p38β and p38δ that carry mutations that modify their activity.

In one embodiment, the variant of p38γ is an active variant of p38γ. An active variant of p38γ is a variant

which does not require activation by the MAP kinase kinases MKK3 and MKK6 in order to exhibit p38γ activity. In one embodiment, the active variant of p38γ is a constitutively active variant of p38γ. A constitutively active variant of p38γ is a variant of p38γ which is continuously active and therefore does not require activation by the MAP kinase kinases MKK3 and MKK6. Typically, a constitutively active variant comprises one or more amino acid substitutions which result in continuous activity. In one embodiment, the constitutively active variant of p38γ comprises the amino acid substitution of D179A. The amino acid sequence of an example of a constitutively active variant of p38γ is shown in Figure 44 (SEQ ID NO: 3). In another embodiment, the constitutive active variant of p38γ may comprise the amino acid substitution of F330L/S. The substitution of F330L/S in p38γ corresponds to the substitution of the constitutive active variant of p38α F327L/S.

In one embodiment, there is provided a method of treating Alzheimer's disease in a subject, comprising administering a nucleic acid sequence which expresses p38γ or a variant thereof, typically a constitutively active variant of p38γ, in neurons of the subject.

In one embodiment, there is provided a method of treating stroke in a subject, comprising administering a nucleic acid sequence which expresses p38γ or a variant thereof, typically a constitutively active variant of p38γ, in neurons of the subject.

In one embodiment, there is provided a method of treating epilepsy in a subject, comprising administering a nucleic acid sequence which expresses p38γ or a variant

thereof, typically a constitutively active variant of p38γ, in neurons of the subject.

In another embodiment, the subject is treated by administering an agent that introduces into neurons of the subject a variant of tau that causes disruption of the tau-dependent signalling complex. As used herein, a "variant of tau" is a tau protein comprising one or more amino acid substitutions, insertions, or deletions, of the full length wild-type tau, wherein the one or more deletions is not more than 100 contiguous amino acids, typically not more than 90, 80, 70, 60, 50, 40, 30, 20, or 10 contiguous amino acids. In one embodiment, the variant of tau comprises one or more amino acid substitutions or insertions of the wild-type tau. In one embodiment, the variant of tau comprises one or more amino acid substitutions of the wild-type tau. In one embodiment, the variant of tau is a phosphomimetic of tau that causes disruption of the tau-dependent signalling complex. As used herein, a phosphomimetic of tau is a variant of tau comprising one or more amino acid substitutions, and which functions in a manner that is the same as, or substantially the same as, that of unsubstituted tau following phosphorylation of the unsubstituted tau at a particular amino acid. A phosphomimetic comprises a phosphomimetic substitution.

As described in the Examples, the inventors have shown that introduction of a T205E variant of tau into hippocampal neurons lowered Aβ-induced toxicity in the neurons. The T205E variant of Tau is a phosphomimetic of Tau phosphorylated at T205. A phosphomimetic substitution is an amino acid substitution in a protein which results in the protein functioning in a manner which is the same

as, or substantially the same as, the unsubstituted protein following phosphorylation of the unsubstituted protein. A phosphomimetic substitution of tau is an amino acid substitution at a site of tau which results in a tau protein that functions in the same, or substantially the same, manner to the wild-type tau following phosphorylation of the wild-type tau, typically at that site.

In one embodiment, the method comprises treating the subject to introduce a phosphomimetic of tau comprising a phosphomimetic substitution of tau that causes disruption of, or reduces formation of, the tau-dependent signalling complex. In one embodiment, the one or more phosphomimetic substitutions are at amino acid residues of the tau protein that are phosphorylated by p38γ. In one embodiment, the phosphomimetic substitution of tau is threonine to glutamic acid at position 205 of tau (T205E), with amino acid numbering based on the longest human tau isoform comprising 441 amino acids. The amino acid sequence of full-length wild-type human tau (SEQ ID NO: 4) and tau T205E (SEQ ID NO: 5) is shown in Figure 45.

Typically, the variant of tau is a variant of human tau. In other embodiments, the variant of tau may be a variant of tau from a non-human mammal. For example, the variant of tau may be a variant of tau from a mouse, dog, cat, pig, cow, rat, non-human primate, goat, sheep.

In one embodiment, there is provided a method of treating Alzheimer's disease in a subject, comprising administering a nucleic acid sequence which expresses tau which differs from wild-type tau in an amino acid substitution of threonine to glutamic acid at position 205 (T205E), in neurons of the subject.

In one embodiment, there is provided a method of treating stroke in a subject, comprising administering a nucleic acid sequence which expresses tau which differs from wild-type tau in an amino acid substitution of threonine to glutamic acid at position 205 (T205E), in neurons of the subject.

In one embodiment, there is provided a method of treating epilepsy in a subject, comprising administering a nucleic acid sequence which expresses tau which differs from wild-type tau in an amino acid substitution of threonine to glutamic acid at position 205 (T205E), in neurons of the subject.

In embodiments in which the agent comprises a nucleic acid that is capable of expressing p38γ or a variant thereof, or the variant of tau, in neurons of the subject, a nucleic acid sequence encoding p38γ or a variant thereof, or the variant of tau, is typically operably linked to regulatory sequence to direct expression of the p38γ, or variant thereof, or the variant of tau, in the neurons of the subject. A nucleic acid that is capable of expressing p38γ or a variant thereof, or a variant of tau, in neurons of a subject may comprise an expression cassette comprising the coding sequence of p38γ or variant thereof, or the variant of tau. An expression cassette is a nucleic acid sequence comprising coding sequence and regulatory sequence which operate together to express a protein encoded by the coding sequence in a cell. "Coding sequence" refers to a DNA or RNA sequence that codes for a specific amino acid sequence. It may constitute an "uninterrupted coding sequence", i.e., lacking an intron, such as in a cDNA, or it may include one or more introns bounded by appropriate splice junctions.

The expression cassette typically includes regulatory sequences. A "regulatory sequence" is a nucleotide sequence located upstream (5' non-coding sequences), within, or downstream (3' non-coding sequences) of a coding sequence, and which influences the transcription, RNA processing or stability, or translation of the associated coding sequence. Regulatory sequences are known in the art and may include, for example, transcriptional regulatory sequences such as promoters, enhancers translation leader sequences, introns, and polyadenylation signal sequences. The coding sequence is typically operably linked to a promoter. A promoter is a DNA region capable under certain conditions of binding RNA polymerase and initiating transcription of a coding sequence usually located downstream (in the 3' direction) from the promoter. The coding sequence may also be operably linked to termination signals. The expression cassette may also include sequences required for proper translation of the coding sequence. The expression cassette including the coding sequence may be chimeric. A "chimeric" vector or expression cassette, as used herein, means a vector or cassette including nucleic acid sequences from at least two different species, or has a nucleic acid sequence from the same species that is linked or associated in a manner that does not occur in the "native" or wild type of the species. The coding sequence in the expression cassette may be under the control of a constitutive promoter or of a regulatable promoter that initiates transcription only in a particular tissue or cell type, or when the host cell is exposed to some particular stimulus. For example, in an expression cassette comprising a nucleic acid encoding p38γ, the coding sequence may be operably linked to a promoter which

is not native to the p38γ gene, such as a promoter that expresses the coding sequence in, or is inducible in, neurons. Examples of suitable neural promoters include synapsin (SYN), calcium/calmodulin-dependent protein kinase (CaMKII), tubulin alpha I (Ta1), neuron-specific enolase (NSE), platelet derived growth factor beta chain (PDGF), MfP, dox, GFAP, Preproenkephalin, dopamine β-hydroxylase (dβH), prolactin, chicken beta actin, prion protein, murine Thy1.2, myelin basic promoter, or any of the above combined with an enhancer, such as a partial cytomegaly virus promoter. Examples of other promoters which may be used to express nucleic acid sequence in neurons include, the SV40 early promoter, mouse mammary tumor virus long terminal repeat (LTR) promoter; adenovirus major late promoter (Ad MLP); a herpes simplex virus (HSV) promoter, a cytomegalovirus (CMV) promoter such as the CMV immediate early promoter region (CMVIE), a rous sarcoma virus (RSV) promoter, synthetic promoters, hybrid promoters, and the like. Inducible or controllable promoters include, for example, promoters whose transcriptional activity is modified in the presence or absence of mifepristone, doxycycline, tetracycline or tamoxifen.

A nucleic acid encoding a protein (coding sequence) is operably linked to a regulatory sequence when it is arranged relative to the regulatory sequence to permit expression of the protein in a cell. For instance, a promoter is operatively linked to a coding region if the promoter helps initiate transcription of the coding sequence.

As used herein, "expression" of a nucleic acid sequence refers to the transcription and translation of a

nucleic acid sequence comprising a coding sequence to produce the polypeptide encoded by the coding sequence.

In one embodiment, the agent is a vector. In such vectors, the nucleic acid sequence encoding p38γ or variant thereof, or the variant of tau, or an expression cassette comprising such sequences, is inserted into an appropriate vector sequence. The term "vector" refers to a nucleic acid sequence suitable for transferring genes into a host cell, such as a neuron. The term "vector" includes plasmids, cosmids, naked DNA, viral vectors, etc. In one embodiment, the vector is a plasmid vector. A plasmid vector is a double stranded circular DNA molecule into which additional sequence may be inserted. The plasmid may be an expression vector. Plasmids and expression vectors are known in the art and described in, for example, Sambrook et al. Molecular Cloning: A Laboratory Manual, 4th Ed. Vol. 1-3, Cold Spring Harbor, N.Y. (2012).

In some embodiments, the vector is a viral vector. Viral vectors comprise viral sequence which permits, depending on the viral vector, viral particle production and/or integration into the host cell genome and/or viral replication. Viral vectors which can be utilized with the methods and compositions described herein include any viral vector which is capable of introducing a nucleic acid into neurons, typically neurons of the brain. Examples of viral vectors include adenovirus vectors; lentiviral vectors; adeno-associated viral vectors; Rabiesvirus vectors; Herpes Simplex viral vectors; SV40; polyoma viral vectors; poxvirus vector.

In one embodiment, the viral vector is an adeno-associated viral (AAV) vector for packaging in an adeno-associated virus. In one embodiment, the AAV vector is a serotype selected from the group consisting of AAV1, AAV2,

AAV3, AAV4, AAV5, AAV6, AAV6.2, AAV7, AAV8, AAV9, AAVrh10, AAVrh20, AAVrh39, AAVrh43, and AAVcy5 vector or variants thereof. In one embodiment, the viral vector is serotype AAV1, AAV9, AAVrh10 or AAVcy5. In one embodiment, the serotype of the AAV vector is AAV1. In another embodiment, the serotype of the AAV vector is AAV9. In another embodiment, the serotype of the AAV vector is AAVrh10. In another embodiment, the serotype of the AAV vector is AAVcy5. The use of recombinant AAV for introducing nucleic acids into cells is known in the art and described in, for example, US20160038613; Grieger and Samulski (2005) Adeno-associated virus as a gene therapy vector: vector development, production and clinical applications, Advances in Biochemical Engineering/Biotechnology 99: 119-145; Methods for the production of recombinant AAV are known in the art and described in, for example, Harasta et al (2015) Neuropsychopharmacology 40: 1969-1978. An example of an adeno-associated viral vector capable of expressing p38γ in neuronal cells is shown in Figures 46 and 48 (SEQ ID NO: 6). An example of an adeno-associated viral vector capable of expressing $p38\gamma^{CA}$ in neuronal cells is shown in Figures 47 and 49 (SEQ ID NO: 7). In one embodiment, the viral vector comprises SEQ ID NO: 6 or 7. In one embodiment, the viral vector comprises SEQ ID NO: 7.

In another embodiment, the viral vector is a lentiviral vector. Methods for production and use of lentiviral vectors are known in the art and described in, for example, Naldini et al. (1996) In vivo gene delivery and stable transduction of nondividing cells by a lentiviral vector, Science, 272:263-267; Lois et al. (2002) Germline transmission and tissue-specific

expression of transgenes delivered by lentiviral vectors, Science,295:868-872; Vogel et al (2004), A single lentivirus vector mediates doxycycline-regulated expression of transgenes in the brain. Hum Gene Ther. 2004;15(2):157-165.

Adenoviruses are also contemplated for use in delivery of nucleic acid agents. Thus, in another embodiment, the viral vector is an adenoviral vector. Adenoviral vectors are known in the art and described in, for example, Kozarsky and Wilson, Current Opinion in Genetics and Development 3:499-503 (1993); Southgate et al. (2008) Gene transfer into neural cells in vitro using adenoviral vectors, Current Protocols in Neuroscience, Unit 4 23, Chapter 4; Akli et al. (1993)Transfer of a foreign gene into the brain using adenovirus vectors. Nature genetics, 3(3): 224-228.

Another aspect provides a vector as described herein, typically a viral vector as described herein.

Viral vectors are typically packaged into viral particles using methods known in the art. The viral particles may then be used to transfer cell lines, including neural cell lines, or neural tissue, either *in vitro* or *in vivo*. Thus, another aspect provides a viral particle comprising a vector described herein.

A further aspect provides an agent as described herein.

The agent described herein may be formulated as a pharmaceutical composition. Accordingly, in another aspect, there is provided a pharmaceutical composition comprising the agent described herein. The composition comprises the agent in a pharmaceutically acceptable carrier. Methods for the formulation of agents with pharmaceutical carriers are known in the art and are

described in, for example, Remington's Pharmaceutical Science, (17th ed. Mack Publishing Company, Easton, Pa. 1985); Goodman & Gillman's: The Pharmacological Basis of Therapeutics (11th Edition, McGraw-Hill Professional, 2005).

Acceptable carriers, diluents and adjuvants are nontoxic to recipients and are preferably inert at the dosages and concentrations employed, and include buffers such as phosphate, citrate, or other organic acids; antioxidants such as ascorbic acid; low molecular weight polypeptides; proteins, such as serum albumin, gelatin, or immunoglobulins; hydrophilic polymers such as polyvinylpyrrolidone; amino acids such as glycine, glutamine, asparagine, arginine or lysine; monosaccharides, disaccharides, and other carbohydrates including glucose, mannose, or dextrins; chelating agents such as EDTA; sugar alcohols such as mannitol or sorbitol; salt-forming counterions such as sodium; and/or nonionic surfactants such as Tween, pluronics or polyethylene glycol (PEG).

Administration of the agent to subject may be by intracranial, intravenous, intraperitoneal, subcutaneous, intramuscular, intranasal or intrathecal injection. Compositions suitable for intracranial, intravenous, intraperitoneal, subcutaneous, intramuscular, intranasal or intrathecal use include sterile aqueous solutions or dispersions and sterile powders for the extemporaneous preparation of sterile injectable solutions or dispersions. The pharmaceutically acceptable carrier can be a solvent or dispersion medium containing, for example, water, ethanol, polyol (for example, glycerol, propylene glycol, liquid polyethylene glycol and the like), suitable mixtures thereof, and vegetable oils. The proper fluidity

can be maintained, for example, by the use of a coating such as lecithin, by the maintenance of the required particle size in the case of a dispersion and by the use of surfactants. The prevention of the action of microorganisms can be brought about by various antibacterial and antifungal agents, for example, parabens, chlorobutanol, phenol, sorbic acid, thimerosal and the like. In many cases it will be preferable to include isotonic agents, for example, sugars or sodium chloride.

In embodiments in which the agent is packaged in a viral particle, the pharmaceutical compositions may comprise viral particles in any concentration that allows the agent to be effective. In such embodiments, the pharmaceutical compositions may comprise the virus particle in an amount of from 0.1% to 99.9% by weight. Pharmaceutically acceptable carriers include water, buffered water, saline solutions such as, for example, normal saline or balanced saline solutions such as Hank's or Earle's balanced solutions), glycine, hyaluronic acid etc.

Titers of viral particles to be administered will vary depending on, for example, the particular vector to be used, the mode of administration, extent of the condition, the individual, and may be determined by methods standard in the art.

The agent described herein may be formulated for introduction into neuronal cells by non-viral methods such as microinjection, electroporation, microparticle bombardment, liposome uptake, nanoparticle-based delivery etc.

In one embodiment, the agents described herein may be formulated in one or more liposomes, lipoplexes, or lipid

nanoparticles. In one embodiment, the agents described herein are formulated in liposomes. Liposomes are unilamellar or multilamellar vesicles which have a membrane formed from a lipophilic material and an aqueous interior. The aqueous portion contains the composition to be delivered. Liposome design may include, for example, opsonins or ligands in order to improve the attachment of liposomes to tissue or to activate events such as, for example, endocytosis.

The formation of liposomes may depend on the physicochemical characteristics such as the agent and the liposomal ingredients, the nature of the medium in which the lipid vesicles are dispersed, the effective concentration of the agent, any additional processes involved during the application and/or delivery of the vesicles, the optimization size, polydispersity and the shelf-life of the vesicles for the intended application, and the batch-to-batch reproducibility and possibility of large-scale production of safe and efficient liposomal products.

Methods for the production of liposomes and lipid nanoparticles for delivery of agents are known in the art, and described in, for example, US 5,264,221.

The term "administering" should be understood to mean providing a compound or agent to a subject in need of treatment.

It will be understood that the specific dose level and frequency of dosage for any particular subject may be varied and will depend upon a variety of factors including, for example, the activity of the specific compound or agent employed, the metabolic stability and length of action of that compound or agent, the age, body weight, general health, sex, diet, mode and time of

administration, drug combination, the severity of the particular condition, and the host undergoing therapy.

Also provided is a kit, comprising a container comprising the agent. The container may be simply a bottle comprising the agent in parenteral dosage form, each dosage form comprising a unit dose of the agent. The kit will further comprise printed instructions. The article of manufacture will comprise a label or the like, indicating treatment of a subject according to the present method. In one form, the article of manufacture may be a container comprising the agent in a form for parenteral dosage. For example, the agent may be in the form of an injectable solution in a disposable container.

As used herein, "treating" means affecting a subject, tissue or cell to obtain a desired pharmacological and/or physiological effect and includes inhibiting the condition, i.e. arresting its development; or relieving or ameliorating the effects of the condition i.e. cause reversal or regression of the effects of the condition.

As used herein, "preventing" means preventing a condition from occurring in a cell or subject that may be at risk of having the condition, but does not necessarily mean that condition will not eventually develop, or that a subject will not eventually develop a condition. Preventing includes delaying the onset of a condition in a cell or subject.

The inventors envisage that p38γ or variants of tau can be used in transgenic animals to assess whether a neurological disease can be treated with the methods described herein.

Accordingly, a further aspect provides a transgenic non-human animal comprising a transgenic nucleic acid sequence which is capable of expressing in neurons of the

transgenic animal p38γ or a variant thereof, or a variant of tau that causes disruption of the tau-dependent signalling complex.

In one embodiment, the transgenic nucleic acid sequence is a nucleic acid sequence capable of expressing p38γ or a variant thereof. In one embodiment, the transgenic nucleic acid sequence is capable of expressing an active variant of p38γ. In one embodiment, the active variant of p38γ is a constitutively active variant of p38γ. In one embodiment, the constitutively active variant of p38γ is $p38\gamma^{CA}$.

The regulatory sequences for expressing the transgene in neurons of the animal are described above.

In one embodiment, the transgenic animal is a mouse. However, it will be understood that the transgenic animal may be any animal, including, for example, a rat, cow, sheep, pig or goat.

Another aspect provides a method of assessing whether a neurological condition can be treated or prevented by a method described herein, comprising the steps of:

(a) providing a test animal suffering from the neurological condition or exhibiting a phenotype which is a model for the neurological condition;

(b) crossing the test animal with a transgenic animal to obtain progeny, the transgenic animal comprising a transgenic nucleic acid sequence which is capable of expressing in neurons of the animal p38γ or a variant thereof, or a variant of tau that causes disruption of the tau-dependent signalling complex; and

(c) assessing the severity of the neurological condition or the phenotype which is a model for the

neurological condition in progeny expressing the transgenic nucleic acid sequence.

In the claims which follow and in the preceding description of the invention, except where the context requires otherwise due to express language or necessary implication, the word "comprise" or variations such as "comprises" or "comprising" is used in an inclusive sense, i.e. to specify the presence of the stated features but not to preclude the presence or addition of further features in various embodiments of the invention.

All publications mentioned in this specification are herein incorporated by reference. It will be appreciated by persons skilled in the art that numerous variations and/or modifications may be made to the invention as shown in the specific embodiments without departing from the spirit or scope of the invention as broadly described. The present embodiments are, therefore, to be considered in all respects as illustrative and not restrictive.

In order to exemplify the nature of the present invention such that it may be more clearly understood, the following non-limiting examples are provided.

Examples

Materials and Methods

Mice. APP23 mice expressing human K670N/M671L mutant APP in neurons (C Sturchler-Pierrat *et al.*, *Proc Natl Acad Sci U S A* **94**, 13287-92 (1997)), Alz17 mice expressing human non-mutant tau in neurons (A Probst *et al.*, *Acta Neuropathol* **99**, 469-81 (2000)), neuron-specific Thy1.2-cre transgenic mice (I Dewachter *et al.*, *J Neurosci* **22**, 3445-53 (2002)), $tau^{-/-}$ (KL Tucker, M Meyer, YA Barde, *Nat Neurosci* **4**, 29-37 (2001)), $p38\alpha^{loxP/loxP}$ (FB Engel *et al.*, *Genes Dev* **19**, 1175-87 (2005)), $p38\beta^{-/-}$ and $p38\gamma^{-/-}$ (AR Pogozelski *et al.*, *PLoS One* **4**, e7934 (2009)), and $p38\delta^{-/-}$ mice (G Sumara *et al.*, *Cell* **136**, 235-48 (2009)) were previously described. Knockouts for p38β, p38γ and p38δ were global without overt phenotypes, while p38α deletion had to be limited to the CNS due to embryonic mortality of global p38α knockout mice. To obtain $p38\alpha^{\Delta neu}$ mice, we crossed $p38\alpha^{loxP/loxP}$ with Thy1.2-cre strain. All lines were maintained on a C57Bl/6 background. Animal experiments were approved by the Animal Ethics Committee of the University of New South Wales. Mice were genotyped by polymerase chain reaction using isopropanol-precipitated DNA from tail biopsies as template. Oligonucleotide primers for genotyping targeted alleles and transgenes by PCR are listed in the following Table 1:

Table 1:

	Forward primer (5'-3')	SEQ ID NO:	Reverse primer (5'-3')	SEQ ID NO::
APP23	GTTCTGCTGCATCTTGGACA	56	GAATTCCGACATGACTCAGG	57
Alz17	GGGTGTCTCCAATGCCTGCTTCTTCAG	58	AAGTCACCCAGCAGGGAGGTGCTCAG	59
*p38α*lox	TCCTACGAGCGTCGGCAAGGTG	60	AGTCCCCGAGAGTTCCTGCCTC	61
p38β	AGAAGATGAAGGTGGAGGAGTACAAGC AAG	62	TAACCCGGATGGCTGACTGTTCCATTTA G	63

p38γ	TGGGCTGCGAAGGTAGAGGTG	64	GTGTCACGTGCTCAGGGCCTG	65
p38δ	ACGTACCTGGGCGAGGCGGCA	66	GCTCAGCTTCTTGATGGCCAC	67
tau^{WT}	CTCAGCATCCCACCTGTAAC	68	CCAGTTGTGTATGTCCACCC	69
tau^{KO}	AAGTTCATCTGCACCACCG	70	TGCTCAGGTAGTGGTTGTCG	71
Thy1.2-Cre	GCGGTCTGGCAGTAAAAACTATC	72	GTGAAACAGCATTGCTGTCACTT	73
Thy1.2-$38\gamma^{CA}$	AAGTCACCCAGCAGGGAGGTG	74	TCGTATGGGTACATGGCCAAAG	75

Generation of transgenic Thy1.2-p38γ^{CA} mice.

The human *p38γ* coding sequence carrying the D179A mutation and an N-terminal hemagglutinin (HA)-tag was amplified by PCR and inserted into the XhoI site of the plasmid pEX12 (Ittner, et al. *Proc. Natl. Acad. Sci. U.S.A.* 105, 15997-16002) (2008)) carrying the *mThy1.2* promoter for neuronal expression using Gibson assembly (Gibson, et al. *Nat. Methods* 6, 343-345 (2009)(Fig. 30A). The construct was excised by restriction digest and transgenic founder mice were generated on a congenic C57Bl/6 background by pronuclear injection (Ittner et al. *Nat. Protoc.* **2**, 1206-1215 (2007)). Tail DNA from founder mice was screened by PCR for genomic transgene insertion and 2 founder lines (*p38γ^{CA}*.3 and *p38γ^{CA}*.4) were established by crossing to C57Bl/6 mice. Normal fertility, survival and Mendelian transgene transmission was observed for both *p38γ^{CA}*.3 and *p38γ^{CA}*.4 lines. Both lines show no overt phenotype. Immunoblots of cortical, hippocampal, and cerebellar brain extracts from transgenic mice confirmed expression of HA-tagged p38γ^{CA} (Fig. 30B).

Seizures.

Seizures were induced with pentylenetetrazole (PTZ, Sigma-Aldrich) as previously described (LM Ittner *et al.*, *Cell* **142**, 387-97 (2010)). Briefly, PTZ was injected i.p. at 30 or 50 mg/kg body weight. Seizures were graded as: 0, no

seizures; 1, immobility; 2, tail extension; 3, forelimb clonus; 4, generalized clonus; 5, bouncing seizures; 6, full extension; 7, status epilepticus.

Spatial learning/memory testing.

Spatial learning/memory was tested in the Morris Water maze paradigm (CV Vorhees, MT Williams, *Nat Protoc* **1**, 848-58 (2006)). Briefly, a custom-built water tank for mouse Morris Water maze (122 cm diameter, 50 cm height) with white non-reflective interior surface in a room with low-light indirect lighting was filled with water (19 - 22 °C) containing diluted non-irritant white dye. Four different distal cues were placed surrounding the tank at perpendicular positions reflecting 4 quadrants. In the target quadrant, a platform ($10cm^2$) was submerged 1 cm below the water surface. Videos were recorded on CCD camera and analyzed using AnyMaze Software. For spatial acquisition, four trials of each 60 seconds were performed per session. The starting position was randomized along the outer edge of the start quadrant for all trials. To test reference memory, probe trials without platform were performed for a trial duration of 60 seconds, and recordings were analyzed for time spent within each quadrant. For visually-cued control acquisition (to exclude vision impairments), a marker was affixed on top of the platform and four trials (60 s) per session were performed. All mice were age and gender-matched and tested at 4 months of age. Mice that displayed continuous floating behavior were excluded. Genotypes were blinded to staff recording trials and analyzing video tracks. Tracking of swim paths was done using the AnyMaze software (Stölting). Average swimming speed was determined to exclude motor impairments.

Touchscreen operant chambers (Campden Instruments) were used with 2 different paradigms to address spatio-temporal memory and learning (differential paired-associates learning, dPAL) or recognition memory/discrimination learning (pairwise discrimination task, PD). Previously described touchscreen chamber protocols were used (Horner et al. *Nat. Protoc.* 8, 1961-1984 (2013)). Mice in dPAL schedule underwent pre-testing procedures and training as follows: food deprivation (to 85 - 90% of initial body weight) and adaptation to handling (day 0 - 4), adaptation to touchscreen boxes (day 4), collect reward (strawberry milk shake, Nippy's) (day 5 -8), panel-pushing to collect reward training (day 9), initial stimulus-dependent touch training (day 10), must touch stimulus training (day 11 - 16), must initiate trial
training (day 17 - 22), punish incorrect touches (day 23 - 26). Followed by either dPAL acquisition for 21 consecutive days (day 27 - 49) or pairwise discrimination task acquisition (day 27 - 31). Maximum time of sessions was set to 60 minutes. Maximum number of trials was set to 36. All training sessions were repeated until mice reached criterion before next training paradigm was started. Criterion was defined as 36 trials within 60 minutes (initial touch training, must touch training, must initiate training) or 27 out of 36 correct trials (punish incorrect touches). Mice with excessive body weight loss were excluded from the protocol.

Behavior and motor testing

Novelty-induced locomotion and anxiety-related behavior was assessed in the open field test paradigm as previously described (Ke, et al. *Acta Neuropathol.* 130, 661-678 (2015)). Briefly, mice were placed individually in 40 x 40

cm^2 boxes in dimly lit sound-insulated enclosures and movements were recorded for 15 minutes. Mice had not been exposed to open field paradigm before. Boxes were wiped with 70 % ethanol between recordings. Movements were tracked using the AnyMaze software (Stölting). Analysis was either accumulated over entire recording period or split in 1-minute bins.

Motor performance was tested on a 5-wheel Rota-Rod treadmill (Ugo Basile) in acceleration mode (5-60rpm) over 120 (aged) or 180 (young) seconds (van Eersel, et al. *Neuropathol. Appl. Neurobiol.* 41, 906-925 (2015)). The longest time each mouse remained on the turning wheel out of 3 attempts per session was recorded. Grip strength was determined as previously described (*Ke et al. (2015)*). Briefly, the force required to pull mice off a metal wire was measured using s grip strength meter (Chatillon, AMETEK). Mice were placed such that they had a double grip on a thin metal wire attached to the meter, and they were pulled away from the meter in a horizontal direction until they let go, and a peak force (N) was recorded at the moment when the mice let go. The highest force from three attempts was recorded.

Calcineurin activity assay

Calcineurin activity in cortical extracts of $p38\gamma^{-/-}$ and $p38\gamma^{+/+}$ littermates was determined by following the manufacturer's instructions (Abcam).

Electroencephalography.

Hippocampal EEG recording in freely moving mice was carried out as previously described (AA Ittner, A Gladbach, J Bertz, LS Suh, LM Ittner, *Acta Neuropathol*

Commun **2**, 149 (2014)). Briefly, wire EEG electrodes of remote telemetric transmitters (DSI) were implanted in mice anesthetized with ketamine/xylazine. The head was fixed in a stereotactic frame (Kopf instruments) and the bregma was located. Bone openings were drilled using a bone micro-drill (Fine Science Tools, F.S.T.) at positions previously described for the hippocampus (x 2.0, y -2.0, z -2 with reference to bregma). Electrodes were inserted at this position with reference electrode placed above the cerebellum (x 0, y -6.0, z 0 from bregma). Electrodes were fixed in place by polyacrylate followed by wound closure and rehydration. Following 10 days of recovery from the surgery, EEGs were recorded with a DSI wireless receiver setup (DSI) with amplifier matrices using the Dataquest A.R.T. recording software at 500 Hz sampling rate (M Weiergraber, M Henry, J Hescheler, N Smyth, T Schneider, *Brain Res Brain Res Protoc* **14**, 154-64 (2005)). Two days after EEG recordings were completed, animals were transcardially perfused with cold phosphate-buffered saline (PBS) and brains extracted for biochemical and histological analysis. Correct placement of electrodes was confirmed by serial sections of paraffin embedded brain tissue stained with hematoxylin-eosin. Only recordings from mice with correct placement of electrodes were included in further analysis.

Analysis of EEG recordings was performed using the NeuroScore software v3.0 (DSI) with integrated spike detection module, to determine spike train duration, frequency and number of spikes per train were obtained. Recordings were screened manually for movement artefacts and only artefact-free EEG passages were used for analysis. Raw local field potentials (LFP) were noise filtered using a powerline noise filter (Neuroscore, DSI).

Spectral analysis (i.e. analysis of signal power at individual frequencies expressed as square of the fast Fourier transform (FFT) magnitude) of intra-ictal sequences was performed using the integrated FFT spectral analysis function of NeuroScore. Frequency bands of theta and gamma wave forms were defined between 4-12 Hz and 25-100 Hz, respectively. Gamma and theta spectral contributions were quantified by area-under-curve (AUC) analysis across the defined frequency band in 8 artefact- and hypersynchronous spike-free sequences per recording (each 1 min in length). Cross-frequency coupling of theta phase and gamma amplitude was performed using MATLAB as previously described (AB Tort, R Komorowski, H Eichenbaum, N Kopell, *J Neurophysiol* **104**, 1195-210 (2010)). Briefly, for cross frequency coupling analysis, raw LFP was noise filtered using a powerline noise filter (Neuroscore, DSI). Noise-filtered LFP was filtered at two frequency ranges of interest for gamma (f_A) and theta (f_p). The phase time series for theta ($\Phi_{fp}(t)$) and the amplitude envelope time series for gamma ($A_{fA}(t)$) were obtained by Hilbert transformation of the filtered LFPs. The combined series [$\Phi_{fp}(t)$, $A_{fA}(t)$] was then generated. After phase binning, the means $\bar{A}_{fA}(j)$ of A_{fA} for each bin j were calculated and normalized using the sum $\sum_{n}^{N} \bar{A}_{n}(j)$ of $\bar{A}_{fA}(j)$ over N bins to generate phase-amplitude distribution $P(j)$. The modulation index is based on calculating the Kullback-Leibler distance D_{KL} between the non-uniform (i.e. coupled) phase-amplitude distribution $P(j)$. The modulation index is based on calculating the Kullback-Leibler distance D_{KL} between the non-uniform (i.e. coupled) phase-amplitude distribution $P(j)$ over all phase bins and the uniform (i.e. uncoupled) distribution $U(j)$.

$$D_{KL}(P,Q) = \sum_{j=1}^{N} P(j) \log\left[\frac{P(j)}{U(j)}\right]$$

The modulation index *MI* is defined as

$$MI = \frac{D_{KL}(P(j),U(j))}{\log(N)}$$

Phase-amplitude distributions and modulation indices were determined from artefact- and hypersynchronous spike-free 8 sequences (each 1 min) per recording.

Synaptosome and post-synaptic density preparation

Purification of synaptosomes from cortical tissue was performed as previously described (Ittner, et al. *Cell* 142, 387-397 (2010)). Briefly, cortical tissue was weighed and homogenized in ice-cold sucrose buffer (0.32M sucrose, 1mM $NaHCO_3$, 1mM $MgCl_2$, 0.5mM $CaCl_2$, protease inhibitors (EDTA-free, Roche)) at 30 mg tissue/ml using a pre-cooled dounce homogenizer. After clearing the homogenate by centrifugation (1,400g, 10 minutes, 4°C), pellets were resuspended in sucrose buffer and centrifuged again (1,400g, 10 minutes, 4°C). Combined supernatants were centrifuged again and supernatant (total brain homogenate) was spun at 13,800g for 10 minutes at 4°C. Pellet was resuspended in sucrose buffer and layered on top of 5% Ficoll (Sigma) and centrifuged at 45,000g for 45 minutes at 4°C. Pellet was resuspended in 5% Ficoll and layered on top of 13% Ficoll and centrifuged at 45,000g for 45 minutes at 4°C. The interface (synaptosomes) was collected, diluted in 5% Ficoll and centrifuged at 45,000g

for 30 minutes at 4°C. Supernatant (non-synaptic) was collected and pellet was resuspended in pH8 buffer (20mM Tris pH8, 1% Triton- X100, 100mM NaCl, 1mM EGTA, 1mM EDTA, 0.5% sodium deoxycholate, 0.1% sodium dodecyl sulfate (SDS), protease inhibitors (EDTA-free, Roche)). After centrifugation at 40,000g for 30 minutes at 4°C, pellets (post-synaptic densities) were resuspended in 5% SDS. The supernatants constituted synaptic non-PSD associated proteins. Protein concentrations for different fractions was determined before preparing samples for Western blotting.

Plasmids.

Plasmids for expression of rat PSD95 (kind gift from Wei-dong Yao; Addgene plasmid #15463), Fyn kinase (kind gift from Filippo Giancotti; Addgene plasmid #16032) and NR2B (kind gift from Robert Malinow; Addgene plasmid #23998), and were obtained from the Addgene depository. For live cell fluorescence confocal imaging, PSD-95 was internally tagged with mCherry between PDZ domains 2 and 3 by megaprime PCR (Bryksinet al. *Biotechniques* 48, 463-465 (2010)) and tau variants were tagged with eGFP by cloning into peGFP-C1 (Clontech).

Coding sequences for human p38α, human p38β and human p38γ were cloned into pcDNA3.1 with an N-terminal HA-tag. Coding sequence for human p38δ was cloned in peGFP-C1. Mutations in *p38* coding sequences for generation of active variants (M Avitzour *et al.*, *FEBS J* **274**, 963-75 (2007)) and variants of p38γ lacking the PDZ motif (ΔPDZm) were generated using the Q5 site-directed mutagenesis kit (NEB). Coding sequence for human tau (441 amino acids) was cloned into pcDNA3.2/V5-DEST (Invitrogen). Phosphorylation-site mutants of tau were generated using

the Q5 site-directed mutagenesis kit (NEB). Oligonucleootide primers for molecular cloning are listed in Table 2.

Table 2

	Forward primer (5'-3')	SEQ ID NO:	Reverse primer (5'-3')	SEQ ID NO:
tauS46D	CCTGAAAGAAgatCCCCTGCAGACCCCC	76	CCAGCGTCCGTGTCACCC	77
tauT50E	TCCCCTGCAGgaaCCCACTGAGG	78	GATTCTTTCAGGCCAGCG	79
tauT52E	GCAGACCCCCgaaGAGGACGGATC	80	AGGGGAGATTCTTTCAGG	81
tauT69E	TGCTAAGAGCgaaCCAACAGCGG	82	TCAGAGGTTTCAGAGCCC	83
tauT71E	GAGCACTCCAgaaGCGGAAGATG	84	TTAGCATCAGAGGTTTCAG	85
tauT111E	CATTGGAGACgaaCCCAGCCTGG	86	CCTGCTTCTTCAGCTGTG	87
tauT153E	GAAGATCGCCgaaCCGCGGGGAG	88	GTTTTACCATCAGCCCCC	89
tauT181E	CGCTCCAAAGgaaCCACCCAGCTC	90	GGCGGGGTTTTTGCTGGA	91
TauS199A	CGGCTACAGCGCCCCCGGCTCCC	92	CTGCGATCCCCTGATTTTGGAG	93
TauS199D	CGGCTACAGCGACCCCGGCTCCC	94	CTGCGATCCCCTGATTTTGGAG	95
tauS202A	CAGCCCCGGCgccCCAGGCACTC	96	CTGTAGCCGCTGCGATCCCCTG	97
tauS202D	CAGCCCCGGCgacCCAGGCACTC	98	CTGTAGCCGCTGCGATCC	99
tauS208D	CACTCCCGGCgacCGCTCCCGCAC	100	CCTGGGGAGCCGGGGCTG	101
tauT212E	CCGCTCCCGCgaaCCGTCCCTTCCAAC	102	CTGCCGGGAGTGCCTGGG	103
tauS235D	TCCACCCAAGgacCCGTCTTCCGC	104	GTACGGACCACTGCCACC	105

TauS404A	TGGGGACACGGCTCCACGGCATC	106	GACACCACTGGCGACTTGTACACG	107
TauS404D	TGGGGACACGGATCCACGGCATC	108	GACACCACTGGCGACTTG	109
TauT205A	CTCCCCAGGCGCTCCCGGCAGCC	110	CCGGGGCTGCTGTAGCCGC	111
TauT205E	CTCCCCAGGCGAACCCGGCAGCCG	112	CCGGGGCTGCTGTAGCCG	113
TauS199AT205A	CCCAGGCGCTCCCGGCAGCCGCTCCCGC	114	GAGCCGGGGGCGCTGTAGCCGCTGCGATCCCC	115
TauS199DT205E	CCCAGGCGAACCCGGCAGCCGCTCCCGC	116	GAGCCGGGGTCGCTGTAGCCGCTGCGATCCCC	117
TauS396A	CGTGTACAAGGCGCCAGTGGTGT	118	ATCTCCGCCCCGTGGTCTG	119
TauS396D	CGTGTACAAGGACCCAGTGGTGTCTGGGG	120	ATCTCCGCCCCGTGGTCT	121
TauS396AS404A	TGGGGACACGGCTCCACGGCATCTCAGCAAT	122	GACACCACTGGCGCCTTGTACACGATCTCCGC	123
TauS396DS404D	TGGGGACACGGACCCACGGCATCTCAGCAAT	124	GACACCACTGGGTCCTTGTACACGATCTCCGC	125
tauS422D	CATGGTAGACgatCCCCAGCTCGCCAC	126	TCGATGCTGCCGGTGGAG	127
tauS199AT205A	CCCAGGCGCTCCCGGCAGCCGCTCCCGC	128	GAGCCGGGGGCGCTGTAGCCGCTGCGATCCCC	129
tauS199DT205E	CCCAGGCGAACCCGGCAGCCGCTCCCGC	130	GAGCCGGGGTCGCTGTAGCCGCTGCGATCCCC	131
tauS396AS404A	TGGGGACACGGCTCCACGGCATCTCAGCAAT	132	GACACCACTGGCGCCTTGTACACGATCTCCGC	133
tauS396DS404D	TGGGGACACGGACCCACGGCATCTCAGCAAT	134	GACACCACTGGGTCCTTGTACACGATCTCCGC	135
mCherry PSD-95	CAAGCCCAGCAATGCCTACCTGAGTGACGTGAGCAAGGGCGAGGAGG	136	CGAGGTTGTGATGTCTGGGGGAGCATAGCTCTTGTACAGCTCGTCCATGCC	137

Adeno-associated virus vectors (von Jonquieres, et al. *PLOS ONE* 8, e65646 (2013)) for neuronal expression (pAM-

CAG) of wildtype (Figure 46, Figure 48 (SEQ ID NO: 6)) and constitutively active (D179A) p38γ (Figure 47, Figure 49 (SEQ ID NO: 7)) or variants of tau were cloned by conventional restriction enzyme cloning. All plasmids were amplified in *E. coli* DH5α or XL-1blue. AAV vectors were propagated in E. coli Stbl3 to avoid recombination events. Constructs were verified by sequencing.

Adeno-associated viruses.

Packaging of rAAV1 vectors was performed as described (AE Harasta *et al.*, *Neuropsychopharmacology* **40**, 1969-78 (2015)). Titres were determined by Quantitative polymerase chain reaction (qPCR). One µl ($1x10^9$ viral particles) of either AAV-SG1-shR or AAV-ctr-shR vector was injected at 3 sites each bilaterally into the brains of cryoanaesthetized neonatal mice as described (G von Jonquieres *et al.*, *PLoS One* 8, e65646 (2013)).

Cell culture.

Primary hippocampal neurons from E16.5 mouse embryos were cultured, using our standard protocol (T Fath, YD Ke, P Gunning, J Gotz, LM Ittner, *Nat Protoc* 4, 78-85 (2009)). Cytotoxicity was determined by measuring LDH release, using a commercial assay (Promega), or by visualization of EthD1 (Thermo Fisher Scientific) added to the cell culture medium 5 min before fixation with 4% PFA/PBS. 293T cells were cultured in DMEM/10%FBS/1%Glutamate/1%P/S (Life Technologies) and transfected by calcium precipitation (A Ittner *et al.*, *J Exp Med* **209**, 2229-46 (2012)). Primary neurons were transduced by AAV infection (AE Harasta *et al.*, *Neuropsychopharmacology* **40**, 1969-78 (2015)).

Live cell confocal imaging and FLIM/FRET analysis

FLIM/FRET measurements were performed using a time resolved, inverted confocal fluorescence microscope (Microtime200, PicoQuant GmbH). Excitation of the donor GFP was via a single-photon fiber coupled pico-second-pulsed diode 473 nm laser (20 MHz repetition rate, 2 ms dwell time, 256 x 256 pixel array) using a 63x water objective (1.25 NA). Fluorescence emission was collected through a 510/32 Semrock BrightLine band pass emission filter onto a single-photon avalanche diode (SPAD) coupled to high speed timing electronics for time-correlated single-photon counting (TCSPC).

Fluorescence images were analysed by phasor plot using the SimFCS software (Globals Software, USA). Briefly, Fourier transformation of the decay curve at each pixel was performed and the resulting transforms were plotted as a 2D histogram. The phasor position for the donor only was determined by measuring the donor in the absence of the acceptor. The FRET samples were measured and the phasor position along the quenching trajectory is calculated according to classical FRET efficiency calculation:

$$E = 1 - \frac{\tau_{DA}}{\tau_D}$$

where E is FRET efficiency, t_D is the fluorescence lifetime of the Donor in absence of acceptor, and t_{DA} is the fluorescence lifetime in the presence of acceptor.

Cell immunofluorescence staining and microscopy

Cell staining was done as previously described ((LM Ittner *et al.*, *Cell* 142, 387-97 (2010))). Briefly, cells were fixed with 4% PFA for 10 min, washed with phosphate

buffered saline (PBS), permeabilised with 0.02% NP-40 and blocked with blocking buffer (3% horse serum/1% bovine albumin in PBS). Primary antibodies diluted in blocking buffer were incubated over-night at 4°C or for 1 hour at room temperature. After washing with PBS, secondary antibodies diluted in blocking buffer with or without addition of DAPI to visualize cell nuclei were incubated for 1 hour at room temperature. Cells were then washed and mounted using anti-fade mounting medium (Prolong Gold, Life Technologies). Secondary antibodies used were coupled to Alexa 488, 555, 568 or 647 dyes (Molecular Probes). Confocal images were acquired on a Zeiss LSM780 confocal microscope with a Plan-Apochromatic 100x 1.4 NA objective or on a Zeiss LSM880 Airyscan confocal microscope with a Plan-Apochromatic 100x 1.4 NA objective using the Zen software (Zeiss). Epifluorescence imaging was done on a BX51 bright field/epifluorescence microscope (UPlanFL N lenses [¥/0.17/FN26.5]: 10x/0.3, 20x/0.5, 40x/0.75, 60x/1.25oil and 100x/1.3oil) equipped with a DP70 color camera (Olympus) using CellSens software (Olympus).

Human brain samples

Human entorhinal cortex tissue samples were received from the New South Wales Brain Tissue Resource Centre at the University of Sydney and the Sydney Brain Bank at Neuroscience Research Australia, which are supported by The University of New South Wales, Neuroscience Research Australia and Schizophrenia Research Institute. Frozen tissue was lysed in phosphate buffered saline (20%w/v) using a rotating dounce homogeniser followed by five 1s sonication bursts at 20% power (Vibra Cell, Sonics). Lysates were centrifuged at 3,000xg for 10 minutes at 4ºC and supernatants were used for analysis. Details on

patients are provided in Table 3. Use of human brain samples was approved by the Human Research Ethics Committees of the University of New South Wales and University of Sydney.

Table 3

Group	Age (y)	gender	PMI	CoD	APOE genotype	Braak
0	93	F	21	cardiac failure	E3/E3	0
0	85	F	23	respiratory failure	E3/E3	0
0	79	M	8	respiratory failure	E2/E3	0
0	89	F	23	metastatic adenocarcinoma	E3/E4	0
0	**86.5±3.0**		**18.8±3.6**			
I/II	78	F	11	respiratory failure	E3/E3	I
I/II	80	M	12	respiratory failure	E3/E3	I
I/II	103	M	20	cardiorespiratory failure	E3/E3	II
I/II	101	F	9	cardiorespiratory failure	E3/E3	II
I/II	88	F	31	cardiorespiratory failure	E3/E3	II
I/II	**90.0±5.2**		**16.6±4.1**			
III/IV	93	F	7	cardiorespiratory failure	E2/E3	III
III/IV	102	F	5	acute renal failure	E2/E3	IV
III/IV	92	F	5	infection	E3/E3	IV
III/IV	76	F	3	cardiac failure	E3/E4	IV
III/IV	**90.8±5.4**		**5.0±0.8**			
V/VI	98	F	11	stroke	E3/E3	VI
V/VI	85	F	10	cardiac failure	E3/E3	VI
V/VI	100	F	4	pneumonia	E3/E4	VI
V/VI	100	F	3	aspiration pneumonia	E3/E3	VI
V/VI	91	F	6	cardiorespiratory failure	E3/E3	VI
V/VI	**94.8±3.0**		**6.8±1.6**			

PMI, post mortem interval; CoD, cause of death; bold values, mean ± SEM of group

Histological Sections and staining

Mice were transcardially perfused with phosphate-buffered saline followed by 4% paraformaldehyde (PFA) and post-fixing in 4% PFA overnight. Tissue was processed in an Excelsior tissue processor (Thermo) for paraffin embedding. Thioflavin S staining to visualize amyloid plaques were performed following a standard protocol (LM Ittner *et al.*, *Cell* 142, 387-97 (2010)). Muscle cross-sections were stained with primary antibodies to laminin (Sigma) as previously described (Ke, et al. *Acta Neuropathol.* 130, 661-678 (2015)). Brain sections from

AAV-injected mice were stained with primary antibody to tau (Tau13; Abcam) or HA-tag (HA-7; Sigma-Aldrich) to visualize viral transgene expression. Serial paraffin sections of human entorhinal cortex samples were obtained from the NSW Brain Bank and stained with a standard Nissl protocol for counting. Neuronal counting was done on an Olympus BX51 microscope equipped with agraticulated ocular (U100H6; Olympus). Neurons with the nucleolus, nucleus and cytoplasm visible within a single plane of the section were considered for counting. Forthe CA fields (CA4-1), three random and non-overlapping fields of view were selected. For the entorhinal cortex, three non-overlapping strips of cortex extending from the pial surface and into the grey-white matter junction were marked for counting. Subsequent cortical counts were then performed across three adjacent graticule fields spanning perpendicularly to the pial surface. Mean cell counts across the section were then normalised into cell density values of neurons per mm2. All tissue sections were imaged on a BX51 bright field/epifluorescence microscope (UPlanFL N lenses [¥/0.17/FN26.5]: 10x/0.3, 20x/0.5, 40x/0.75, 60x/1.25oil and 100x/1.3oil) equipped with a DP70 color camera (Olympus).

Western Blotting

Western blotting was performed as previously described (A Ittner *et al.*, *J Exp Med* 209, 2229-46 (2012)). Bands were visualized by chemiluminescence on X-ray films or ChemiDoc MP (Biorad). Densitometric quantification of Western blot results was performed using ImageJ 2.0.0-rc-49/1.51d (NIH). Antibodies used in this study were: anti-NR1 (Chemicon), anti-NR2B (Santa Cruz), antiphosphoTyrosine1473-NR2B (Affinity BioReagents), anti-

PSD95 (Millipore), anti-Fyn (Santa Cruz), anti-phospho-Y418 Fyn (Invitrogen), anti-phospho-Y529 Fyn (Invitrogen), anti-APP (22C11), anti-Aβ (6E10), anti-tau (DAKO), anti-tau (tau-1, Millipore), anti-tau (Tau13, Abcam), anti-phospho-Serine199 tau (Abcam), anti-phospho-Serine202 tau (Abcam), anti-phospho-Threonine205 tau (Abcam), antiphospho-Threonine212 tau (Abcam), anti-phospho-Serine214 tau (Millipore), anti-phospho-Threonine231 tau (Abcam), anti-phospho-Serine235 tau (Abcam), anti-phospho-Serine356 tau (Abcam), anti-phospho-Serine396 tau (Abcam), anti-phospho-Serine404 tau (Millipore), anti-phospho-Serine422 tau (Millipore), PHF-1 (phospho-Serine396-phospho-Serine404 tau; kind gift by P. Davies), anti-p38alpha (Cell Signaling), anti-p38beta (Santa Cruz), anti-p38gamma (R&D), anti-p38delta (R&D), anti-phosphoThreonine180/Tyrosine182-p38 (Cell Signaling Technologies), anti-Flag (M2, Sigma), anti-HA7 (Sigma), anti-V5 (Invitrogen), anti-MAP2 (mouse Abcam), anti-MAP2 (chicken: Abcam), anti-β3 tubulin (Covance), anti-NeuN (Abcam), anti-Debrin (Sigma), anti-Synaptophysin (Abcam), anti-αsynuclein (Sigma), anti-glyceraldehyde dehydrogenase (anti-GAPDH, Millipore).

Immunoprecipitation.

Immunoprecpitation was performed from cell or tissue lysates as previously described (LM Ittner *et al.*, *Cell* 142, 387-97 (2010)). Briefly, cells were lysed in pTNN buffer (20mM Tris pH7.4, 150mM NaCl, 1mM EDTA, 1mM Na3VO4, 1mM NaF, 1mM glycerophosphate, 2.5mM $Na_2H_2P_2O_7$, 1mM PMSF, protease inhibitors (Complete, Roche), 1% NP-40 substitute (Sigma-Aldrich)) on ice. Lysates were cleared by centrifugation (16,000×g/10 min/4°C). Protein

concentration was determined (DC Protein Assay, BioRad) and 200µg of lysate incubated with antibody (1:400) for 3 h on a rotator at 4°C. Equilibrated and blocked protein G-beads (Life Technologies) were incubated with lysates for 45 min on a rotator at 4°C. Beads were then washed 3 times and incubated in sample buffer for 5 min at 95°C before SDS-PAGE. Cortical or hippocampal tissues were homogenized in RIPA buffer (20mM Tris pH8.0, 150mM NaCl, 1mM EDTA, 1mM Na3VO4, 1mM NaF, 1mM glycerophosphate, 2.5 mM sodium pyrophosphate, 1mM PMSF, protease inhibitors (Complete, Roche), 1% NP-40 substitute (Sigma-Aldrich), SDS, sodium deoxycholate) and subjected to immunoprecipitation as outlined above. Quantitative densitometric analysis was performed using Image J2.0.0-rc-49/1.5ld (NIH) and levels for immunoprecipiations of PSD-95/tau/Fyn complexes were expressed relative to immunopreciptateed PSD-95 protein levels.

Microscale thermophoresis (MST)

Tau variants were purified as GST-fusion proteins from E. coli BL21DE3pLys (Promega) using glutathione resin (GE Healthcare) followed by concentration and buffer exchange using ultrafiltration spin columns (10,000 molecular weight cut-off; Vivaspin, Sartorius). eGFP-PSD-95 was expressed in 293T cells and lysates were prepared in TNN buffer (20 mM Tris pH7.4, 150 mM sodium chloride, 1% NP40 substitute, sodium orthovanadate, sodium pyrophosphate, glycerophosphate, sodium fluoride, protease inhibitors (Complete; Roche)) 48 h after transfection. Concentrations of fusion proteins were determined by absorbance measurements (Nanodrop 2000C; Thermo-Fisher) using molar extinction coefficients. Thermophoresis of GFP-PSD-95 was measured on a Monolith NT115 (Nanotemper technologies)

using 50 % LED power and 20 % MST power with 5 s pre-MST and 30 s MST-time with serials dilutions (1:1) of GST-tau (starting concentration 9 µM). Thermophoresis and temperature-jump normalized fluorescence curves from three independent experiments were expressed as fraction of the bound state of the fluorophores-tagged protein (Wienken et al. *Nat. Commun.* 1, 100 (2010)). Thermophoresis was plotted as a function of tau concentration and non-linear curves fitting to determine experimental equilibrium dissociation constants (KD) was performed using sum-of-squares minimization (Marquardt method; Graphpad Prism 6).

Kinase assay.

Recombinant proteins were expressed in bacteria and purified as previously described (A Ittner *et al.*, *J Exp Med* 209, 2229-46 (2012)). Purity of proteins was assessed by SDS-PAGE and Coomassie staining. Kinase assay reactions were performed as previously described (A Ittner *et al.*, *J Exp Med* 209, 2229-46 (2012)). Briefly, 0.5µg recombinant p38γ was mixed with 1µg of recombinant human tau in kinase reaction buffer (Promega) and incubated for 30 min at 30°C. Kinase reactions were stopped by addition of sample buffer and incubation for 5 min at 95°C.

Mass spectrometry

Phospho-peptide mapping of tau after in vitro p38γ kinase reactions was done as previously described (Dolai, et al. *Cancer Res.* **76**, 2766-2777 (2016), Thingholm, et al. *Nat. Protoc.* **1**, 1929-1935 (2006)). Briefly, kinase treated protein extracts containing tau were reduced with 3mM tris(2-carboxyethyl)phosphine (TCEP, 56oC, 10min), alkylated with 6 mM iodoacetamide (ambient temp, 30min), buffer exchanged and concentrated using 100mM ammonium

bicarbonate and 3kDa spin-filters (Amicon Ultra-4 centrifugal filters, Merck KGaA, Darmstadt, Germany) followed by trypsin digest (25:1 w/w protein:trypsin ratio, 16h, 37oC). A portion of the material was enriched for phosphopeptides using Titansphere Phos-TiO kit, with TiO2 Spin tips (GL Sciences, Tokyo, Japan), following the manufacturer's protocol. Phosphopeptide enriched and non-enriched samples were analysed by LC-MS/MS using Orbitrap mass spectrometers (LTQ-Orbitrap Velos with CID and ETD activation modes and HCD on the QExactive Plus: Thermo Electron, Bremen, Germany) to maximize identification of phosphopeptides. Chromatography was carried out by nano-LC (Dionex UltiMate 3000 HPLC, Thermo Scientific, Waltham, USA) with autosampler system (Dionex, Amsterdam, Netherlands). Peptides (1-7µL injected) were initially captured on a C18 cartridge (Acclaim PepMap 100, 5µm 100 Å, Thermo Scientific Dionex, Waltham, USA), switching to a capillary column (10cm) containing C18 reverse phase packing (Reprosil-Pur, 1.9 µm, 200 Å, Dr. Maisch GmbH, Ammerbuch-Entringen, Germany), supported within a column heater (45°C, Sonation GmbH, Germany). Peptides were eluted using a 40min gradient of buffer A (H_2O:CH_3CN of 98:2 containing 0.1% formic acid) to 45% buffer B (H_2O:CH_3CN of 20:80 containing 0.1% formic acid) at 200nL/min, with high voltage applied at the column inlet. Mass spectrometer settings were: electrospray voltage 2000V, capillary temperature 275 - 300°C, positive ion mode, data dependent acquisition mode with a survey scan acquired (*m/z* 375-1750) and up to ten multiply charged ions (charge state ≥ 2+) isolated for MS/MS fragmentation (counts > 2500 for CID, >5000 for ETD and intensity threshold of 8.0x104 for HCD). Nitrogen was used as HCD collision gas and fluoranthene anion reagent for ETD. Peak lists were

generated from the raw data using MASCOT Distiller (Matrix Science, London, England) and searched using the MASCOT search engine (version 2.5, Matrix Science) and the NCBInr database (downloaded 24-10-15) using *homo sapiens* taxonomy. Search parameters were: peptide tolerance of ± 4ppm and MS/MS tolerances of ± 0.4 Da for CID and ETD or ± 0.05 Da for HCD, variable modifications were carbamidomethyl cys, met oxidation, phospho (ST) and phospho (Y), peptide charge of 2+, 3+, and 4+, enzyme specificity trypsin with up to three missed cleavages allowed.

Aβ preparation.

Aβ42 (Bachem) was prepared and pre-aggregated at a concentration of 100 µM as described (MP Lambert *et al.*, *Proc Natl Acad Sci U S A* 95, 6448-53 (1998)). Briefly, hexafluoro-2-propanol (Sigma) dissolved and evaporated Aβ was reconstituted in dimethyl sulfoxide (Sigma) at 5mM and then diluted in phenol-red free F-12 medium (Invitrogen) to a final concentration of 100µM, followed by brief vortexing and incubation at 4ºC for 24 hours. Further dilutions were done in culture medium.

Aβ levels and pathology.

Aβ40 and Aβ42 and levels were determined by ELISA as previously described (LM Ittner *et al.*, *Cell* 142, 387-97 (2010)). Plaque load was determined as previously described (LM Ittner *et al.*, *Cell* 142, 387-97 (2010)).

Statistical analysis.

Statistical analysis was performed using Graphpad Prizm Version 6.0 (Student's t test or ANOVA). Linear regression and correlation analysis was done by sum of-squares

minimization. Survival data were analyzed by log-rank Mantel-Cox testing. All values are presented as mean ± standard error of the mean (SEM).

Results

To understand the molecular contributions of p38 kinases to AD, we first challenged mice with individual deletion of *p38α*, *p38β*, *p38γ* or *p38δ* (Fig. 1) by inducing excitotoxic seizures with pentylenetetrazole (PTZ), an approach that has been instrumental in understanding excitotoxicity in AD mouse models (*7*, *8*). The results are shown in Figs. 2A, 6A, 6B and 6C. Surprisingly, neither neuronal deletion of *p38α* (*p38α*Δneu), nor knockout of *p38β* or *p38δ* changed seizure latency and severity after PTZ administration, suggesting they have no modulatory role in acute excitotoxicity. In contrast, *p38γ* depletion ($p38\gamma^{-/-}$) markedly enhanced sensitivity to PTZ-induced seizures (Fig. 2A and fig. 6A, B and C). Pan-p38 inhibition increased severity and reduced latency of PTZ-induced seizures in wild-type mice similar to changes in $p38\gamma^{-/-}$, suggesting p38γ but not p38α/β/δ contribute to acute excitotoxicity. Consistent with a role in post-synaptic signaling, only p38γ localized to dendritic spines and post-synaptic densities of cultured neurons (Fig. 2B). p38α and p38β were found in soma and dendrite shafts, while p38δ was not detectable in neurons. Taken together, only p38γ localizes to the post-synaptic compartment and limits PTZ-induced excitotoxicity.

To test whether the effects of p38γ depletion on PTZ-induced seizures would also impact on Aβ-induced deficits in AD mouse models, we crossed $p38\gamma^{-/-}$ mice with mutant APP expressing APP23 mice. These APP23.$p38\gamma^{-/-}$ mice were

assessed for seizure sensitivity by administering PTZ. The results are shown in Fig. 7. The increased sensitivity of APP23 mice to PTZ-induced seizures was further augmented in APP23.$p38\gamma^{-/-}$ mice (fig. 7A-C). APP23 mice are characterized by premature mortality, memory deficits, neuronal circuit aberrations with epileptiform brain activity, and Aβ plaque pathology (Ittner et al., Cell 142, 387-397 (2010);) Ittner, et al., Acta Neuropathol. Commun. 2, 149 (2014); Sturchler-Pierrat et al., Proc. Natl. Acad. Sci. U.S.A. 94, 13287-13292 (1997)). While Aβ formation and plaque pathology were comparable in brains of APP23.$p38\gamma^{-/-}$ and APP23.$p38\gamma^{+/+}$ mice, deletion of *p38γ* aggravated the premature mortality of APP23 mice, and 82% of APP23.$p38\gamma^{-/-}$ mice died by 8 months of age (Fig. 2C). $p38\gamma^{-/-}$ mice showed normal survival (Fig. 2C). Memory deficits in APP23.$p38\gamma^{-/-}$ were significantly more severe compared to those of APP23.$p38\gamma^{+/+}$ mice, as assessed in the Morris-water maze paradigm (Fig. 2D-F, fig. 8A-C), in differential paired associate learning (dPAL) (Fig. 21) and in a pairwise discrimination task (Fig. 22). In contrast, $p38\gamma^{-/-}$ mice showed wild-type-like memory performance and motor function. Memory deficits were associated with neuronal circuit aberrations and hypersynchronous epileptiform brain activity in APP transgenic lines (*10*), including APP23 (*14*). Electroencephalography (EEG) of APP23.$p38\gamma^{-/-}$ showed more frequent spontaneous seizure spike trains and interictal hypersynchronous discharges than APP23.$p38\gamma^{+/+}$ recordings (Fig. 2G-I). As can be seen from Fig. 2G, virtually no spike activity was found in $p38\gamma^{-/-}$ and $p38\gamma^{+/+}$ mice. Theta (4-8Hz) and gamma (25-100Hz) oscillations, both critical measures of hippocampal network activity related to learning and memory (*18, 19*), are altered in

APP transgenic mice (*14*). Accordingly, theta spectral power was shifted to lower frequencies (4-8Hz) in APP23.*p38γ*$^{+/+}$ and more so APP23.*p38γ*$^{-/-}$ mice, while gamma spectral power was increased compared to *p38γ*$^{-/-}$ and *p38γ*$^{+/+}$ mice (fig. 9A-G). Hippocampal cross frequency coupling (CFC) through theta-phase modulation of gamma power (*18*) correlates with memory performance in rodents and humans (*20, 21*), and is impaired in APP23 mice (*14*). Interictal EEG traces showed CFC of similar magnitude at ~8Hz in *p38γ*$^{+/+}$ and *p38γ*$^{-/-}$ mice, but a marked impairment in APP23.*p38γ*$^{+/+}$ and virtual depletion 1 in APP23.*p38γ*$^{-/-}$ littermates (Fig. 2J), suggesting p38γ depletion further exacerbates compromised CFC in APP23 mice. Similarly, synchrony of phase-amplitude distribution and theta phase was markedly reduced in APP23.*p38γ*$^{+/+}$, and virtually absent in APP23.*p38γ*$^{-/-}$ mice compared to *p38γ*$^{+/+}$ and *p38γ*$^{-/-}$ mice (fig. 9). Consequently, the modulation index, a robust measure of CFC (*21*), was significantly lower in APP23.*p38γ*$^{-/-}$ recordings as compared with *p38γ*$^{+/+}$ and *p38γ*$^{-/-}$ or even APP23.*p38γ*$^{+/+}$ (Fig. 2K).

p38γ levels were determined in extracts from brains of humans without Alzheimer's disease (Braak 0) and from humans with different neuropatholocial disease stages ranging from Braak I to Braak VI (Table 3). The results are shown in Fig. 23A and 23B. As can be seen from Fig. 23A and 23B, p38γ levels were markedly reduced in humans as AD advances.

In summary, p38γ modulates excitotoxicity, neuronal circuit synchronicity, premature mortality and memory deficits in APP23 mice, without changes in Aβ. In addition, p38γ levels are reduced in APP23 mice and humans suffering from AD.

To determine if levels of tau affect the excitotoxicity-limiting effects of p38γ *in vivo*, we crossed non-mutant human tau-expressing Alz17 mice (*22*) with *p38γ*$^{-/-}$ mice, to challenge these mice with PTZ. The results are shown in Fig. 3A-C. As can be seen from Fig. 3A-C, while tau expression did not affect seizure thresholds in Alz17.*p38γ*$^{+/+}$ mice, Alz17.*p38γ*$^{-/-}$ mice presented with significantly enhanced seizure progression and severity compared to *p38γ*$^{-/-}$ mice (Fig. 3A-C). Conversely, crossing *p38γ*$^{-/-}$ with tau-deficient *tau*$^{-/-}$ mice, revealed similar protection from PTZ-induced seizures in *tau*$^{-/-}$.*p38γ*$^{-/-}$ and *tau*$^{-/-}$.*p38γ*$^{+/+}$ mice (Fig. 3D-F).

To determine whether the Aβ toxicity-limiting effects of p38γ were tau-dependent, APP23.p38γ$^{-/-}$ mice were crossed with tau$^{-/-}$ mice, and the resulting crosses assessed for survival, memory deficit and neuronal network disfunction. The results are shown in Fig. 3G-3I, 24, 25, 26A, 26B, 27, 28A and B, and 29). The exacerbating effects of p38γ loss on reduced survival, memory deficits, and neuronal network dysfunction of APP23 mice were virtually abolished in APP23.p38γ$^{-/-}$.tau$^{-/-}$ mice. These data also show that, compared with APP23 mice, APP23.p38γ$^{-/-}$ animals had aggravated memory deficits that persisted with aging. In contrast, as noted above, increasing tau levels in p38γ$^{-/-}$ mice (brought about by crossing with non-mutant tau-expressing Alz17 mice) significantly enhanced PTZ-induced seizures in Alz17.p38γ$^{-/-}$ mice. Conversely, when compared to tau$^{-/-}$.p38γ$^{+/+}$ mice, tau$^{-/-}$.p38γ$^{-/-}$ animals showed similar protection from PTZ-induced seizures. Taken together, the effects of p38γ on excitotoxicity and Aβ toxicity are tau-dependent.

Tau resides in a post-synaptic signaling complex with Fyn and PSD-95 that mediates Aβ-induced excitotoxicity (*8*). Interaction of tau, Fyn and PSD95 in Alz17.*p38γ*$^{-/-}$ brains was enhanced compared to Alz17.*p38γ*$^{+/+}$ mice (Fig. 4A, B), consistent with their increased sensitivity to PTZ-induced seizures. Conversely, no PSD-95/tau/Fyn complexes could be isolated from *tau*$^{-/-}$ and *tau*$^{-/-}$ *p38γ*$^{-/-}$ brains. Strikingly, increased p38γ levels compromised, and expression of a constitutive active variant of p38γ (p38γ^{CA}) completely disrupted, PSD-95/tau/Fyn interaction in cells (Fig. 4C and D). Pan-p38 inhibition stopped p38γ and p38γ^{CA}-induced disruption of PSD-95/tau/Fyn complexes, furthermore indicating that p38γ activity is required (Fig. 4E and F). PSD-95 co-purified more tau and Fyn from *p38γ*$^{-/-}$ than *p38γ*$^{+/+}$ brains, suggesting increased PSD-95/tau/Fyn complex formation in the absence of p38γ (Fig. 4G and H). PTZ transiently increased PSD-95/tau/Fyn complex formation in *p38γ*$^{+/+}$ animals, and even further in *p38γ*$^{-/-}$ mice. Similarly, PSD-95/tau/Fyn complex formation was markedly increased in APP23.*p38γ*$^{-/-}$ compared to APP23.*p38γ*$^{+/+}$ and *p38γ*$^{-/-}$ brains (Fig. 4I and J). Consistent with increased PSD-95/tau/Fyn complex formation, Fyn-mediated phosphorylation of NR2B at Y1472, that facilitates interaction of PSD-95 and NR2B (*23*, *24*), was increased in *p38γ*$^{-/-}$ brains. Similarly, p38γ and p38γ^{CA} expression reduced Y1472-phosphorylation of NR2B.

Importantly, neither p38αCA, p38βCA nor p38δCA reduced NR2B phosphorylation, indicating that regulation of PSD-95/tau/Fyn complexes is a non-redundant function of p38γ. Interestingly, both p38γ and p38γ^{CA} interacted with PSD-95 (Fig. 4C), which was abolished by deleting the C-terminal

PDZ interaction motif from p38γ and p38γ^{CA} (Fig. 10A). Both p38γ and p38γ^{CA} also interacted with tau (Fig. 10B). Since, p38γ and more so p38γ^{CA} disrupted PSD-95/tau interaction in the absence of Fyn overexpression (Fig. 10C), but neither disrupted tau/Fyn interaction (Fig. 10D), p38γ appears to regulate PSD-95/tau/Fyn complexes at the level of PSD-95/tau interaction.

While p38γ phosphorylates tau at multiple epitopes during long-term *in vitro* kinase assays, possibly contributing to tau hyperphosphorylation (*25*), the temporal profile of p38γ-induced tau phosphorylation in acute signaling, including excitotoxicity, remained unknown. Using recombinant tau for short-term *in vitro* kinase reactions, we tested phosphorylation of a range of SP and TP sites, using available phosphorylation site-specific antibodies (Fig. 11A). Tau was phosphorylated strongly at serine (S) 199 and threonine (T) 205, and less at S396 and S404, but not at other sites tested (Fig. 11B). Site-specificity was confirmed by individually mutating S199, T205, S396 and S404 to alanine, which abolished p38γ-induced tau phosphorylation tau at the mutated sites *in vitro* (Fig. 11C). Mass spectrometric analysis of tau in kinase reactions confirmed these 4 sites, and an additional fourteen low abundant sites. Co-expression of p38γ or p38γ^{CA} and tau revealed that p38γ predominantly phosphorylated tau at T205 and to a lesser degree at S199, but barely at S396 and S404 in cells (Fig. 5A). Similarly, T205 (and less so S199 and S396) were phosphorylated in p38γ^{CA} transgenic mice. Phosphorylated T205 (pT205) increased after PTZ treatment of p38γ$^{+/+}$ animals but was virtually abolished in p38γ$^{-/-}$ mice,

whereas pS199, pS396 and pS404 were induced in both p38$\gamma^{+/+}$ and p38$\gamma^{-/-}$ mice. Similarly, pT205 was markedly reduced in APP23.p38$\gamma^{-/-}$ animals compared with APP23.p38$\gamma^{+/+}$ mice. Consistently, phosphorylation of T205 in primary neurons was markedly reduced by pan-p38 inhibition, while S199 phosphorylation remained unaffected. Taken together, these data indicate that T205 is a primary site in tau phosphorylation by p38γ.

To determine the functional relevance of tau phosphorylation by p38γ at S199 and T205, we generated phosphorylation-mimicking (S199D and T205E) and -preventing (S199A and T205A) tau variants. We also prepared phosphorylation mimicking mutants of all other sites identified by mass spectrometry and assessed all mutants for their ability to co-purify with PSD-95, tau and Fyn. The results are shown in Fig. 5B, 5C and Fig. 31. PSD-95 co-purified with Fyn and all mutants except T205E. In this regard, T205E coprecipitated significantly less with PSD-95 as compared with PSD-95 as compared with non-mutant and T205A tau, while all other phosphorylation mimicking mutants of all other identified sites had no effect on PSD-95/tau/Fyn interaction. Microscale thermophoresis and glutathione S-transferase-pulldown in vitro and fluorescence lifetime imaging microscopy (FLIM)-fluorescence resonance energy transfer (FRET) analysis in live cells confirmed the markedly compromised interaction of T205E tau with PSD-95. The T205E mutation did not hinder tau/Fyn interaction. These data suggests that phosphorylation of tau at T205 is sufficient to disrupt interaction with PSD-95. T205E and T205A mutations did not compromise tau/Fyn interaction. Importantly, p38γ^{CA}

disrupted PSD-95/tau/Fyn complexes in the presence of non-mutant tau, but had no effects when T205A tau was co-expressed (Fig. 5D and E). In contrast, phospho-mimicking and -preventing S396 or S404 variants of tau had no effect on PSD-95/tau/Fyn interaction (Fig. 5C). Taken together, this suggests that p38γ regulates PSD-95/tau/Fyn complexes via phosphorylation of tau at T205.

Disruption of NR/PSD-95/tau/Fyn complexes prevented exitotoxicity and Aβ-induced toxicity in primary neurons and APP23 mice (*8*). Hence, phosphorylation of tau at T205 should mitigate or reduce Aβ-induced neurotoxicity. To test this, we used AAV-mediated gene transfer to express wild-type, T205A or T205E tau at similar levels in primary neurons (fig. 12). Challenge with Aβ induced cell death in wild-type and T205A, but virtually not in T205E human tau-expressing hippocampal neurons, as indicated by increased LDH release (Fig. 5F) or EthD1 uptake (fig. 12A). H_2O_2-treatment exerted the same level of cytotoxicity in neurons irrespectively of the tau variant expressed. To test whether increasing levels or activity of p38γ in neurons similarly confer protection from Aβ toxicity, we expressed p38γ, $p38\gamma^{CA}$ or a GFP control in primary neurons (Fig. 5G and Fig. 13). Both, expressed p38γ and $p38\gamma^{CA}$ enriched in dendritic spines, similar to endogenous p38γ. Neurons expressing p38γ and more so $p38\gamma^{CA}$ were significantly more resistant to Aβ-induced cell death compared to controls (Fig. 5H). Neither expression of p38γ nor p38γCA limited H_2O_2-induced cell death. In summary, expression of site-specific phosphorylation-mimicking T205E tau or increasing p38γ activity mitigated the toxic effects of Aβ in hippocampal neurons. Remaining Aβ toxicity in the presence of T205E tau or $p38\gamma^{CA}$ was

possibly due to endogenous tau, or alternative pathways (*9*).

To determine if increased neuronal p38γ levels and/or activity limits excitotoxicity *in vivo*, we used AAV-mediated gene transfer to express p38γ, p38γ^{CA} or a GFP control in forebrains of newborn wild-type mice (fig. 14) and challenged them with PTZ at 2 months of age. Expression of p38γ *in vivo* moderately, but significantly decreased progression of PTZ-induced seizures in 2 month-old mice, with a trend towards reduction of mean seizure severity, compared to GFP expressing mice (Fig. 5I, J and fig. 15). p38γ^{CA} expression profoundly increased the latency to develop severe seizures in response to PTZ administration, and significantly decreased the mean seizure severity as compared with control mice (Fig. 5I, J and fig. 15). Expression levels of p38γ and p38γ^{CA} varied between mice as expected from AAV-mediated gene expression, with levels of p38γ being on average higher than those of p38γ^{CA} (Fig. 14B). Interestingly, levels of both p38γ and p38γ^{CA} and seizure latency slopes showed positive linear correlation (p38γ: R2 = 0.483, *P* = 0.0832, s = 65.23 ± 30.20; p38γCA: R2 = 0.707, *P* = 0.0023, s = 215.1 ± 48.96), with a significantly pronounced level-dependent protective effect of p38γ^{CA} over p38γ expression (F = 6.8407, *P* = 0.0214) (Fig. 5K). Thus, levels of active p38γ kinase *in vivo* determine susceptibility to excitotoxic signals.

Memory deficits in APP23.AAV$^{p38\gamma CA}$ were significantly less severe compared to those of APP23.AAV^{GFP} mice, as assessed in the Morris-water maze paradigm (Figs. 16-18).

APP23.AAV$^{p38\gamma CA}$ mice showed memory performance similar to wild-type memory performance (AAV^{GFP}, AAV$^{p38\gamma CA}$). Adeno-associated virus (AAV)- mediated expression of WT and T205A, but not T205E tau or green fluorescent protein (GFP), in the forebrains of tau$^{-/-}$ mice enhanced PTZ-induced seizures (Fig. 19). In contrast, expression of p38g^{CA} in WT mice using AAV or in Thy1.2-p38γ^{CA} transgenic mice decreased PTZ-induced seizures. AAV-mediated p38γ^{CA} expression in APP23 mice rescued memory deficits and network aberrations (Fig. 34-38); the same was true for crossing APP23 with Thy.1.2-p38γ^{CA} transgenic mice (Figs. 39-41). In summary, the levels of active p38γ kinase and tau phosphorylation at T205 determined susceptibility to excitotoxicity and Aβ toxicity.

Tau is a key mediator of deficits in APP transgenic mice (*7*, *8*), and tau has been suggested to transmit detrimental signals of Aβ in neurons by becoming aberrantly phosphorylated (*4*, *27*). Here, we show that tau is part of an intrinsic molecular pathway involving phosphorylation at T205 mediated by p38γ to inhibit excito- and Aβ toxicity. While we formally cannot exclude further non-tested sites being phosphorylated by p38γ, our data with T205A/E tau suggest that phosphorylation at T205 is key to modulating post-synaptic PSD-95/tau/Fyn complexes. Tau is required for the toxicity-limiting effects of p38γ, as *p38γ* depletion failed to exacerbate seizures in *tau*$^{-/-}$*.p38$\gamma^{-/-}$* mice. Although other kinases might target T205 on tau in disease or physiologically (*28-30*), the very distinct localization of PSD-95, tau and p38γ in a complex at the post-synapse indicates a specific and spatially

compartmentalized role of p38γ downstream of synaptic NR activation.

While different roles have been characterized for other p38 kinases, the function of p38γ remained understudied. Here, our study revealed an unprecedented function of p38γ in the brain, by showing its involvement in tau-mediated Aβ toxicity, memory deficits and survival in AD mice. Its distinct spatial expression in post-synapses and unique sequence features, when compared to neuronally expressed p38α/β, likely contribute to this non-redundant function of p38γ in neurons. p38α/β have been described as downstream mediators of excito- (*11*) and Aβ toxicity (*12*, *13*). Therefore and importantly, the p38γ function in excito- and Aβ toxicity we describe here is distinct from and opposite to p38a/β.

In summary, our work suggests that phosphorylation of tau at T205 is part of an Aβ toxicity-inhibiting response. This is contrary to the current view that tau phosphorylation downstream of Aβ toxicity is a purely pathological response (*27*). However, it is in line with the idea that tau is involved in normal physiologic signaling events in neurons likely involving NR signal transduction (*9*). Finally, we have identified p38γ as an unprecedented Aβ-toxicity limiting signaling factor, which modulates tau-dependent excitotoxicity by site-specific phosphorylation of tau and controlling post-synaptic PSD-95/tau/Fyn complexes. This provides new insight into post-synaptic processes involved in early AD pathogenesis and may contribute to future drug development.

References

1. C Ballatore, VM Lee, JQ Trojanowski, *Nature reviews. Neuroscience* 8, 663-72 (2007).
2. C Haass, DJ Selkoe, *Nature reviews. Molecular cell biology* 8, 101-12 (2007).
3. K Iqbal, F Liu, CX Gong, C Alonso Adel, I Grundke-Iqbal, *Acta Neuropathol* 118, 53-69 (2009).
4. EM Mandelkow, E Mandelkow, *Cold Spring Harb Perspect Med* 2, a006247 (2012).
5. ES Musiek, DM Holtzman, *Nat Neurosci* 18, 800-6 (2015).
6. M Rapoport, HN Dawson, LI Binder, MP Vitek, A Ferreira, *Proc Natl Acad Sci U S A* 99, 6364-9 (2002).
7. ED Roberson *et al.*, *Science* 316, 750-4 (2007).
8. LM Ittner *et al.*, *Cell* 142, 387-97 (2010).
9. L Mucke, DJ Selkoe, *Cold Spring Harb Perspect Med* 2, a006338 (2012).
10. JJ Palop, L Mucke, *Nat Neurosci* 13, 812-8 (2010).
11. GE Hardingham, H Bading, *Nature reviews. Neuroscience* 11, 682-96 (2010).
12. Q Wang, DM Walsh, MJ Rowan, DJ Selkoe, R Anwyl, *J Neurosci* 24, 3370-8 (2004).
13. S Li *et al.*, *J Neurosci* 31, 6627-38 (2011).
14. AA Ittner, A Gladbach, J Bertz, LS Suh, LM Ittner, *Acta Neuropathol Commun* 2, 149 (2014).
15. MA Fabian *et al.*, *Nat Biotechnol* 23, 329-36 (2005).
16. MB Menon, S Dhamija, A Kotlyarov, M Gaestel, *Autophagy*, 0 (2015).
17. C Sturchler-Pierrat *et al.*, *Proc Natl Acad Sci U S A* 94, 13287-92 (1997).
18. G Buzsaki, EI Moser, *Nat Neurosci* 16, 130-8 (2013).
19. R Goutagny, J Jackson, S Williams, *Nat Neurosci* 12, 1491-3 (2009).
20. RT Canolty *et al.*, *Science* 313, 1626-8 (2006).
21. AB Tort, RW Komorowski, JR Manns, NJ Kopell, H Eichenbaum, *Proc Natl Acad Sci USA* 106, 20942-7 (2009).

22. A Probst *et al.*, *Acta Neuropathol* 99, 469-81 (2000).
23. Y Rong, X Lu, A Bernard, M Khrestchatisky, M Baudry, *J Neurochem* 79, 382-90 (2001).
24. M Aarts *et al.*, 1 *Science* 298, 846-50 (2002).
25. M Goedert *et al.*, *FEBS Lett* 409, 57-62 (1997).
26. S Mondragon-Rodriguez *et al.*, *J Biol Chem* 287, 32040-53 (2012).
27. LM Ittner, J Gotz, *Nature reviews. Neuroscience* 12, 65-72 (2011).
28. JZ Wang, Q Wu, A Smith, I Grundke-Iqbal, K Iqbal, *FEBS Lett* 436, 28-34 (1998).
29. V Buee-Scherrer, M Goedert, *FEBS Lett* 515, 151-4 (2002).
30. A Cavallini *et al.*, *J Biol Chem* 288, 23331-47 (2013).

CLAIMS:

1. A method of treating or preventing a neurological condition mediated by a tau-dependent signalling complex in neurons of a subject, comprising treating the subject to:
   a. promote phosphorylation of one or more amino acid residues of tau, wherein the phosphorylation of the amino acid residues causes disruption of the tau-dependent signalling complex in neurons of the subject; or
   b. introduce a variant of tau that causes disruption of the tau-dependent signalling complex in neurons of the subject.

2. The method of claim 1, wherein treating the subject comprises administering an agent which:
   a. promotes phosphorylation of one or more amino acid residues of tau, wherein the phosphorylation of the amino acid residues causes disruption of the tau-dependent signalling complex; or
   b. introduces a variant of tau that causes disruption of the tau-dependent signalling complex in neurons of the subject.

3. The method of claim 1, wherein the one or more amino acid residues of tau is threonine at position 205 of tau (T205).

4. The method of any one of claims 1 to 3, wherein the subject is treated by administering an agent that elevates p38γ activity, or the activity of a variant of p38γ, in neurons of the subject.

5. The method of claim 4, wherein the agent comprises p38γ or a variant thereof, or a nucleic acid that is capable of expressing p38γ or a variant thereof in neurons of the subject.

6. The method of claim 4 or 5, wherein the agent comprises a nucleic acid that is capable of expressing p38γ or a variant thereof in neurons of the subject.

7. The method of any one of claims 4 to 6, wherein p38γ comprises the amino acid sequence of SEQ ID NO: 2.

8. The method of any one of claims 4 to 7, wherein the variant of p38γ comprises an amino acid sequence that is at least 60%, 65%, 70%, 75%, 80%, 85%, 90%, 95 or 99% identical to the amino acid sequence of p38γ (SEQ ID NO: 2).

9. The method of any one of claims 4 to 8, wherein the variant of p38γ comprises a PDZ interaction motif.

10. The method of any one of claims 4 to 9, wherein the variant of p38γ is a constitutively active variant of p38γ.

11. The method of claim 10, wherein the constitutively active variant of p38γ ($p38\gamma^{CA}$) comprises SEQ ID NO: 3.

12. The method of any one of claims 1 to 11, wherein the tau-dependent signalling complex comprises PSD-95 and tau.

13. The method of any one of claims 1 to 12, wherein the tau-dependent signalling complex comprises PSD-95, tau and FYN.

14. The method of any one of claims 1 to 13, wherein the neurological condition is selected from the group consisting of Alzheimer's disease, stroke and epilepsy.

15. A method of treating or preventing a neurological condition mediated by a tau-dependent signalling complex in neurons of a subject, comprising administering an agent which elevates p38γ activity, or the activity of a variant of p38γ, in the neurons of the subject.

16. The method of claim 15, wherein the agent comprises p38γ or a variant thereof, or a nucleic acid that is capable of expressing p38γ or a variant thereof in neurons of the subject.

17. The method of claim 15 or 16, wherein the agent comprises a nucleic acid that is capable of expressing p38γ or a variant thereof in neurons of the subject.

18. The method of any one of claims 15 to 17, wherein the variant of p38γ comprises an amino acid sequence that

is at least 60%, 70%, 75%, 80%, 85%, 90%, 95 or 99% identical to the amino acid sequence of p38γ (SEQ ID NO: 2).

19. The method of any one of claims 15 to 18, wherein the variant of p38γ comprises a PDZ interaction motif.

20. The method of any one of claims 15 to 19, wherein the variant of p38γ is a constitutively active variant of p38γ ($p38\gamma^{CA}$).

21. The method of claim 20, wherein the constitutively active variant comprises SEQ ID NO: 3.

22. The method of any one of claims 15 to 21, wherein the tau-dependent signalling complex comprises PSD-95 and tau.

23. The method of any one of claims 15 to 22, wherein the tau-dependent signalling complex comprises PSD-95, tau and FYN.

24. The method of any one of claims 15 to 23, wherein the neurological condition is selected from the group consisting of Alzheimer's disease, stroke and epilepsy.

25. A vector for treating or preventing a neurological condition mediated by a tau-dependent signalling complex in neurons of a subject, comprising:

a. a nucleic acid sequence encoding p38γ or a variant thereof; or

b. a nucleic acid sequence encoding a variant of tau that causes disruption of the tau-dependent signalling complex in neurons of the subject.

26. The vector of claim 25, wherein the nucleic acid sequence is operably linked to a regulatory sequence for expressing the p38γ or a variant thereof, or the variant of tau, in neurons of the subject.

27. The vector of claim 25 or 26, wherein the vector is a viral vector.

28. The vector of claim 27, wherein the viral vector is an adeno-associated viral (AAV) vector.

29. The vector of claim 28, wherein the AAV vector is AAV1, AAV9, AAVrh10 or AAVcy5.

30. An adeno-associated viral vector for treating or preventing a neurological condition mediated by a tau-dependent signalling complex in neurons of a subject, comprising:

a. a nucleic acid sequence encoding p38γ or a variant thereof; or

b. a nucleic acid sequence encoding a variant of tau that causes disruption of the tau-dependent signalling complex in neurons of the subject.

31. The vector of claim 30, wherein the nucleic acid encoding p38γ or a variant thereof, or variant of tau,

is operably linked to regulatory sequence for expressing the p38γ or a variant thereof, of the variant of tau, in neurons of the subject.

32. The vector of any one of claims 25 to 31, wherein the variant of p38γ comprises an amino acid sequence which is at least 60%, 65%, 70%, 75%, 80%, 85%, 90%, 95 or 99% identical to the amino acid sequence of p38γ (SEQ ID NO: 1).

33. The vector of any one of claims 25 to 32, wherein the variant of p38γ comprises a PDZ interaction motif.

34. The vector of any one of claims 25 to 33, wherein the variant of p38γ is a constitutively active mutant of p38γ.

35. The vector of claim 34, wherein the constitutively active mutant of p38γ comprises SEQ ID NO: 3.

36. The vector of any one of claims 25 to 35, wherein the tau-dependent signalling complex comprises PSD-95 and tau.

37. The vector of any one of claims 25 to 36, wherein the tau-dependent signalling complex comprises PSD-95, tau and FYN.

38. The vector of any one of claims 25 to 37, wherein the neurological condition is selected from the group consisting of Alzheimer's disease, stroke and epilepsy.

39. A composition comprising the vector of any one of claims 25 to 38.

40. A method of disrupting a signalling complex comprising PSD-95, tau and FYN in a neuron, comprising contacting the neuron with an agent which:
    a. promotes phosphorylation of one or more amino acid residues of the tau, wherein the phosphorylation of the amino acid residues causes disruption of the signalling complex; or
    b. introduces a variant of tau that causes disruption of the tau-dependent signalling complex.

41. The method of claim 40, wherein the amino acid residue of tau that causes disruption of, or reduces formation of, the tau-dependent signalling complex is threonine at position 205 of tau (T205).

42. The method of claim 40, wherein the neuron is contacted with an agent that elevates p38γ activity, or the activity of a variant of p38γ, in the neuron.

43. The method of claim 41, wherein the agent comprises p38γ or a variant thereof, or a nucleic acid that is capable of expressing p38γ or a variant thereof, in the neuron.

44. The method of claim 39 or 42, wherein the agent comprises a nucleic acid that is capable of expressing p38γ, or a variant thereof, in the neuron.

45. The method of any one of claims 41 to 43, wherein p38γ comprises the amino acid sequence of SEQ ID NO: 2.

46. The method of any one of claims 41 to 43, wherein the variant of p38γ comprises an amino acid sequence that is at least 60%, 65%, 70%, 75%, 80%, 85%, 90%, 95 or 99% identical to the amino acid sequence of p38γ (SEQ ID NO: 1).

47. The method of any one of claims 41 to 43, wherein the variant of p38γ comprises a PDZ interaction motif.

48. The method of any one of claims 41 to 43, wherein the variant of p38γ is a constitutively active mutant of p38γ.

49. The method of claim 47, wherein the constitutively active mutant of p38γ ($p38\gamma^{CA}$) comprises an amino acid substitution of aspartic acid to alanine at position 179 of p38γ.

50. The method of any one of claims 39 to 48, wherein the neuron is in a subject.

51. A method of treating Alzheimer's disease in a subject comprising introducing into neurons of the subject:

a. a nucleic acid capable of expressing p38γ, or a variant thereof; or

b. a nucleic acid capable of expressing a variant of tau that causes disruption of the tau-dependent signalling complex.

52. A method of treating stroke in a subject, comprising introducing into neurons of the subject:

a. a nucleic acid capable of expressing p38γ, or a variant thereof; or

b. a nucleic acid capable of expressing a variant of tau that causes disruption of the tau-dependent signalling complex.

53. A method of treating epilepsy in a subject, comprising introducing into neurons of the subject:

a. a nucleic acid capable of expressing p38γ, or a variant thereof; or

b. a nucleic acid capable of expressing a variant of tau that causes disruption of the tau-dependent signalling complex.

54. An agent which: (a) promotes phosphorylation of one or more amino acid residues of tau, wherein the phosphorylation of the amino acid residues causes disruption of the tau-dependent signalling complex in neurons of the subject; or (b) introduces a variant of tau that causes disruption of the tau-dependent signalling complex in neurons of the subject, for use in the treating or preventing a neurological condition mediated by a tau-dependent signalling complex in neurons of a subject.

55. An agent which elevates p38γ activity, or the activity of a variant of p38γ, in neurons of a subject, for use

in the treating or preventing a neurological condition mediated by a tau-dependent signalling complex in neurons of a subject.

56. An agent which: (a) promotes phosphorylation of one or more amino acid residues of tau, wherein the phosphorylation of the amino acid residues causes disruption of the tau-dependent signalling complex in neurons of the subject; or (b) introduces a variant of tau that causes disruption of the tau-dependent signalling complex in neurons of the subject, for use in disrupting, or reducing formation of, a signalling complex comprising PSD-95, tau and FYN in a neuron.

57. An agent which: (a) promotes phosphorylation of one or more amino acid residues of tau, wherein the phosphorylation of the amino acid residues causes disruption of the tau-dependent signalling complex in neurons of the subject; or (b) introduces a variant of tau that causes disruption of the tau-dependent signalling complex in neurons of the subject, for use in treating Alzheimer's disease in a subject.

58. An agent which: (a) promotes phosphorylation of one or more amino acid residues of tau, wherein the phosphorylation of the amino acid residues causes disruption of the tau-dependent signalling complex in neurons of the subject; or (b) introduces a variant of tau that causes disruption of the tau-dependent signalling complex in neurons of the subject, for use in treating stroke in a subject.

59. An agent which: (a) promotes phosphorylation of one or more amino acid residues of tau, wherein the

phosphorylation of the amino acid residues causes disruption of the tau-dependent signalling complex in neurons of the subject; or (b) introduces a variant of tau that causes disruption of the tau-dependent signalling complex in neurons of the subject, for use in treating epilepsy in a subject.

Figure 1

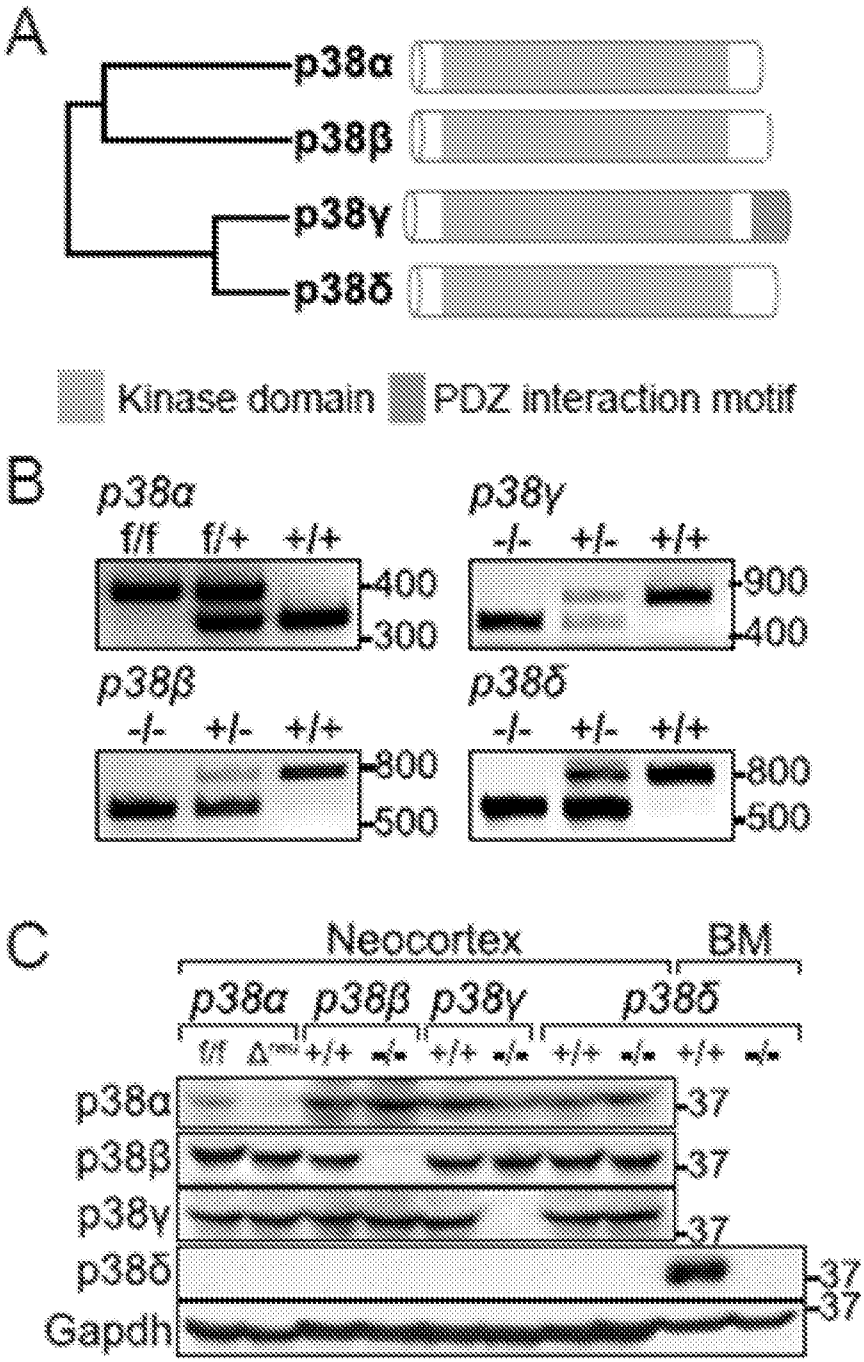
A
p38α
p38β
p38γ
p38δ
Kinase domain
PDZ interaction motif
B
p38α
f/f f/+ +/+
400
300
p38γ
-/- +/- +/+
900
400
p38β
-/- +/- +/+
800
500
p38δ
-/- +/- +/+
800
500
C
Neocortex
BM
p38α p38β p38γ p38δ
f/f Δ+/+ -/- +/+ -/- +/+ -/- +/+ -/-
p38α
p38β
p38γ
p38δ
Gapdh
37
37
37
37
37

Figure 2A

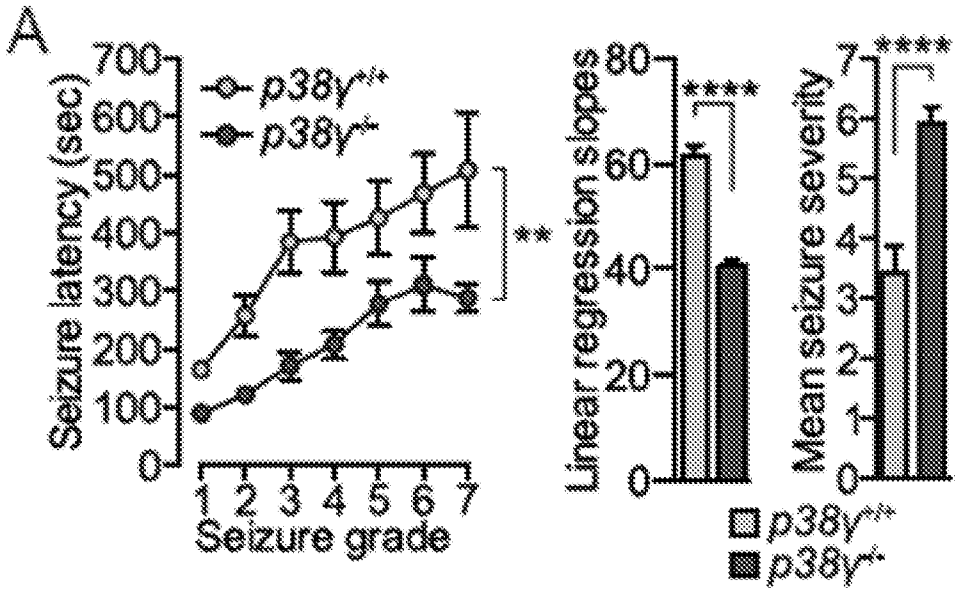
A
Seizure latency (sec)
700
600
500
400
300
200
100
0
p38γ+/+
p38γ-/-
**
1 2 3 4 5 6 7
Seizure grade
Linear regression slopes
80
60
40
20
0
****
Mean seizure severity
7
6
5
4
3
2
1
0
****
p38γ+/+
p38γ-/-

Figure 2B

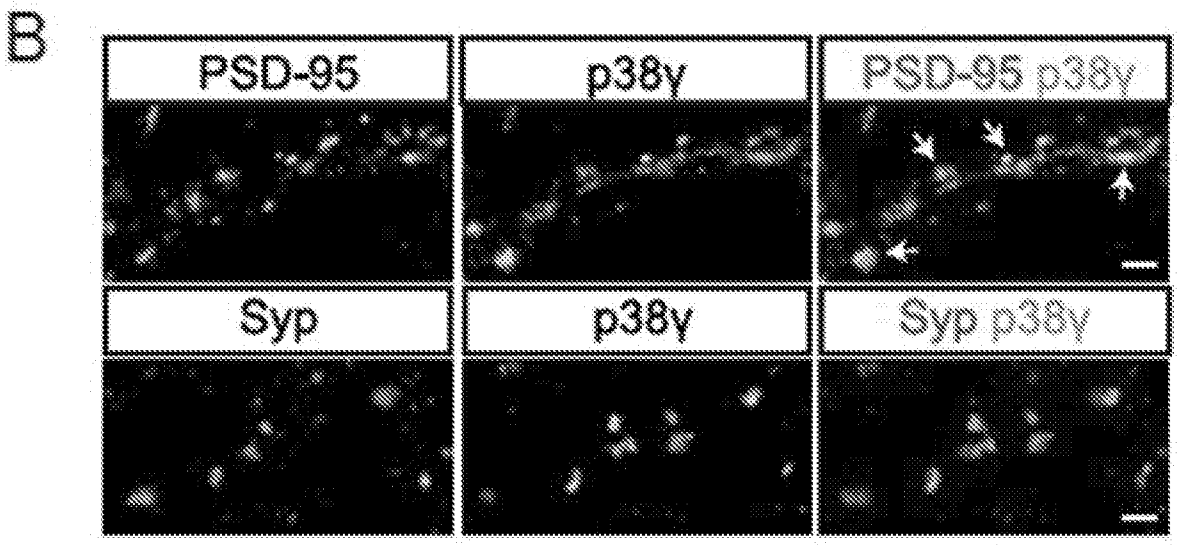

FIGURE 2C

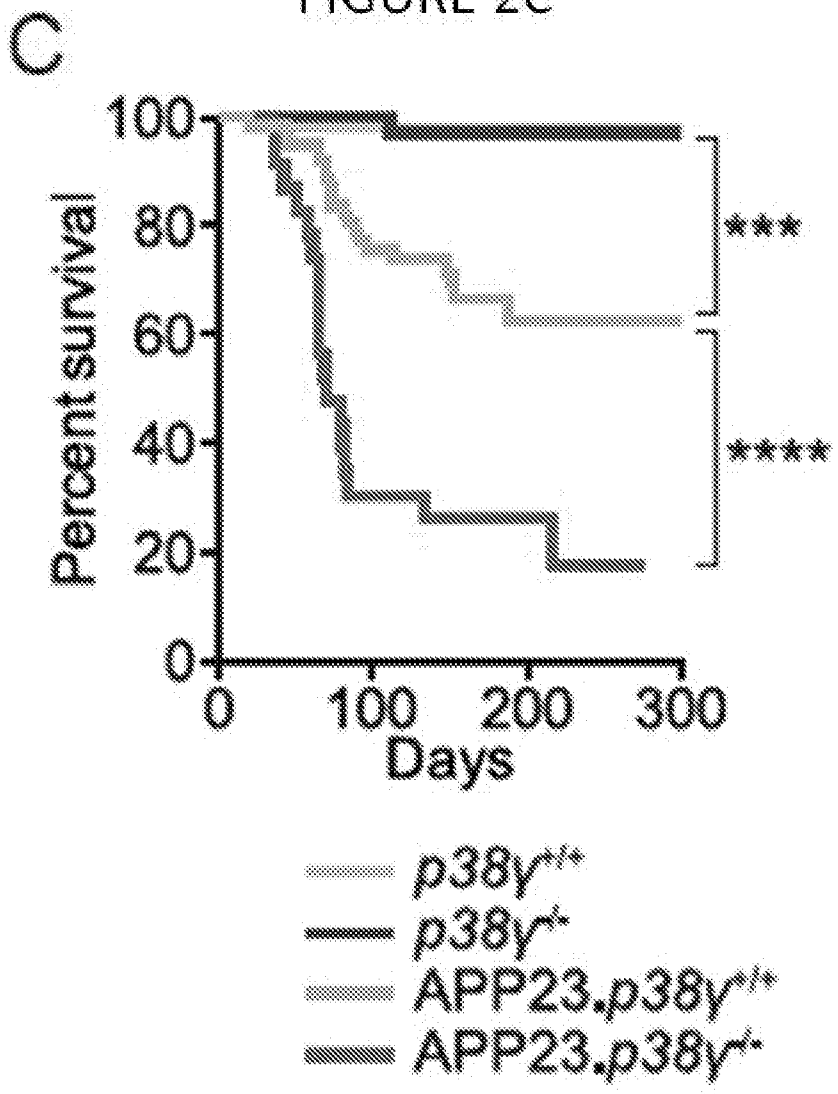
C
100
80
60
40
20
0
Percent survival
0
100
200
300
Days
***
****
p38γ+/+
p38γ-/-
APP23.p38γ+/+
APP23.p38γ-/-

Figure 2D

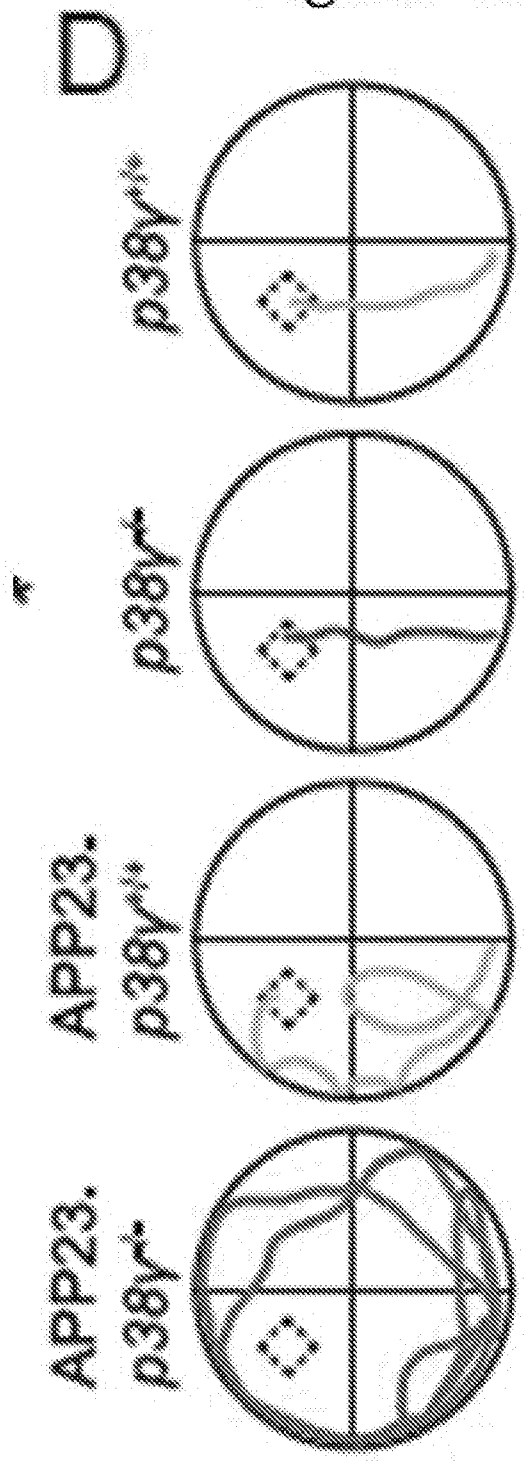

Figure 2E

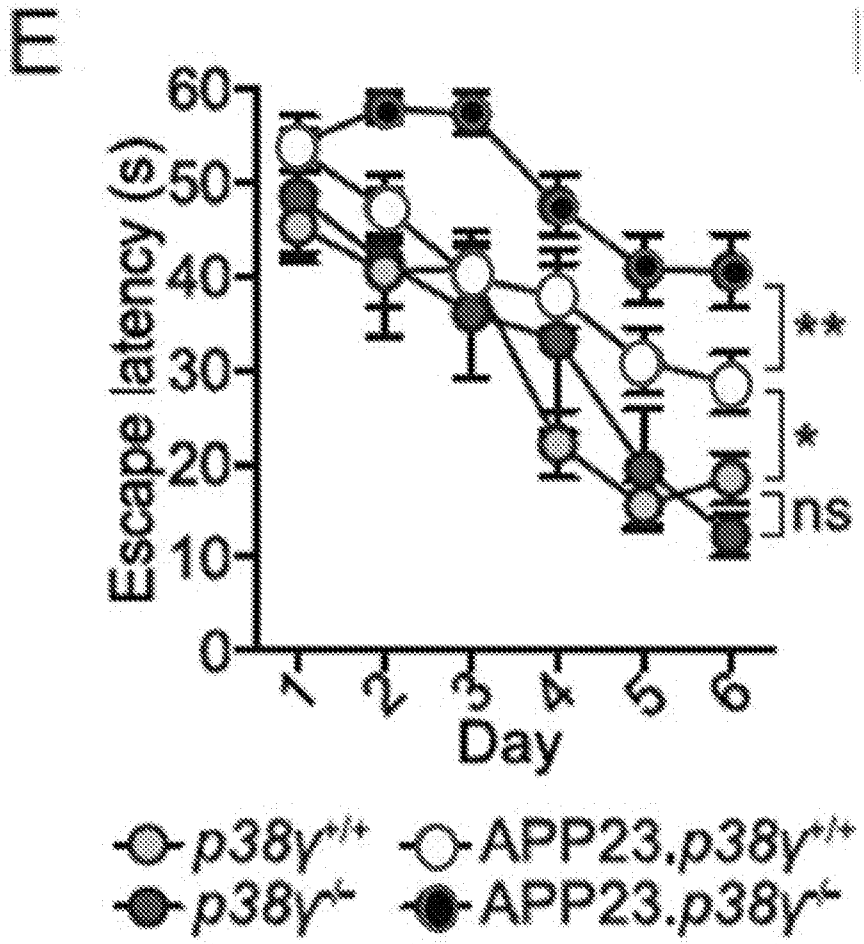
E
Escape latency (s)
60
50
40
30
20
10
0
1
2
3
4
5
6
Day
**
*
ns
p38γ+/+
p38γ-/-
APP23.p38γ+/+
APP23.p38γ-/-

Figure 2F

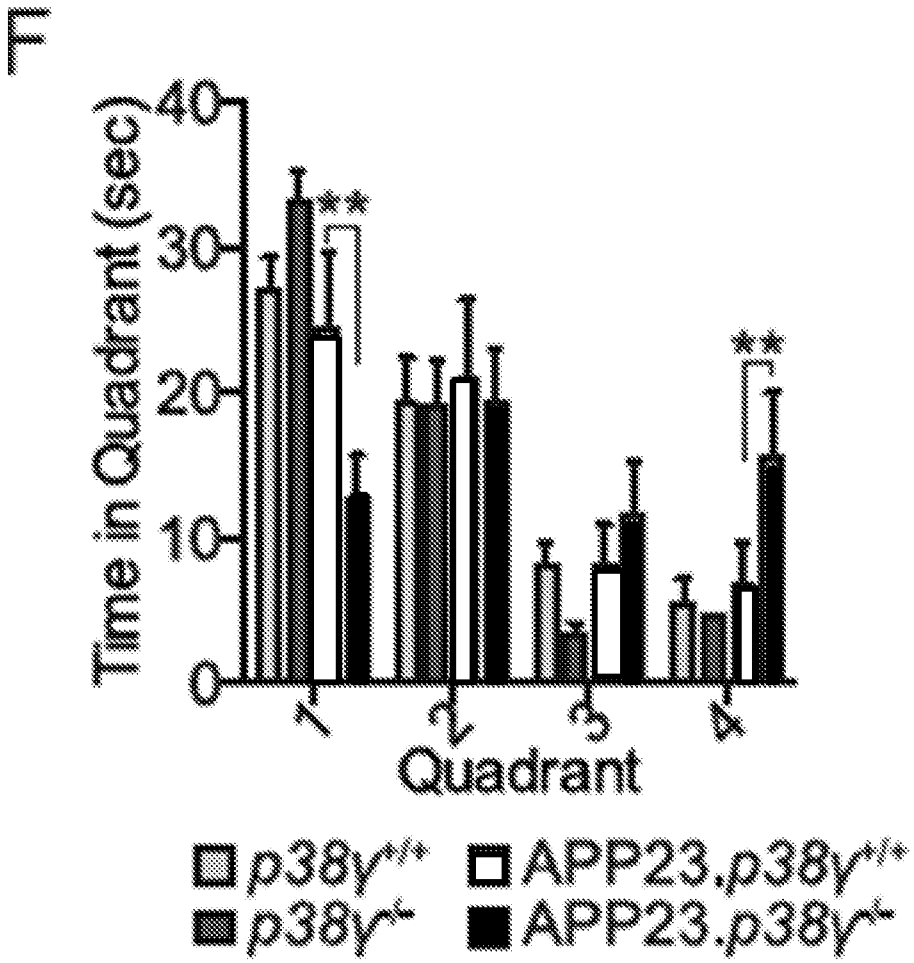
F
Time in Quadrant (sec)
40
30
20
10
0
**
**
1
2
3
4
Quadrant
p38γ+/+
p38γ-/-
APP23.p38γ+/+
APP23.p38γ-/-

Figure 2G

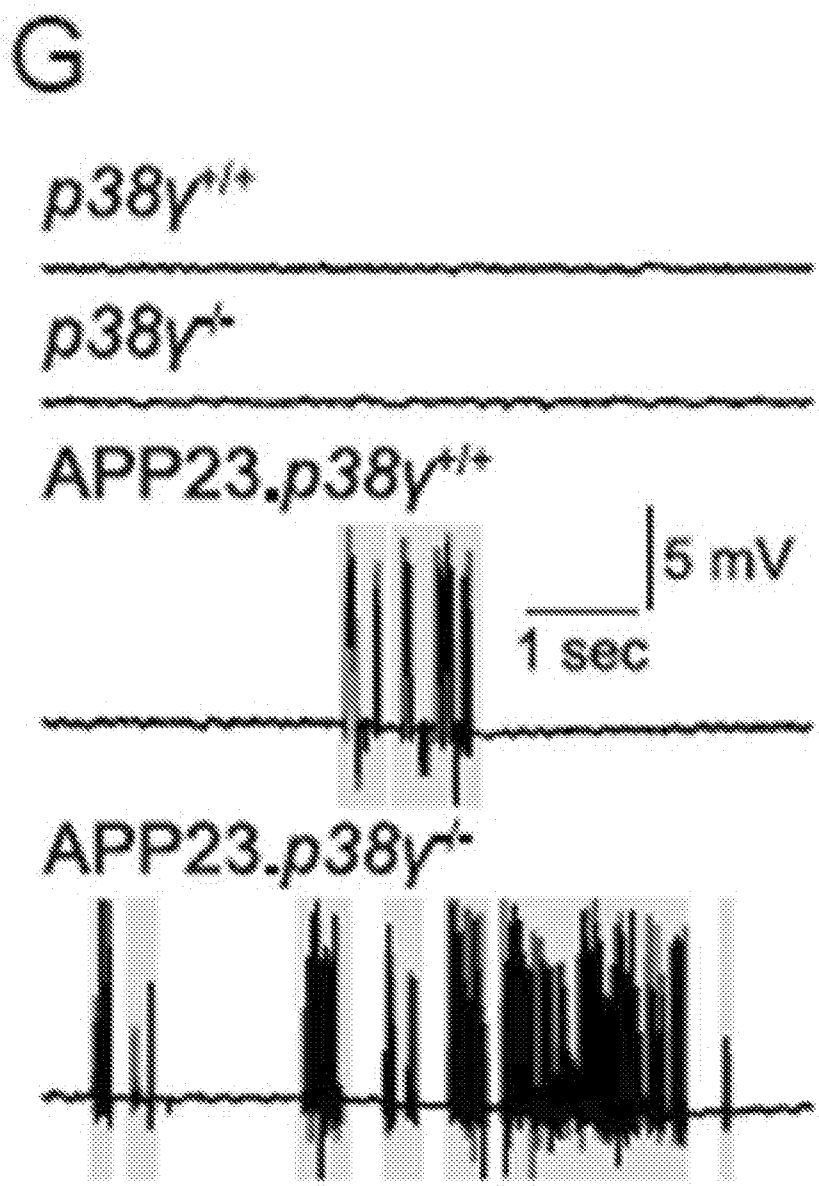

Figures 2H and 2I

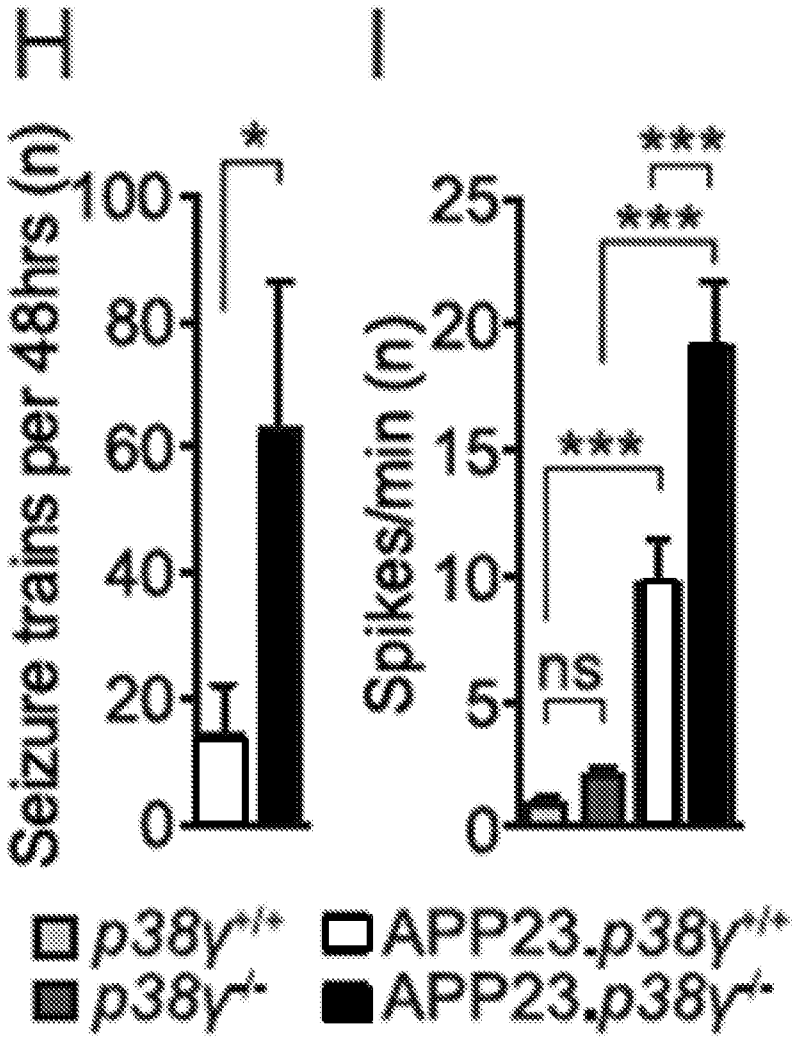

Figure 2J

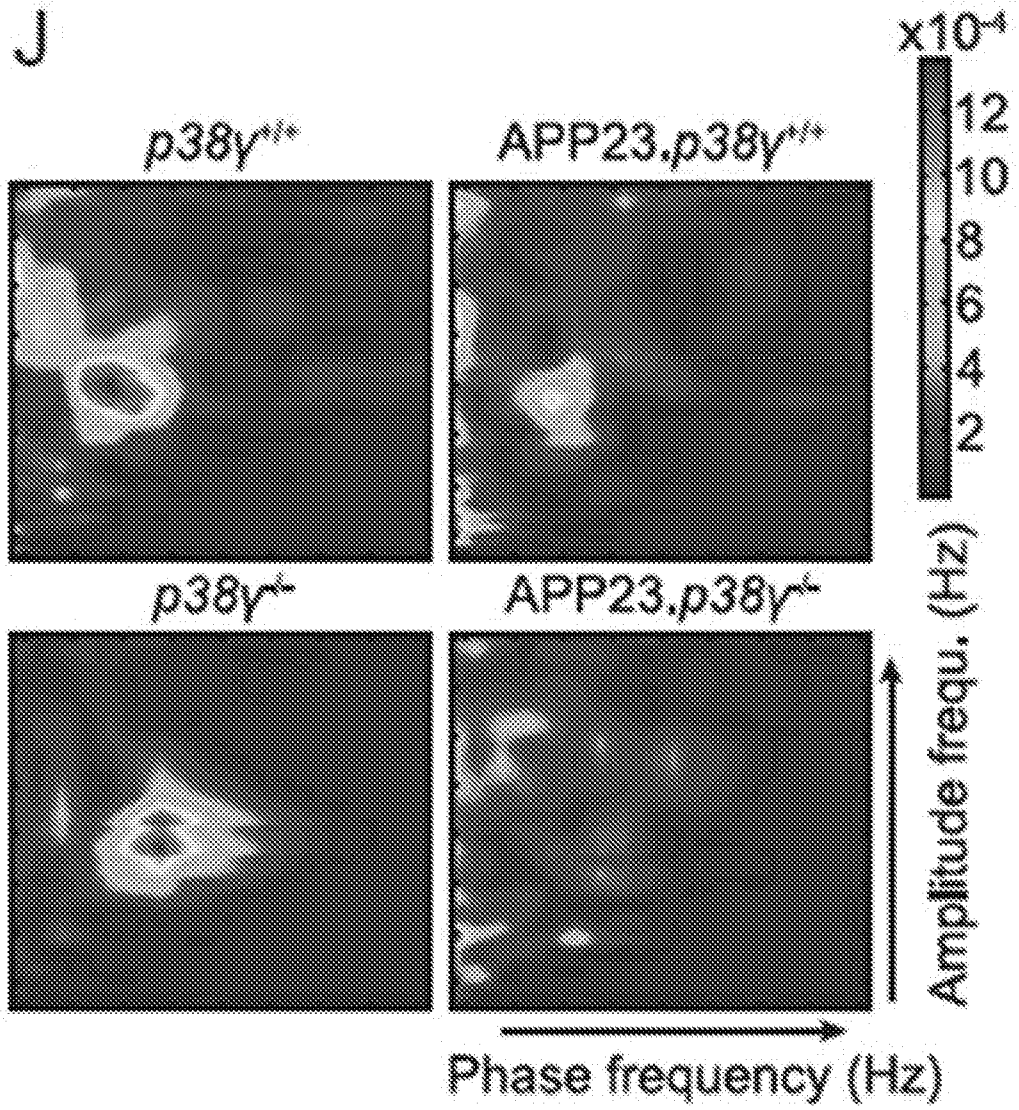
J
x10⁻⁴
12
10
8
6
4
2
p38γ+/+
APP23.p38γ+/+
p38γ-/-
APP23.p38γ-/-
Amplitude frequ. (Hz)
Phase frequency (Hz)

Figure 2K

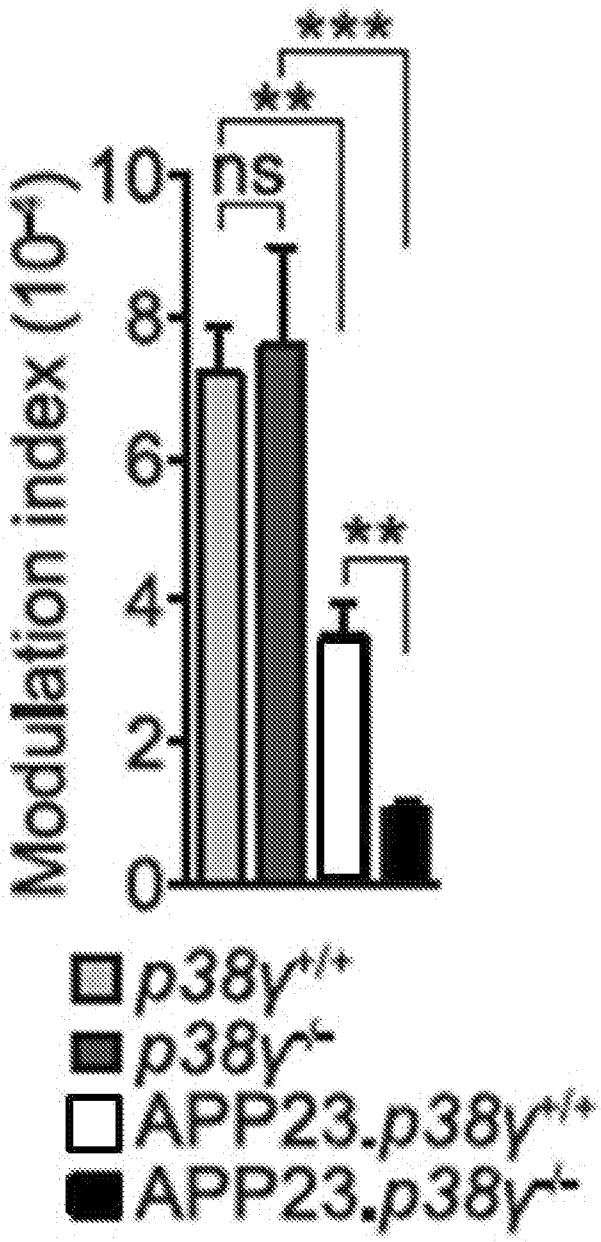
K
***
**
ns
**
Modulation index (10⁻¹)
10
8
6
4
2
0
p38γ+/+
p38γ-/-
APP23.p38γ+/+
APP23.p38γ-/-

Figure 3

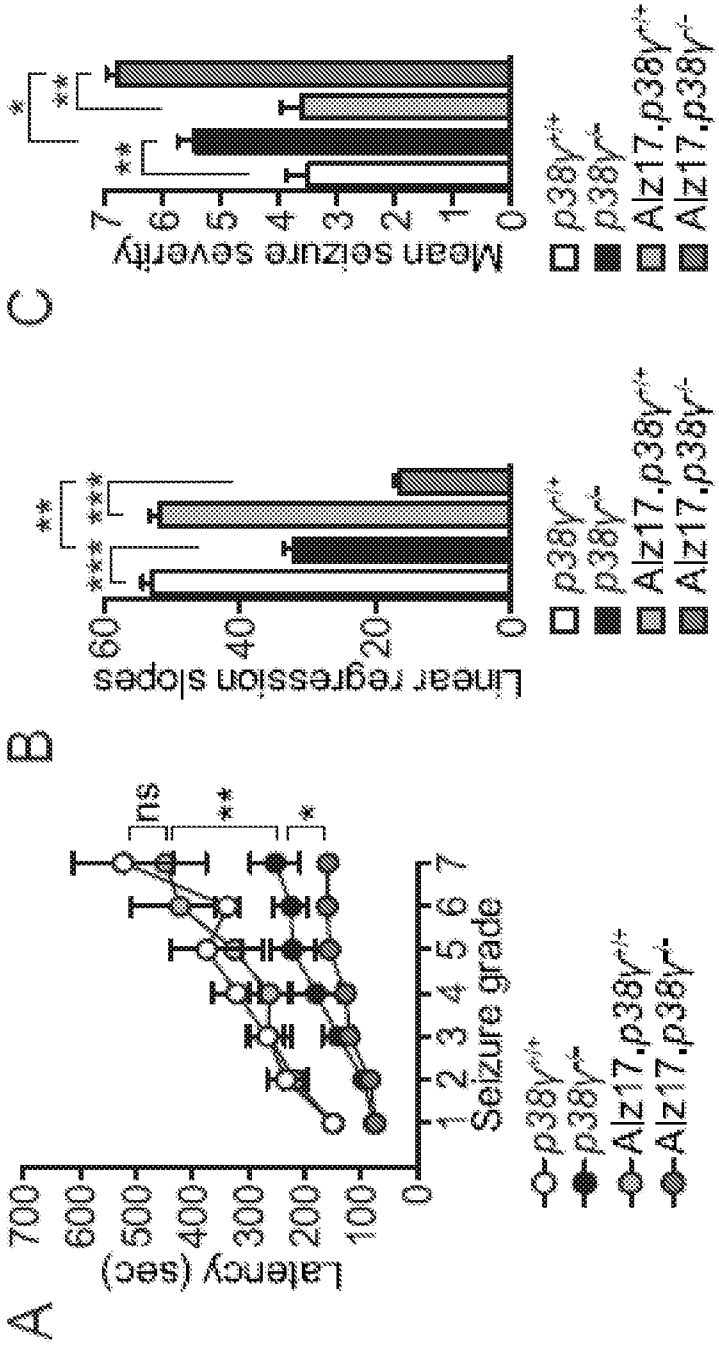
A
latency (sec)
700
600
500
400
300
200
100
0
1 2 3 4 5 6 7
Seizure grade
ns
**
*
p38γ+/+
p38γ-/-
Alz17.p38γ+/+
Alz17.p38γ-/-
B
Linear regression slopes
60
40
20
0
***
***
**
C
Mean seizure severity
7 6 5 4 3 2 1 0
**
**
*

Figure 3 cont.

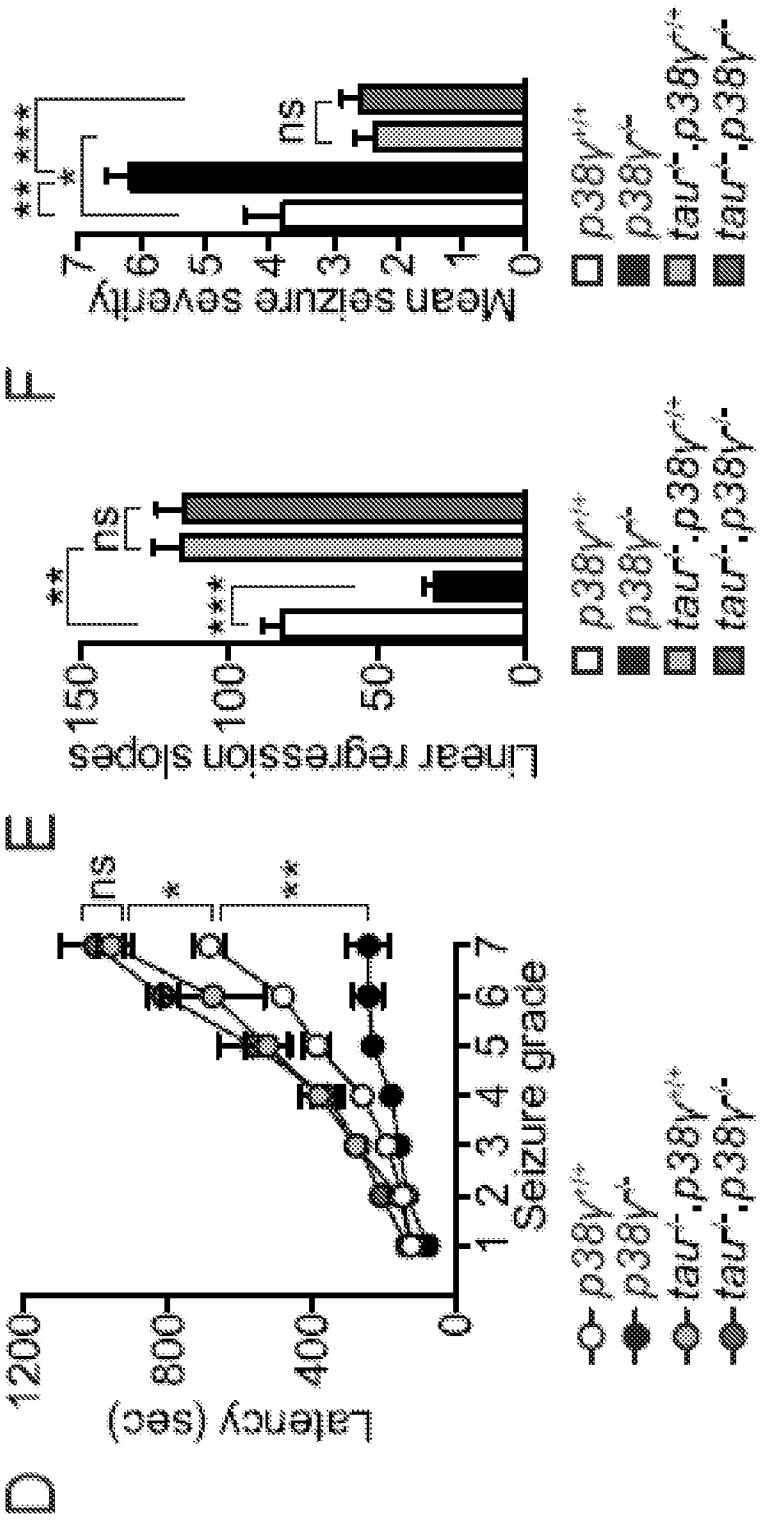

Figure 3 cont.

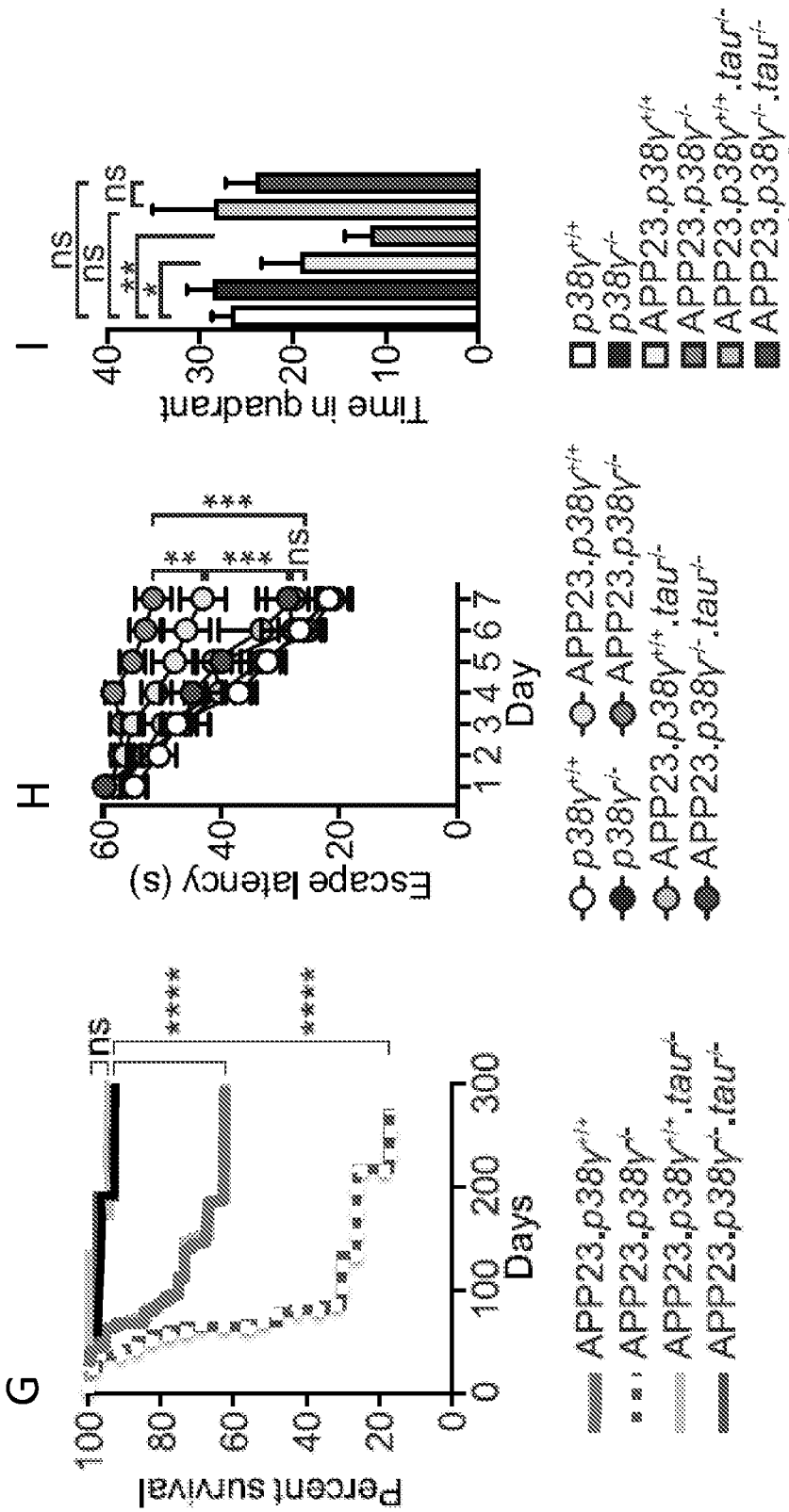

Figure 4

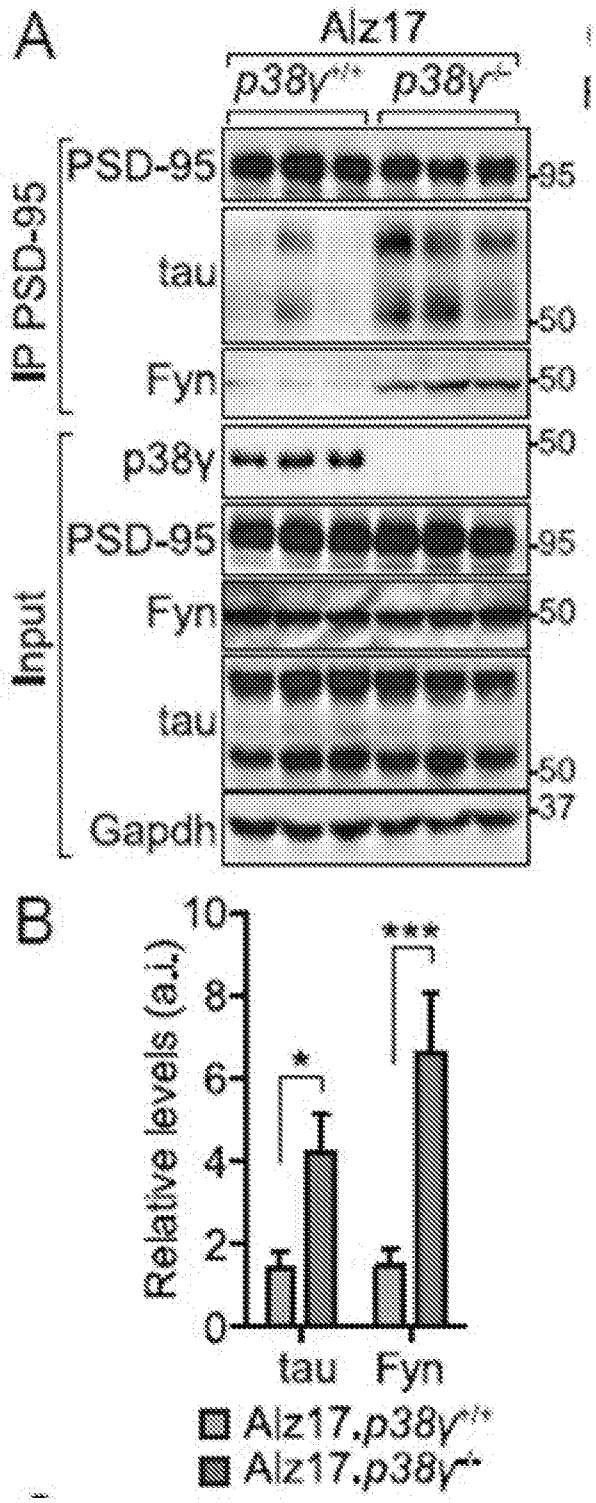
A
Alz17
p38γ+/+
p38γ-/-
IP PSD-95
PSD-95
tau
Fyn
Input
p38γ
PSD-95
Fyn
tau
Gapdh
95
50
50
50
95
50
50
37
B
Relative levels (a.u.)
10
8
6
4
2
0
*
***
tau
Fyn
Alz17.p38γ+/+
Alz17.p38γ-/-

Figure 4 cont.

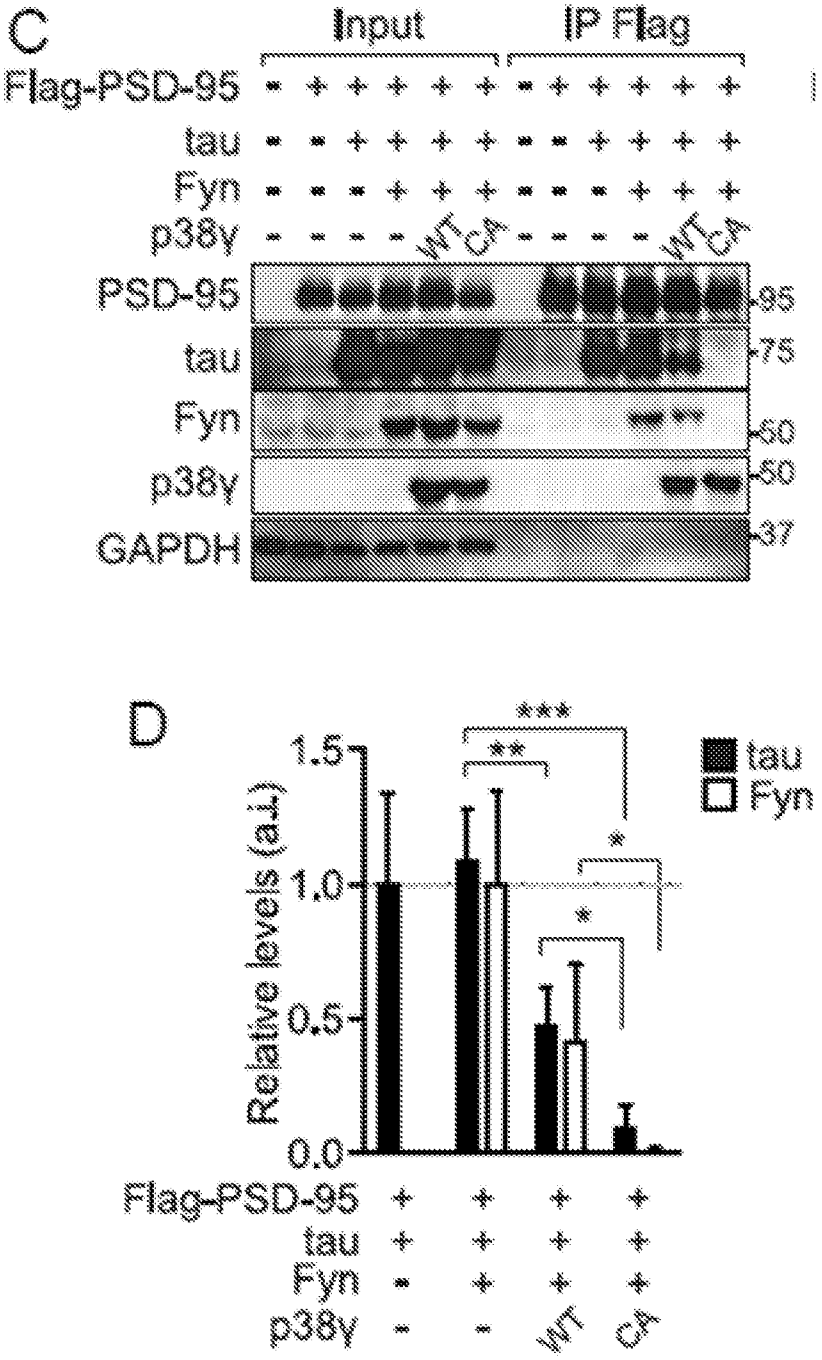

Figure 4 cont.

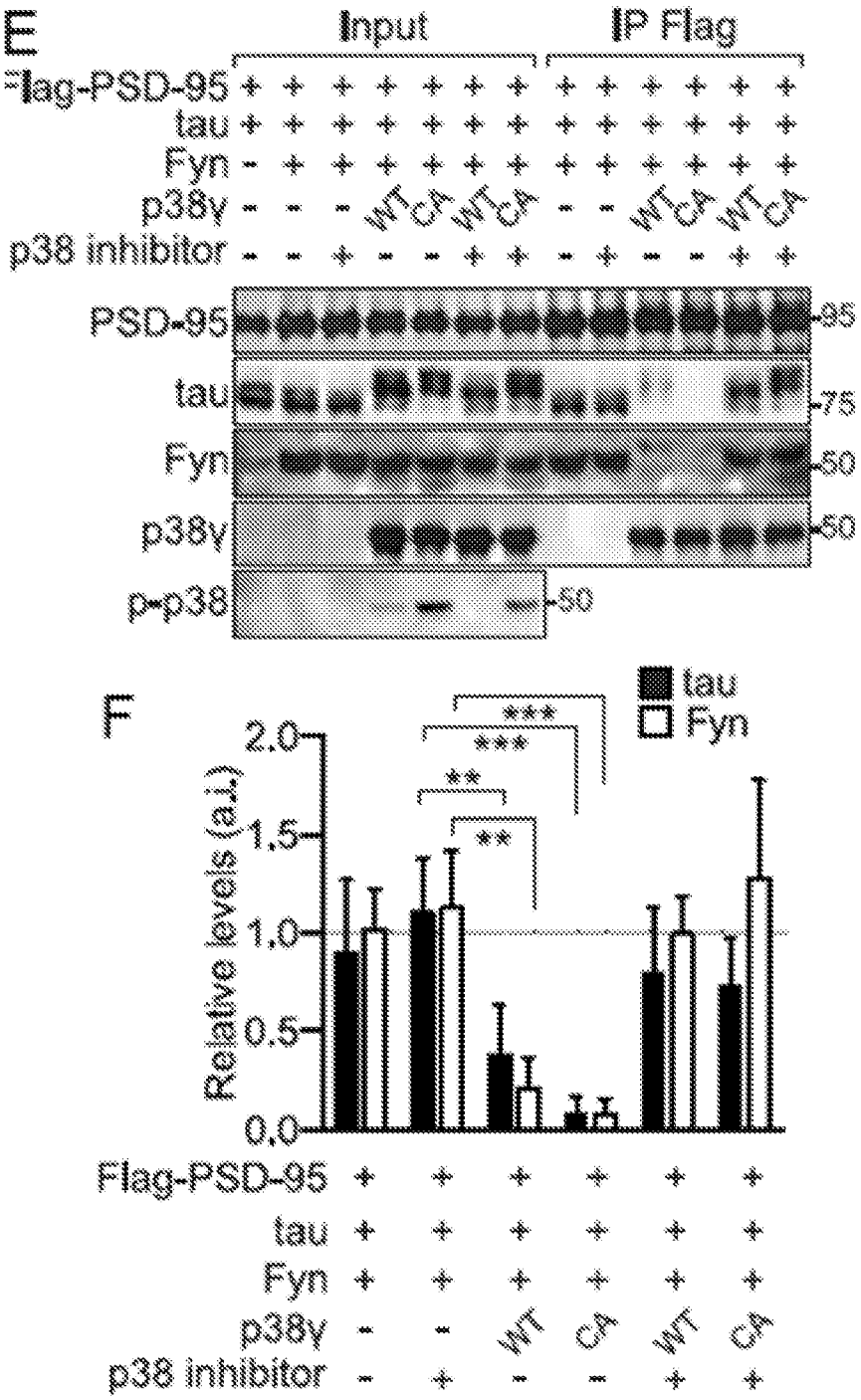

Figure 4 cont.

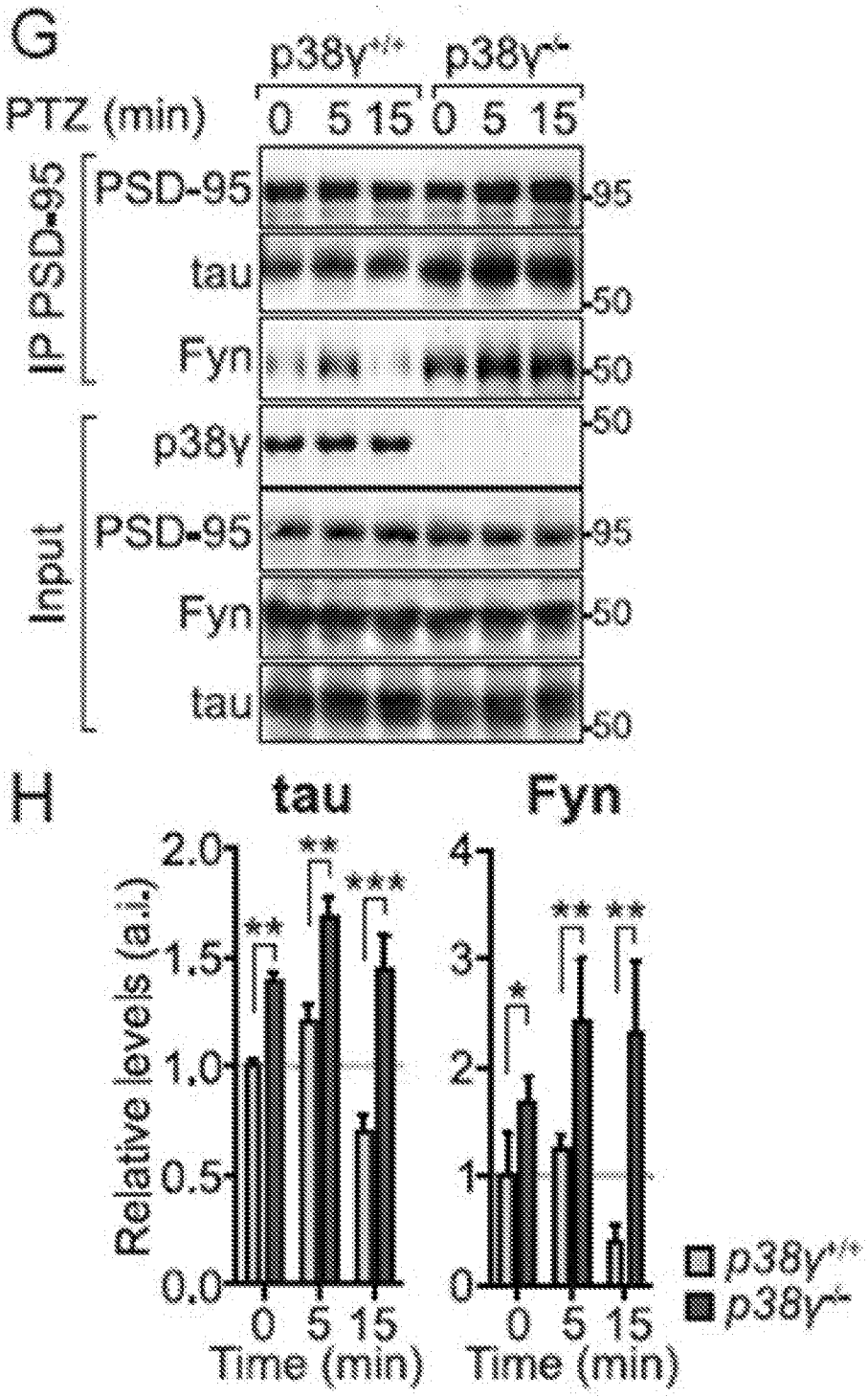

Figure 4 cont.

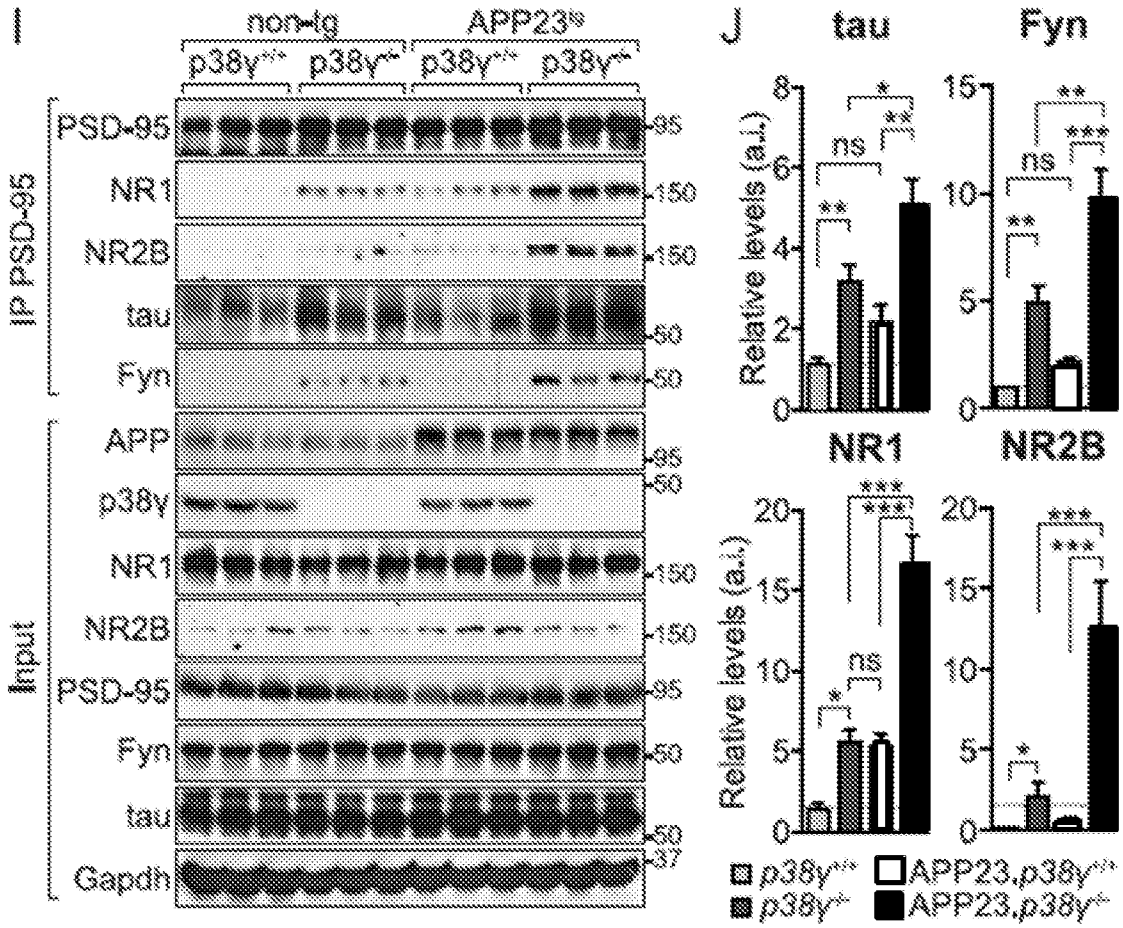

Figure 5

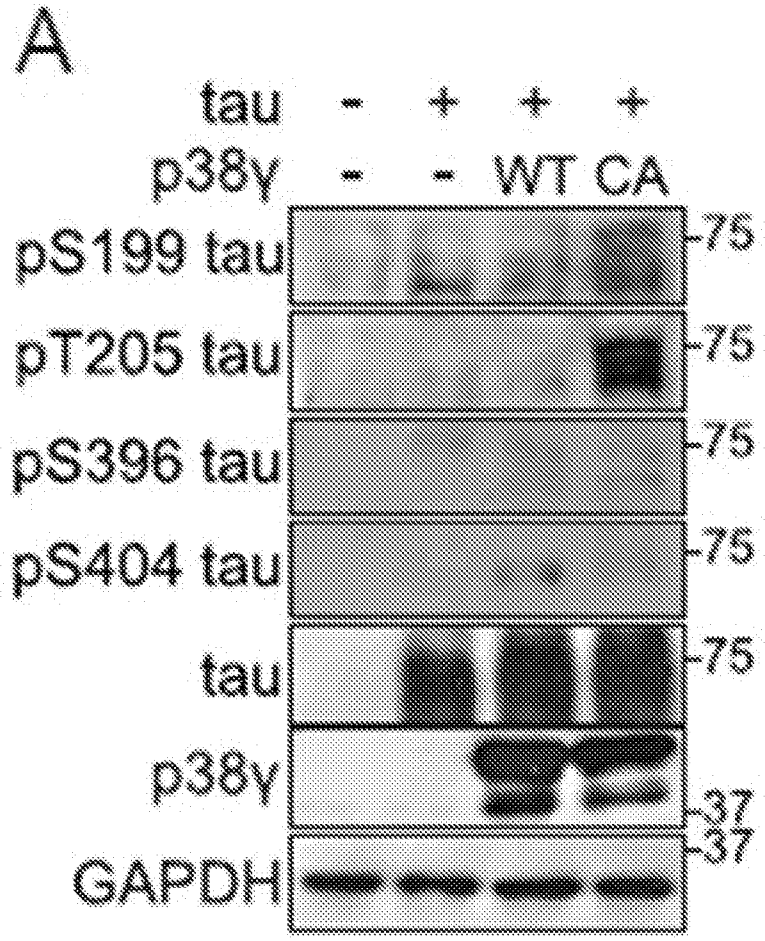
A
tau - + + +
p38γ - - WT CA
pS199 tau
pT205 tau
pS396 tau
pS404 tau
tau
p38γ
GAPDH
75
75
75
75
75
37
37

Figure 5 cont.

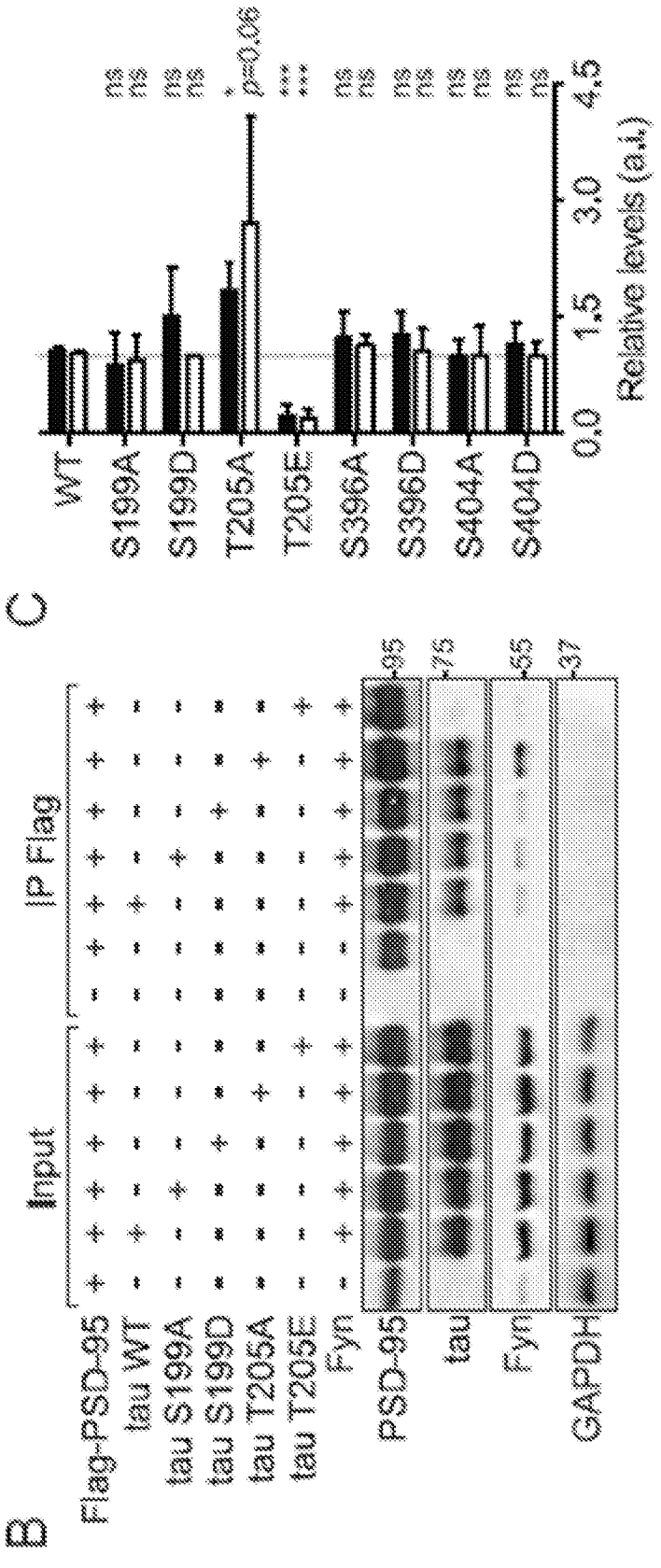

Figure 5 cont.

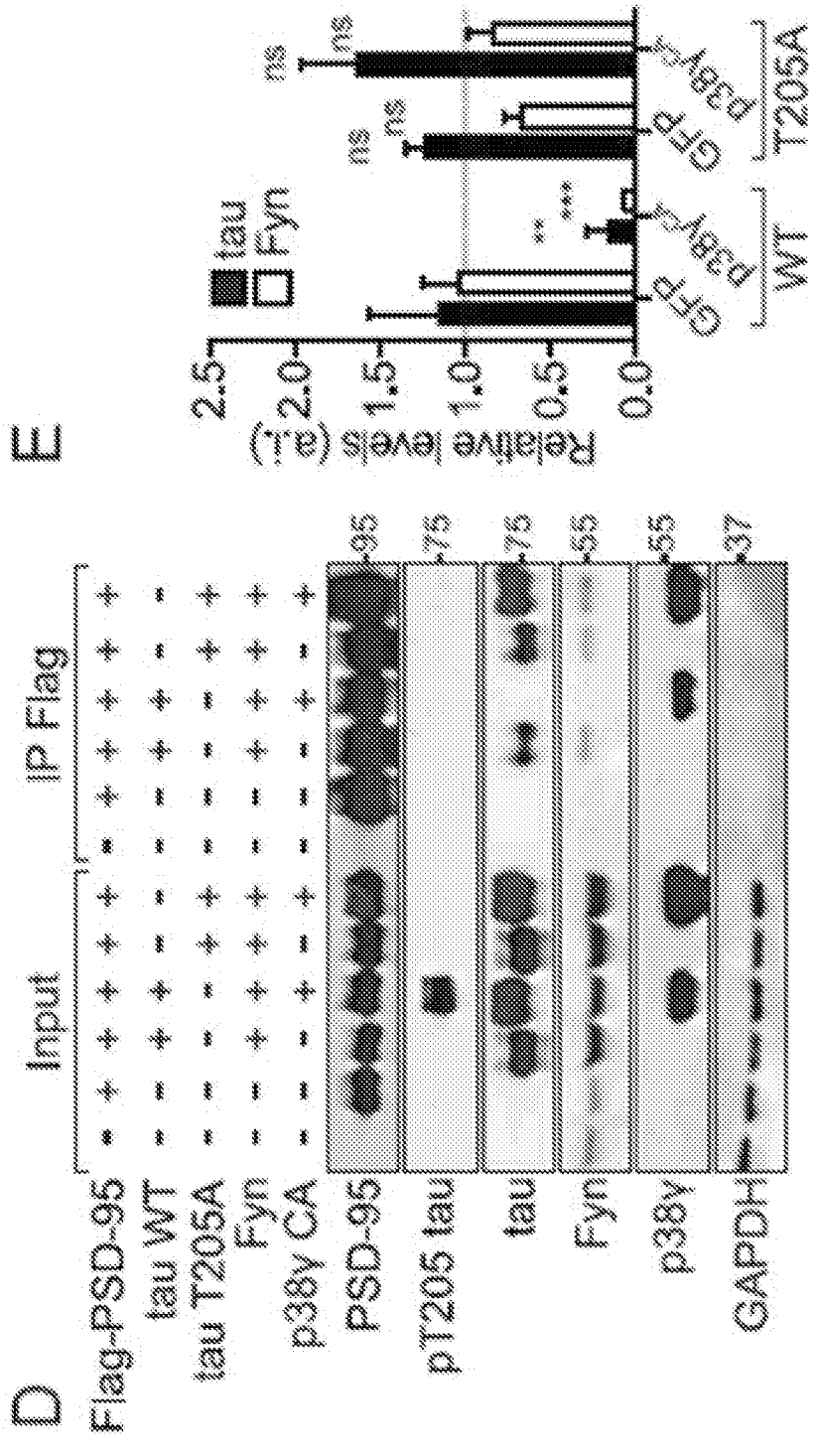

Figure 5 cont.

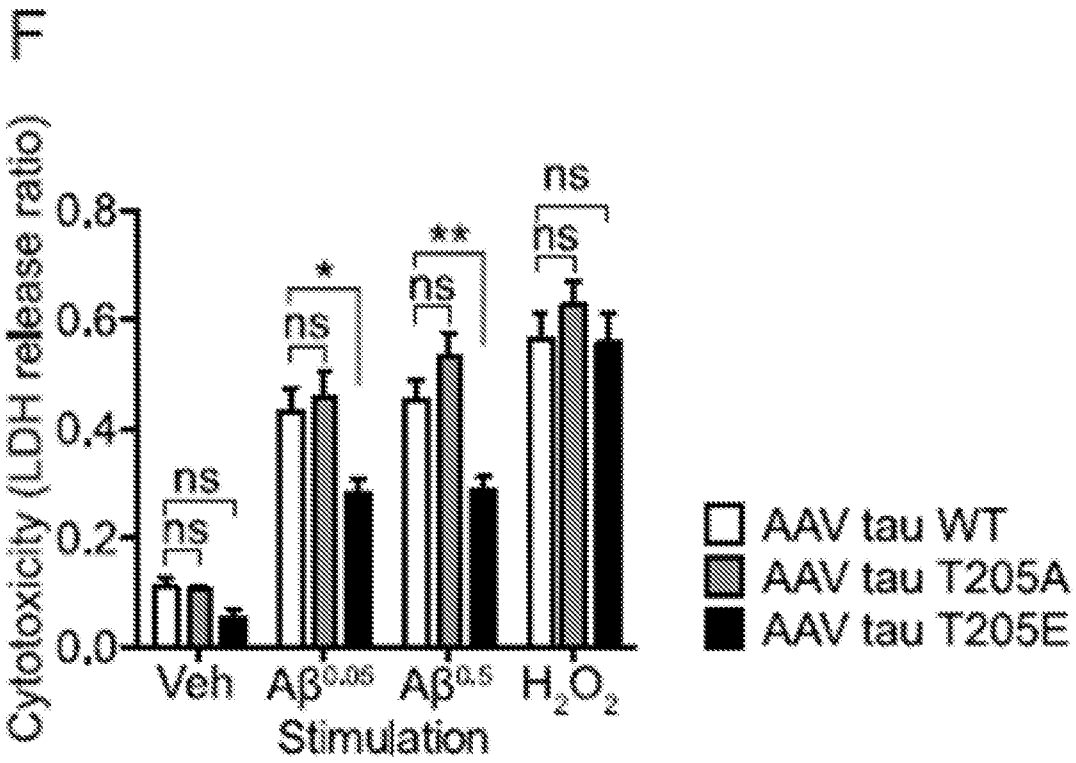

Figure 5 cont.

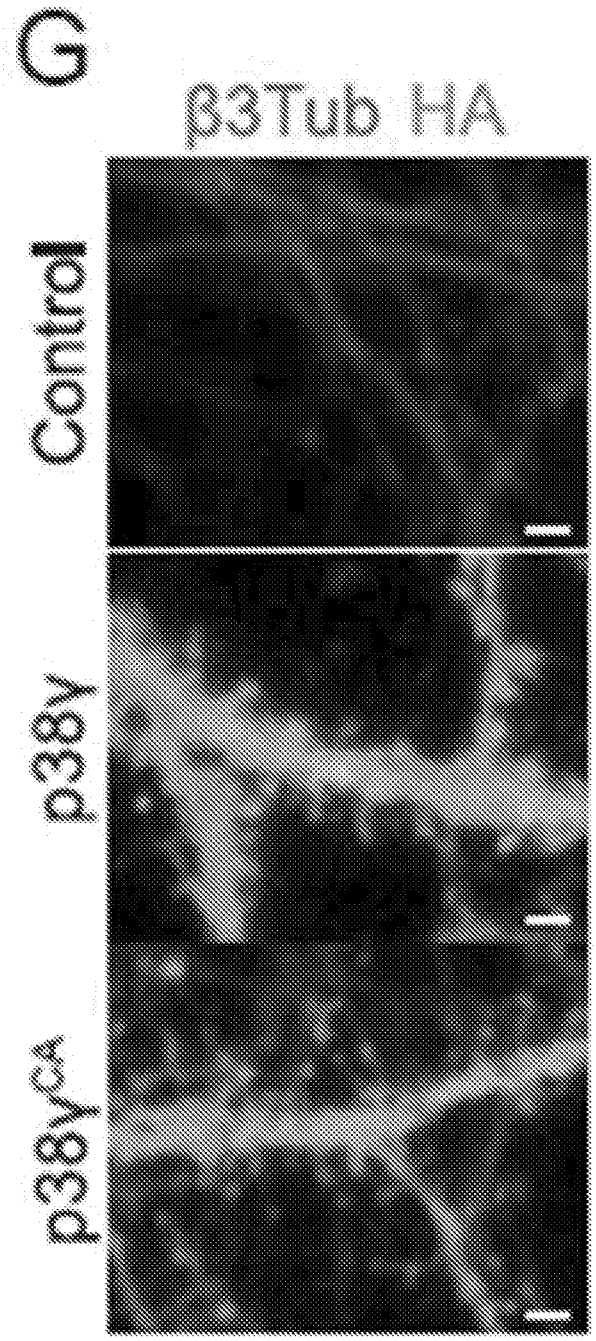

Figure 5 cont.

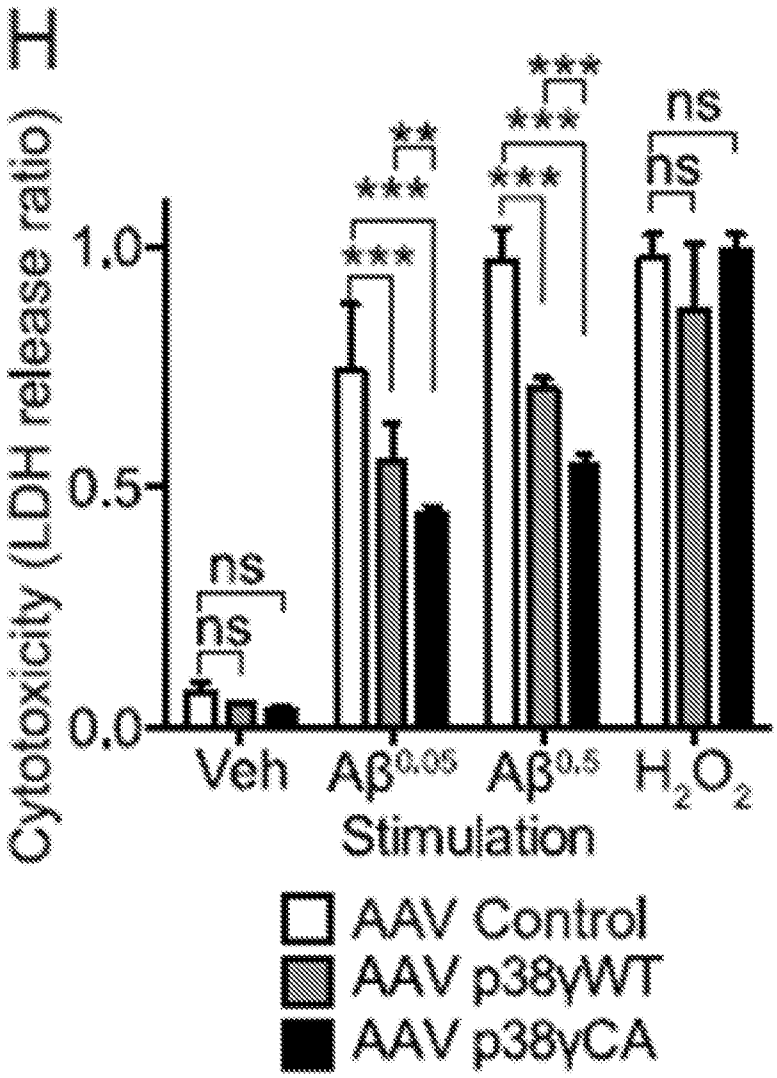

Figure 5 cont.

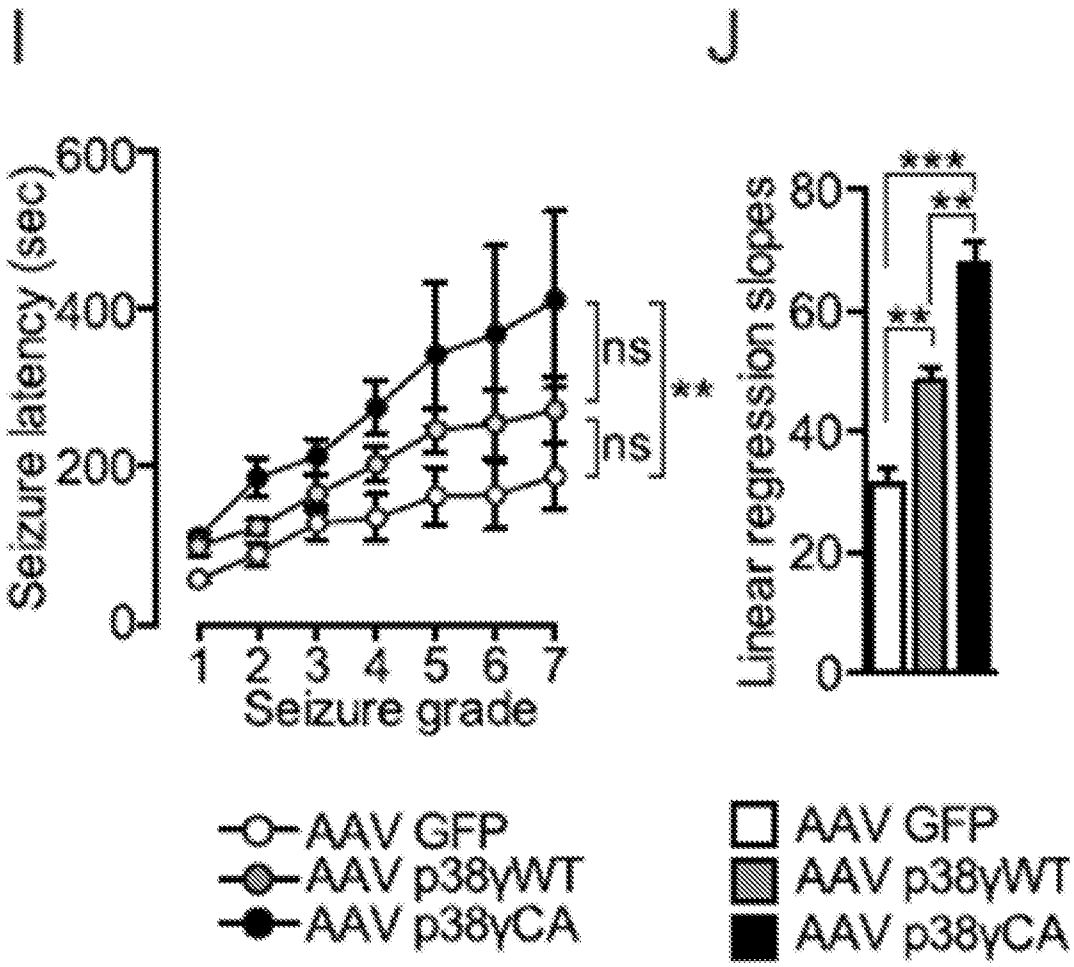

Figure 5 cont.

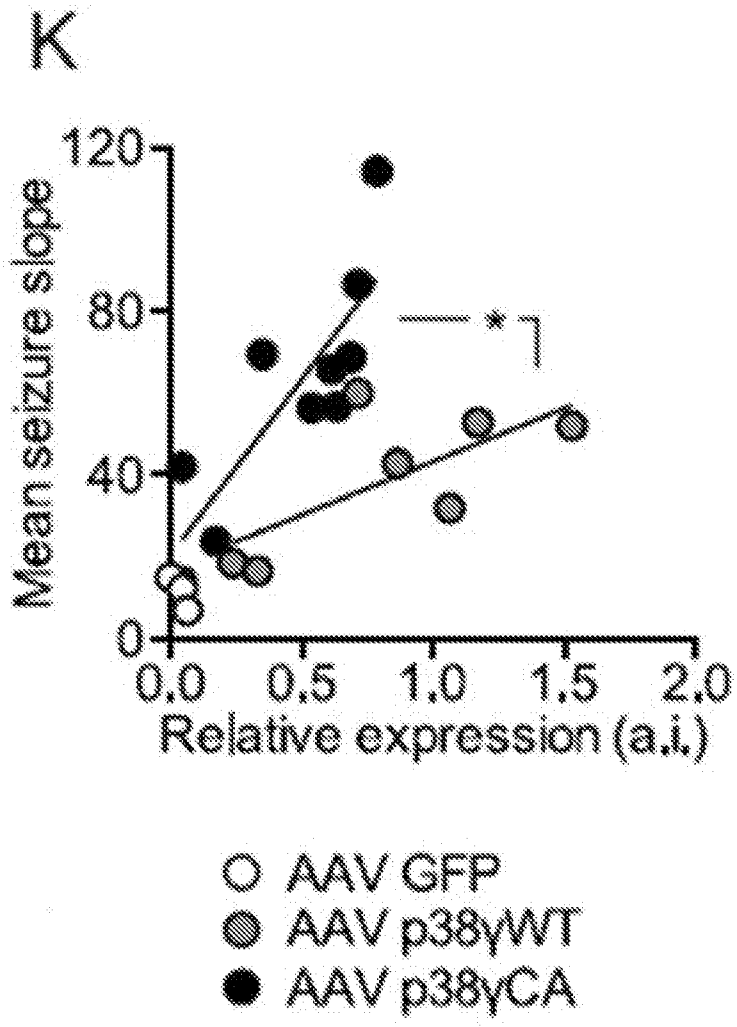

Figure 6

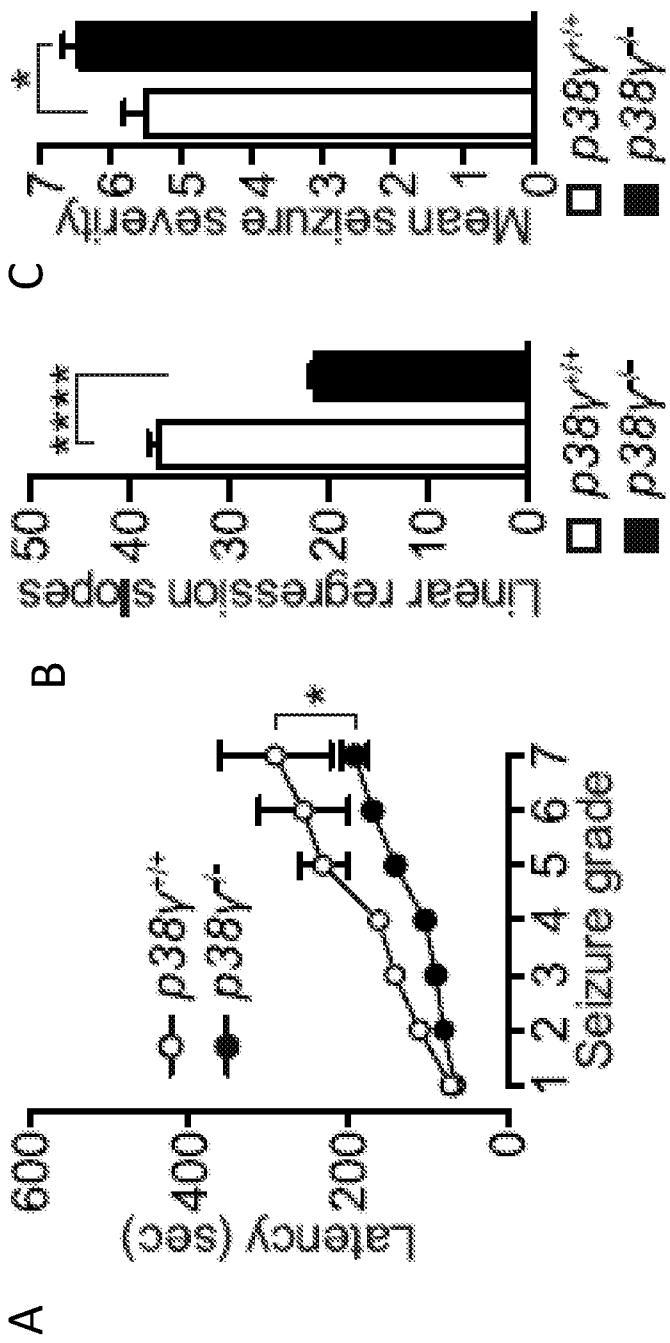
A
Latency (sec)
600
400
200
0
p38γ+/+
p38γ-/-
*
1 2 3 4 5 6 7
Seizure grade
B
Linear regression slopes
50
40
30
20
10
0
****
p38γ+/+
p38γ-/-
C
Mean seizure severity
7
6
5
4
3
2
1
0
*
p38γ+/+
p38γ-/-

Figure 7

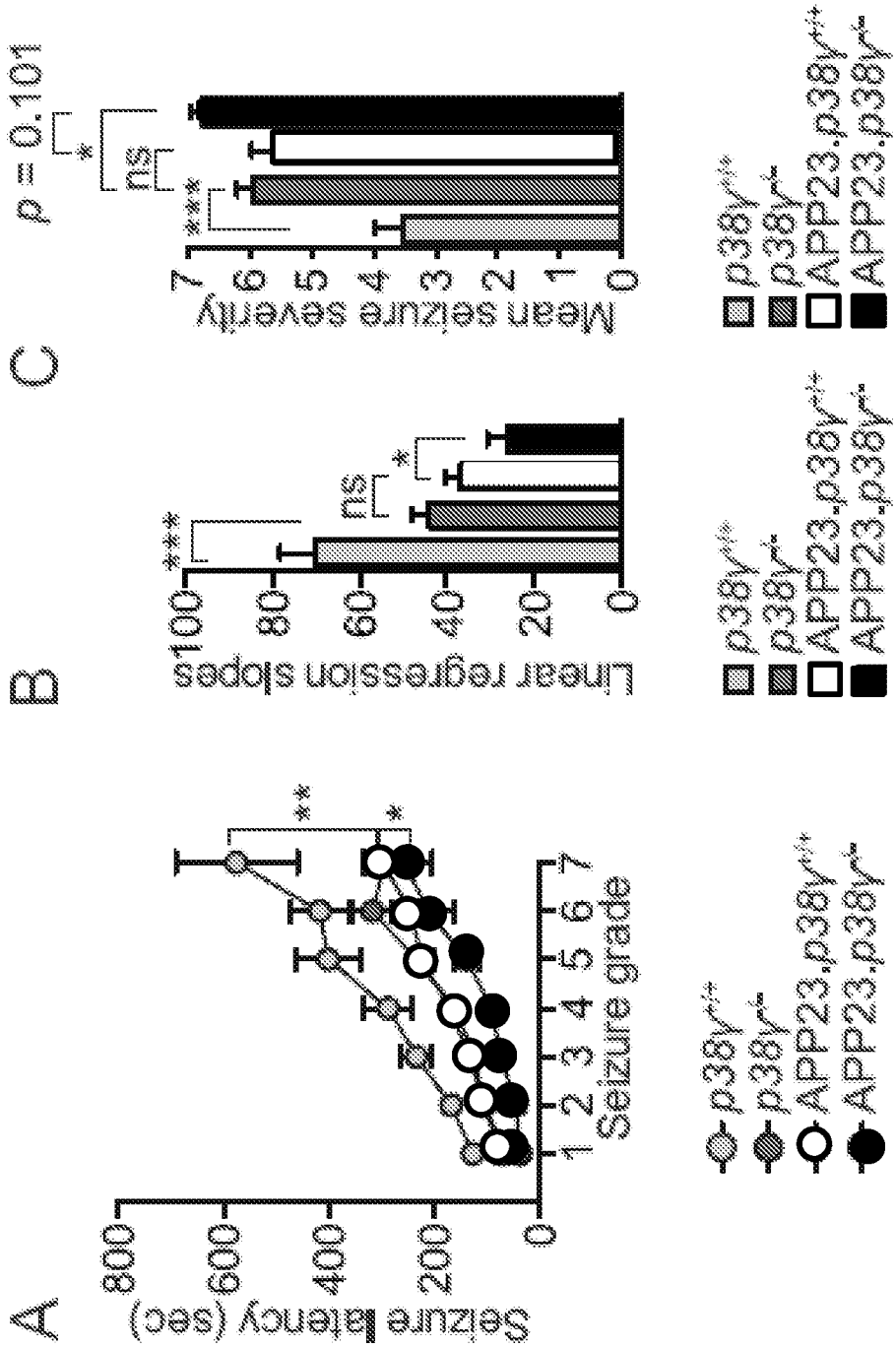
A
Seizure latency (sec)
800
600
400
200
0
1 2 3 4 5 6 7
Seizure grade
**
*
p38γ+/+
p38γ-/-
APP23.p38γ+/+
APP23.p38γ-/-
B
Linear regression slopes
100
80
60
40
20
0
***
ns
*
p38γ+/+
p38γ-/-
APP23.p38γ+/+
APP23.p38γ-/-
C
p = 0.101
Mean seizure severity
7 6 5 4 3 2 1 0
***
ns
*
p38γ+/+
p38γ-/-
APP23.p38γ+/+
APP23.p38γ-/-

Figure 8

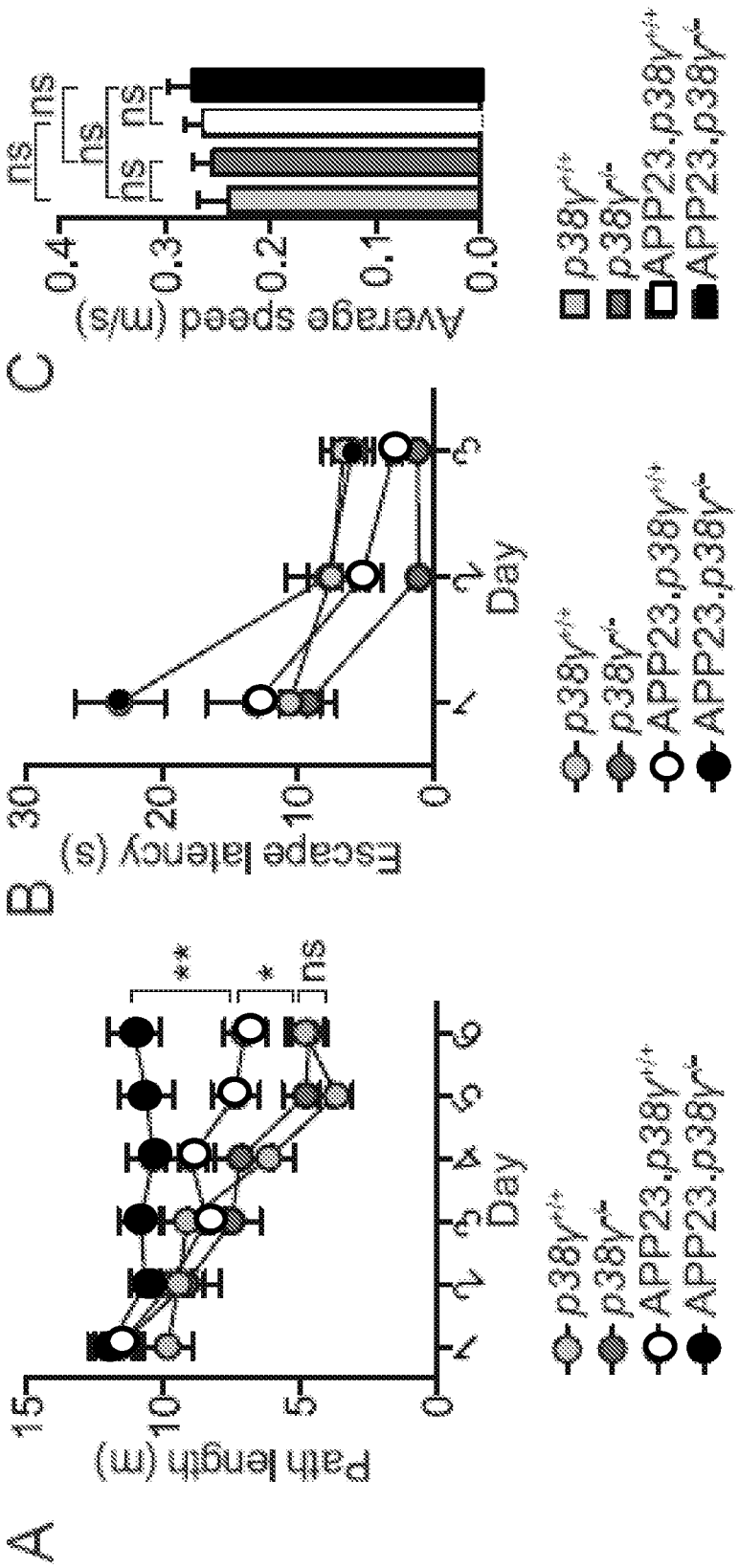
A
Path length (m)
15
10
5
0
1
2
3
4
5
6
Day
**
*
ns
p38γ+/+
p38γ-/-
APP23.p38γ+/+
APP23.p38γ-/-
B
Escape latency (s)
30
20
10
0
1
2
3
Day
p38γ+/+
p38γ-/-
APP23.p38γ+/+
APP23.p38γ-/-
C
Average speed (m/s)
0.4
0.3
0.2
0.1
0.0
ns
ns
ns
ns
ns
p38γ+/+
p38γ-/-
APP23.p38γ+/+
APP23.p38γ-/-

Figure 9

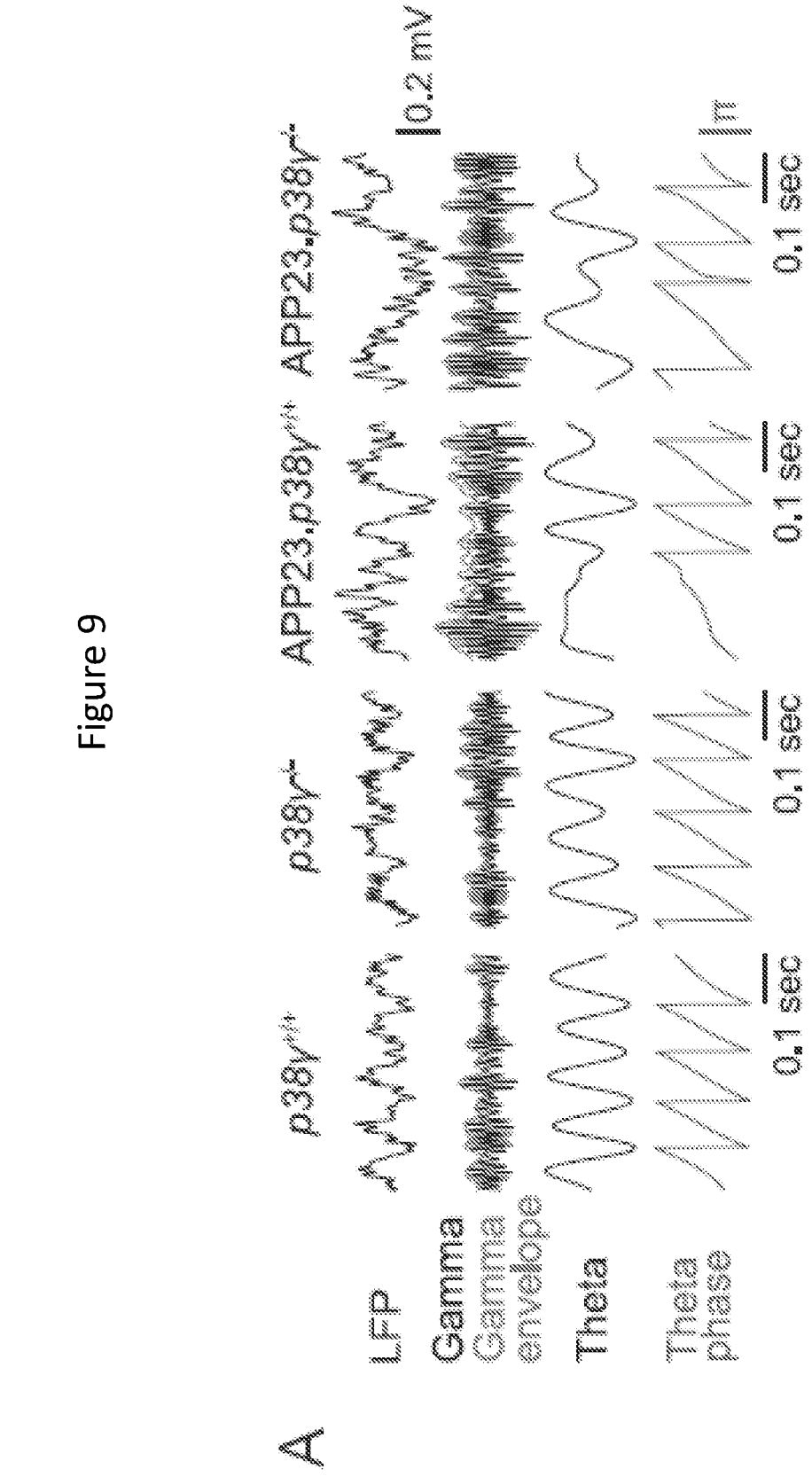
A
LFP
Gamma
Gamma envelope
Theta
Theta phase
p38γ+/+
p38γ-/-
APP23.p38γ+/+
APP23.p38γ-/-
0.2 mV
0.1 sec
0.1 sec
0.1 sec
π

Figure 9 cont.

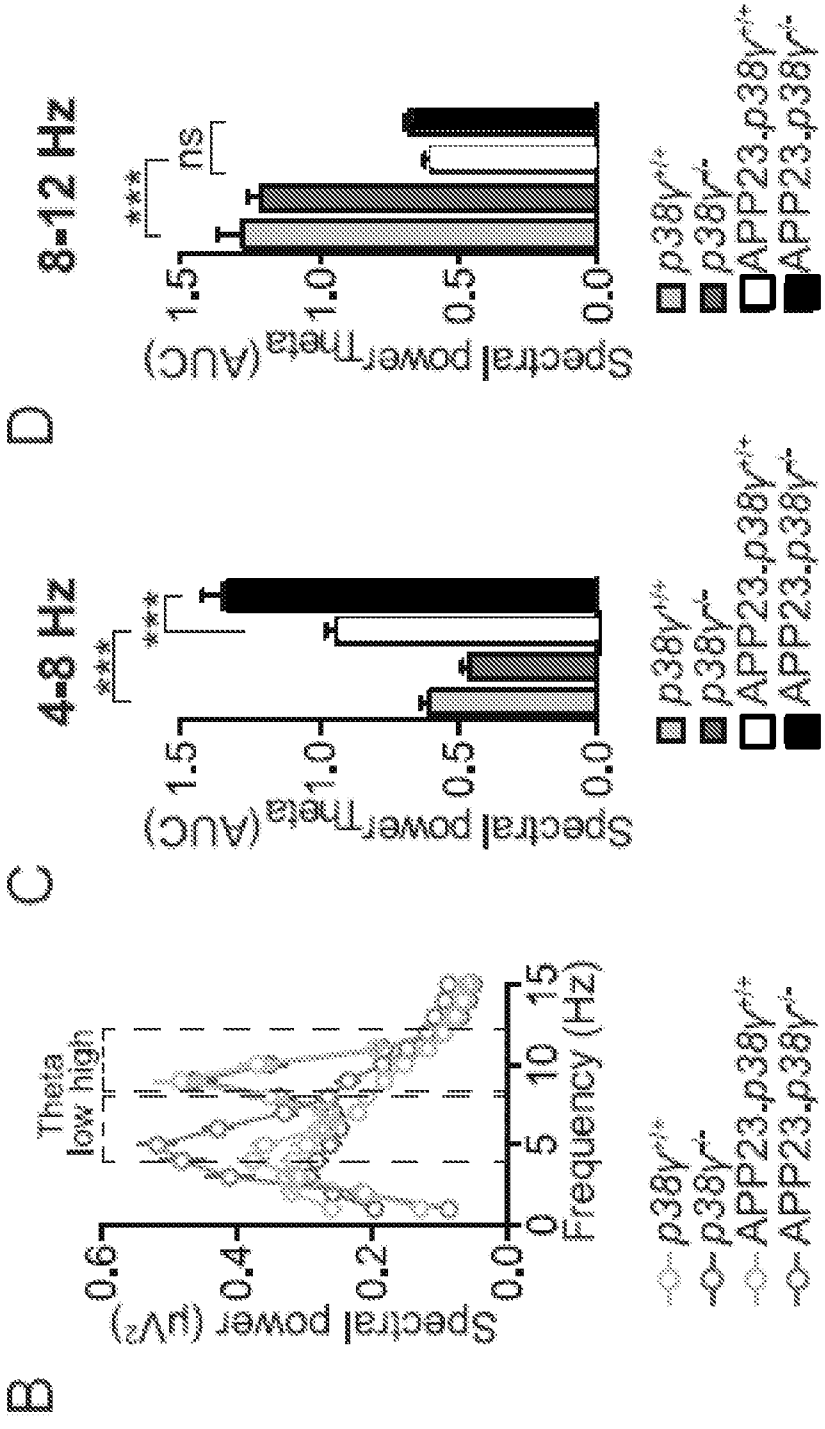

Figure 9 cont.

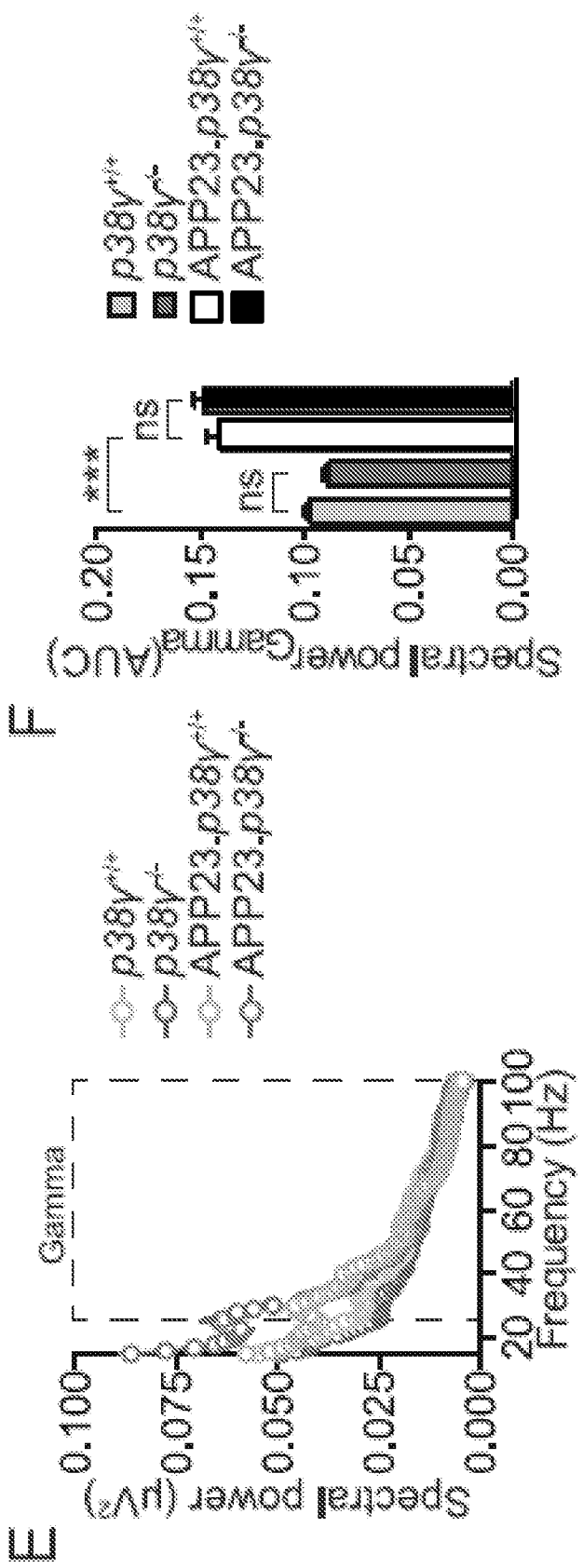

Figure 9 cont.

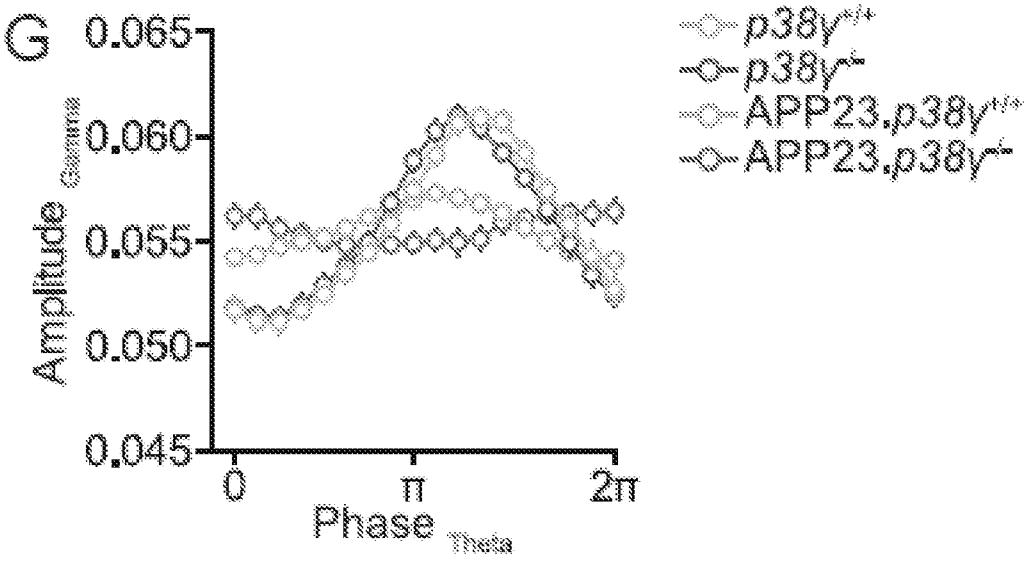

Figure 10

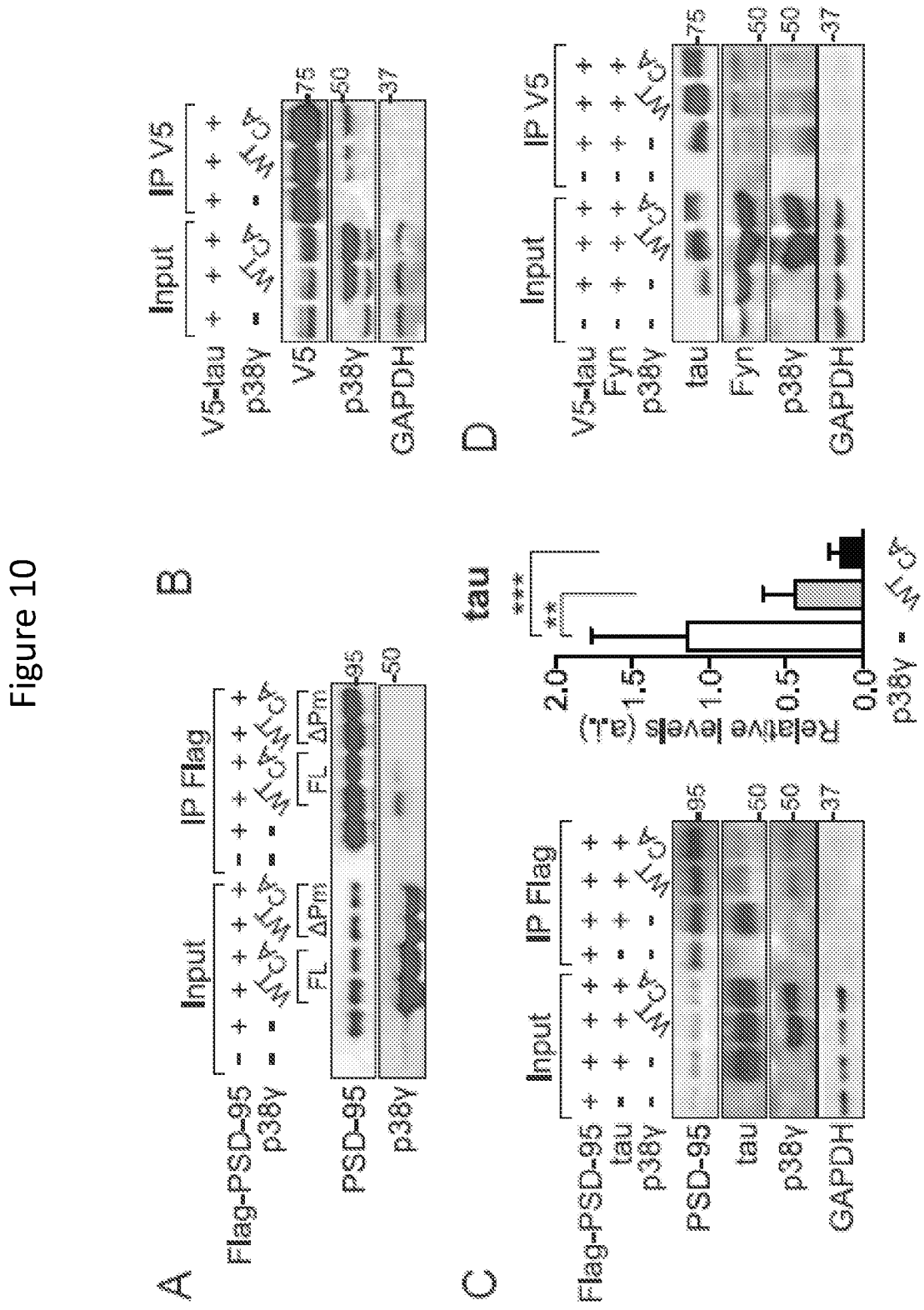
A
Input
IP Flag
Flag-PSD-95
p38γ
FL
ΔPm
PSD-95
p38γ
B
Input
IP V5
V5-tau
p38γ
V5
p38γ
GAPDH
C
tau
Input
IP Flag
Flag-PSD-95
tau
p38γ
PSD-95
tau
p38γ
GAPDH
Relative levels (a.u.)
p38γ
D
Input
IP V5
V5-tau
Fyn
p38γ
tau
Fyn
p38γ
GAPDH

Figure 11

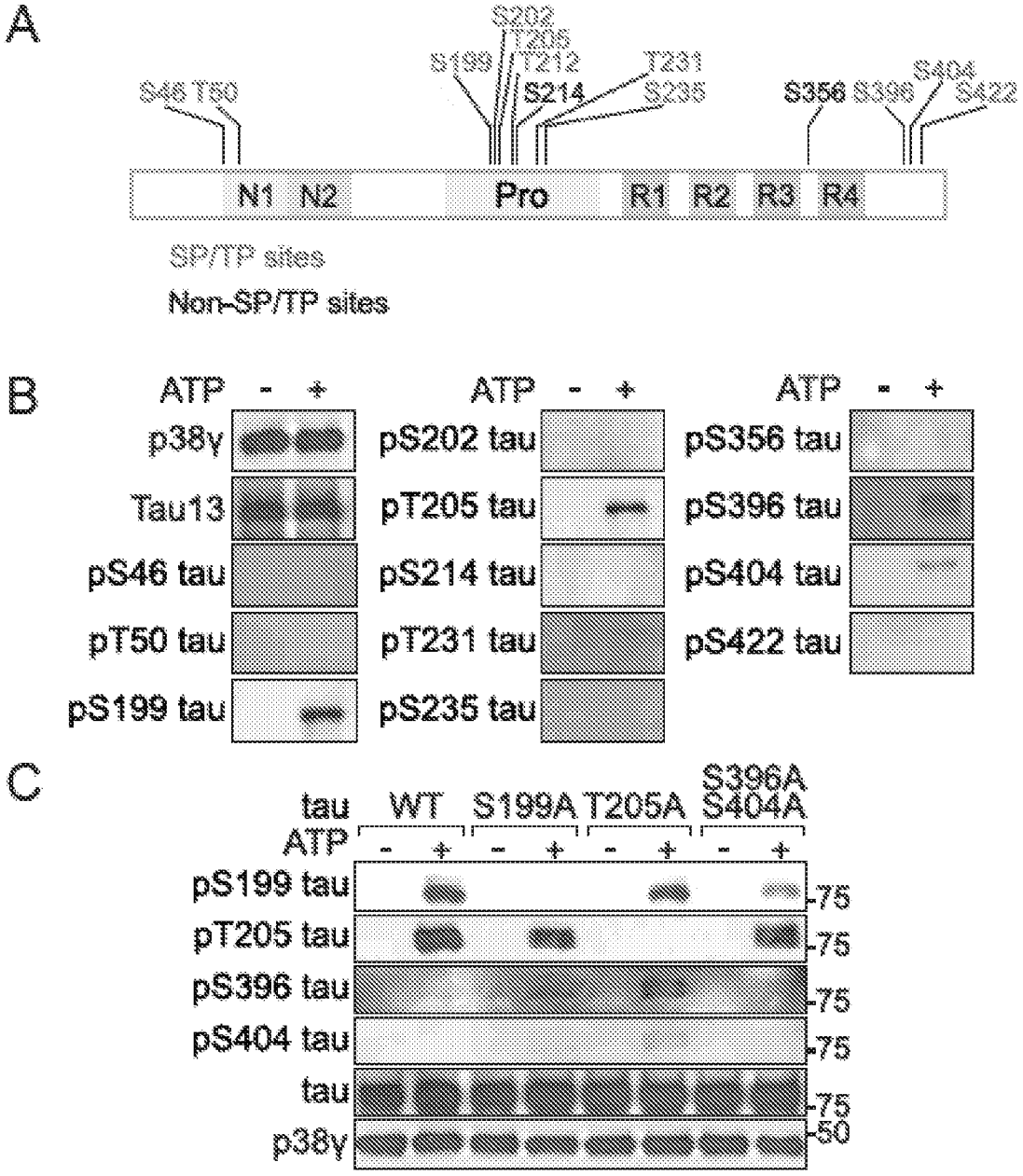
A
S202
T205
S199
T212
T231
S214
S235
S46 T50
S356 S396
S404
S422
N1 N2
Pro
R1 R2 R3 R4
SP/TP sites
Non-SP/TP sites
B
ATP - +
p38γ
Tau13
pS46 tau
pT50 tau
pS199 tau
pS202 tau
pT205 tau
pS214 tau
pT231 tau
pS235 tau
pS356 tau
pS396 tau
pS404 tau
pS422 tau
C
tau WT S199A T205A S396A S404A
ATP - + - + - + - +
pS199 tau
pT205 tau
pS396 tau
pS404 tau
tau
p38γ
75
75
75
75
75
50

Figure 12

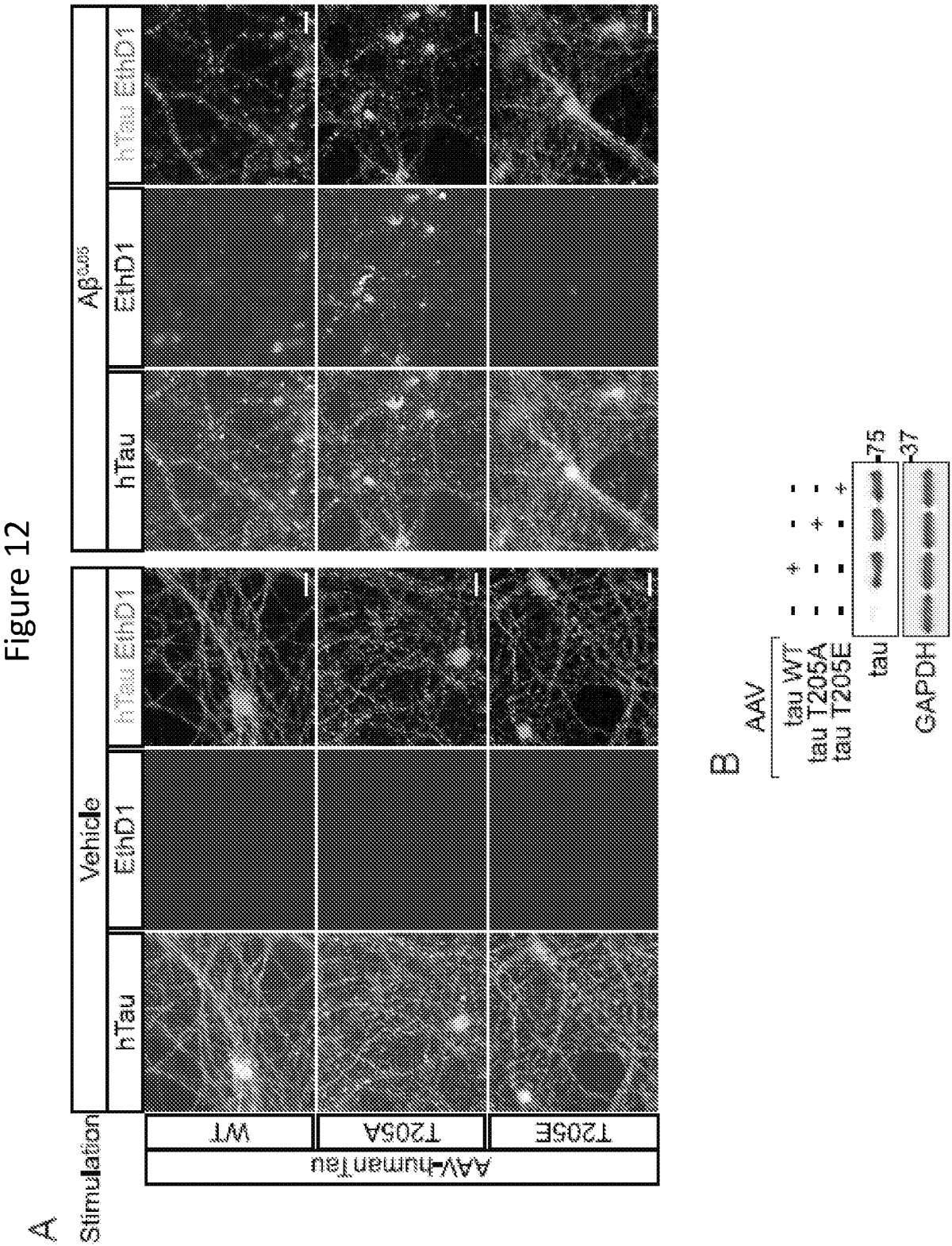
A
Stimulation
Vehicle
Aβ1-42
AAV-humanTau
hTau
EthD1
hTau EthD1
WT
T205A
T205E
B
AAV
tau WT
tau T205A
tau T205E
tau
GAPDH
75
37

Figure 13

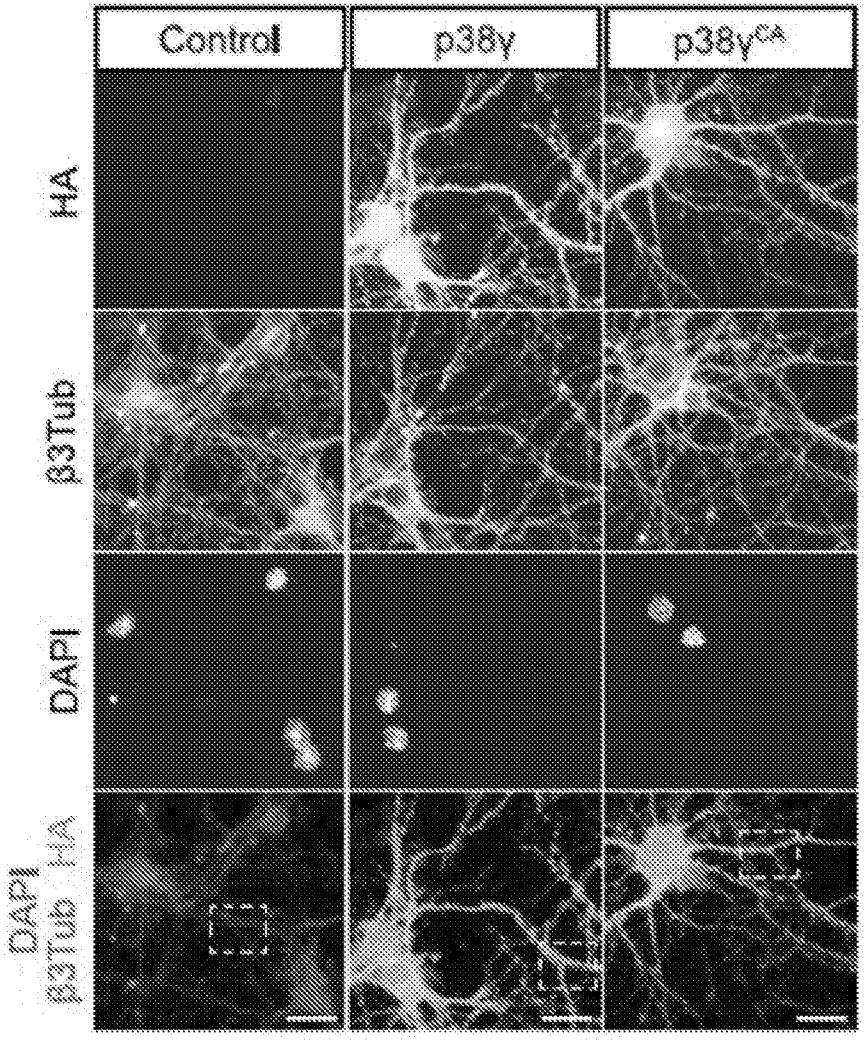

Figure 14

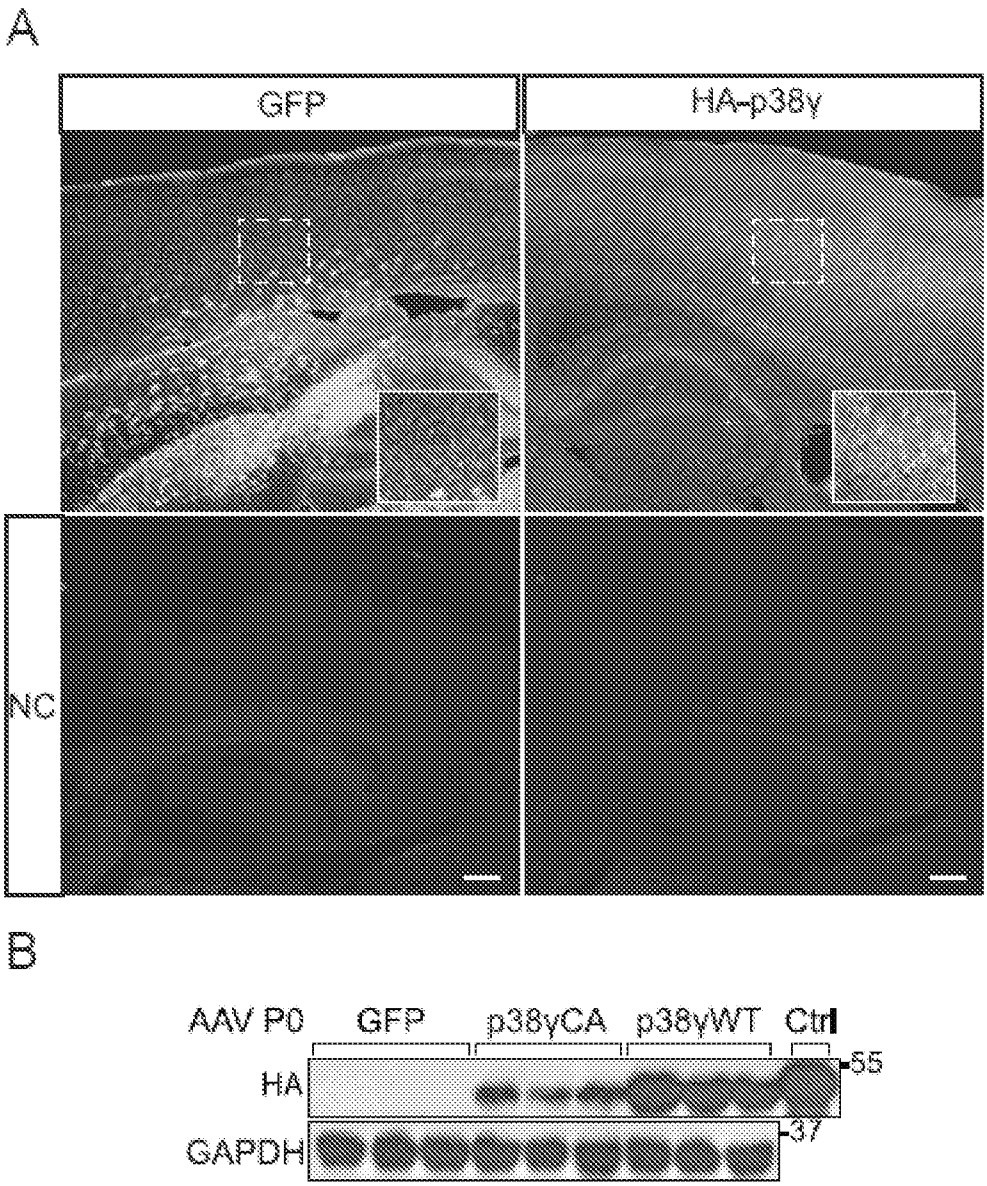

Figure 15

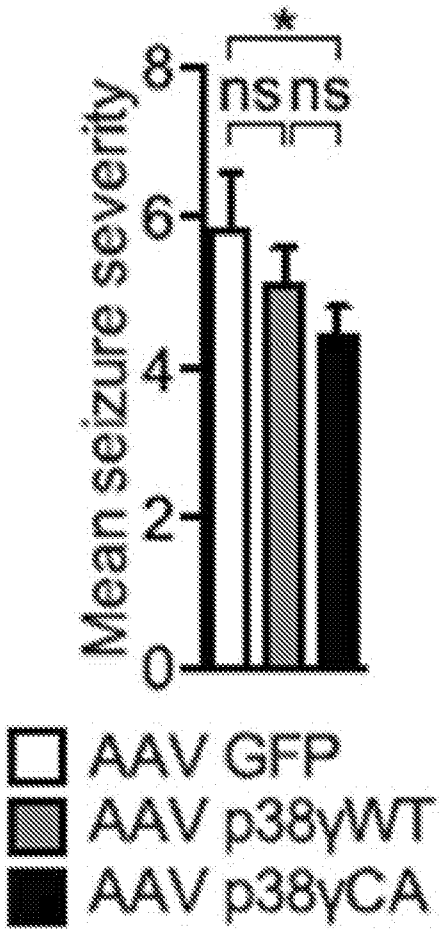
*
ns ns
Mean seizure severity
8
6
4
2
0
AAV GFP
AAV p38γWT
AAV p38γCA

Figure 16

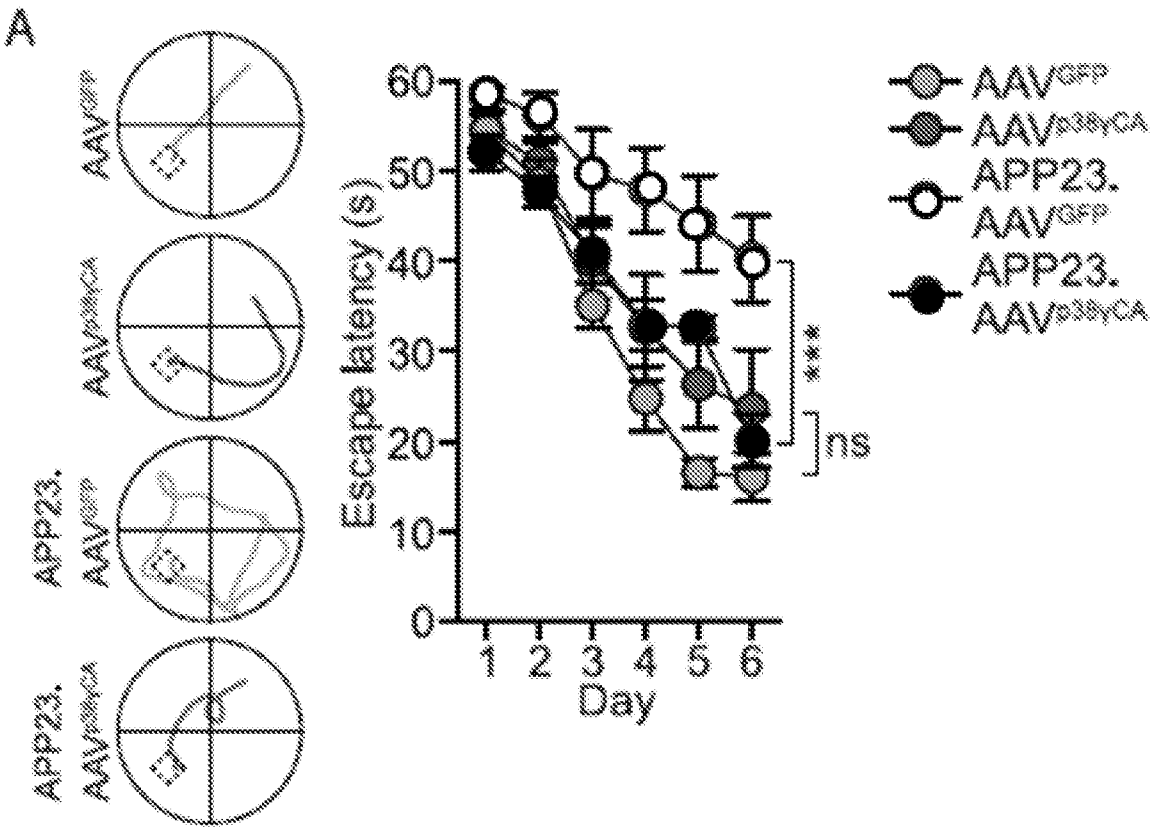
A
AAVGFP
AAVp38γCA
APP23. AAVGFP
APP23. AAVp38γCA
Escape latency (s)
60
50
40
30
20
10
0
1 2 3 4 5 6
Day
***
ns
AAVGFP
AAVp38γCA
APP23. AAVGFP
APP23. AAVp38γCA

Figure 17

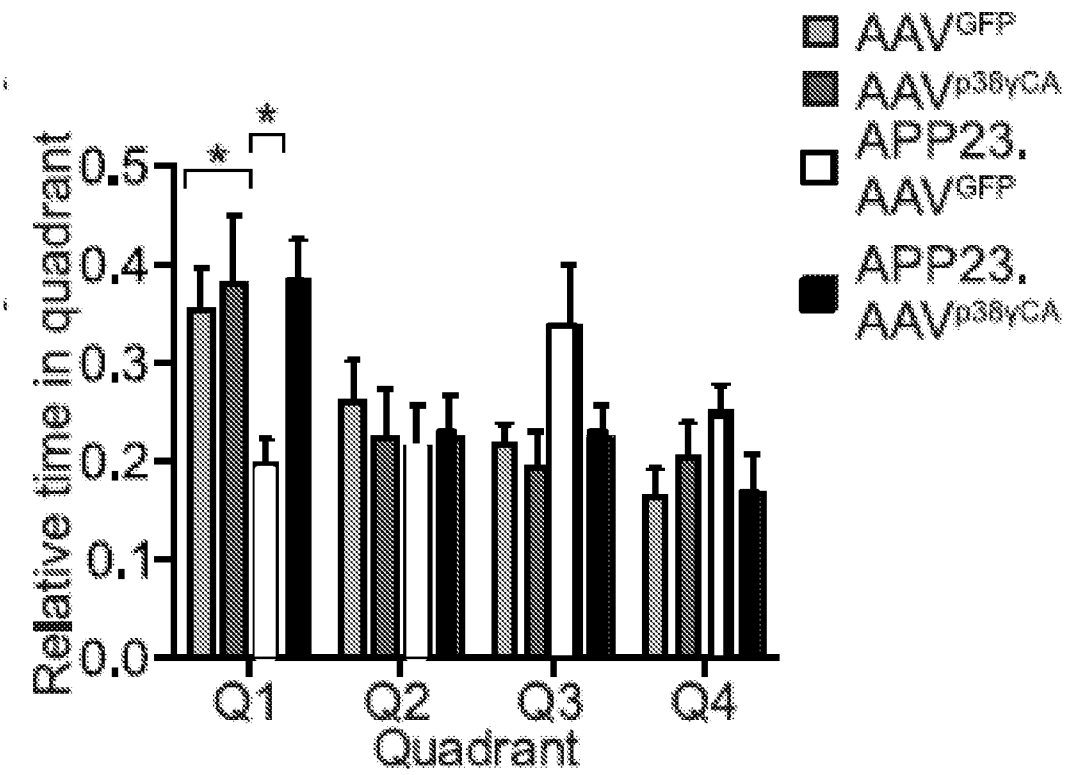
AAVGFP
AAVp38γCA
APP23. AAVGFP
APP23. AAVp38γCA
Relative time in quadrant
0.0
0.1
0.2
0.3
0.4
0.5
*
*
Q1
Q2
Q3
Q4
Quadrant

Figure 18

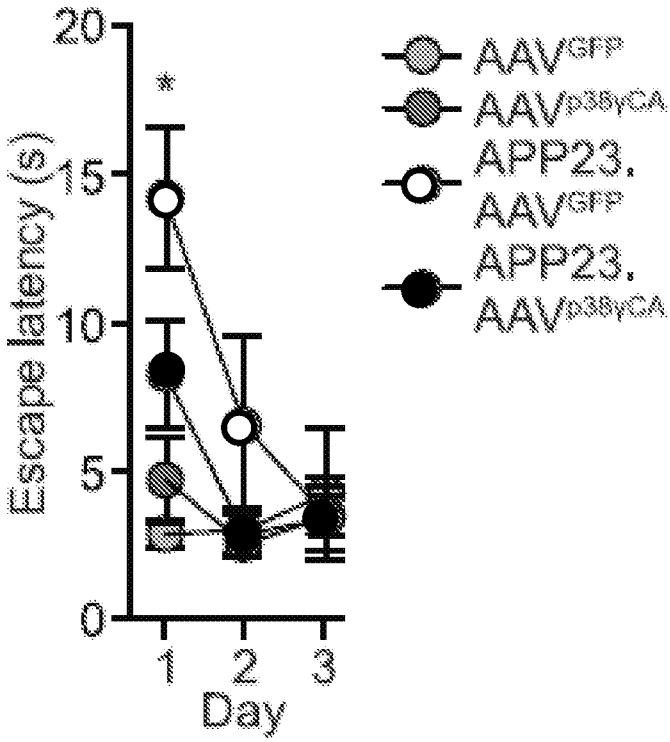
20
15
10
5
0
Escape latency (s)
*
1
2
3
Day
AAVGFP
AAVp38γCA
APP23, AAVGFP
APP23, AAVp38γCA

Figure 19

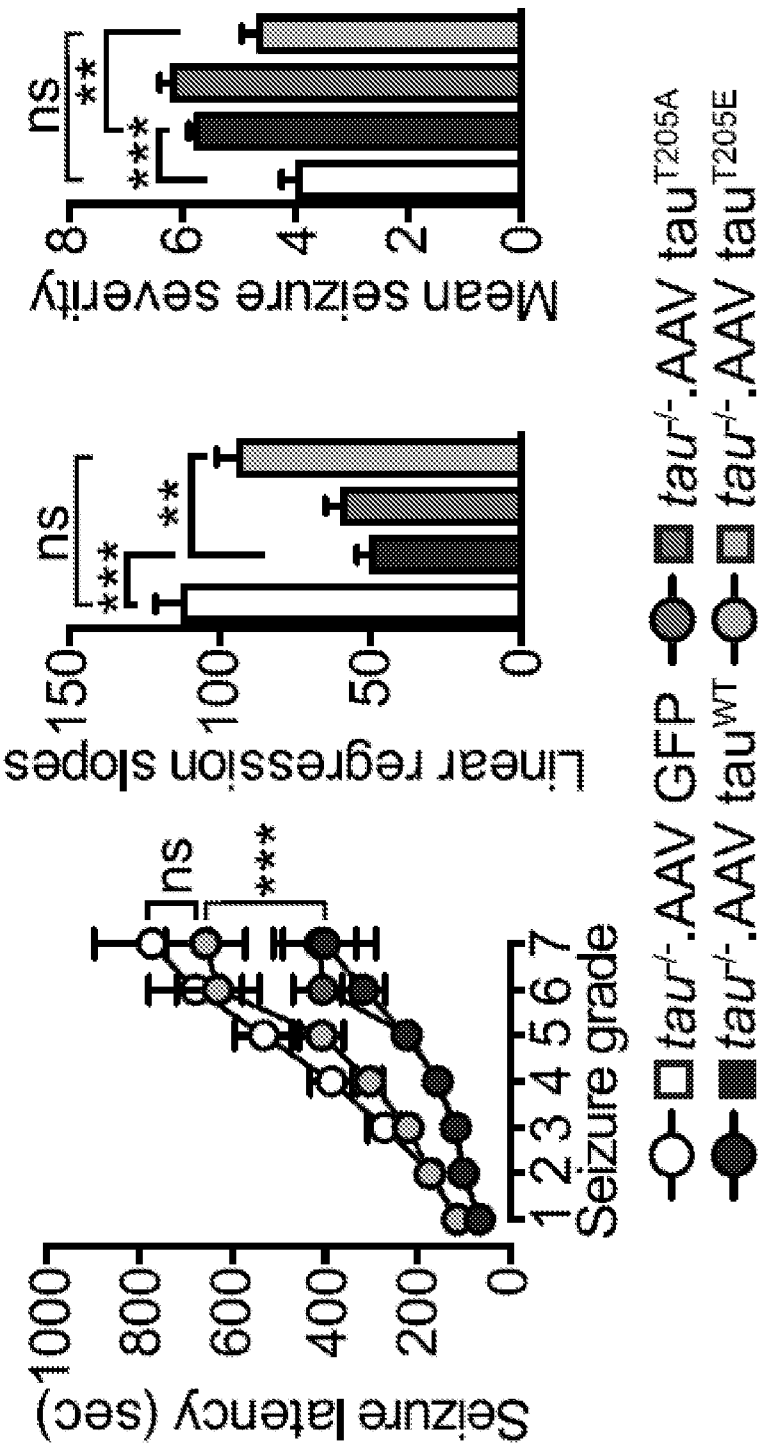
A
B
C
Seizure latency (sec)
1000
800
600
400
200
0
ns
***
1 2 3 4 5 6 7
Seizure grade
linear regression slopes
150
100
50
0
ns
***
**
Mean seizure severity
8
6
4
2
0
ns
**
***
taur/-.AAV GFP
taur/-.AAV tauWT
taur/-.AAV tauT205A
taur/-.AAV tauT205E

Figure 20

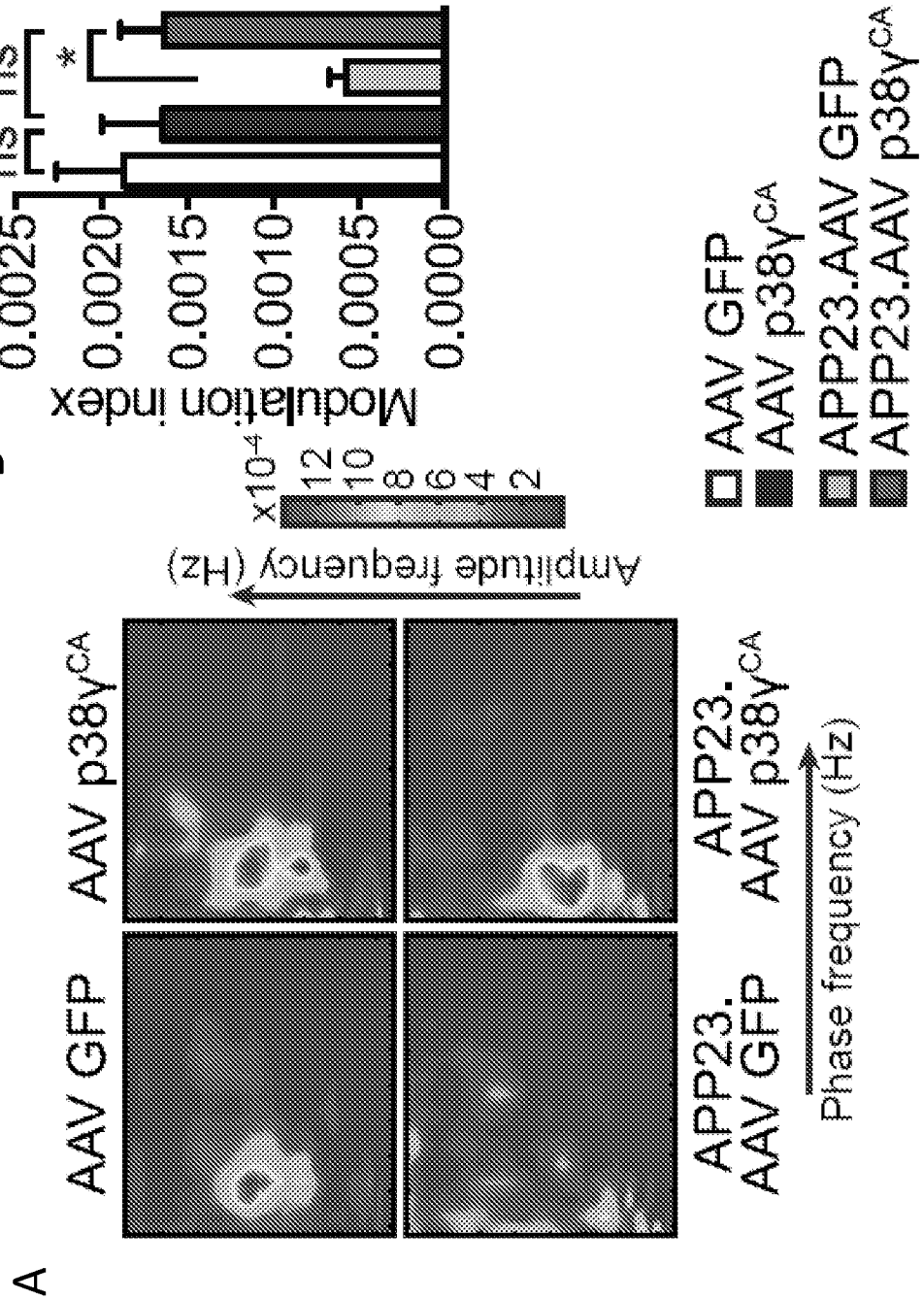
A
AAV GFP
AAV p38γCA
APP23.
AAV GFP
APP23.
AAV p38γCA
Phase frequency (Hz)
Amplitude frequency (Hz)
x10-4
12
10
8
6
4
2
B
Modulation index
0.0025
0.0020
0.0015
0.0010
0.0005
0.0000
ns
ns
*
AAV GFP
AAV p38γCA
APP23.AAV GFP
APP23.AAV p38γCA

Figure 21

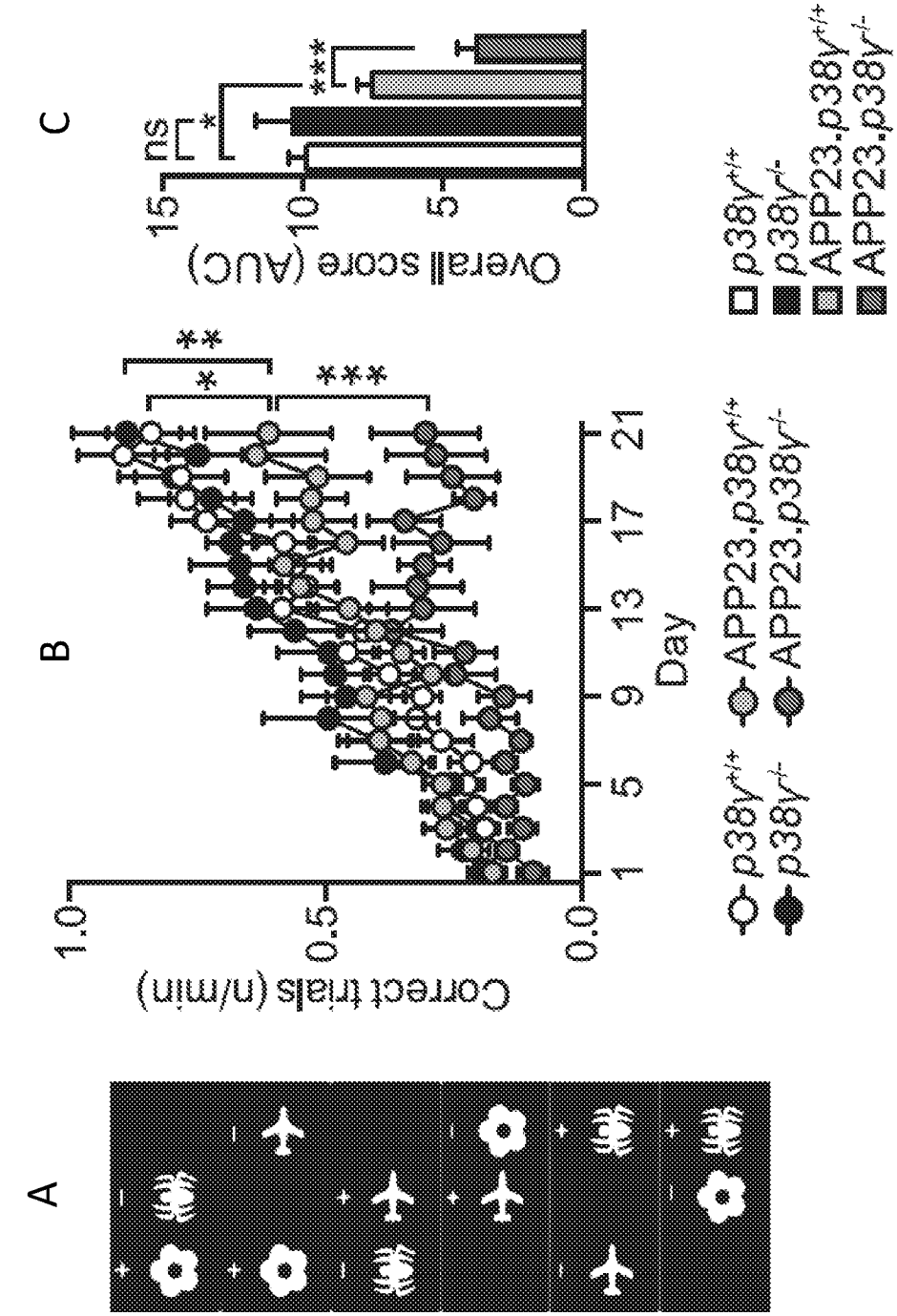
A
B
C
Correct trials (n/min)
1.0
0.5
0.0
1
5
9
13
17
21
Day
**
*
***
Overall score (AUC)
15
10
5
0
ns
*
***
p38γ+/+
p38γ-/-
APP23.p38γ+/+
APP23.p38γ-/-

Figure 22

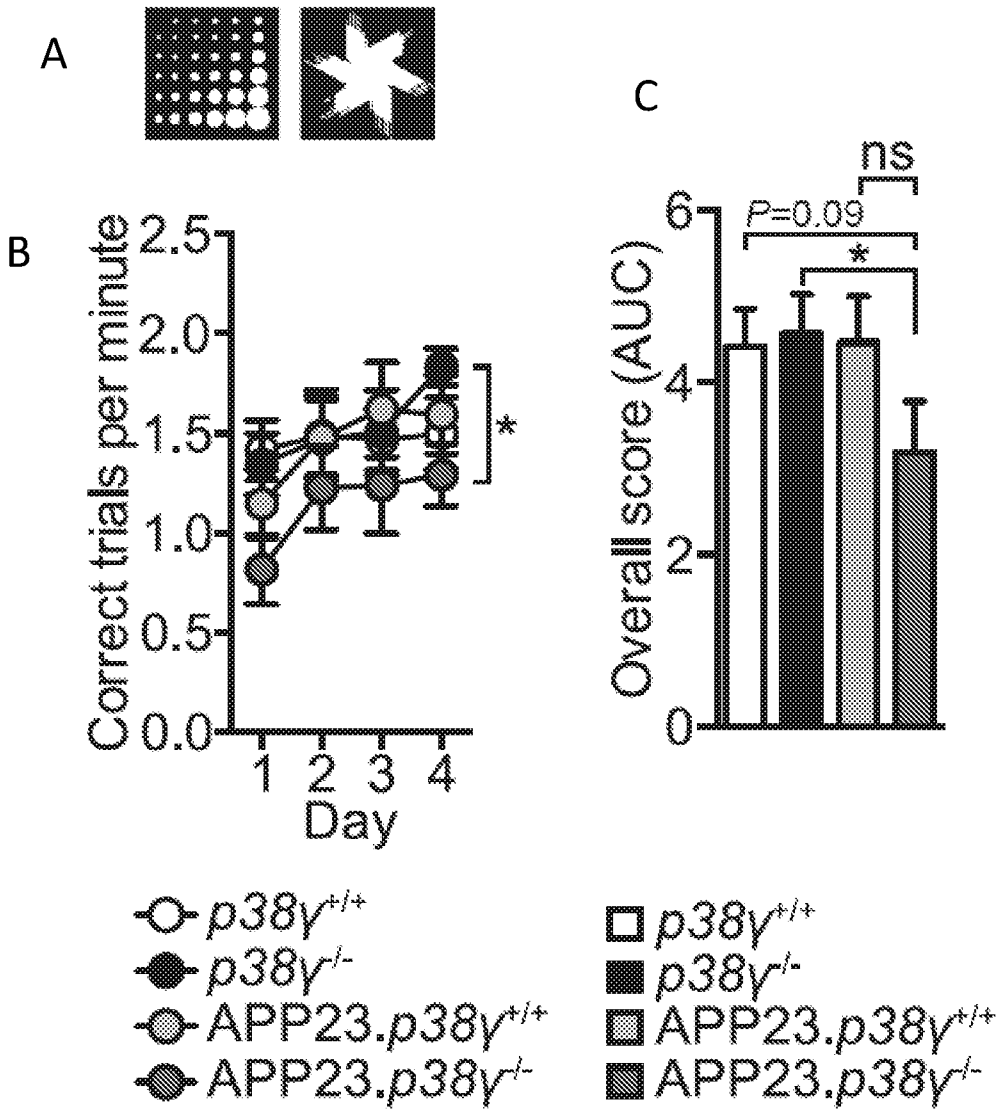
A
B
C
Correct trials per minute
2.5
2.0
1.5
1.0
0.5
0.0
1 2 3 4
Day
*
Overall score (AUC)
6
4
2
0
P=0.09
ns
*
p38γ+/+
p38γ-/-
APP23.p38γ+/+
APP23.p38γ-/-
p38γ+/+
p38γ-/-
APP23.p38γ+/+
APP23.p38γ-/-

Figure 23

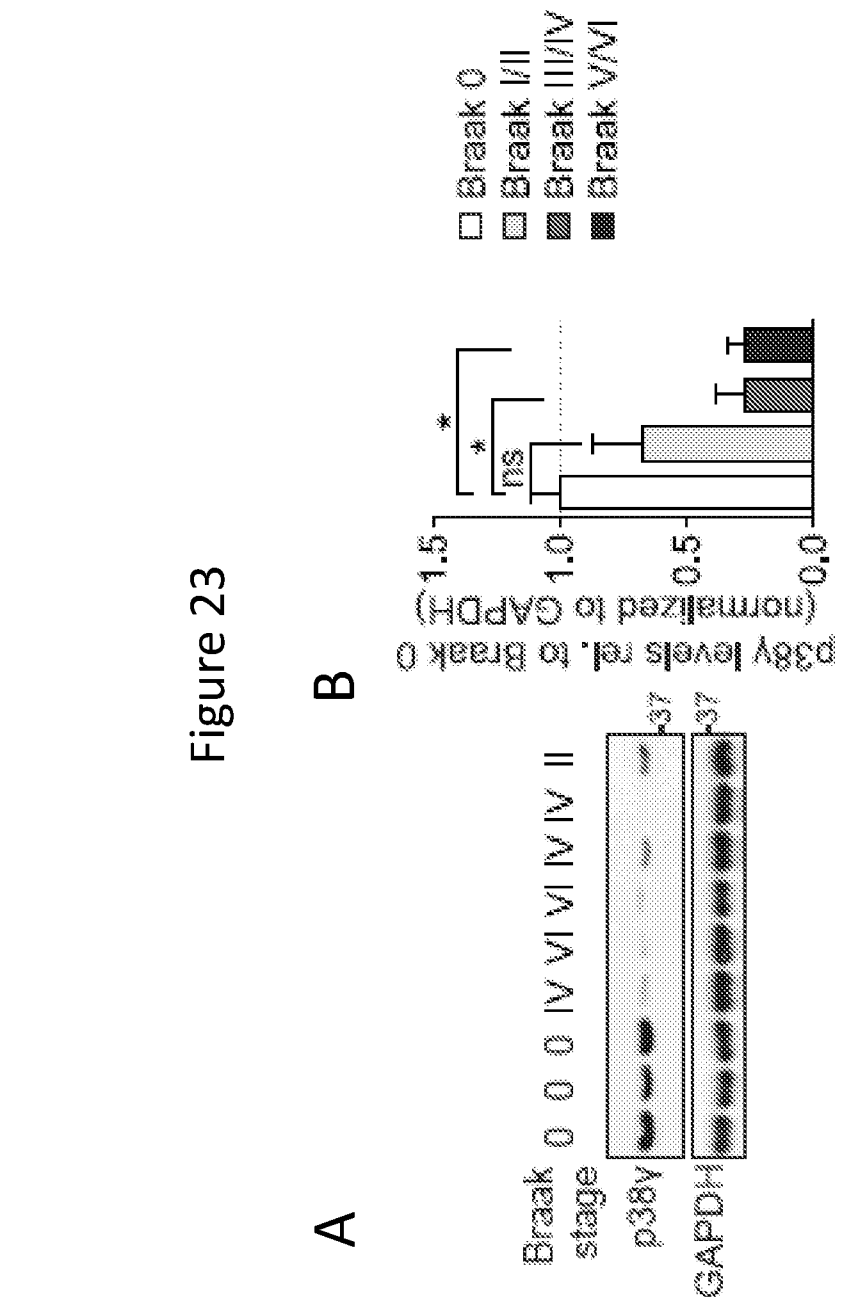
A
Braak stage
0 0 0 IV VI VI IV II
p38γ
GAPDH
37
37
B
p38γ levels rel. to Braak 0 (normalized to GAPDH)
1.5
1.0
0.5
0.0
ns
*
*
Braak 0
Braak I/II
Braak III/IV
Braak V/VI

Figure 24

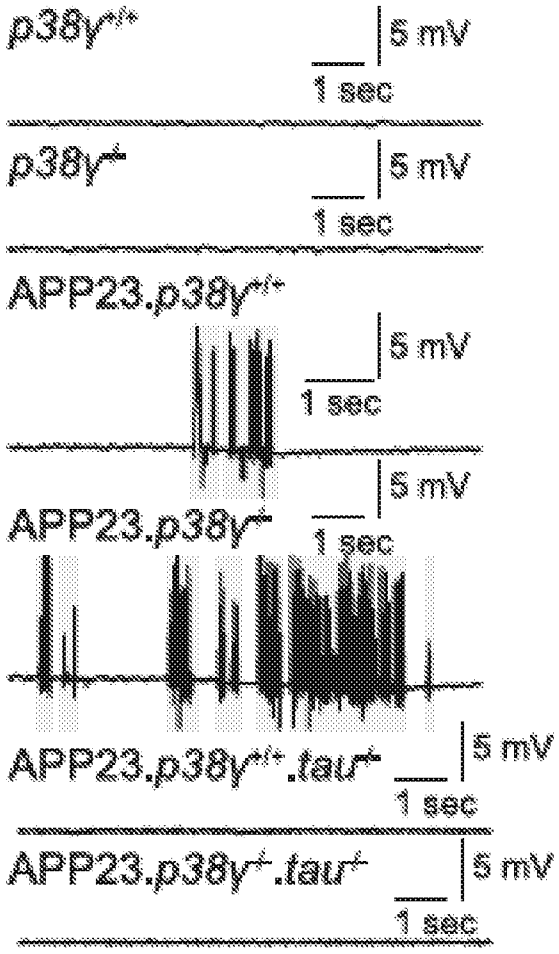
p38γ+/+
5 mV
1 sec
p38γ-/-
5 mV
1 sec
APP23.p38γ+/+
5 mV
1 sec
5 mV
APP23.p38γ-/-
1 sec
APP23.p38γ+/+.tau-/-
5 mV
1 sec
APP23.p38γ-/-.tau-/-
5 mV
1 sec

Figure 25

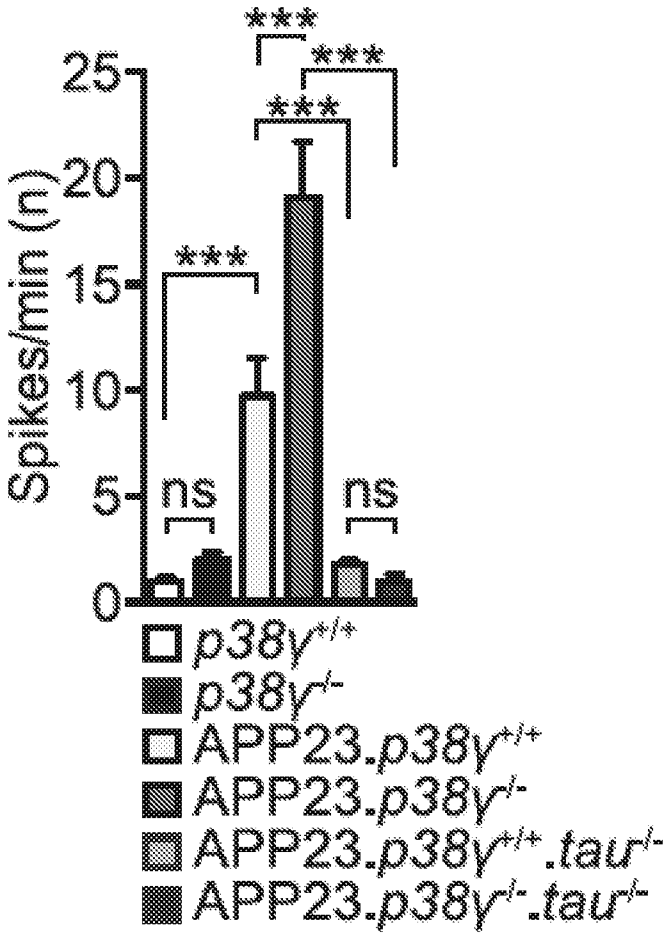
***
***
***
***
25
20
15
10
5
0
Spikes/min (n)
ns
ns
p38γ+/+
p38γ-/-
APP23.p38γ+/+
APP23.p38γ-/-
APP23.p38γ+/+.tau-/-
APP23.p38γ-/-.tau-/-

Figure 26

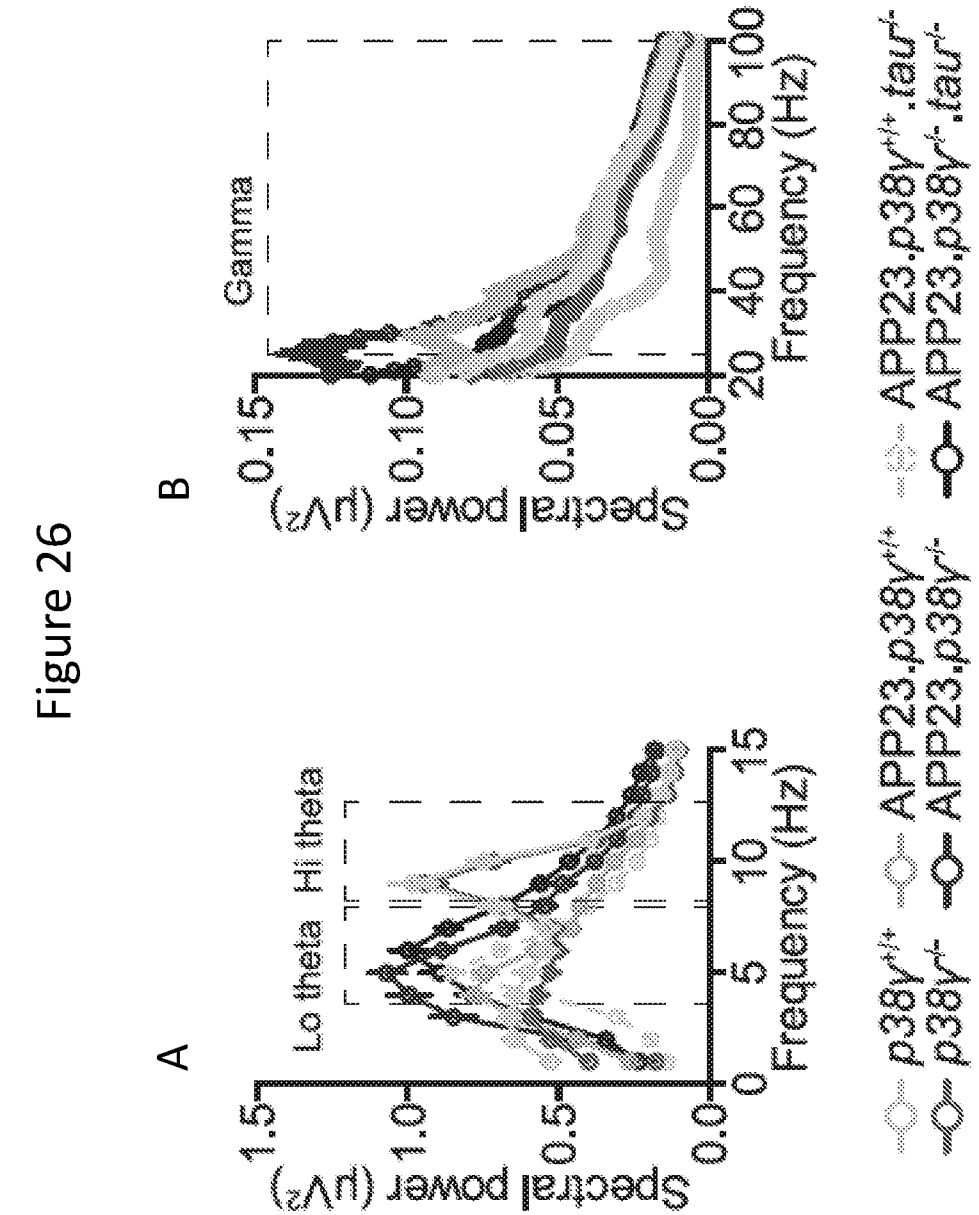
A
B
Lo theta
Hi theta
Gamma
Spectral power (μV²)
Frequency (Hz)
p38γ+/+
APP23.p38γ+/+
APP23.p38γ+/+.tau-/-
p38γ-/-
APP23.p38γ-/-
APP23.p38γ-/-.tau-/-

Figure 27

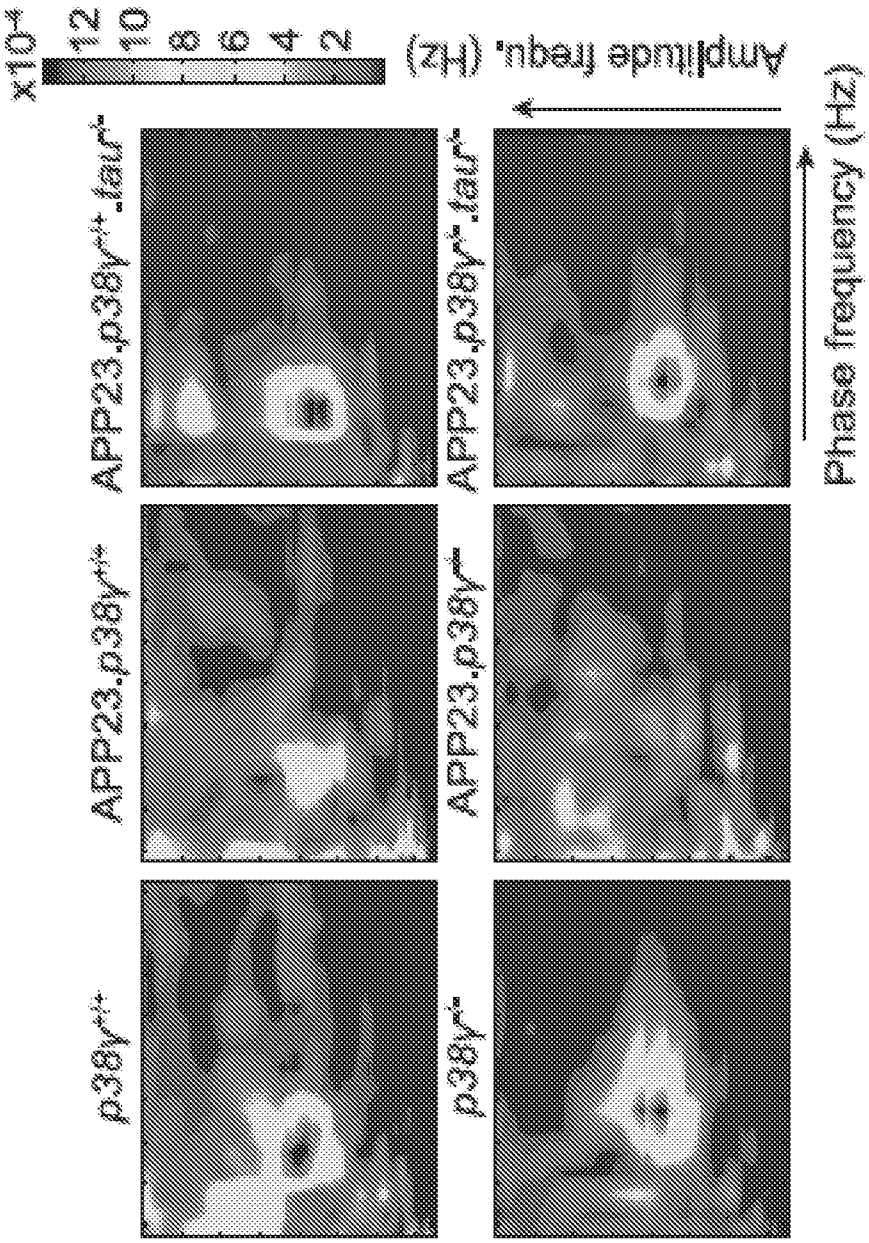
x10-4
12
10
8
6
4
2
Amplitude frequ. (Hz)
Phase frequency (Hz)
p38γ+/+
APP23.p38γ+/+
APP23.p38γ+/+.tau-/-
p38γ-/-
APP23.p38γ-/-
APP23.p38γ-/-.tau-/-

Figure 28

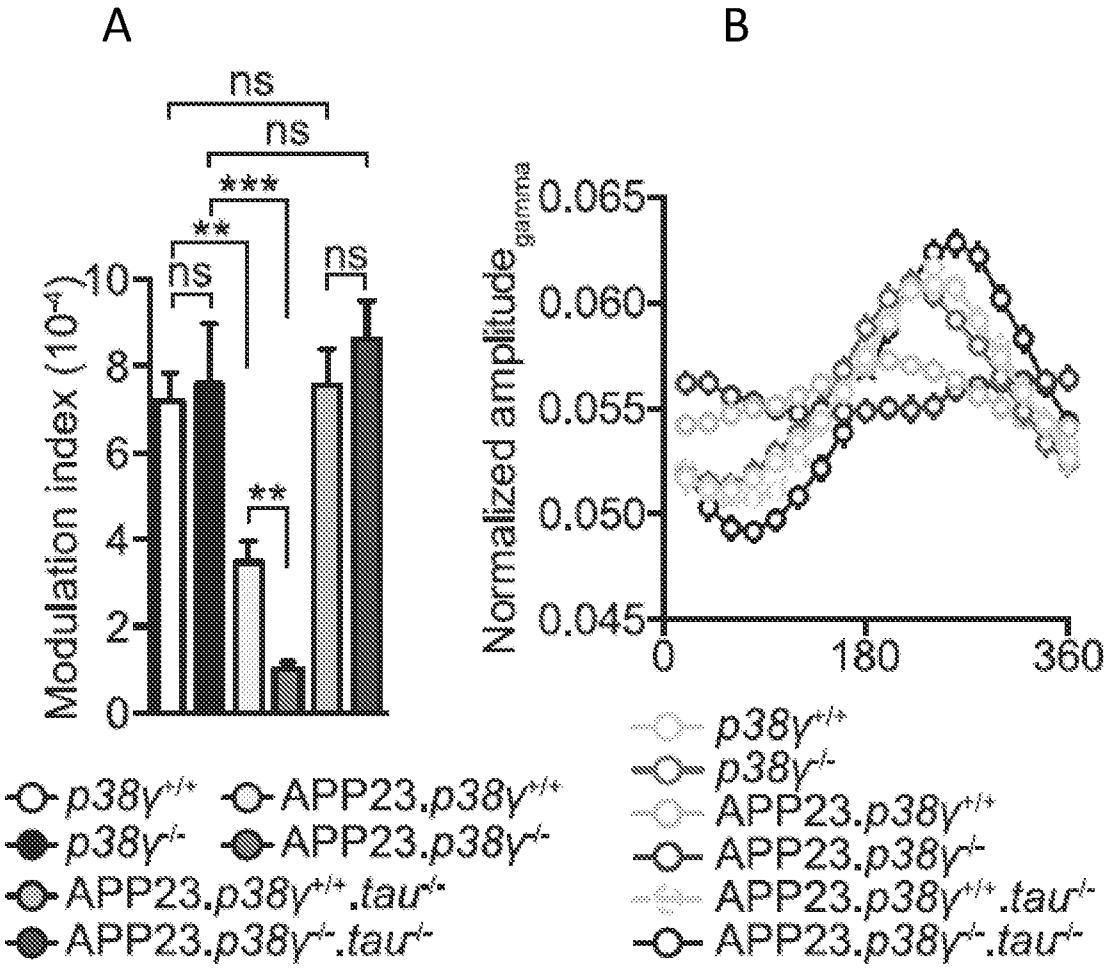
A
B
ns
ns
***
**
ns
ns
**
Modulation index (10^{-4})
0
2
4
6
8
10
Normalized amplitude gamma
0.045
0.050
0.055
0.060
0.065
0
180
360
p38γ+/+
p38γ-/-
APP23.p38γ+/+
APP23.p38γ-/-
APP23.p38γ+/+.tau-/-
APP23.p38γ-/-.tau-/-

Figure 29

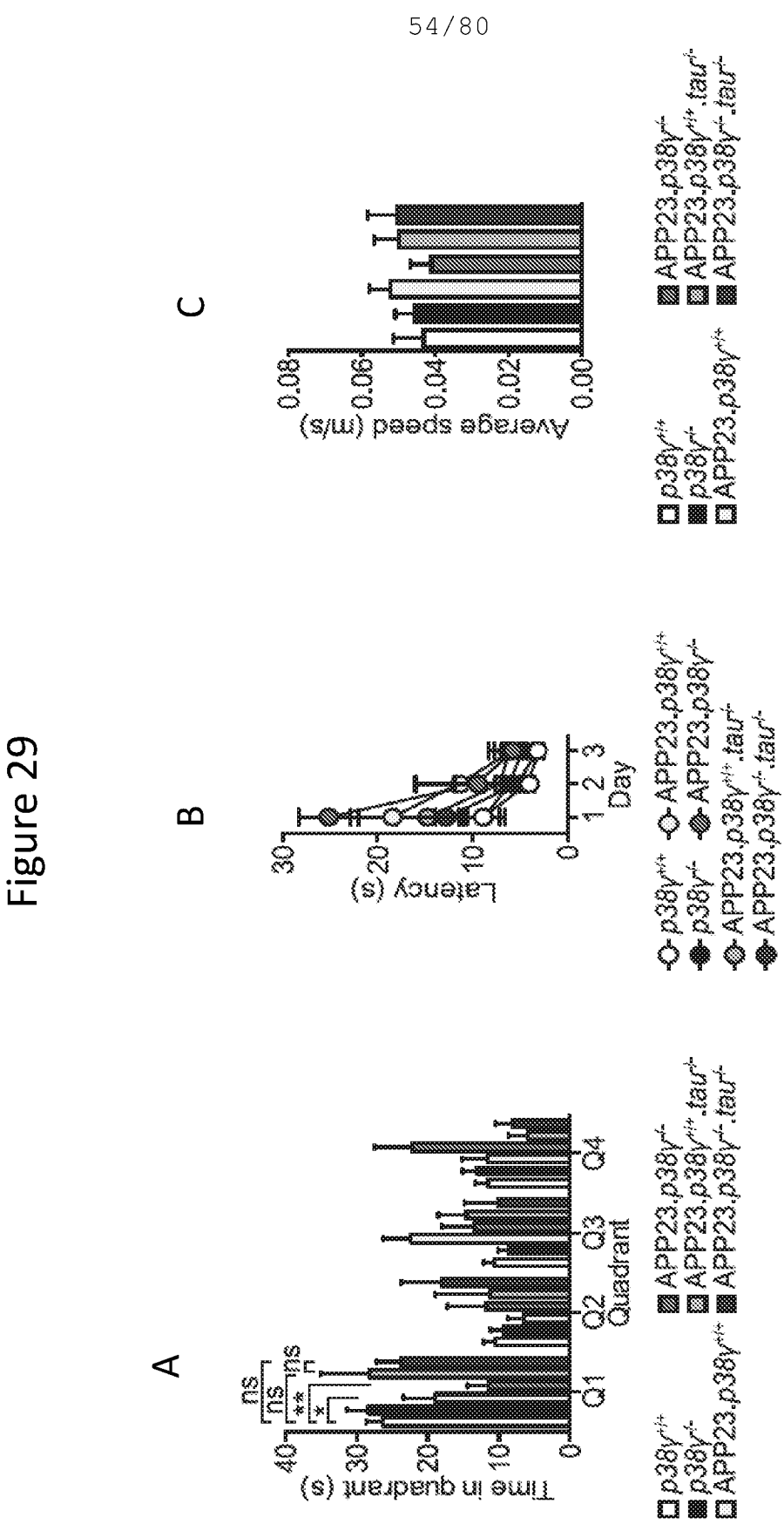
A
B
C
Time in quadrant (s)
Q1
Q2
Q3
Q4
Quadrant
ns
ns
**
*
Latency (s)
Day
Average speed (m/s)
p38γ+/+
p38γ-/-
APP23.p38γ+/+
APP23.p38γ-/-
APP23.p38γ+/+.tau-/-
APP23.p38γ-/-.tau-/-

Figure 30

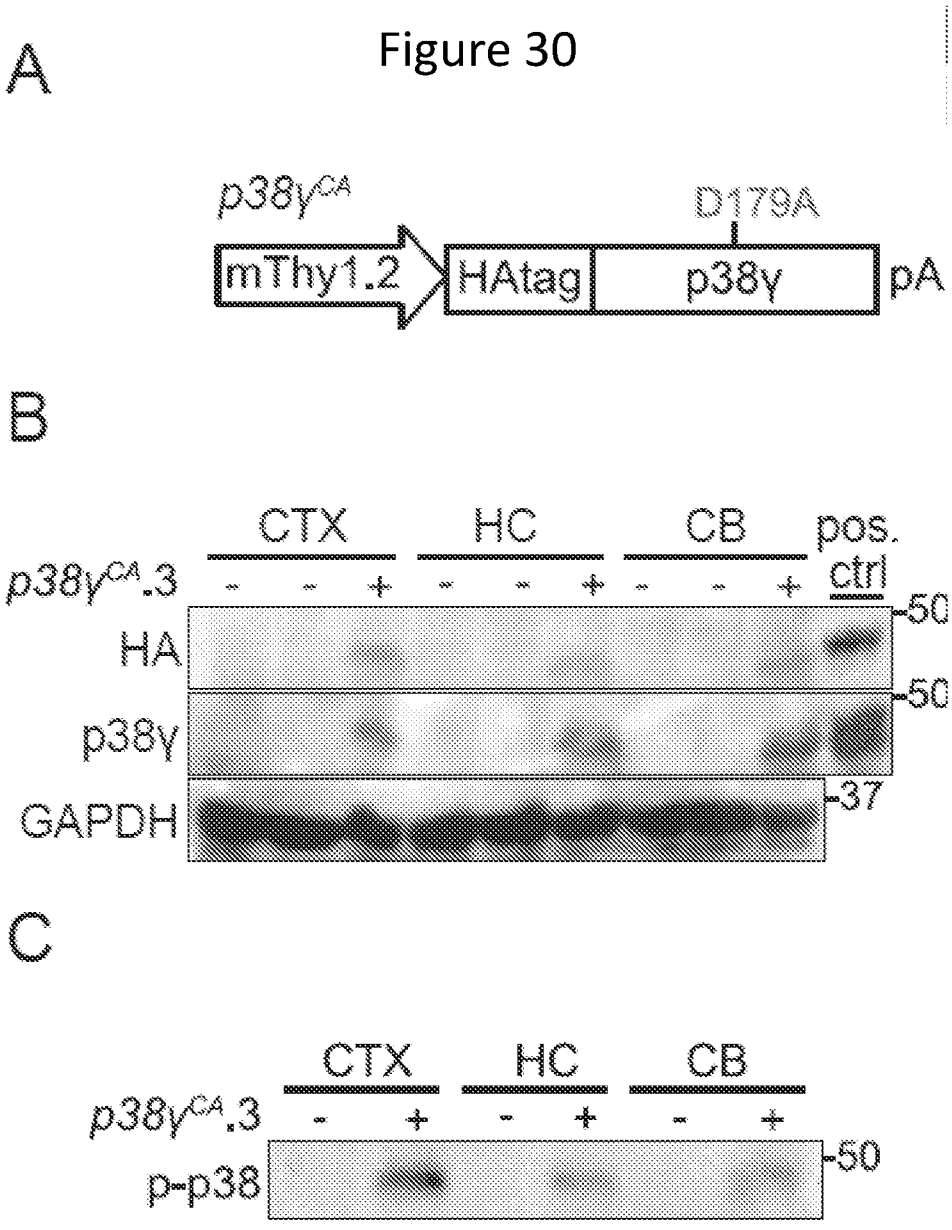
A
p38γCA
D179A
mThy1.2
HAtag
p38γ
pA
B
CTX
HC
CB
pos.
p38γCA.3
- - + - - + - - +
ctrl
HA
p38γ
GAPDH
50
50
37
C
CTX
HC
CB
p38γCA.3
- + - + - +
p-p38
50

Figure 31

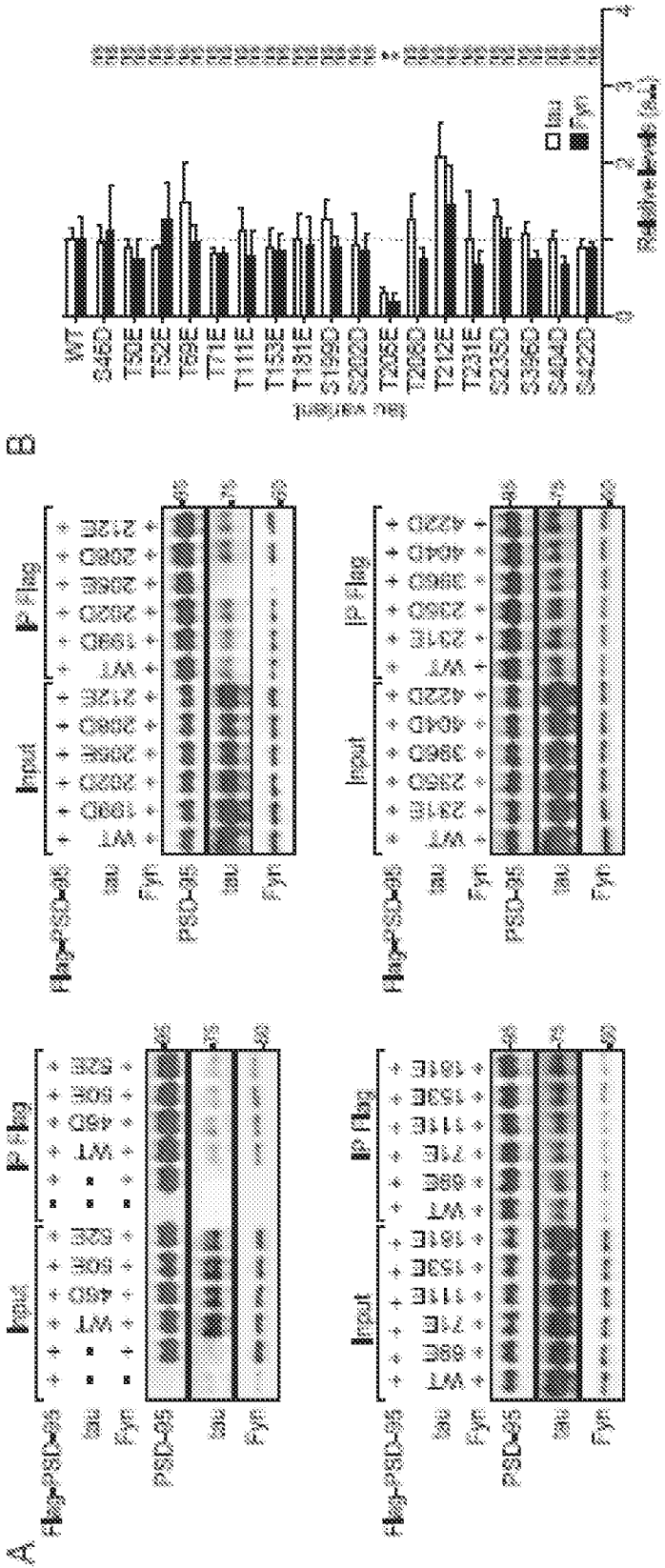
A
B
Input
IP flag
Flag-PSD-95
PSD-95
Lau
Fyn
WT
S48D
T92E
T92E
T69E
T71E
T111E
T153E
T181E
S199D
S202D
T205E
T206D
T212E
T201E
S233D
S396D
S404D
S422D

Figure 32

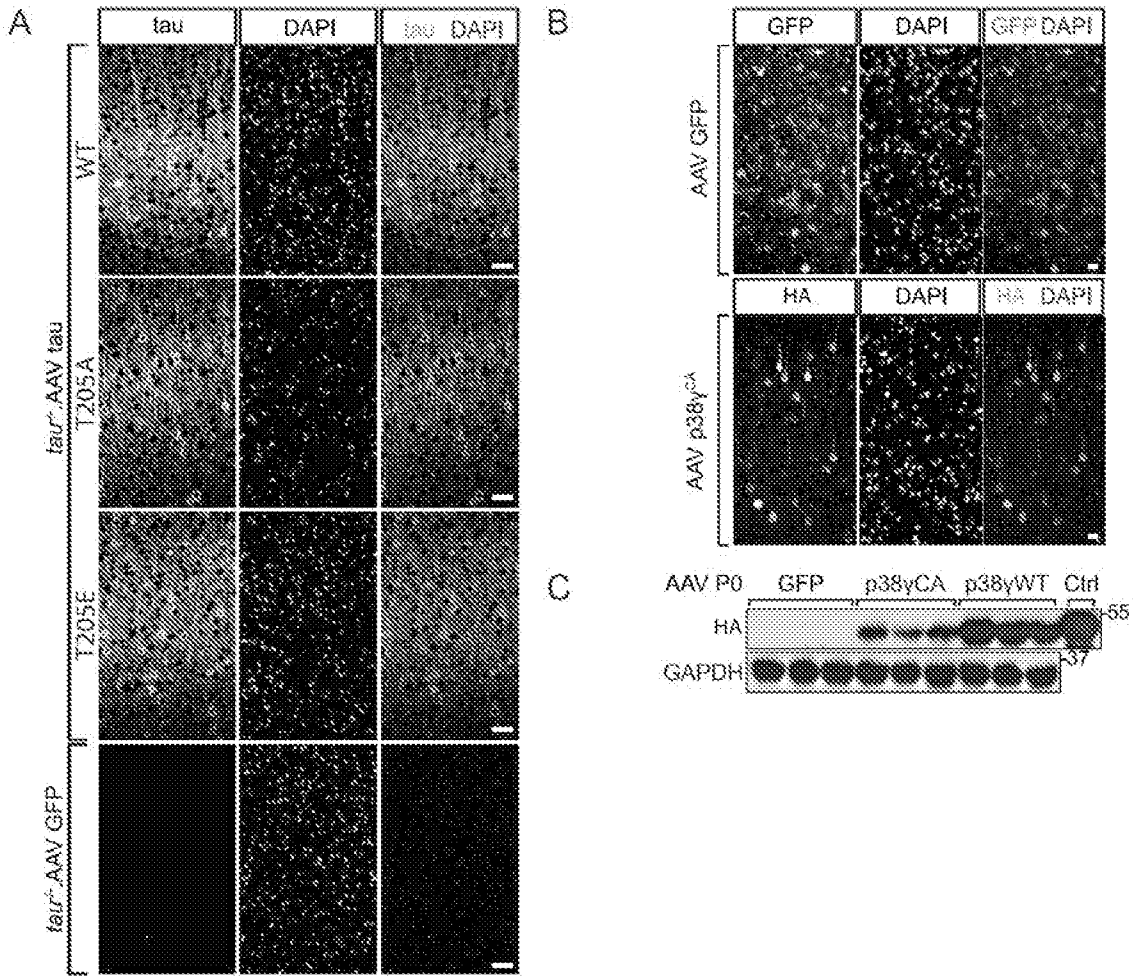
A
tau
DAPI
tau DAPI
WT
T205A
T205E
tau-/- AAV tau
tau-/- AAV GFP
B
GFP
DAPI
GFP DAPI
AAV GFP
HA
DAPI
HA DAPI
AAV p38γCA
C
AAV P0
GFP
p38γCA
p38γWT
Ctrl
HA
GAPDH
55
37

Figure 33

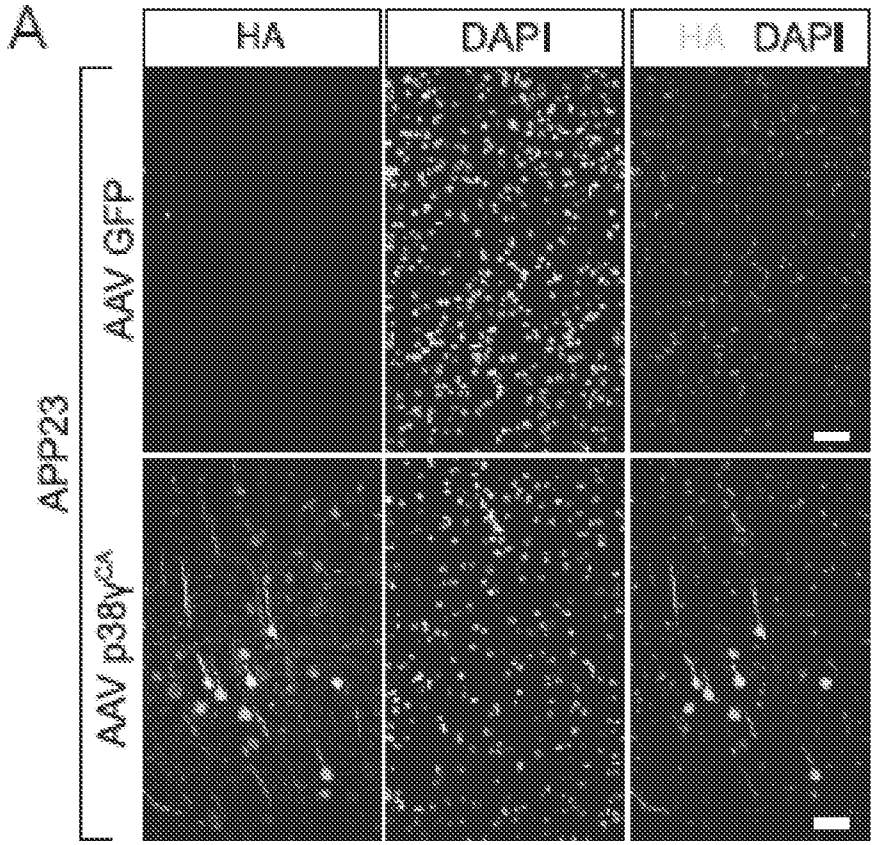

Figure 34

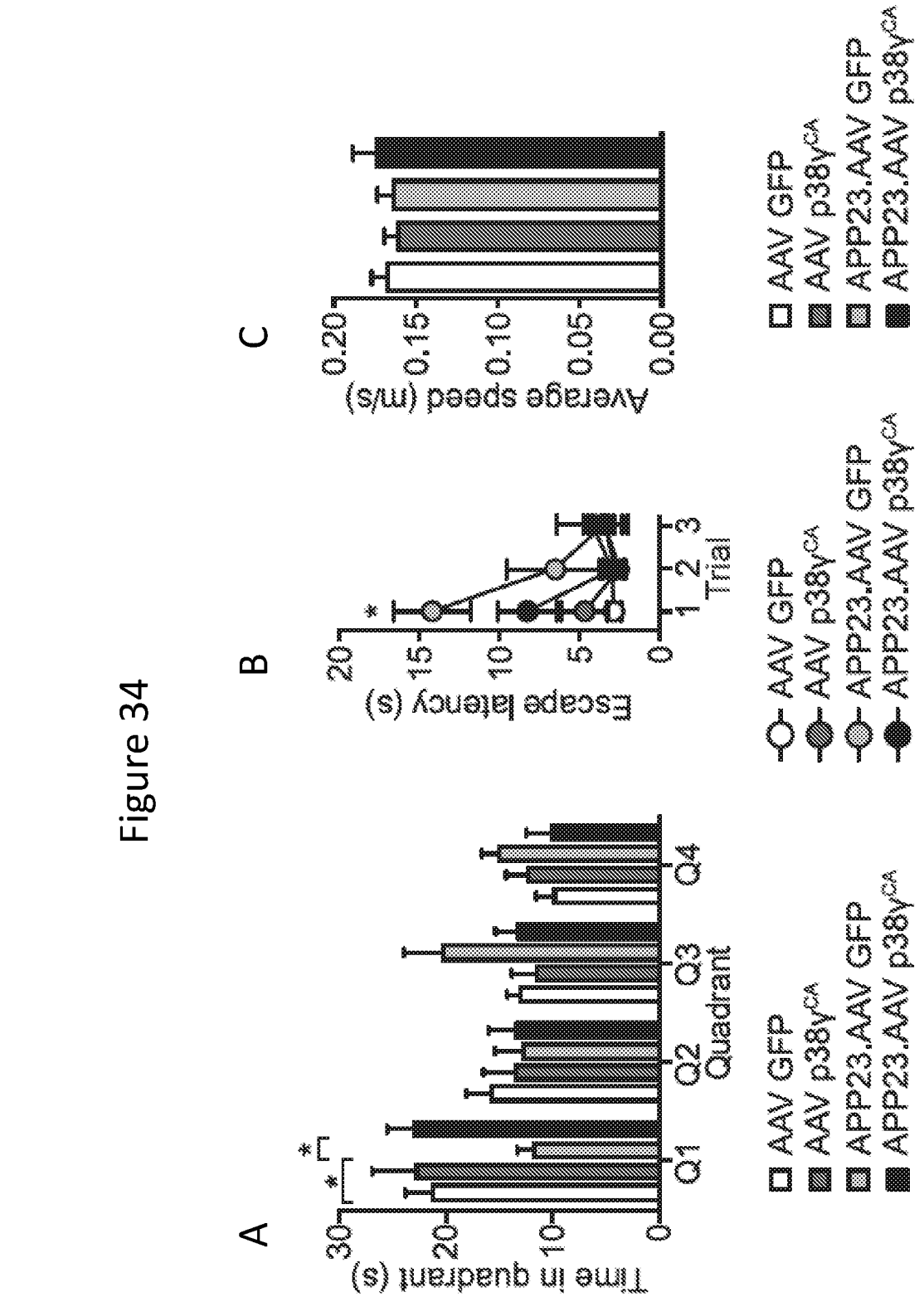
A
B
C
Time in quadrant (s)
Q1
Q2
Q3
Q4
Quadrant
Escape latency (s)
Trial
Average speed (m/s)
AAV GFP
AAV p38γ^CA
APP23.AAV GFP
APP23.AAV p38γ^CA

Figure 35

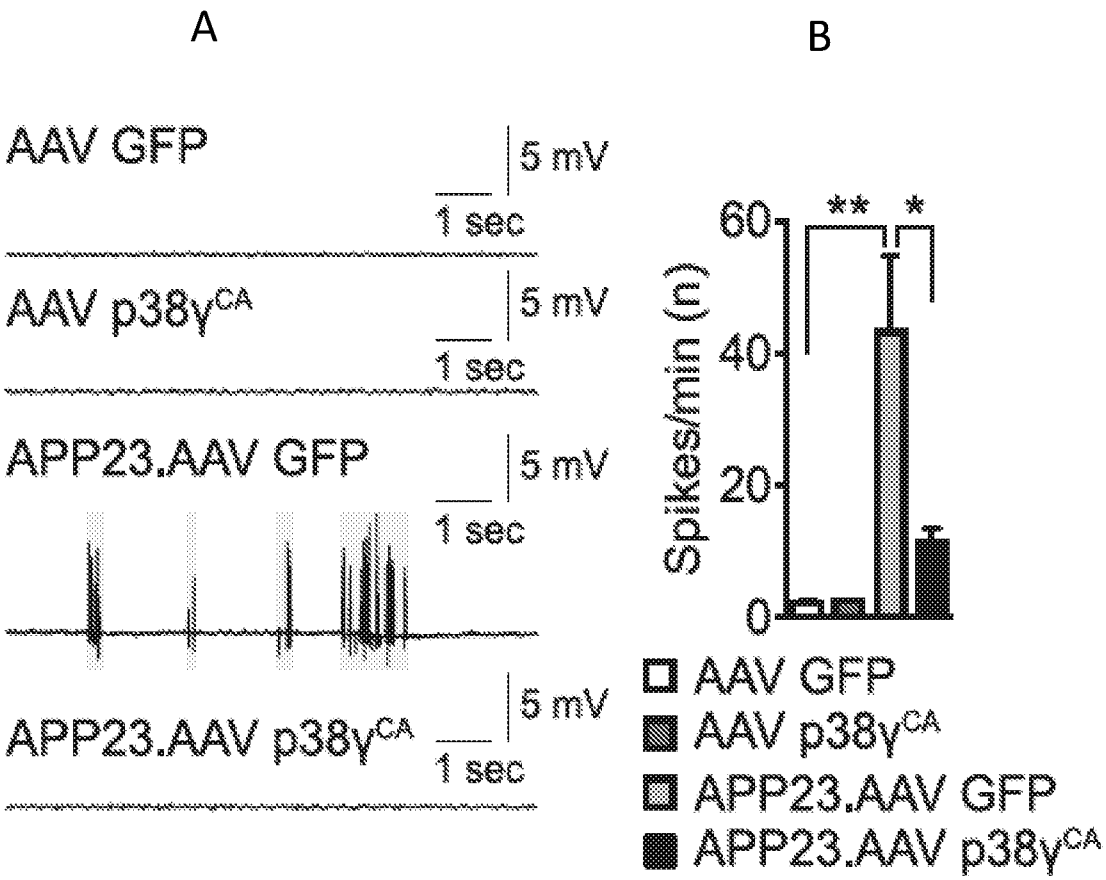
A
B
AAV GFP
5 mV
1 sec
AAV p38γCA
5 mV
1 sec
APP23.AAV GFP
5 mV
1 sec
APP23.AAV p38γCA
5 mV
1 sec
Spikes/min (n)
60
40
20
0
**
*
AAV GFP
AAV p38γCA
APP23.AAV GFP
APP23.AAV p38γCA

Figure 36

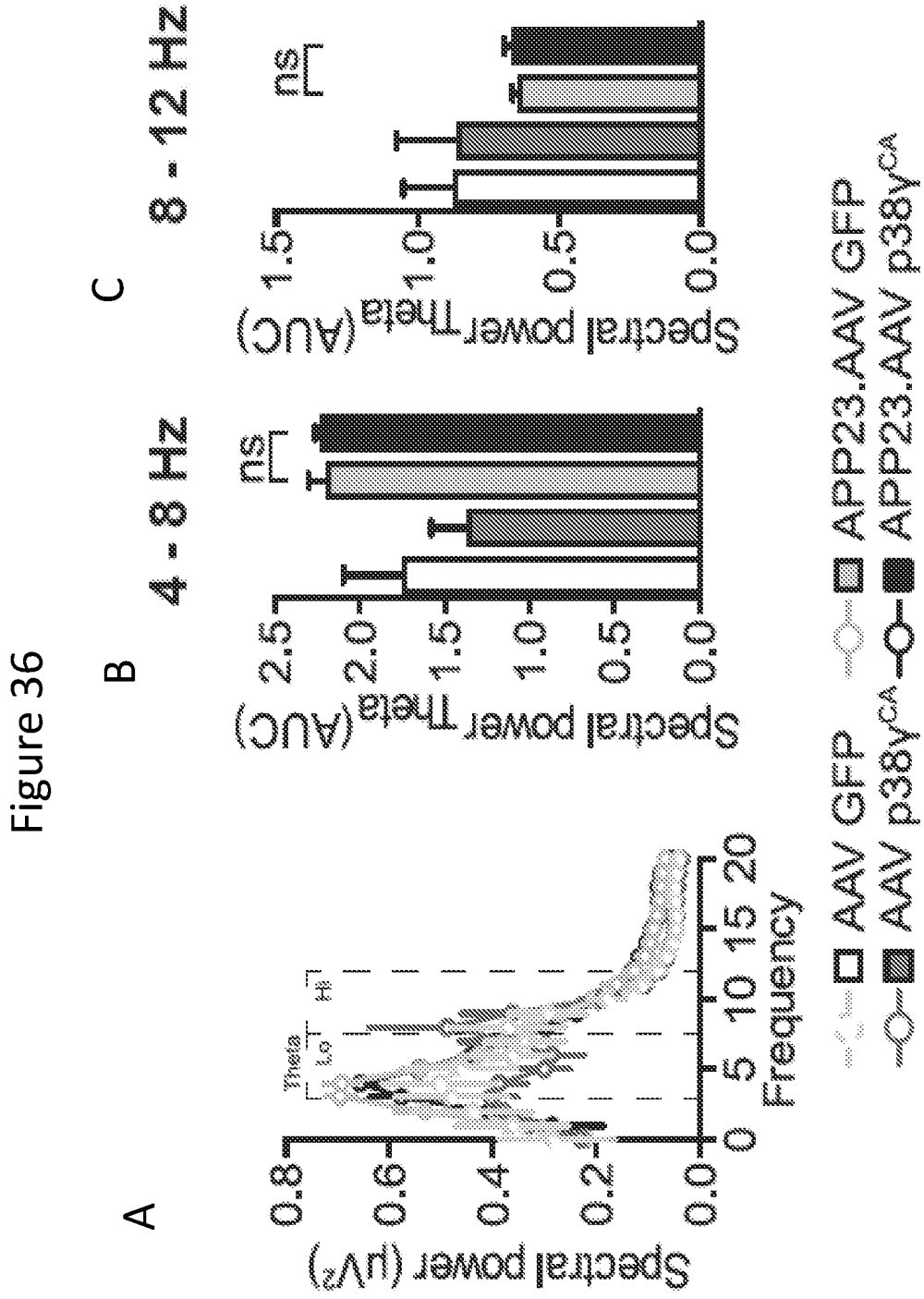
A
B
C
4 - 8 Hz
8 - 12 Hz
ns
ns
Spectral power Theta (AUC)
Spectral power Theta (AUC)
Spectral power (μV²)
Frequency
Theta
AAV GFP
AAV p38γ^CA
APP23.AAV GFP
APP23.AAV p38γ^CA

Figure 37

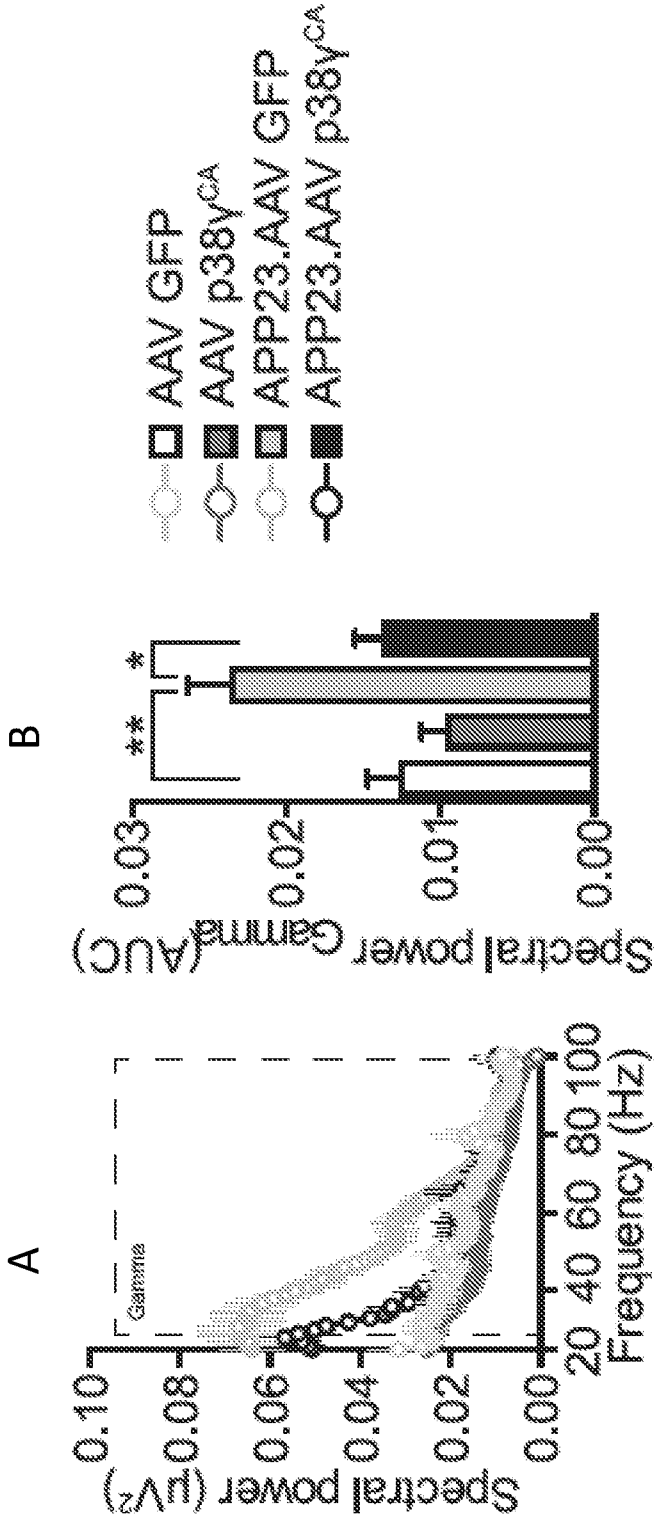
A
Gamma
Spectral power (μV²)
0.10
0.08
0.06
0.04
0.02
0.00
20 40 60 80 100
Frequency (Hz)
B
Spectral power Gamma (AUC)
0.03
0.02
0.01
0.00
**
*
AAV GFP
AAV p38γCA
APP23.AAV GFP
APP23.AAV p38γCA

Figure 38

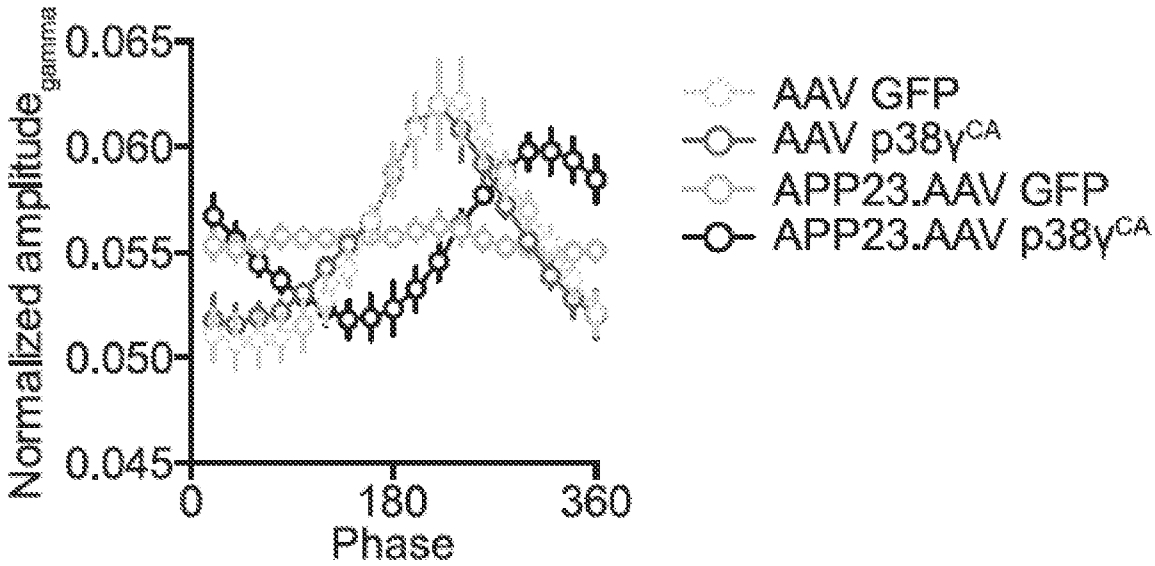
Normalized amplitude gamma
0.065
0.060
0.055
0.050
0.045
0
180
360
Phase
AAV GFP
AAV p38γCA
APP23.AAV GFP
APP23.AAV p38γCA

Figure 39

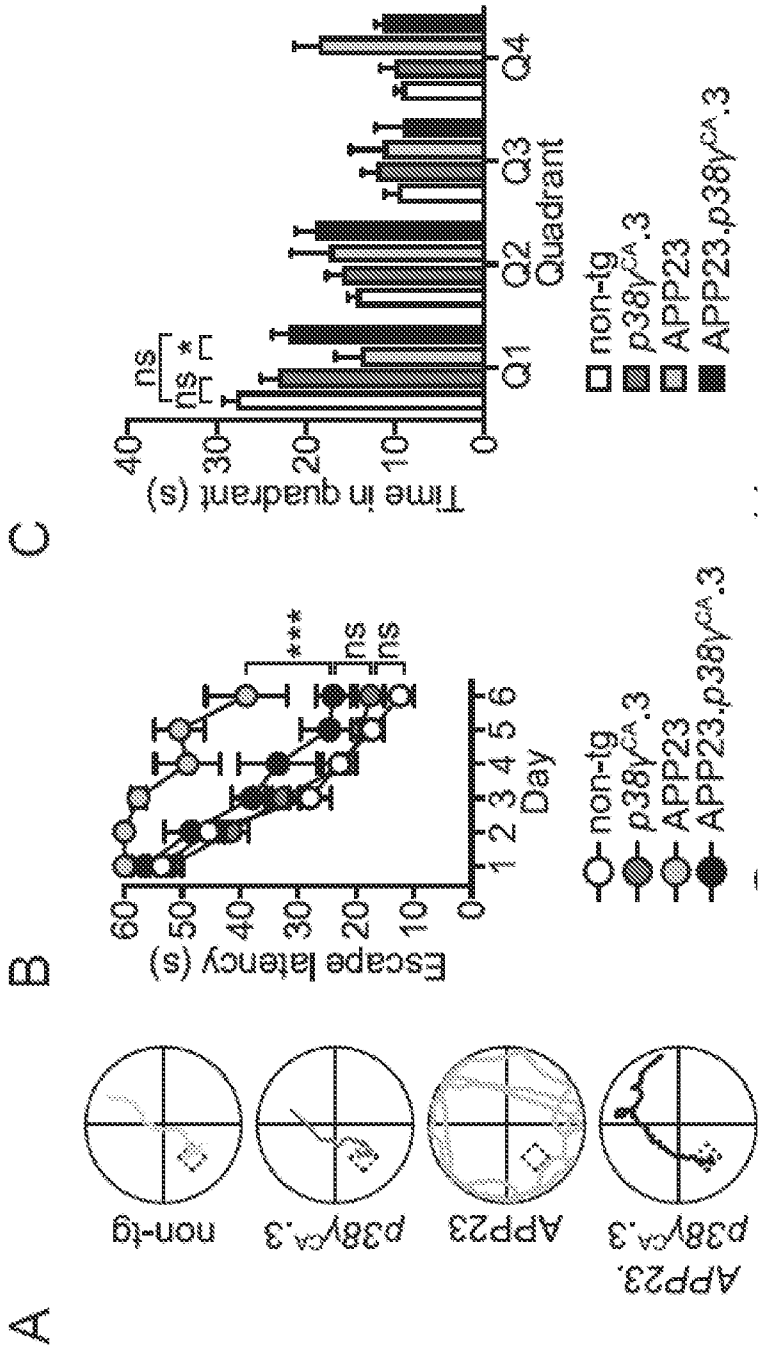
A
non-tg
p38γCA.3
APP23
APP23.p38γCA.3
B
Escape latency (s)
Day
non-tg
p38γCA.3
APP23
APP23.p38γCA.3
***
ns
ns
C
Time in quadrant (s)
Quadrant
Q1
Q2
Q3
Q4
ns
ns
*

Figure 39 cont.

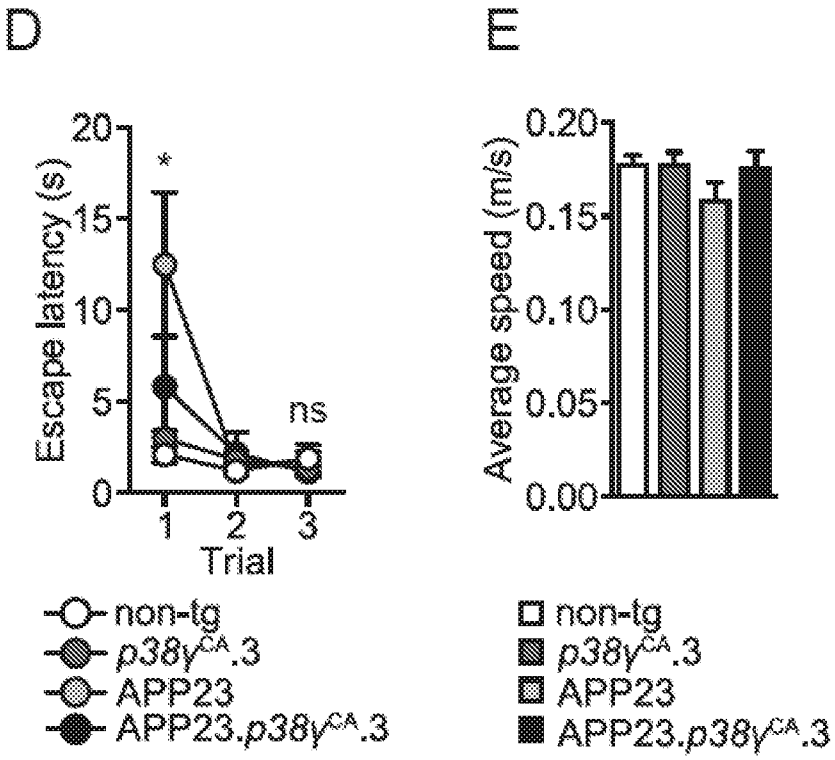

Figure 40

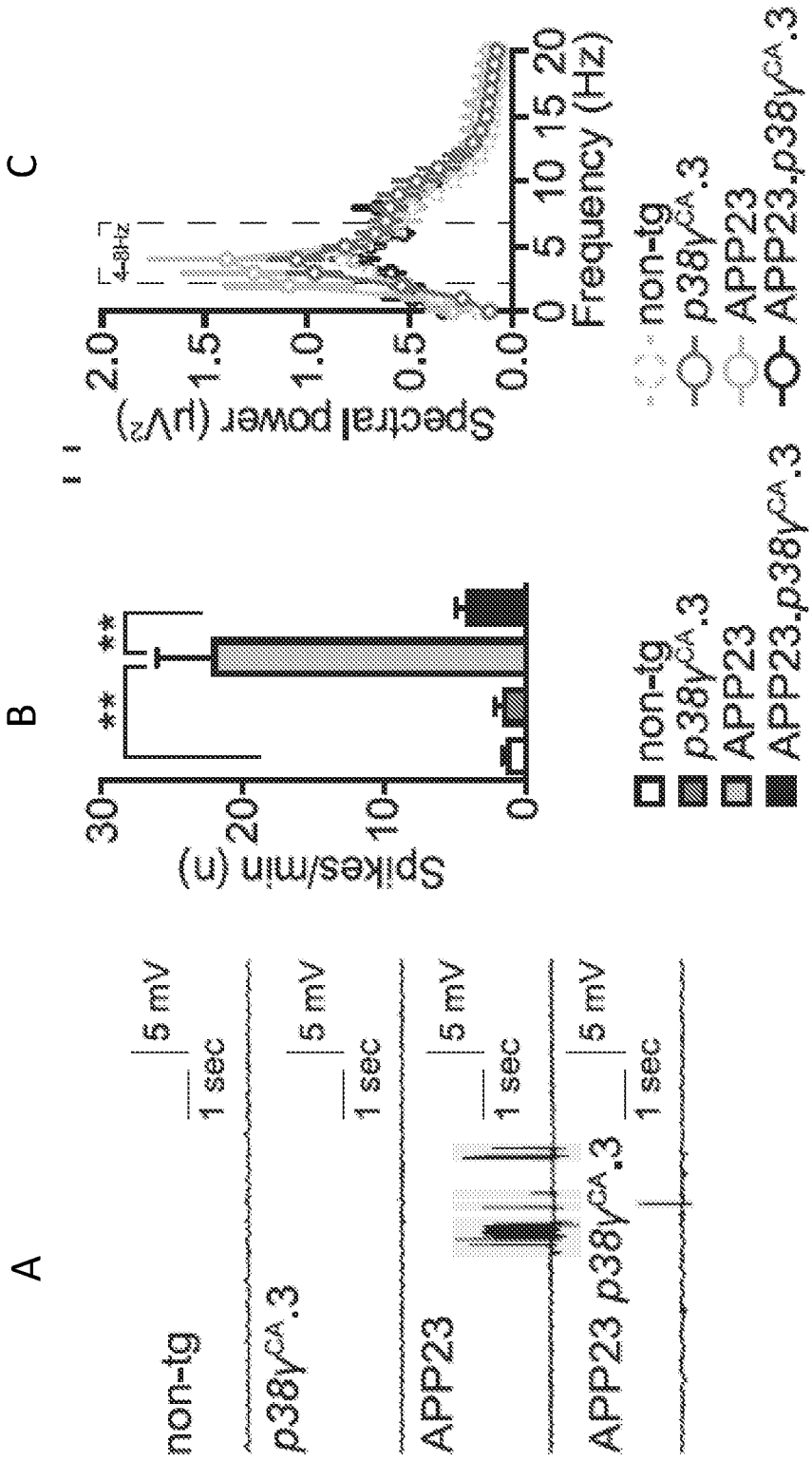
A
non-tg
p38γCA.3
APP23
APP23 p38γCA.3
5 mV
1 sec
B
Spikes/min (n)
30
20
10
0
**
**
C
Spectral power (μV²)
2.0
1.5
1.0
0.5
0.0
4–8Hz
0 5 10 15 20
Frequency (Hz)
non-tg
p38γCA.3
APP23
APP23.p38γCA.3

Figure 40 cont.

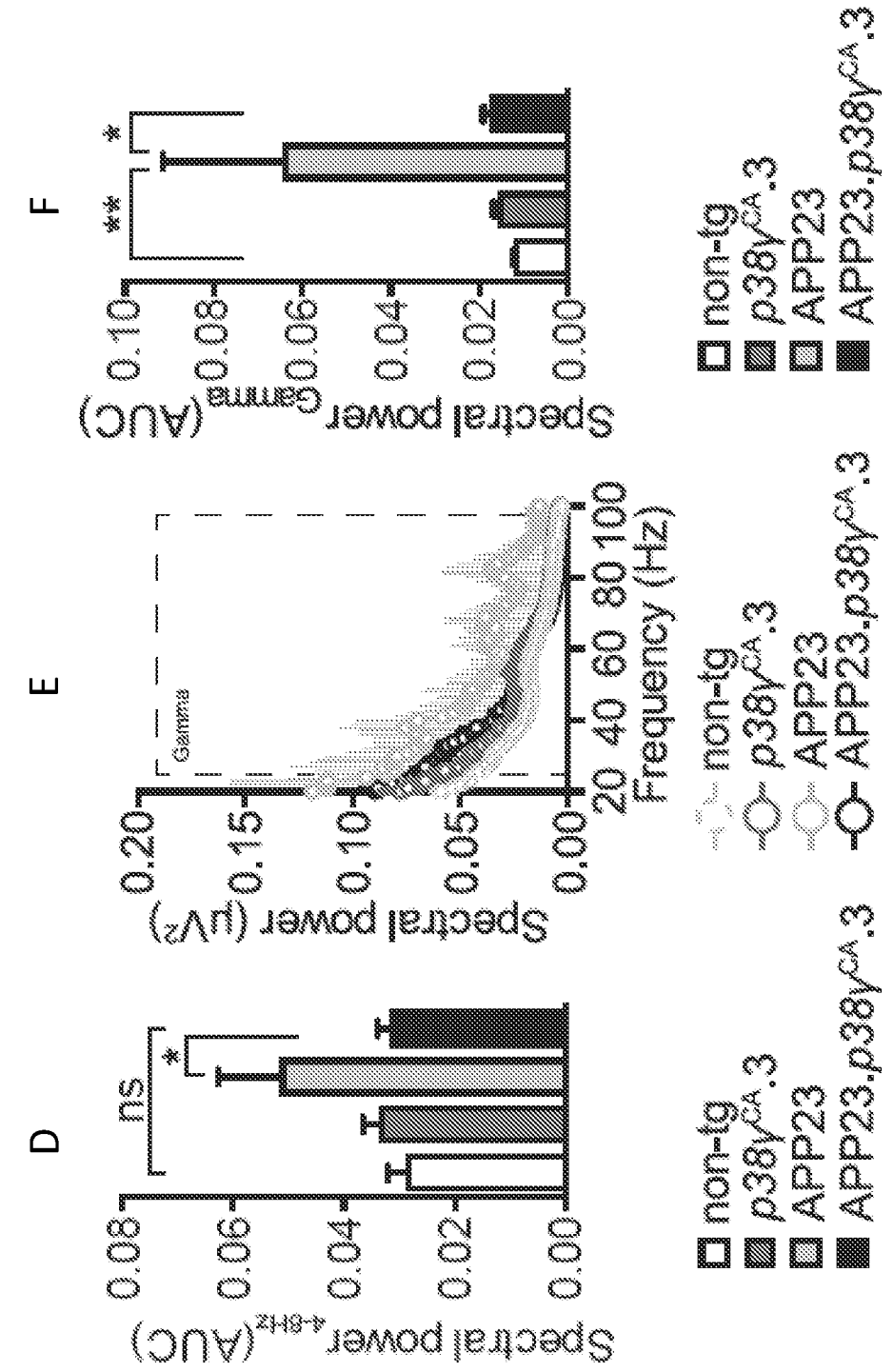

Figure 41

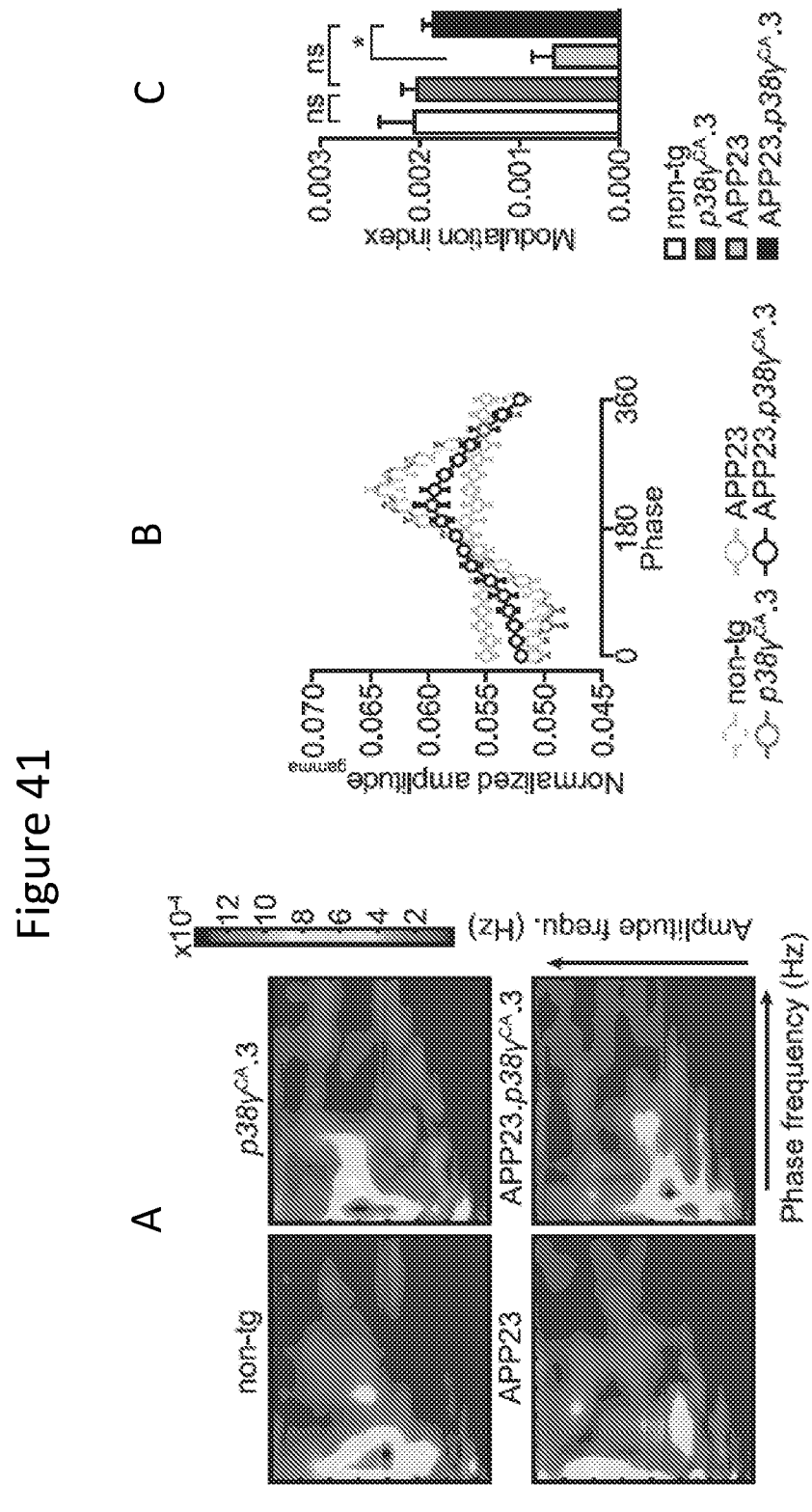
A
non-tg
p38γCA.3
APP23
APP23.p38γCA.3
x10-4
12
10
8
6
4
2
Amplitude frequ. (Hz)
Phase frequency (Hz)
B
Normalized amplitude
gamma
0.070
0.065
0.060
0.055
0.050
0.045
0
180
360
Phase
non-tg
p38γCA.3
APP23
APP23.p38γCA.3
C
Modulation index
0.003
0.002
0.001
0.000
ns
ns
*
non-tg
p38γCA.3
APP23
APP23.p38γCA.3

Figure 42

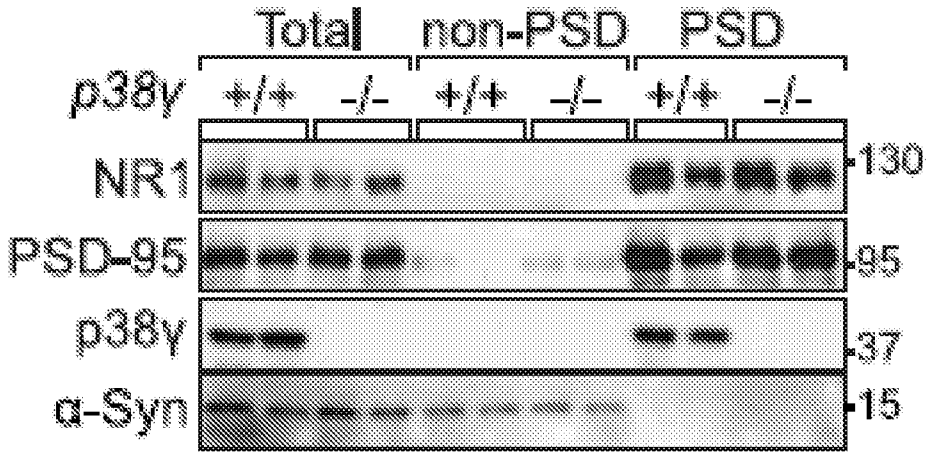

Figure 43

Human p38γ

A

```
ATGAGCTCTCCGCCGCCCGCCCGCAGTGGCTTTTACCGCCAGGAGGTGACCAAGACGGCCTGGGAGGTGCGCGCCGTGTA
CCGGGACCTGCAGCCCGTGGGCTCGGGCGCCTACGGCGCGGTGTGCTCGGCCGTGGACGGCCGCACCGGCGCTAAGGTGG
CCATCAAGAAGCTGTATCGGCCCTTCCAGTCCGAGCTGTTCGCCAAGCGCGCCTACCGCGAGCTGCGCCTGCTCAAGCAC
ATGCGCCACGAGAACGTGATCGGGCTGCTGGACGTATTCACTCCTGATGAGACCCTGGATGACTTCACGGACTTTTACCT
GGTGATGCCGTTCATGGGCACCGACCTGGGCAAGCTCATGAAACATGAGAAGCTAGGCGAGGACCGGATCCAGTTCCTCG
TGTACCAGATGCTGAAGGGGCTGAGGTATATCCACGCTGCCGGCATCATCCACAGAGACCTGAAGCCCGGCAACCTGGCT
GTGAACGAAGACTGTGAGCTGAAGATCCTGGACTTCGGCCTGGCCAGGCAGGCAGACAGTGAGATGACTGGGTACGTGGT
GACCCGGTGGTACCGGGCTCCCGAGGTCATCTTGAATTGGATGCGCTACACGCAGACGGTGGACATCTGGTCTGTGGGCT
GCATCATGGCGGAGATGATCACAGGCAAGACGCTGTTCAAGGGCAGCGACCACCTGGACCAGCTGAAGGAGATCATGAAG
GTGACGGGGACGCCTCCGGCTGAGTTTGTGCAGCGGCTGCAGAGCGATGAGGCCAAGAACTACATGAAGGGCCTCCCCGA
ATTGGAGAAGAAGGATTTTGCCTCTATCCTGACCAATGCAAGCCCTCTGGCTGTGAACCTCCTGGAGAAGATGCTGGTGC
TGGACGCGGAGCAGCGGGTGACGGCAGGCGAGGCGCTGGCCCATCCCTACTTCGAGTCCCTGCACGACACGGAAGATGAG
CCCCAGGTCCAGAAGTATGATGACTCCTTTGACGACGTTGACCGCACACTGGATGAATGGAAGCGTGTTACTTACAAAGA
GGTGCTCAGCTTCAAGCCTCCCCGGCAGCTGGGGGCCAGGGTCTCCAAGGAGACGCCTCTGTGA
```

B

```
MSSPPPARSGFYRQEVTKTAWEVRAVYRDLQPVGSGAYGAVCSAVDGRTGAKVAIKKLYR        60
PFQSELFAKRAYRELRLLKHMRHENVIGLLDVFTPDETLDDFTDFYLVMPFMGTDLGKLM       120
KHEKLGEDRIQFLVYQMLKGLRYIHAAGIIHRDLKPGNLAVNEDCELKILDFGLARQADS       180
EMTGYVVTRWYRAPEVILNWMRYTQTVDIWSVGCIMAEMITGKTLFKGSDHLDQLKEIMK       240
VTGTPPAEFVQRLQSDEAKNYMKGLPELEKKDFASILTNASPLAVNLLEKMLVLDAEQRV       300
TAGEALAHPYFESLHDTEDEPQVQKYDDSFDDVDRTLDEWKRVTYKEVLSFKPPRQLGAR       360
VSKETPL                                                             367
```

Figure 44

$p38\gamma^{CA}$ (D179A)

```
MSSPPPARSGFYRQEVTKTAWEVRAVYRDLQPVGSGAYGAVCSAVDGRTGAKVAIKKLYR    60
PFQSELFAKRAYRELRLLKHMRHENVIGLLDVFTPDETLDDFTDFYLVMPFMGTDLGKLM   120
KHEKLGEDRIQFLVYQMLKGLRYIHAAGIIHRDLKPGNLAVNEDCELKILDFGLARQA**A**S   180
EMTGYVVTRWYRAPEVILNWMRYTQTVDIWSVGCIMAEMITGKTLFKGSDHLDQLKEIMK   240
VTGTPPAEFVQRLQSDEAKNYMKGLPELEKKDFASILTNASPLAVNLLEKMLVLDAEQRV   300
TAGEALAHPYFESLHDTEDEPQVQKYDDSFDDVDRTLDEWKRVTYKEVLSFKPPRQLGAR   360
VSKETPL                                                         367
```

Figure 45

Human tau

```
  1 MAEPRQEFEV MEDHAGTYGL GDRKDQGGYT MHQDQEGDTD AGLKESPLQT PTEDGSEEPG
 61 SETSDAKSTP TAEDVTAPLV DEGAPGKQAA AQPHTEIPEG TTAEEAGIGD TPSLEDEAAG
121 HVTQARMVSK SKDGTGSDDK KAKGADGKTK IATPRGAAPP GQKGQANATR IPAKTPPAPK
181 TPPSSGEPPK SGDRSGYSSP GSPGTPGSRS RTPSLPTPPT REPKKVAVVR TPPKSPSSAK
241 SRLQTAPVPM PDLKNVKSKI GSTENLKHQP GGGKVQIINK KLDLSNVQSK CGSKDNIKHV
301 PGGGSVQIVY KPVDLSKVTS KCGSLGNIHH KPGGGQVEVK SEKLDFKDRV QSKIGSLDNI
361 THVPGGGNKK IETHKLTFRE NAKAKTDHGA EIVYKSPVVS GDTSPRHLSN VSSTGSIDMV
421 DSPQLATLAD EVSASLAKQG L
```

Human tau T205E

```
  1 MAEPRQEFEV MEDHAGTYGL GDRKDQGGYT MHQDQEGDTD AGLKESPLQT PTEDGSEEPG
 61 SETSDAKSTP TAEDVTAPLV DEGAPGKQAA AQPHTEIPEG TTAEEAGIGD TPSLEDEAAG
121 HVTQARMVSK SKDGTGSDDK KAKGADGKTK IATPRGAAPP GQKGQANATR IPAKTPPAPK
181 TPPSSGEPPK SGDRSGYSSP GSPGEPGSRS RTPSLPTPPT REPKKVAVVR TPPKSPSSAK
241 SRLQTAPVPM PDLKNVKSKI GSTENLKHQP GGGKVQIINK KLDLSNVQSK CGSKDNIKHV
301 PGGGSVQIVY KPVDLSKVTS KCGSLGNIHH KPGGGQVEVK SEKLDFKDRV QSKIGSLDNI
361 THVPGGGNKK IETHKLTFRE NAKAKTDHGA EIVYKSPVVS GDTSPRHLSN VSSTGSIDMV
421 DSPQLATLAD EVSASLAKQG L
```

Figure 46

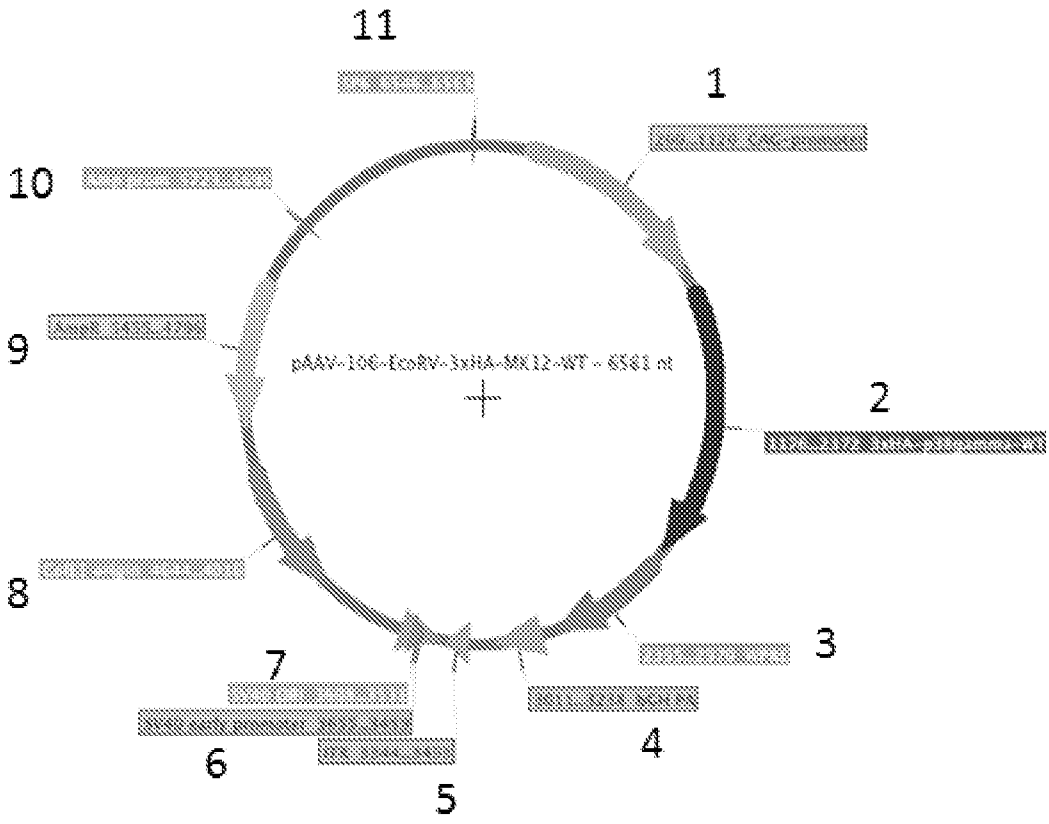

Figure 47

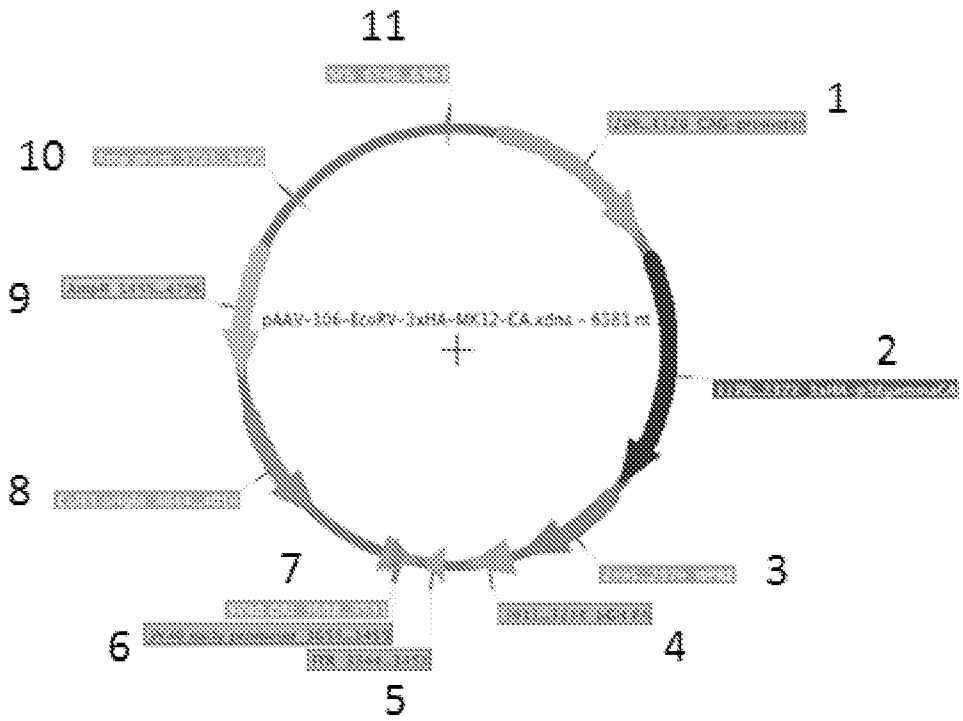

Figure 48

pAAV-CAG-106-3xHA-p38gamma(MAPK12)-wt

tagctgcgcgctcgctcgctcactgaggccgcccgggcaaagcccgggcgtcgggcga
cctttggtcgcccggcctcagtgagcgagcgagcgcgcagagagggagtggccaactc
catcactaggggttccttgtagttaatgattaacccgccatgctacttatctacgtag
ccatgctctaggtaccgggccccccctAgaggtAgacggtatcTTCCCATAGTAACGC
CAATAGGGACTTTCCATTGACGTCAATGGGTGGACTATTTACGGTAAACTGCCCACTT
GGCAGTACATCAAGTGTATCATATGCCAAGTACGCCCCCTATTGACGTCAATGACGGT
AAATGGCCCGCCTGGCATTATGCCCAGTACATGACCTTATGGGACTTTCCTACTTGGC
AGTACATCTACGTATTAGTCATCGCTATTACCATGGGTCGAGGTGAGCCCCACGTTCT
GCTTCACTCTCCCCATCTCCCCCCCCTCCCCACCCCCAATTTTGTATTTATTTATTTT
TTAATTATTTTGTGCAGCGATGGGGGCGGGGGGGGGGGGGCGCGCCAGGCGGGGC
GGGGCGGGGCGAGGGGCGGGGCGGGGCGAGGCGGAGAGGTGCGGCGGCAGCCAATCAG
AGCGGCGCGCTCCGAAAGTTTCCTTTTATGGCGAGGCGGCGGCGGCGGCGGCCCTATA
AAAAGCGAAGCGCGCGGCGGGCGGGAGTCGCTGCGTTGCCTTCGCCCCGTGCCCCGCT
CCGCGCCGccTCCGCGCCCGCCGCCCCGGCTCTGACTGACCGCGTTACTCCCACAGGT
GAGCGGGCGGGACGGCCCTTCTCCTCCGGGCTGTAATTAGCGCTTGGTTTAATGACGG
CTTGTTTCTTTTCTGTGGCTGCGTGAAAGCCTTGAGGGGCTCCGGGAGGGCCCTTTGT
GCGGGGGGAGCGGCTCGGGGCTGTCCGCGGGGGGACGGCTGCCTTCGGGGGGGACGGG
GCAGGGCGGGGTTCGGCTTCTGGCGTGTGACCGGCGGCTCTAGAGCCTCTGCTAACCA
TGTTCATGCCTTCTTCTTTTTCCTACAGCTCCTGGGCAACGTGCTGGTTATTGTGCTG
TCTCATCATTTTGGCAAAGAATTGGATCCACTCGAGTGGAGCTCGCGACTAGTCGATT
CGAATTCGATagctTATGTACCCATACGATGTTCCAGATTACGCCATGTACCCATACG
ATGTTCCAGATTACGCCATGTACCCATACGATGTTCCAGATTACGCCATGGGGAGCTC
TCCGCCGCCCGCCCGCAGTGGCTTTTACCGCCAGGAGGTGACCAAGACGGCCTGGGAG
GTGCGCGCCGTGTACCGGGACCTGCAGCCCGTGGGCTCGGGCGCCTACGGCGCGGTGT
GCTCGGCCGTGGACGGCCGCACCGGCGCTAAGGTGGCCATCAAGAAGCTGTATCGGCC
CTTCCAGTCCGAGCTGTTCGCCAAGCGCGCCTACCGCGAGCTGCGCCTGCTCAAGCAC
ATGCGCCACGAGAACGTGATCGGGCTGCTGGACGTATTCACTCCTGATGAGACCCTGG
ATGACTTCACGGACTTTTACCTGGTGATGCCGTTCATGGGCACCGACCTGGGCAAGCT
CATGAAACATGAGAAGCTAGGCGAGGACCGGATCCAGTTCCTCGTGTACCAGATGCTG
AAGGGGCTGAGGTATATCCACGCTGCCGGCATCATCCACAGAGACCTGAAGCCCGGCA
ACCTGGCTGTGAACGAAGACTGTGAGCTGAAGATCCTGGACTTCGGCCTGGCCAGGCA
GGCAGACAGTGAGATGACTGGGTACGTGGTGACCCGGTGGTACCGGGCTCCCGAGGTC
ATCTTGAATTGGATGCGCTACACGCAGACGGTGGACATCTGGTCTGTGGGCTGCATCA
TGGCGGAGATGATCACAGGCAAGACGCTGTTCAAGGGCAGCGACCACCTGGACCAGCT
GAAGGAGATCATGAAGGTGACGGGGACGCCTCCGGCTGAGTTTGTGCAGCGGCTGCAG
AGCGATGAGGCCAAGAACTACATGAAGGGCCTCCCCGAATTGGAGAAGAAGGATTTTG
CCTCTATCCTGACCAATGCAAGCCCTCTGGCTGTGAACCTCCTGGAGAAGATGCTGGT
GCTGGACGCGGAGCAGCGGGTGACGGCAGGCGAGGCGCTGGCCCATCCCTACTTCGAG
TCCCTGCACGACACGGAAGATGAGCCCCAGGTCCAGAAGTATGATGACTCCTTTGACG
ACGTTGACCGCACACTGGATGAATGGAAGCGTGTTACTTACAAAGAGGTGCTCAGCTT
CAAGCCTCCCCGGCAGCTGGGGGCCAGGGTCTCCAAGGAGACGCCTCTGTGATctagA
TCAAGCTTATCgataatcaacctctggattacaaaatttgtgaaagattgactggtat
tcttaactatgttgctccttttacgctatgtggatacgctgctttaatgcctttgtat
catgctattgcttcccgtatggctttcattttctcctccttgtataaatcctggttgc

Figure 48 cont.

tgtctctttatgaggagttgtggcccgttgtcaggcaacgtggcgtggtgtgcactgt
gtttgctgacgcaacccccactggttggggcattgccaccacctgtcagctcctttcc
gggactttcgctttcccccctccctattgccacggcggaactcatcgccgcctgccttg
cccgctgctggacaggggctcggctgttgggcactgacaattccgtggtgttgtcggg
gaaGCTGAcgtcctttccAtggctgctcgcctgtgttgccacctggattctgcgcggg
acgtccttctgctacgtcccttcggccctcaatccagcggaccttccttcccgcggcc
tgctgccggctctgcggcctcttccgcgtcttcgccttcgccctcagacgagtcggat
ctccctttgggccgcctccccgcatcgataccgtcgactcgctgatcagcctcgactg
tgccttctagttgccagccatctgttgtttgcccctcccccgtgccttccttgaccct
ggaaggtgccactcccactgtcctttcctaataaaatgaggaaattgcatcgcattgt
ctgagtaggtgtcattctattctgggggggtggggtggggcaggacagcaaggggagg
attgggaagacaatagcaggcatgctggggatgcggtgggctctatggcttctgaggc
ggaaagaaccagctggggctcgactagagcatggctacgtagataagtagcatggcgg
gttaatcattaactacaaggaacccctagtgatggagttggccactccctctctgcgc
gctcgctcgctcactgaggccgggcgaccaaaggtcgcccgacgcccgggctttgccc
gggcggcctcagtgagcgagcgagcgcgcagagcttttgcaaaagcctaggcctcca
aaaaagcctcctcactacttctggaatagctcagaggccgaggcggcctcggcctctg
cataaataaaaaaaattagtcagccatggggcggagaatgggcggaactgggcggagt
tagggggcgggatgggcggagttaggggcgggactatggttgctgactaattgagatgc
atgctttgcatacttctgcctgctggggagcctggggactttccacacctggttgc
tgactaattgagatgcatgctttgcatacttctgcctgctggggagcctggggacttt
ccacaccctaactgacacacattccacagctgcattaatgaatcggccaacgcgcggg
gagaggcggtttgcgtattgggcgctcttccgcttcctcgctcactgactcgctgcgc
tcggtcgttcggctgcggcgagcggtatcagctcactcaaaggcggtaatacggttat
ccacagaatcaggggataacgcaggaaagaacatgtgagcaaaaggccagcaaaaggc
caggaaccgtaaaaaggccgcgttgctggcgtttttccataggctccgccccctgac
gagcatcacaaaaatcgacgctcaagtcagaggtggcgaaacccgacaggactataaa
gataccaggcgtttccccctggaagctccctcgtgcgctctcctgttccgaccctgcc
gcttaccggatacctgtccgcctttctcccttcgggaagcgtggcgctttctcatagc
tcacgctgtaggtatctcagttcggtgtaggtcgttcgctccaagctgggctgtgtgc
acgaaccccccgttcagcccgaccgctgcgccttatccggtaactatcgtcttgagtc
caacccggtaagacacgacttatcgccactggcagcagccactggtaacaggattagc
agagcgaggtatgtaggcggtgctacagagttcttgaagtggtggcctaactacggct
acactagaagaacagtatttggtatctgcgctctgctgaagccagttaccttcggaaa
aagagttggtagctcttgatccggcaaacaaaccaccgctggtagcggtggttttttt
gtttgcaagcagcagattacgcgcagaaaaaaaggatctcaagaagatcctttgatct
tttctacggggtctgacgctcagtggaacgaaaactcacgttaagggattttggtcat
gagattatcaaaaaggatcttcacctagatccttttaaattaaaaatgaagttttaaa
tcaatctaaagtatatatgagtaaacttggtctgacagttaccaatgcttaatcagtg
aggcacctatctcagcgatctgtctatttcgttcatccatagttgcctgactccccgt
cgtgtagataactacgatacgggagggcttaccatctggccccagtgctgcaatgata
ccgcgagacccacgctcaccggctccagatttatcagcaataaaccagccagccggaa
gggccgagcgcagaagtggtcctgcaactttatccgcctccatccagtctattaattg
ttgccgggaagctagagtaagtagttcgccagttaatagtttgcgcaacgttgttgcc
attgctacaggcatcgtggtgtcacgctcgtcgtttggtatggcttcattcagctccg

Figure 48 cont.

gttcccaacgatcaaggcgagttacatgatcccccatgttgtgcaaaaaagcggttag
ctccttcggtcctccgatcgttgtcagaagtaagttggccgcagtgttatcactcatg
gttatggcagcactgcataattctcttactgtcatgccatccgtaagatgcttttctg
tgactggtgagtactcaaccaagtcattctgagaatagtgtatgcggcgaccgagttg
ctcttgcccggcgtcaatacgggataataccgcgccacatagcagaactttaaaagtg
ctcatcattggaaaacgttcttcggggcgaaaactctcaaggatcttaccgctgttga
gatccagttcgatgtaacccactcgtgcacccaactgatcttcagcatcttttacttt
caccagcgtttctgggtgagcaaaaacaggaaggcaaaatgccgcaaaaaagggaata
agggcgacacggaaatgttgaatactcatactcttccttttcaatattattgaagca
tttatcagggttattgtctcatgagcggatacatatttgaatgtatttagaaaaataa
acaaatagggttccgcgcacatttccccgaaaagtgccacctgacgtctaagaaacc
attattatcatgacattaacctataaaaataggcgtatcacgaggccctttcgtctcg
cgcgtttcggtgatgacggtgaaaacctctgacacatgcagctcccggagacggtcac
agcttgtctgtaagcggatgccgggagcagacaagcccgtcagggcgcgtcagcgggt
gttggcgggtgtcggggctggcttaactatgcggcatcagagcagattgtactgagag
tgcaccattcgacgctctcccttatgcgactcctgcattaggaagcagcccagtagta
ggttgaggccgttgagcaccgccgccgcaaggaatggtgcatgcaaggagatggcgcc
caacagtcccccggccacggggcctgccaccatacccacgccgaaacaagcgctcatg
agcccgaagtggcgagcccgatcttccccatcggtgatgtcggcgatataggcgccag
caaccgcacctgtggcgccggtgatgccggccacgatgcgtccggcgtagaggatctg
gctagcgatgaccctgctgattggttcgctgaccatttccgggtgcgggacggcgtta
ccagaaactcagaaggttcgtccaaccaaaccgactctgacggcagtttacgagagag
atgatagggtctgcttcagtaagccagatgctacacaattaggcttgtacatattgtc
gttagaacgcggctacaattaatacataaccttatgtatcatacacatacgatttagg
tgacactatagaatacacggaattaattc

Figure 49

pAAV-CAG-106-3xHA-p38gamma(MAPK12)-ca

tagctgcgcgctcgctcgctcactgaggccgcccgggcaaagcccgggcgtcgggcga
cctttggtcgcccggcctcagtgagcgagcgagcgcgcagagagggagtggccaactc
catcactaggggttccttgtagttaatgattaacccgccatgctacttatctacgtag
ccatgctctaggtaccgggccccccctAgaggtAgacggtatcTTCCCATAGTAACGC
CAATAGGGACTTTCCATTGACGTCAATGGGTGGACTATTTACGGTAAACTGCCCACTT
GGCAGTACATCAAGTGTATCATATGCCAAGTACGCCCCCTATTGACGTCAATGACGGT
AAATGGCCCGCCTGGCATTATGCCCAGTACATGACCTTATGGGACTTTCCTACTTGGC
AGTACATCTACGTATTAGTCATCGCTATTACCATGGGTCGAGGTGAGCCCCACGTTCT
GCTTCACTCTCCCCATCTCCCCCCCCTCCCCACCCCCAATTTTGTATTTATTTATTTT
TTAATTATTTTGTGCAGCGATGGGGGCGGGGGGGGGGGGGCGCGCGCCAGGCGGGGC
GGGGCGGGGCGAGGGGCGGGGCGGGGCGAGGCGGAGAGGTGCGGCGGCAGCCAATCAG
AGCGGCGCGCTCCGAAAGTTTCCTTTTATGGCGAGGCGGCGGCGGCGGCGGCCCTATA
AAAAGCGAAGCGCGCGGCGGGCGGGAGTCGCTGCGTTGCCTTCGCCCCGTGCCCCGCT
CCGCGCCGccTCCGCGCCCGCCGCCCCGGCTCTGACTGACCGCGTTACTCCCACAGGT
GAGCGGGCGGGACGGCCCTTCTCCTCCGGGCTGTAATTAGCGCTTGGTTTAATGACGG
CTTGTTTCTTTTCTGTGGCTGCGTGAAAGCCTTGAGGGGCTCCGGGAGGGCCCTTTGT
GCGGGGGGAGCGGCTCGGGGCTGTCCGCGGGGGGACGGCTGCCTTCGGGGGGGACGGG
GCAGGGCGGGGTTCGGCTTCTGGCGTGTGACCGGCGGCTCTAGAGCCTCTGCTAACCA
TGTTCATGCCTTCTTCTTTTTCCTACAGCTCCTGGGCAACGTGCTGGTTATTGTGCTG
TCTCATCATTTTGGCAAAGAATTGGATCCACTCGAGTGGAGCTCGCGACTAGTCGATT
CGAATTCGATagctTATGTACCCATACGATGTTCCAGATTACGCCATGTACCCATACG
ATGTTCCAGATTACGCCATGTACCCATACGATGTTCCAGATTACGCCATGGGGAGCTC
TCCGCCGCCCGCCCGCAGTGGCTTTTACCGCCAGGAGGTGACCAAGACGGCCTGGGAG
GTGCGCGCCGTGTACCGGGACCTGCAGCCCGTGGGCTCGGGCGCCTACGGCGCGGTGT
GCTCGGCCGTGGACGGCCGCACCGGCGCTAAGGTGGCCATCAAGAAGCTGTATCGGCC
CTTCCAGTCCGAGCTGTTCGCCAAGCGCGCCTACCGCGAGCTGCGCCTGCTCAAGCAC
ATGCGCCACGAGAACGTGATCGGGCTGCTGGACGTATTCACTCCTGATGAGACCCTGG
ATGACTTCACGGACTTTTACCTGGTGATGCCGTTCATGGGCACCGACCTGGGCAAGCT
CATGAAACATGAGAAGCTAGGCGAGGACCGGATCCAGTTCCTCGTGTACCAGATGCTG
AAGGGGCTGAGGTATATCCACGCTGCCGGCATCATCCACAGAGACCTGAAGCCCGGCA
ACCTGGCTGTGAACGAAGACTGTGAGCTGAAGATCCTGGACTTCGGCCTGGCCAGGCA
GGCAGCCAGTGAGATGACTGGGTACGTGGTGACCCGGTGGTACCGGGCTCCCGAGGTC
ATCTTGAATTGGATGCGCTACACGCAGACGGTGGACATCTGGTCTGTGGGCTGCATCA
TGGCGGAGATGATCACAGGCAAGACGCTGTTCAAGGGCAGCGACCACCTGGACCAGCT
GAAGGAGATCATGAAGGTGACGGGGACGCCTCCGGCTGAGTTTGTGCAGCGGCTGCAG
AGCGATGAGGCCAAGAACTACATGAAGGGCCTCCCCGAATTGGAGAAGAAGGATTTTG
CCTCTATCCTGACCAATGCAAGCCCTCTGGCTGTGAACCTCCTGGAGAAGATGCTGGT
GCTGGACGCGGAGCAGCGGGTGACGGCAGGCGAGGCGCTGGCCCATCCCTACTTCGAG
TCCCTGCACGACACGGAAGATGAGCCCCAGGTCCAGAAGTATGATGACTCCTTTGACG
ACGTTGACCGCACACTGGATGAATGGAAGCGTGTTACTTACAAAGAGGTGCTCAGCTT
CAAGCCTCCCCGGCAGCTGGGGGCCAGGGTCTCCAAGGAGACGCCTCTGTGATctagA
TCAAGCTTATCgataatcaacctctggattacaaaatttgtgaaagattgactggtat
tcttaactatgttgctccttttacgctatgtggatacgctgctttaatgcctttgtat
catgctattgcttcccgtatggctttcattttctcctccttgtataaatcctggttgc

Figure 49 cont.

tgtctctttatgaggagttgtggcccgttgtcaggcaacgtggcgtggtgtgcactgt
gtttgctgacgcaacccccactggttggggcattgccaccacctgtcagctcctttcc
gggactttcgctttccccctccctattgccacggcggaactcatcgccgcctgccttg
cccgctgctggacaggggctcggctgttgggcactgacaattccgtggtgttgtcggg
gaaGCTGAcgtcctttccAtggctgctcgcctgtgttgccacctggattctgcgcggg
acgtccttctgctacgtcccttcggccctcaatccagcggaccttccttcccgcggcc
tgctgccggctctgcggcctcttccgcgtcttcgccttcgccctcagacgagtcggat
ctccctttgggccgcctccccgcatcgataccgtcgactcgctgatcagcctcgactg
tgccttctagttgccagccatctgttgtttgcccctcccccgtgccttccttgaccct
ggaaggtgccactcccactgtcctttcctaataaaatgaggaaattgcatcgcattgt
ctgagtaggtgtcattctattctgggggggtggggtggggcaggacagcaaggggagg
attgggaagacaatagcaggcatgctggggatgcggtgggctctatggcttctgaggc
ggaaagaaccagctggggctcgactagagcatggctacgtagataagtagcatggcgg
gttaatcattaactacaaggaacccctagtgatggagttggccactccctctctgcgc
gctcgctcgctcactgaggccgggcgaccaaaggtcgcccgacgcccgggctttgccc
gggcggcctcagtgagcgagcgagcgcgcagagcttttgcaaaagcctaggcctcca
aaaaagcctcctcactacttctggaatagctcagaggccgaggcggcctcggcctctg
cataaataaaaaaaattagtcagccatggggcggagaatgggcggaactgggcggagt
taggggcgggatgggcggagttaggggcgggactatggttgctgactaattgagatgc
atgctttgcatacttctgcctgctggggagcctggggactttccacacctggttgctg
actaattgagatgcatgctttgcatacttctgcctgctggggagcctggggactttcc
acaccctaactgacacacattccacagctgcattaatgaatcggccaacgcgcgggga
gaggcggtttgcgtattgggcgctcttccgcttcctcgctcactgactcgctgcgctc
ggtcgttcggctgcggcgagcggtatcagctcactcaaaggcggtaatacggttatcc
acagaatcaggggataacgcaggaaagaacatgtgagcaaaaggccagcaaaaggcca
ggaaccgtaaaaaggccgcgttgctggcgtttttccataggctccgccccctgacga
gcatcacaaaaatcgacgctcaagtcagaggtggcgaaacccgacaggactataaaga
taccaggcgtttcccccctggaagctccctcgtgcgctctcctgttccgaccctgccgc
ttaccggatacctgtccgcctttctcccttcgggaagcgtggcgctttctcatagctc
acgctgtaggtatctcagttcggtgtaggtcgttcgctccaagctgggctgtgtgcac
gaaccccccgttcagcccgaccgctgcgccttatccggtaactatcgtcttgagtcca
acccggtaagacacgacttatcgccactggcagcagccactggtaacaggattagcag
agcgaggtatgtaggcggtgctacagagttcttgaagtggtggcctaactacggctac
actagaagaacagtatttggtatctgcgctctgctgaagccagttaccttcggaaaaa
gagttggtagctcttgatccggcaaacaaaccaccgctggtagcggtggtttttttgt
ttgcaagcagcagattacgcgcagaaaaaaaggatctcaagaagatcctttgatcttt
tctacggggtctgacgctcagtggaacgaaaactcacgttaagggattttggtcatga
gattatcaaaaaggatcttcacctagatccttttaaattaaaaatgaagttttaaatc
aatctaaagtatatatgagtaaacttggtctgacagttaccaatgcttaatcagtgag
gcacctatctcagcgatctgtctatttcgttcatccatagttgcctgactccccgtcg
tgtagataactacgatacgggagggcttaccatctggccccagtgctgcaatgatacc
gcgagacccacgctcaccggctccagatttatcagcaataaaccagccagccggaagg
gccgagcgcagaagtggtcctgcaactttatccgcctccatccagtctattaattgtt
gccgggaagctagagtaagtagttcgccagttaatagtttgcgcaacgttgttgccat

Figure 49 cont.

tgctacaggcatcgtggtgtcacgctcgtcgtttggtatggcttcattcagctccggt
tcccaacgatcaaggcgagttacatgatcccccatgttgtgcaaaaaagcggttagct
ccttcggtcctccgatcgttgtcagaagtaagttggccgcagtgttatcactcatggt
tatggcagcactgcataattctcttactgtcatgccatccgtaagatgcttttctgtg
actggtgagtactcaaccaagtcattctgagaatagtgtatgcggcgaccgagttgct
cttgcccggcgtcaatacgggataataccgcgccacatagcagaactttaaaagtgct
catcattggaaaacgttcttcggggcgaaaactctcaaggatcttaccgctgttgaga
tccagttcgatgtaacccactcgtgcacccaactgatcttcagcatcttttactttca
ccagcgtttctgggtgagcaaaaacaggaaggcaaaatgccgcaaaaaagggaataag
ggcgacacggaaatgttgaatactcatactcttccttttcaatattattgaagcatt
tatcagggttattgtctcatgagcggatacatatttgaatgtatttagaaaaataaac
aaatagggttccgcgcacatttccccgaaaagtgccacctgacgtctaagaaaccat
tattatcatgacattaacctataaaaataggcgtatcacgaggccctttcgtctcgcg
cgtttcggtgatgacggtgaaaacctctgacacatgcagctcccggagacggtcacag
cttgtctgtaagcggatgccgggagcagacaagcccgtcagggcgcgtcagcgggtgt
tggcgggtgtcggggctggcttaactatgcggcatcagagcagattgtactgagagtg
caccattcgacgctctcccttatgcgactcctgcattaggaagcagcccagtagtagg
ttgaggccgttgagcaccgccgccgcaaggaatggtgcatgcaaggagatggcgccca
acagtcccccggccacggggcctgccaccatacccacgccgaaacaagcgctcatgag
cccgaagtggcgagcccgatcttccccatcggtgatgtcggcgatataggcgccagca
accgcacctgtggcgccggtgatgccggccacgatgcgtccggcgtagaggatctggc
tagcgatgaccctgctgattggttcgctgaccatttccgggtgcgggacggcgttacc
agaaactcagaaggttcgtccaaccaaaccgactctgacggcagtttacgagagagat
gatagggtctgcttcagtaagccagatgctacacaattaggcttgtacatattgtcgt
tagaacgcggctacaattaatacataaccttatgtatcatacacatacgatttaggtg
acactatagaatacacggaattaattc

INTERNATIONAL SEARCH REPORT

International application No.
PCT/AU2017/050180

A. CLASSIFICATION OF SUBJECT MATTER

A61K 38/17 (2006.01) A61P 25/28 (2006.01) A61P 25/08 (2006.01) A61P 9/10 (2006.01)

According to International Patent Classification (IPC) or to both national classification and IPC

B. FIELDS SEARCHED

Minimum documentation searched (classification system followed by classification symbols)

Documentation searched other than minimum documentation to the extent that such documents are included in the fields searched

Electronic data base consulted during the international search (name of data base and, where practicable, search terms used)

Databases: WPIAP, EPODOC, MEDLINE, CAPLUS, EMBASE, BIOSIS, Esp@cenet, Pubmed, and internal databases provided by IP Australia

Keywords: Tau, MAPT, DDPAC, FTDP-17, PPND, PPP1R103, p38 gamma, ERK6, SAPK-3, MAPK-12, Fyn, PSD-95, SAP-90, phosphorylate, phospho-mimic, pseudo-phospho, T205, Adeno-associated virus, and similar terms, as well as SEQ ID NO. 2 and 3 and the Applicant's and Inventor's names.

C. DOCUMENTS CONSIDERED TO BE RELEVANT

Category*	Citation of document, with indication, where appropriate, of the relevant passages	Relevant to claim No.
	Documents are listed in the continuation of Box C	

[X] Further documents are listed in the continuation of Box C [X] See patent family annex

* Special categories of cited documents:

"A" document defining the general state of the art which is not considered to be of particular relevance

"E" earlier application or patent but published on or after the international filing date

"L" document which may throw doubts on priority claim(s) or which is cited to establish the publication date of another citation or other special reason (as specified)

"O" document referring to an oral disclosure, use, exhibition or other means

"P" document published prior to the international filing date but later than the priority date claimed

"T" later document published after the international filing date or priority date and not in conflict with the application but cited to understand the principle or theory underlying the invention

"X" document of particular relevance; the claimed invention cannot be considered novel or cannot be considered to involve an inventive step when the document is taken alone

"Y" document of particular relevance; the claimed invention cannot be considered to involve an inventive step when the document is combined with one or more other such documents, such combination being obvious to a person skilled in the art

"&" document member of the same patent family

Date of the actual completion of the international search	Date of mailing of the international search report
16 May 2017	16 May 2017
Name and mailing address of the ISA/AU	**Authorised officer**
AUSTRALIAN PATENT OFFICE PO BOX 200, WODEN ACT 2606, AUSTRALIA Email address: pct@ipaustralia.gov.au	Christina van Broekhoven AUSTRALIAN PATENT OFFICE (ISO 9001 Quality Certified Service) Telephone No. 0262833196

INTERNATIONAL SEARCH REPORT C (Continuation). DOCUMENTS CONSIDERED TO BE RELEVANT		International application No. PCT/AU2017/050180
Category*	Citation of document, with indication, where appropriate, of the relevant passages	Relevant to claim No.
X	Buee-Scherre, V. et al. 2002 "Phosphorylation of microtubule-associated protein tau by stress-activated protein kinases in intact cells" FEBS Letters, Vol. 515, pp. 151-154 see pp. 151, Abstract and Discussion	25, 26, 36-39, 54-59
X	Goedert, M. et al 1997 "Phosphorylation of microtubule-associated protein tau by stress-activated protein kinases" FEBS Letters, Vol. 409, pp. 57-62 see pp. 57, Abstract and Discussion	25, 26, 36-39, 54-59
X	Sabio, G. et al. 2004 "Stress- and mitogen-induced phosphorylation of the synapse-associated protein SAP90/PSD-95 by activation of SAPK3/p38γ and ERK1/ERK2" Biochem. J. Vol. 380, pp. 19-30 see pp. 20	25, 26, 36-39, 54-59
X	WO 2007/094867 A2 (GE HEALTHCARE UK LIMITED) 23 August 2007 see pp. 10 and 12 and claims	25-28, 30-31, 36-39, and 54-59
X	Long, D. et al. 2010 "p38g mitogen-activated protein kinase suppresses chondrocyte production of MMP-13 in response to catabolic stimulation", Osteoarthritis and Cartilage, Vol. 18, pp. 1203-1210 see pp. 1204-5	25, 26, 32-39, and 54-59
X	Rankin, C. et al. 2005 "Pseudo-phosphorylation of tau at Ser202 and Thr205 affects tau filament formation", Molecular Brain Research, Vol. 138, pp. 84-93 see pp. 85, Abstract and Discussion	25, 36-39, and 54-59
A	Jeganathan, S. et al. 2008 "Proline-directed Pseudo-phosphorylation at AT8 and PHF1 Epitopes Induces a Compaction of the Paperclip Folding of Tau and Generates a Pathological (MC-1) Conformation" The Journal of Biological Chemistry Vol. 283, No. 46, pp. 32066-32076 see, pp.32067, Abstract and Discussion	1-59
A	Pooler, A. et al. 2012 "Dynamic association of tau with neuronal membranes is regulated by phosphorylation" Neurobiology of Aging, Vol. 33, pp. 431.e27-431.e38 see, Figure 6, Abstract and Discussion	1-59
A	Sun, Q. et al. 2009 "Pseudo-hyperphosphorylation causing AD-like changes in tau has significant effects on its polymerization" Biochemistry, Vol. 48, No. 25, pp. 6002-6011 see, Abstract, Results and Discussion	1-59
A	WO 2007/062167 A2 (INTERMUNE, INC.) 31 May 2007 see Examples and Claims	1-59
A	WO 2012/009442 A2 (MERCK SHARP & DOHME CORP.) 19 January 2012 see Examples and Claims	1-59
A	WO 2008/124066 A1 (THE J. DAVID GLADSTONE INSTITUTE) 16 October 2008 see Examples and Claims	1-59
A	Tenreiro, S. et al. 2014 "Protein phosphorylation in neurodegeneration: friend or foe?" Frontiers in Molecular Neuroscience, Vol. 7, Article 42, pp. 1-30 see pp. 10-19	1-59
	Ittner, L. et al 2010 "Dendritic function of tau mediates amyloid-beta toxicity in Alzheimer's disease mouse models." Cell, Vol. 142, No. 3, pp. 387-97	

INTERNATIONAL SEARCH REPORT C (Continuation). DOCUMENTS CONSIDERED TO BE RELEVANT		International application No. **PCT/AU2017/050180**
Category*	Citation of document, with indication, where appropriate, of the relevant passages	Relevant to claim No.
A	see Discussion	1-59
A	WO 2013/086583 A1 (THE UNIVERSITY OF SYDNEY) 20 June 2013 see Examples and Claims	1-59

INTERNATIONAL SEARCH REPORT Information on patent family members	International application No. **PCT/AU2017/050180**

This Annex lists known patent family members relating to the patent documents cited in the above-mentioned international search report. The Australian Patent Office is in no way liable for these particulars which are merely given for the purpose of information.

Patent Document/s Cited in Search Report		Patent Family Member/s	
Publication Number	**Publication Date**	**Publication Number**	**Publication Date**
WO 2007/094867 A2	23 August 2007	WO 2007094867 A2	23 Aug 2007
		EP 1941044 A2	09 Jul 2008
		JP 2009513150 A	02 Apr 2009
		US 2008227131 A1	18 Sep 2008
WO 2007/062167 A2	31 May 2007	WO 2007062167 A2	31 May 2007
		AU 2006318428 A1	31 May 2007
		BR PI0618939 A2	13 Sep 2011
		CA 2630752 A1	31 May 2007
		CN 101360750 A	04 Feb 2009
		EP 1960405 A2	27 Aug 2008
		EP 2426134 A2	07 Mar 2012
		JP 2009517390 A	30 Apr 2009
		KR 20080076968 A	20 Aug 2008
		US 2011034495 A1	10 Feb 2011
WO 2012/009442 A2	19 January 2012	WO 2012009442 A2	19 Jan 2012
		AU 2011279221 A1	31 Jan 2013
		AU 2011279221 B2	11 Jun 2015
		AU 2012282825 A1	16 Jan 2014
		AU 2012282825 B2	26 May 2016
		AU 2013355359 A1	21 May 2015
		BR 112014000671 A2	14 Feb 2017

Due to data integration issues this family listing may not include 10 digit Australian applications filed since May 2001.

INTERNATIONAL SEARCH REPORT Information on patent family members	International application No. **PCT/AU2017/050180**

This Annex lists known patent family members relating to the patent documents cited in the above-mentioned international search report. The Australian Patent Office is in no way liable for these particulars which are merely given for the purpose of information.

Patent Document/s Cited in Search Report		Patent Family Member/s	
Publication Number	**Publication Date**	**Publication Number**	**Publication Date**
		CA 2805414 A1	19 Jan 2012
		CA 2840976 A1	17 Jan 2013
		CA 2891627 A1	12 Jun 2014
		CN 103140500 A	05 Jun 2013
		CN 103140500 B	09 Sep 2015
		CN 103782171 A	07 May 2014
		CN 103782171 B	14 Dec 2016
		EP 2593475 A2	22 May 2013
		EP 2593475 B1	02 Mar 2016
		EP 2732286 A1	21 May 2014
		EP 2732289 A2	21 May 2014
		EP 2928561 A1	14 Oct 2015
		JP 2013542914 A	28 Nov 2013
		JP 5934203 B2	15 Jun 2016
		JP 2014521089 A	25 Aug 2014
		JP 2016502553 A	28 Jan 2016
		KR 20130135831 A	11 Dec 2013
		KR 20140072019 A	12 Jun 2014
		MX 2013000490 A	21 Feb 2013
		MX 338640 B	25 Apr 2016
		MX 2014000480 A	23 Jun 2014
		RU 2013106270 A	20 Aug 2014
		RU 2014105172 A	20 Aug 2015
		US 2013130288 A1	23 May 2013
		US 9176151 B2	03 Nov 2015
		US 2015023952 A1	22 Jan 2015
		US 9309309 B2	12 Apr 2016
		US 2015260731 A1	17 Sep 2015
		US 9310383 B2	12 Apr 2016
		US 2013089537 A1	11 Apr 2013
		US 9320793 B2	26 Apr 2016
		US 2013052670 A1	28 Feb 2013
		US 2013115227 A1	09 May 2013
		US 2014120037 A1	01 May 2014
		US 2015320860 A1	12 Nov 2015
		WO 2013009667 A1	17 Jan 2013

Due to data integration issues this family listing may not include 10 digit Australian applications filed since May 2001.

INTERNATIONAL SEARCH REPORT Information on patent family members	International application No. **PCT/AU2017/050180**

This Annex lists known patent family members relating to the patent documents cited in the above-mentioned international search report. The Australian Patent Office is in no way liable for these particulars which are merely given for the purpose of information.

Patent Document/s Cited in Search Report		Patent Family Member/s	
Publication Number	**Publication Date**	**Publication Number**	**Publication Date**
		WO 2013009703 A2	17 Jan 2013
		WO 2014089149 A1	12 Jun 2014
WO 2008/124066 A1	16 October 2008	WO 2008124066 A1	16 Oct 2008
		CA 2682497 A1	16 Oct 2008
		EP 2145014 A1	20 Jan 2010
		EP 2145014 B1	12 Dec 2012
		EP 2578692 A1	10 Apr 2013
		EP 2578692 B1	08 Jun 2016
		JP 2010525303 A	22 Jul 2010
		JP 5721426 B2	20 May 2015
		JP 2015107972 A	11 Jun 2015
		JP 5997241 B2	28 Sep 2016
		US 2014065206 A1	06 Mar 2014
		US 9084813 B2	21 Jul 2015
		US 2012198573 A1	02 Aug 2012
		US 9198982 B2	01 Dec 2015
		US 2008249058 A1	09 Oct 2008
WO 2013/086583 A1	20 June 2013	WO 2013086583 A1	20 Jun 2013
		US 2015017657 A1	15 Jan 2015

End of Annex

Due to data integration issues this family listing may not include 10 digit Australian applications filed since May 2001.